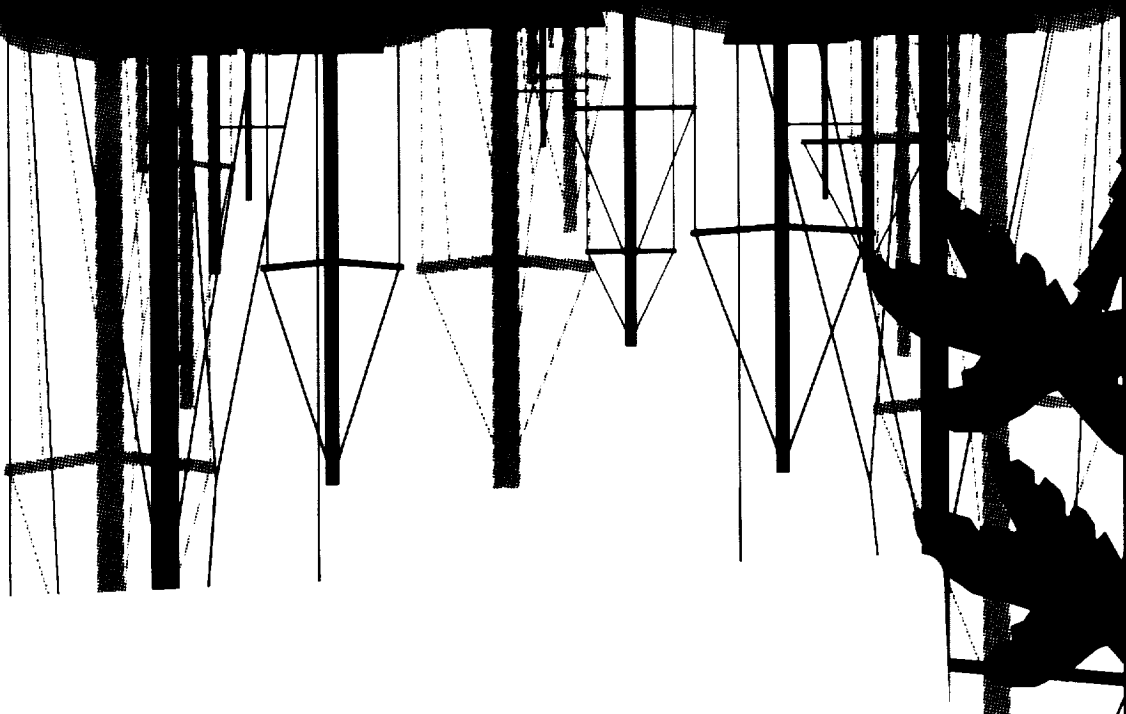


# PRESENTATION ORAL



63/76 0122332

(NASA) 206 P

Unclass

N93-11684

1992

(NASA-CR-190919) ICCG-10: TENTH  
INTERNATIONAL CONFERENCE ON CRYSTAL  
GROWTH. ORAL PRESENTATION ABSTRACTS

Sheraton Harbor Island Hotel  
San Diego, California, USA  
August 16 - 21, 1992

TENTH INTERNATIONAL CONFERENCE  
ON CRYSTAL GROWTH

# ICCG-10

NAGW-3079

NASA-CR-190919



ICCG-10

---

**ICCG-10**  
**ORAL PRESENTATION ABSTRACTS**

**INDEX**

**ORGANIZATION**

ORGANIZING COMMITTEES .....	i
INTERNATIONAL ADVISORY BOARD .....	ii
IOCG OFFICERS/EXECUTIVE COMMITTEE .....	ii
IOCG COUNCILORS/GENERAL ASSEMBLY .....	iii
ICCG-10 CORPORATE SPONSORS .....	iii
ICCG-10 GOVERNMENT SPONSORS .....	iii

**CONFERENCE SCHEDULE and PROGRAM .....** Blue Pages

**ABSTRACTS**

SESSION 1 .....	1
SESSION 2 .....	27
SESSION 3 .....	51
SESSION 4 .....	77
SESSION 5 .....	97
SESSION 6 .....	125
SESSION 7 .....	149
SESSION 8 .....	151
SESSION 9 .....	179

**AUTHOR INDEX .....** 197

**ACTIVITIES LOCATION**

**LOCATION MAP .....** inside back cover

## ORGANIZING COMMITTEES

	CHAIRPERSONS	COMMITTEE PERSONS
CONFERENCE CO-CHAIRMEN:	W.A. Bonner J.F. Wenckus	
TECHNICAL PROGRAM:	R.S. Feigelson R.F. Sekerka	Reviewers M. Brown, R. Brown, C. Bugg, B. Chai, T. Ciszek, S. Coriell, M. DiGiuseppe, E. Giess, M. Glicksman, R. Hopkins, A. Jordan, E. Monberg, P. Morris, G. Nancollas, K. Nassau, H. Olsen, J. Olson, F. Ponce, F. Rosenberger, L. Schneemeyer, D. Shaw, G. Sloan, G. Stringfellow, A. Witt.
LOCAL ARRANGEMENTS:	A.L. Gentile R.R. Monchamp	F.P. Doty, H. Olsen, L. Rothrock, B. Wechsler.
INDUSTRIAL EXHIBIT:	L. Colombo S. Samuelson	
FINANCE:	T. Kuech	Subject Chairpersons (Partial List)
PROCEEDINGS EDITORS:	J.B. Mullin T. Surek	J. Abell, I. Alexander, K. Barraclough, R. Belt, K. Bertness, G. Blom, M. Brown, B. Chai, K. Cheng, T. Ciszek, S. Coriell, R. DeMattie, J. Derby, A. Elliot, V. Fratello, E. Giess, M. Glicksman, R. Hopkins, D. Hurle, D. Kaiser, J. Kalejs, R. McConnell, A. McPherson, E. Monberg, P. Morris, D. Nason, M. Pusey, K. Ravi, R. Reynolds, F. Rosenberger, H. Schaake, L. Schneemeyer, F. Szofran
CORPORATE SPONSORSHIP:	F.A. Halden G.M. Loiacono	
GOVERNMENT SPONSORSHIP:	E.A. Giess A.F. Witt	
PUBLICITY:	M.A. DiGiuseppe J.C. Jacco	
PHOTO EXHIBIT:	R. Andrews P. Morris	
IOCG AWARDS:	B. Cockayne	
ACCOMPANYING PERSONS PROGRAM:	Arlene Bonner Patricia Brandle Madlyn Monchamp Alleen Wenckus	
CRYSTAL EXHIBIT:	R. Belt L.R. Rothrock	
ISSCG-8 COMMITTEE:	L. Boatner E. Bourret K.A. Jackson	
CONFERENCE SECRETARIAT	C. David Brandle	

**INTERNATIONAL ADVISORY BOARD**

BRAZIL: O.N. Mesquita  
BULGARIA: D. Nenow  
CANADA: F. Weinberg  
CHINA: M.-H. Jiang and N.-B. Ming  
CZECHOSLOVAKIA: B. Brezina  
DENMARK: A.N. Christensen  
FRANCE: R. Kern and B. Mutaftschiev  
GERMANY: G. Kuhn, P. Rudolph, W. Tolksdorf and H. Wenzl  
HUNGARY: J. Paitz  
INDIA: P. Ramasamy  
ISRAEL: L. Ben-Dor  
ITALY: C. Paorici  
JAPAN: H. Komatsu, T. Nishinaga and I. Sunagawa  
KOREA: K.K. Orr  
MEXICO: H. Riveros  
ROMANIA: Z. Schleit  
RUSSIA: A.A. Chernov, E.I. Givargizov and F.A. Kuznetsov  
SPAIN: R. Rodriguez-Clemente  
SWITZERLAND: D. Rytz  
THE NETHERLANDS: P. Bennema, L.J. Gilling and G.M. van Rosmalen  
UNITED KINGDOM: K.G. Barracough, B. Cockayne and P.M. Dryburgh  
UNITED STATES OF AMERICA: G. Cullen, R.A. Laudise, G.H. Olsen, R. Reynolds and F. Rosenberger

**INTERNATIONAL ORGANIZATION FOR CRYSTAL GROWTH**

**OFFICERS**

President: B. Cockayne (ENGLAND)  
Vice President: A.A. Chernov (RUSSIA)  
Vice President: R.F. Sekerka (USA)  
Secretary: M. Schieber (ISRAEL)  
Treasurer: E. Kaldis (SWITZERLAND)  
Past President: R. Kern (FRANCE)

**IOCG EXECUTIVE COMMITTEE MEMBERS**

K.W. Benz (GERMANY)	W.A. Bonner (USA)
R.S. Feigelson (USA)	D.T.J. Hurle (UK)
M.-H. Jiang (CHINA)	H. Komatsu (JAPAN)
R.A. Laudise (USA)	B. Mutaftschiev (FRANCE)
T. Nishinaga (JAPAN)	V.V. Osiko (RUSSIA)
C. Paorici (ITALY)	G.M. van Rosmalen (THE NETHERLANDS)
I. Sunagawa (JAPAN)	J.F. Wenckus (USA)

**IOCG COUNCILORS REPRESENTING NATIONAL ORGANIZATIONS  
and GENERAL ASSEMBLY**

FRANCE: A. Baronnet, J.J. Metois and B. Mutaftschiev

GERMANY: M. Krohn, G. Kuhn, P. Rudolph, W. Tolksdorf H. Walcher and H. Wenzl

HUNGARY: E. Lendvay

INDIA: P. Ramasamy and S.M.D. Rao

ISRAEL: A. Horowitz

ITALY: C. Paorici

JAPAN: T. Nishinaga, T. Ogawa and I. Sunagawa

KOREA: H. Kim, Y.S. Kim and K.K. Orr

RUSSIA: A.A. Chernov, P.P. Fedorov and F.A. Kuznetsov

SPAIN: R. Rodriguez-Clemente

SWITZERLAND: J. Hulliger and E. Kaldis

THE NETHERLANDS: J.W.M. van Kessel and J.A.M. Meijer

UNITED KINGDOM: P.M. Dryburgh, S.E.B. Gould and D.T.J. Hurle

UNITED STATES OF AMERICA: W. Bonner, C.D. Brandle and T. Surek

IUPAC: T.S. West

IUCr: A.I. Hordvik

GENERAL ASSEMBLY: P. Bennema, S. Kimura, O.N. Mesquita, N.-B. Ming, and D. Nenow

**ICCG-10 CORPORATE SPONSORS**

Airtron/Synoptics

AKZO

Allied Signal Corporation

Bertram Laboratories

Ceres Corporation

Cleveland Crystals

Crystal Associates Inc.

Crystal Technology Inc.

Crystal Systems

Deltronic Crystal Industries

DuPont Corporation

Eastman Kodak Company

Engelhard Industries

Epitaxx

Fujian Castech Crystals

Hewlett-Packard

Hughes Research Laboratories

Johnson Matthey Corporation

Keon Optics

Laser Diode Inc.

Magnesium Elektron Inc

MEMC Electronic Materials

MR Semicon

Philips Laboratories

Quantum Technology

Saint Gobain

Sandoz Produkte AG Inc.

Texas Instruments, Inc.

Virgo Optics

Westinghouse S.T.C.

Zirconia Sales

**US GOVERNMENT SPONSORS**

Air Force Office of Scientific Research

Army Research Office

National Aeronautics and Space Administration

National Renewable Energy Laboratory

National Science Foundation

Oak Ridge National Laboratory

Office of Naval Research

Office of Naval Research - Europe

Wright Laboratories, Wright-Patterson Air Force Base



## CONFERENCE SCHEDULE

	TECHNICAL PROGRAM				SOCIAL EVENTS & ACCOMPANYING PERSONS SCHEDULE
Sunday Afternoon					Registration
Sunday Evening					Welcome Reception
Monday Morning	<b>Session 1A</b> Fundamentals of Nucleation and Growth	<b>Session 1B</b> Non-Linear Optical Crystals I	<b>Session 1C</b> Silicon Growth	<b>Session 1D</b> Halide Growth	* Introducing San Diego
Monday Noon	IOCG Executive	Committee Meeting			
Monday Afternoon	<b>Session 2A</b> Fundamentals of Nucleation and Growth	<b>Session 2B</b> Non-linear Optical Crystals II	<b>Session 2C</b> III-V Bulk Growth I	<b>Session 2D</b> Quasi Crystals and Special Topics	* San Diego by Land and Sea
Monday Evening					Vendor's Reception
Tuesday Morning	<b>Session 3A</b> Growth Mechanisms	<b>Session 3B</b> Non-linear Optical Crystals III	<b>Session 3C</b> III-V Bulk Growth II	<b>Session 3D</b> Superconductors I (Substrates)	
Tuesday Noon	IOCG Council	Meeting			
Tuesday Afternoon	<b>Session 4A</b> Convection and Segregation	<b>Session 4B</b> Laser Crystals I Fluorides	<b>Session 4C</b> III-V Epitaxial Growth I	<b>Session 4D</b> Superconductors II	* Shopping in La Jolla
Tuesday Evening	Poster Session # 1		Poster Session # 2		
Wednesday Morning	<b>Session 5A</b> Convection and Convective Instabilities	<b>Session 5B</b> Laser Crystals II Oxides and Garnets	<b>Session 5C</b> III-V Epitaxial Growth II	<b>Session 5D</b> Superconductors III	* Mexican Cooking Demonstration
Wednesday Afternoon & Evening					Balboa Park Promenade
Thursday Morning	<b>Session 6A</b> Morphological Stability	<b>Session 6B</b> Oxide Crystal Growth	<b>Session 6C</b> Wide Bandgap Materials (GaN, SiC etc)	<b>Session 6D</b> Aqueous Solution I (Bio-material)	
Thursday Afternoon	<b>Session 7</b> Plenary Session				
	Poster Session #3		Poster Session # 4		
	IOCG General Assembly Meeting				
Thursday Evening					Conference Banquet
Friday Morning	<b>Session 8A</b> Dendritic Growth and Patterns	<b>Session 8B</b> II-VI Growth I	<b>Session 8C</b> Wide Bandgap Materials (Diamond)	<b>Session 8D</b> Aqueous Solution II (Organic & Phosphate)	* Good-Bye Social
Friday Afternoon	<b>Session 9A</b> Surface Roughening and Particle Formation	<b>Session 9B</b> II-VI Growth II/Ternary Semiconductors	<b>Session 9C</b> Special Techniques	<b>Session 9d</b> Aqueous Solution III (Industrial Crystals)	
After Last Session	Closing		Ceremony		

\* ACCOMPANY PERSONS PROGRAM ACTIVITY

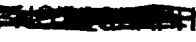
ORIGINAL PAGE  
COLOR

## MONDAY MORNING - AUGUST 17, 1992

### SESSION 1

8:00	<b>OPENING CEREMONIES - Grand Ballroom</b> Session Chairperson - B. Cockayne, UK			
8:30 *	Dynamics, Stability and Control of Czochralski Growth, D.T.J. Hurle, UK			
9:15	BREAK			
<b>Session 1 A - Cuyamaca Room</b>				
<b><u>FUNDAMENTALS OF NUCLEATION AND GROWTH I</u></b>				
<p>Session Chairpersons - F. Rosenberger, USA and B. Mutaftschiev, France</p>				
9:30 *	Molecular Dynamics Simulations of Crystal Growth from the Vapor George Glimer AT&T Bell Laboratories, USA			
10:00 *	The Defect Mechanism of Crystal Growth and its Kinetics N.-B. Ming Nanjing University, PR China			
10:30	COFFEE BREAK			
10:45	Models for the Early Stages of Nucleation H. Riveros, E. Cabrera, M. Gally, C. Ruiz-Mejia, and J. Fujioka University Nacional Autonoma de Mexico, Mexico			
11:00	Nucleation and Growth of Fine Crystals from Supercritical Fluids E. M. Berends, O. S. L. Bruylants and G. M. van Rosmalen Delft University of Technology, The Netherlands			
11:15	Crystallization of Amorphous Germanium on Metal Film T. Okabe, S. Saito and T. Wada Toyama University, Japan			
11:30	Visualization of Sub-Critical Crystalline Particles: Their Behavior in Growth of KDP Crystal in Aqueous Solution L. Lian, L. Taigin, K. Sakai, T. Agawa, and I. Sunagawa Gakushuin University, Institute for Physical and Chemical Research and Yamanashi Institute of Gemology Arts, Japan			
11:45	Metastable State Relaxation Near the Binodal Line A. S. Myerson and A. F. Izmalov Polytechnic University, USA			
12:00 *	Tailor-Made Auxiliary Molecules for Controlling Growth and Nucleation of Organic Crystals M. Lahav and L. Leiserowitz Weizmann Institute of Science, Israel			
<b>Session 1 B - Laguna Room</b>				
<b><u>NON-LINEAR OPTICAL CRYSTALS I</u></b>				
<p>Session Chairpersons - P. Morris, USA and M.-H. Jiang, PR China</p>				
9:30 *	Growth, Defects and Properties of Nonlinear Optical Oxide Crystals Patricia A. Morris DuPont Company, USA			
10:00	Hydrothermal Growth of Potassium Titanyl Arsenate (KTA) In Large Autoclaves R. F. Bell and J. B. Ings Litton Systems, Inc., USA			
10:15	Growth of $\text{KTiOAsO}_4$ (KTA) and $\text{CsTiOAsO}_4$ (CTA) Crystals From New Molten-Salt System C. Luo, K. Gu, J. Li, C. Zheng, Q. Xie, and F. Luo Southwest Institute of Technical Physics, P.R. China			
10:30	COFFEE BREAK			
10:45	Growth and Properties of the Nonlinear Optical Crystal $\text{CsTiOAsO}_4$ L.K. Cheng DuPont Corporation, USA			
11:00	Investigations of the Flux Crystallization Processes and Properties of $\text{KTiOPO}_4$ and $\text{LiB}_3\text{O}_5$ V. A. Maslov, L. A. Olkhovaya, V. V. Osiko, and E. A. Shcherbakov General Physics Institute, Russia			
11:15	Surface Stability of Lithium Triborate Crystal Grown from Excess Boric Oxide Solutions E. Bruck, R. J. Raymakers, R. K. Route and R. S. Feigelson Stanford University, USA			
11:30	$\beta\text{-BaB}_2\text{O}_4$ Single Crystal Growth by Czochralski Method using an $\alpha\text{-BaB}_2\text{O}_4$ and a $\beta\text{-BaB}_2\text{O}_4$ Single Crystal H. Kouta, S. Imoto and Y. Kuwano NEC Corporation, Japan			
11:45	Growth and Properties of New TB Type Photorefractive Crystals H. Chen, D. Sun, Q. Jiang, and Y. Song Shandong University, PR China			

\* Indicates Invited Speaker

ORIGINAL PAGE  
COLOR 

## MONDAY MORNING - AUGUST 17, 1992

### SESSION 1

8:00 **OPENING CEREMONIES- Grand Ballroom**  
 Session Chairperson - B. Cockayne, UK

8:30 \* Dynamics, Stability and Control of Czochralski Growth, D.T.J. Hurle, UK

9:15 **BREAK**

#### Session 1 C - Palomar Room

##### SILICON GROWTH

Session Chairperson - E. Blakeslee, USA and J. Wilkes, UK

9:30 Point Defect, Carbon and Oxygen Complexing in Polycrystalline Silicon  
 J. P. Kalejs  
 Mobil Solar Energy Corp., USA

9:45 Characterization of Interstitial Oxygen Striations in Silicon Single Crystals  
 I. Fusegawa, H. Yamagishi, H. Takayama, E. Iono, and K. Takano  
 Shin-Etsu Handotai Co., Ltd., Japan

10:00 Detection of Microdefects Near Surface and Inside of Ultra-Thin Semiconductor Crystals by Light Scattering and Interference Methods  
 L. Tailing, K. Toyoda, L. Lian, N. Nango, and T. Ogawa  
 Institute of Physical Chemical Research, Gaskushium University, and Ratoc Systems Engineering Co. LTD, Japan

10:15 Development of a Nondestructive Bulk Micro-Defect Analyzer for Silicon Wafers  
 K. Moriya, H. Wada and K. Hirai  
 Mitsui Mining & Smelting Co., Ltd., Japan

10:30 COFFEE BREAK

10:45 Study of the Characteristics of Crystal Temperature in a CZ-Puller - through Simulation and Experiment  
 T. Fujiwara, S. Inami, S. Miyahara, S. Kobayashi, T. Kubo, and H. Fujiwara  
 Sumitomo Metal Industries, Ltd., Japan

11:00 In-Situ Observation of Surface Tension Driven Flow on the Molten Silicon Surface  
 K. Kakimoto, M. Watanabe, M. Eguchi, and T. Hibiya  
 NEC Corporation, Japan

11:15 In-Situ Observation of the Convection on the Surface of Silicon Melt  
 H. Yamagishi, I. Fusegawa, E. Iino, and K. Takano  
 Shin-Etsu Handotai Co., Ltd., Japan

11:30 Gravity Effect on Liquid Phase Epitaxy of Silicon  
 H. Kanai, S. Motoyama, M. Kimura, A. Tanaka, and T. Sukegawa  
 Shizuoka University and New Japan Radio Co. LTD, Japan

11:45 Growth of Thin Crystalline Silicon Layers for Photovoltaic Device Use  
 T. F. Ciszek, R. Burrows and T. H. Wang  
 National Renewable Energy Lab, USA

12:00 Misfit Dislocation Formation and Interaction in Ge on (001) Si  
 M. Albrecht and H. P. Strunk  
 University of Erlangen, Germany

12:15 Intrinsic and Impurity Point Defect Aggregation in Silicon Crystal Pulling  
 V. V. Voronkov  
 Institute of Rare Metals, Russia

9:30 \* Recent Advances in Bulk Crystal Growth from the Vapor  
 E. Kaldis and M. Plechotka  
 ETH - Zurich, Switzerland

10:00 Purification and Growth of BaFBr and Identification of Radiation-Produced Electron and Hole Centers in Oxygen-Containing BaFBr  
 R. S. Eachus, W. G. McDowell, R. H. D. Nuttall, M. T. Olm, F. K. Koschnick, Th. Hangleiter, and J.-M. Spaeth  
 Eastman Kodak Company, USA and University of Paderborn, Germany

10:15 COFFEE BREAK

10:30 The Growth of Ag Doped PbBr<sub>2</sub> Crystals using Coupled Vibrational Stirring  
 R. C. DeMattel and R. S. Feigelson  
 Stanford University, USA

10:45 Precise Measurements of the Mass Transport Rate of Mercuric Iodide in the Vapour Phase  
 M. Plechotka and E. Kaldis  
 ETH - Zurich, Switzerland

11:00 Thermo-Convective Effects During Vapor-Phase Growth of Mercurous Chloride Crystals  
 M. E. Glicksman, G. T. Kim, O. C. Jones, and J. T. Lin  
 Rensselaer Polytechnic Institute, USA

11:15 Morphology and Characterization of Solution Grown Mercuric Iodide Crystals  
 K. Baskar and P. Ramasamy  
 Anna University, India

11:30 Characterization of Trapping Levels in Solution Grown and PCG Mercuric Iodide Single Crystals  
 T. Pal, S. L. Sharma and H. N. Acharya  
 Indian Institute of Technology, India

11:45 Characterization of Modified Pyrochlores CsMFeF<sub>6</sub> (M=Mn,Co,Zn)  
 K. S. Raju and B. M. Wanklyn  
 University of Madras, India and Oxford University, UK

12:00 Growth of Some V-VI-VII Group Compounds From Vapour  
 R. Ganesh, D. Arivuoli and P. Ramasamy  
 Anna University, India

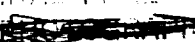
12:15 Automated Pulling from the Melt - The Effective Method of Growing Large Alkali Halide Single Crystals for Optical and Scintillation Applications  
 L. G. Eidelman, V. I. Gorlitsky, V. G. Protsenko, A. V. Radkevich, and V. V. Trofimenco  
 Institute for Single Crystals, Ukraine

#### Session 1 D - White Wings Room

##### HALIDE GROWTH

Session Chairpersons- N.B. Singh, USA and E. Kaldis, Switzerland

\* Indicates Invited Speaker

ORIGINAL PAGE  
 COLOR 

MONDAY AFTERNOON - AUGUST 17, 1992

SESSION 2

Grand Ballroom

Session Chairperson - S. Corieff, USA

1:45 \* Convective Instabilities in Melt Growth Configuration, Georg Müller, University of Erlangen-Nürnberg, Germany

2:30 BREAK

Session 2 A - Cuyamaca Hall

FUNDAMENTALS OF NUCLEATION AND GROWTH II

Session Chairpersons - R. Kern, France and  
K.Tsukamoto, Japan

2:45 \* In-Situ Observation of Interface Kinetics and Flow Dynamics  
Katsuo Tsukamoto  
Tohoku University, Japan

3:15 Non-Equilibrium Phase Transformations in Two Component Systems  
K. A. Jackson, G. H. Glümer and D. E. Temkin  
University of Arizona, USA, AT&T Bell Laboratories, USA and  
Research Institute of Metallurgy, Russia

3:30 A New Model of Effective Segregation Coefficient  
A. G. Ostrogorsky and G. Müller  
Columbia University, USA and Universität Erlangen-Nürnberg, Germany

3:45 COFFEE BREAK

4:00 \* Surface Roughening and Melting: Models and Relevance for Crystal  
Growth  
J.P. van der Eerden  
University of Utrecht, The Netherlands

4:30 Kinetical Roughening and Roughening Transition in Odd-Numbered  
Normal Alkanes  
X.-Y. Liu and P. Bennema  
University of Nijmegen, The Netherlands

4:45\* Computer Modelling  
T.A. Cherepanova  
Center for Microelectronics, Latvia

5:15 Mapping of Crystal Growth onto the 6-Vertex Model: Growth Mode and  
Surface Roughness  
M. Kotria and A. C. Levi  
University of Genova, Italy

Session 2 B - Laguna Room

NON-LINEAR OPTICAL CRYSTALS II

Session Chairpersons - P. Bordui, USA and  
D. Rytz, Switzerland

2:45 \* Growth of Large Size KNbO<sub>3</sub> Crystals and Epitaxial Layers of  
KTa<sub>(1-x)</sub>Nb<sub>x</sub>O<sub>3</sub>  
J. Hulliger, R. Gutmann and H. Wuerz  
Institute of Quantum Electronics, ETH, Switzerland

3:15 Defect Structure in Transition Metal Ion Doped Photorefractive KNbO<sub>3</sub>  
Crystals  
X. Ma and D. Shen  
Research Institute of Synthetic Crystals, PR China

3:30 COFFEE BREAK

3:45 Electric Field Poling of Potassium Niobate Crystals  
R. H. Jarman and B. C. Johnson  
Amoco Technology Company, USA

4:00 Growth and Characterization of Off-congruent LiNbO<sub>3</sub> Single Crystals  
Grown by Double Crucible Method  
Y. Furukawa, M. Sato, K. Kitamura, F. Nitanda, and K. Ito  
Hitachi Metals, Ltd. and National Institute for Research in Inorganic  
Materials, Japan

4:15 Stoichiometric LiNbO<sub>3</sub> Single Crystal Growth by Double Crucible  
Czochralski Method Using Automatic Powder Supply System  
K. Kitamura, J. K. Yamamoto, N. Iyi, S. Kimura, and T. Hayashi  
National Institute for Research in Inorganic Materials and ASGAL Co. LTD,  
Japan

4:30 LiNbO<sub>3</sub> Single Crystal Growth from Li-Rich Melts by the Continuous  
Charging and Double Crucible Czochralski Methods  
M. Sakamoto, S. Kan, Y. Okano, K. Hoshikawa, and T. Fukuda  
Tohoku University, Japan

4:45 Physical Property Variation of Molten Lithium Niobate by Doping with  
Magnesium Oxide  
E. Tokiaki, K. Terashima and S. Kimura  
ERATO, Research Dev Corp, Japan

\* Indicates invited Speaker

ORIGINAL PAGE  
COLOR

## MONDAY AFTERNOON - AUGUST 17, 1992

### SESSION 2

#### Grand Ballroom

Session Chairperson - S. Coriell

1:45 \* Convective Instabilities in Melt Growth Configuration, Georg Müller, University of Erlangen-Nürnberg, Germany

2:30 BREAK

#### Session 2 C - Palomar Room

##### III-V BULK GROWTH I

Session Chairpersons - A. G. Elliot, USA and  
H. Wenzl, Germany

2:45 \* Advances in Preparation of GaAs and InP Crystals by LEC Method  
Roberto Fornari  
MASPEC-CNR Institute, Italy

3:15 MLEK Crystal Growth of (100) Indium Phosphide  
D. F. Bliss, R. M. Hilton, and J. A. Adamski  
Hanscom Air Force Base and Parke Mathematical Laboratories, USA

3:30 A Thermal Stress Theory of Dislocation Reduction in the Vertical  
Gradient Freeze (VGF) Growth of GaAs  
A. S. Jordan, E. M. Monberg and J. E. Clemans  
AT&T Bell Labs and Engineering Research Center, USA

3:45 COFFEE BREAK

4:00 LEC Growth of Large GaAs Single Crystals  
M. Shibata, T. Suzuki, T. Inada, and S. Kuma  
Hitachi Cable, Ltd., Japan

4:15 Heat Transfer During GaAs of Bulk Single Crystal by the Liquid  
Encapsulated Vertical Bridgman Technique  
T. Suzuki, Y. Okano, K. Hoshikawa, and T. Fukuda  
Tohoku University, Japan

4:30 Consecutive Thermal Cooling Cycle Effect of  
Liquid-Encapsulated-Czochralski GaAs Crystal Growth on the  
Crystallographic Uniformity  
Y. Saito  
Toshiba Corporation, Japan

4:45 GaAs and CdTe Crystal Growth by the VZM Technique  
R. L. Henry, P. E. R. Nordquist and R. J. Gorman  
Naval Research Laboratory, USA

#### Session 2 D - "White Wings" Room

##### QUASI CRYSTALS AND SPECIAL TOPICS

Session Chairpersons - A.R. Kortan, USA and  
W. A. Bonner, USA

2:45 \* Growth of Perfect Quasicrystals: From Curiosity to Reality  
Ahmet R. Kortan  
AT&T Bell Labs, USA

3:15 On the Morphology of AlCuFe Quasicrystals and Related Phases  
K. Balzuweit and H. Meekes  
University of Nijmegen, The Netherlands

3:30 COFFEE BREAK

3:45 Generalization of Morphological Hartman-Perdok Theory to Modulated  
and Quasi Crystals  
P. Bennema, K. Balzuweit, J. P. van den Eerden, M. Kremers, H. Meekes,  
M. A. Verheijen, and L. J. P. Vogels  
University of Nijmegen, The Netherlands

4:00 \* Residual Melt Analysis  
Brian Cockayne  
DRA Malvern, UK

4:15

4:30 Temperature Difference in Radial Direction of Czochralski Copper Crystals  
Y. Imashimizu and J. Watanabe  
Akita University, Japan

4:45 Fundamental Aspects of Particle Engulfment by a Solidifying Front  
M. Yemmou, M. A. Azouni and G. Petre  
National Center of Scientific Research- Meudon, France and ULB, Belgium

5:00 Mechanism of Growth of Organic Hourglass Inclusions: Old Materials with  
Photonic Applications  
B. Kahr, M. Nyman and J. K. Chow  
Purdue University, USA

5:15 Properties and Surface Morphology of Indium Tin Oxide Films Prepared  
by Electron Shower Method  
H. Yumoto, J. Hatano, T. Watanabe, K. Fujikawa, and H. Sato  
The Science University of Japan, Japan

\* Indicates Invited Speaker

ORIGINAL PAGE  
COLOR [REDACTED]

## TUESDAY MORNING - AUGUST 18, 1992

### SESSION 3

**Grand Ballroom**  
Session Chairperson - K. Jackson, USA

8:00 \* Studies on Crystal Growth and Thin Layer Formation by TEAS and STM, B. Mutaftschiev, University of Paris, France

8:45 BREAK

#### Session 3 A - Cuyamaca Room

##### GROWTH MECHANISMS

Session Chairperson - K. Jackson, USA and  
P. Bennema, The Netherlands

9:00 \* Growth Mechanisms and Morphology of Crystals  
P. Bennema  
Nijmegen Universiteit, The Netherlands

9:30 \* Face Statistics on the Dissolution Forms of Garnet Crystals  
E. Hartmann and E. Beregi  
Research Laboratory for Crystal Physics and Research Institute for  
Telecommunications, Hungary

10:00 COFFEE BREAK

10:15 Elementary Processes of Dissolution; (101) ADP Face  
P. G. Vekilov, Yu. G. Kuznetsov, and A. A. Chernov  
Institute of Physical Chemistry, Bulgaria and Institute of Crystallography,  
Russia

10:30 Interstep Interaction in Solution Growth (101) ADP Face  
P. G. Vekilov, Yu. G. Kuznetsov, and A. A. Chernov  
Institute of Crystallography, Moscow

10:45 \* Atomic Force Microscopy of Lysozyme Single Crystals  
S. D. Durbin and W. E. Carlson  
Carleton College, USA

11:15 Growth Mechanism of Long Chain Molecular Crystals on KCl  
Substrate Due to Annealing  
M. Yamanaka, K. Mirura, K. Yase, K. Sato, and K. Inaoka  
Hiroshima University and Yuge Mercantile Marine College, Japan

11:30 \* In-Situ X-ray Topography and Interferometry to Study Solution Growth  
Mechanisms  
Yurii Georgy Kuznetsov  
Institute of Crystallography, Russia

#### Session 3 B - Laguna Room

##### NON-LINEAR OPTICAL CRYSTALS III

Session Chairpersons - R. Route, USA and  
J. Hulliger, Switzerland

9:00 \* Defect Structure in  $\text{LiNbO}_3$  with Different Compositions  
N. Iyi, K. Kitamura, F. Izumi, J. K. Yamamoto, H. Hayashi, H. Asano, and  
S. Kimura  
National Institute for Research, ASGAL Co. LTD, and University of  
Tsukuba, Japan

9:15 Partitioning of Intrinsic Species During Phase Equilibria and Crystallization  
of  $\text{LiNbO}_3$  Melts  
S. Uda and W. A. Tiller  
Stanford University, USA

9:30 Control of Crystal-Melt Interface Shape During Growth of Lithium Niobate  
Single Crystals  
A. Hirata, M. Tashibana, T. Sugimoto, Y. Okano, and T. Fukuda  
Waseda University and Tohoku University, Japan

9:45 \* Organic-on-Inorganic Semiconductor Molecular Beam Epitaxy  
Norbert Karl  
Universitat Stuttgart, Germany

10:15 COFFEE BREAK

10:30 Growth of a First Organic Photorefractive Crystal  
J. Hulliger and Y. Schumacher  
Swiss Federal Institute of Technology, Switzerland

10:45 High Efficiency Agile Laser Materials: Binary Organic Crystals  
N. B. Singh, T. Henningsen, R. Hamacher, E. P. Supertzi, R. H. Hopkins, R.  
Mazelsky, F. K. Hopkins, and D. E. Zelmon  
Westinghouse Electric Corporation, USA

11:00 The Growth, Structural and Optical Characterisation of Large Area, Single

Crystalline Thin Films of 3-Nitroaniline (mNA)

J. N. Sherwood and G. S. Simpson

University of Strathclyde, UK

11:15 Crystal Growth and Characterisation of the Electro-Optic Material,  
3-(1,1-Dicyanoethyl)-1-Phenyl-4, 5-Dihydro-1H-Pyrazole  
P. Halfpenny, J. N. Sherwood, S. N. Black, R. J. Davey, and P. R. Morley  
ICI Chemicals & Polymers, Ltd., UK

11:30 ZnGeP<sub>2</sub> Crystal Growth Studies using the Horizontal Gradient Freeze  
Technique  
P. G. Schunemann and T. M. Pollak  
Lockheed Sanders, Inc., USA

11:45\* New Approaches to Nonlinear Optical Materials  
M. M. Fejer  
Stanford University, USA

\* Indicates Invited Speaker

ORIGINAL PAGE  
COLOR [REDACTED]

## TUESDAY MORNING - AUGUST 18, 1992

### SESSION 3

#### **Grand Ballroom**

Session Chairperson - K. Jackson, USA

8:00 \* Studies on Crystal Growth and Thin Layer Formation by TEAS and STM, B. Mutaitschlev, University of Paris, France

8:45 BREAK

#### Session 3 C - Palomar Room

##### III-V BULK GROWTH II

Session Chairpersons - A. F. Witt, USA and  
K. Sangwal, Poland

9:00 \* THM Growth of Binary and Ternary III-V Semiconductor Single Crystals  
K.W. Benz  
Albert-Ludwigs-Universitat Freiburg, Germany

9:30 Growth of  $Al_xGa_{(1-x)}Sb$  and  $GaSb$  Bulk Crystals with Liquid Phase  
Electro Epitaxy (LPEE)  
G. Bischoff and K. W. Benz  
Albert-Ludwigs-Universitat Freiburg, Germany

9:45 InGaAs Mixed Crystals Grown by Gradient Freeze, Vertical Bridgman  
and Rotary Bridgman Methods  
Y. Hayakawa, M. Ando, T. Ozawa, T. J. Anderson, P. H. Holloway, B.  
Pathaney, and M. Kumagawa  
Shizouka University, Japan and University of Florida, USA

10:00 COFFEE BREAK

10:15 \* Growth and Characterization of  $GaSb$  Single Crystals  
F. Morvic  
Institute of Physics, Czechoslovakia

10:45 Non-Invasive Bulk Characterization of  $GaAs$  and  $Si$  Wafers  
A. F. Witt  
Massachusetts Institute of Technology, USA

11:00 Dislocation Distribution on X-ray Topographs: Residual Strain and  
Composition and Impurity Effect in LEC  $GaAs$   
Y. Saito  
Toshiba Corporation, Japan

11:15 Novel Approaches to Crystal Growth of Bulk Ternary Solid Solutions  
J. J. Venkrbec, Z. Cecil, V. Rosicka, J. Kohout, J. Sedlacek,  
Z. Kodejs, and P. Pacak  
Czech Technical University, Institute of Radioelectronics, Institute of  
Inorganic Chemistry, Czechoslovakia

11:30 Mathematical Modelling and Control System Design of the Czochralski  
and LEC Process  
G. A. Satunkin and A. G. Leonov  
Institute of Microelectronics Technology and High Purity Materials, Russia

#### Session 3 D - "White Wings" Room

##### SUPERCONDUCTORS I (SUBSTRATES)

Session Chairpersons - C. D. Brandle, USA and  
H. J. Scheel, Switzerland

9:00 \* Substrates for High Tc Superconductors  
Hans J. Scheel  
CRISTALLOGENESE - IMO, Switzerland

9:30 Congruent Composition for Growth of Lanthanum Aluminate  
G. W. Berkstresser, A. J. Valentino and C. D. Brandle  
AT&T Bell Labs, USA

9:45 Vertical Gradient-Freeze Growth of Aluminate Crystals to Provide  
Substrates for High-Temperature Superconducting Films  
R. E. Fahey, A. J. Strauss and A. C. Anderson  
MIT Lincoln Laboratories, USA

10:00 Microanalytical Characterization of Flux Grown  $LaAlO_3$  Single Crystals  
A. K. Razdan, P. N. Kotru and B. M. Wanklyn  
University of Jammu, India and Oxford University, UK

10:15 COFFEE BREAK

10:30 Anomalies in Crystal Growth by Czochralski Technique  
A. Pejaczewska and P. Byszewski  
Institute of Physics and Institute of Electronic Materials Technology,  
Poland

10:45 Flux Growth of Single Crystals of  $Nd_yPr_{(1-y)}GaO_3$  Solid Solutions  
H. Dabkowska, A. Dabkowski and J. E. Greedan  
McMaster University, Canada

11:00 Investigation of the Growth of Neighbrite,  $NaMgF_3$ ,  
S. Sengupta, A. Cassanho and H. P. Jensen  
Massachusetts Institute of Technology, USA

11:15 Single Crystal Growth of Rare-Earth Galates and Epitactic Growth Nature  
of High-Tc Superconducting YBCO Thin Films on Them  
S. Miyazawa, M. Sasaura, and M. Mukaid  
Nippon Telegraph & Telephone Corp, Japan

11:30 LPE of High-Tc Superconductors  
C. Klemenz and H. J. Scheel  
CRISTALLOGENESE - IMO, Switzerland

\* Indicates Invited Speaker

ORIGINAL PAGE  
COLOR 

## TUESDAY AFTERNOON - AUGUST 18, 1992

### SESSION 4

#### Grand Ballroom

Session Chairperson - G. Stringfellow, USA

1:45 \* In-situ Analysis of Organometallic Vapor Phase Epitaxy using Grazing Incidence X-ray Scattering, D.W. Kisker, IBM, USA

2:30 BREAK

#### Session 4 A - Cuyamaca Hall

##### CONVECTION AND SEGREGATION

Session Chairpersons - R. A. Brown, USA and  
J. J. Favier, France

2:45 \* The Boundary Layer Concept; A Key to Segregation Phenomena In  
Crystal Growth from the Melt  
J. J. Favier, J. P. Garandet and D. Camel  
Centre d'Etudes Nucleaires de Grenoble, France

3:15 Analysis of the Bridgman Growth of Semi-transparent Crystals  
S. Brandon and J. J. Derby  
University of Minnesota, USA

3:30 Radial Segregation In Floating-Zone Crystal Growth  
C. W. Lan and S. Kou  
University of Wisconsin-Madison, USA

3:45 COFFEE BREAK

4:00 Fluid Patterns in the Diffusive Field Surrounding a Growing Crystal  
J. M. Garcia-Ruiz and F. Otalora  
Inst Andaluz de Geologia Mediterranea, Spain

4:15 Characterization of the Onset of Turbulence in Liquid Tin in a Bridgman  
Configuration  
D. J. Knuteson, A. L. Fripp, W. J. Debnam, Jr., G. A. Woodell and  
R. Narayanan  
NASA-Langley Research Center and University of Florida, USA

4:30 Effect of Turbulence Modelling on the Predictions of an Integrated  
Thermal-Capillary Model for Czochralski Crystal Growth  
T. A. Kinney and R. A. Brown  
Massachusetts Institute of Technology, USA

4:45 Control of Radiative Heat Transfer in Shaped Semi-Transparent Crystals  
Being Pulled from the Melt  
V.S. Yuferev, M. G. Vasil'ev, E. N. Kolesnikova and L.A. Stefanova  
A.F. Ioffe Phys-Tech Institute, Russia

#### Session 4 B - Laguna Room

##### LASER CRYSTALS I (FLUORIDES)

Session Chairpersons - R. Belt, USA and  
V. V. Osiko, Russia

2:45 \* Recent Developments of New Laser Crystals  
Bruce Chai  
University of Florida, USA

3:15 CaCl<sub>2</sub>:Sm<sup>3+</sup> Crystal Growth and Spectroscopy  
J. P. Chaminade, A. Garcia, A. Oppenlander, J. C. Vial, and  
R. M. Macfarlane  
Laboratoire de Chimie du Solide du CNRS, Laboratoire de Spectrometre  
Physique, France and IBM Almaden Research Center, USA

3:30 COFFEE BREAK

3:45 New Fluoride Crystals for Laser Applications  
A. Cassanho and H. P. Jenssen  
Massachusetts Institute of Technology, USA

4:00 Three-Dimensional Heat Transfer During the Seeding of LiCAF Single  
Crystals in a Modified Bridgman System  
S. Brandon and J. J. Derby  
University of Minnesota and Lawrence Livermore National Laboratory,  
USA

4:15 Growth of High-Quality Yb-Doped Fluoro-Apatite for Advanced Laser  
Applications  
W. L. Kway, S. A. Payne, W. F. Krupke, L. D. DeLoach, L. K. Smith, and J.  
B. Tassano  
Lawrence Livermore National Laboratory, USA

4:30 Characterization of the LiSrAlF<sub>6</sub>-LiSrCrF<sub>6</sub> Solid-Solution for Cr-Laser  
Applications  
W. L. Kway, B. Rupp, S. A. Payne, W. F. Krupke, L. K. Smith, L. D.  
DeLoach, and J. B. Tassano  
Lawrence Livermore National Laboratory

\* Indicates Invited Speaker

## TUESDAY EVENING - AUGUST 18, 1992

#### Exhibit Hall

8:00 Poster Sessions # 1 and # 2

CRIMSON COLOR  
COLOR

## TUESDAY AFTERNOON - AUGUST 18, 1992

### SESSION 4

#### **Grand Ballroom**

Session Chairperson - G. Stringfellow, USA

1:45 \* In-situ Analysis of Organometallic Vapor Phase Epitaxy using Grazing Incidence X-ray Scattering, D.W. Kisker, IBM

2:30 BREAK

#### Session 4 C - Palomar Room

##### III-V EPITAXIAL GROWTH I

Session Chairpersons - G. B. Stringfellow, USA and  
J. Nishizawa, Japan

2:45 \* Novel Precursors for Organometallic Vapor Phase Epitaxy  
G.B. Stringfellow  
University of Utah, USA

3:15 The Modeling of MOVPE GaAs Growth from  $(C_2H_5)_2GaCl$  and  $AsH_3$ ,  
Assuming Thermodynamic Equilibrium at the Growth Front  
M. Hierlemann and T. F. Kuech  
University of Wisconsin, USA

3:30 MOVPE Growth of InGaAsP Using EDMin, TBP and TBA For Optical  
Devices  
M. Ogasawara and Y. Imamura  
NTT Integrated Opto-Electronics Lab, Japan

3:45 COFFEE BREAK

4:00 MOCVD Growth of InAs from Monoethyl Arsine  
R. J. Egan  
Macquarie University, Australia

4:15 The Growth of InSb Using Alternate Organometallic Sb Sources  
R. M. Biefeld  
Sandia National Laboratories, USA

4:30 Study on Interfaces of MOVPE  $GeAs/Al_xGa_{1-x}As$  Quantum  
Heterostructures  
X. Xu, H. Ren, B. Huang, S. Liu, and M. Jiang  
Shandong University, PR China

4:45 Novel Characterization Techniques to Obtain Basic Semiconductor  
Properties in Epitaxial Crystals and Quantum Well Structure  
B. K. Meyer, C. Wetzel, P. Omling, and F. Scholz  
Technical University Munich, University of Lund and University Stuttgart,  
Germany

5:00 Absolutely Stable Strained Superlattices: Formation Via Coherent  
Phase Separation of Semiconductor Alloys  
I. P. Ipatova, V. G. Malyskin, A. Yu. Maslov, and V. A. Shchukin  
A. F. Ioffe Physical Technical Institute, Russia

#### Session 4 D - "White Wings" Room

##### SUPERCONDUCTORS II

Session Chairperson - S. Abell, UK &  
L. Schneemeyer, USA

2:45 \* Single Source MOCVD of Epitaxial Oxide Thin Films  
R. Hiskes, S.A. DiCarolis, R.D. Jacobowitz, Z. Lu, R.S. Feigelson  
and J.L. Young  
Hewlett Packard Laboratories, Stanford University and University of  
California- Los Angles, USA

3:15 Solid Source MOCVD For Oxide Thin Film Growth  
Z. Lu, R. S. Feigelson, R. K. Route, S. A. Decarolis, and R. Hiskes  
Stanford University and Hewlett Packard Laboratories, USA

3:30 COFFEE BREAK

3:45 OMVCD Growth of  $YBa_2Cu_3O_7$  Thin Films on  $SrTiO_3$  And  $LaAlO_3$ ,  
W.J. DeSisto, R.L. Henry, H.S. Newman, M.S. Osofsky  
and V. C. Cestone  
Naval Research Laboratory, USA

4:00 Growth of Epitaxial  $Bi_xSr_2Ca_{n-1}CuO_{2n+4}$  Films by Pulsed Laser Ablation  
S. Zhu, D. H. Lowndes, B. Chakoumakos, R. Feenstra, and X.-Y. Zheng  
Oak Ridge National Laboratory and University of Tennessee, USA

4:15 \* Growth of Superconducting Whiskers in Bismuth System  
I. Matsubara, H. Yamashita and T. Kawai  
Government Industrial Research Institute and Osaka University, Japan

4:45 Detailed Study on High  $T_c$  Phase of  $BiSrCaCuO$  From High Temperature  
Solutions  
S. Miyashita, H. Komatsu, T. Inoue, S. Hayashi, H. Horuchi, and S. Sueno  
Tohoku University, University of Tokyo and University of Tsukuba, Japan

5:00 Crystal Growth and Superconductivity of  $Bi_{1-x}Pb_{0.3}Sr_2CaCu_2O_8$   
L. Zhang, J. Z. Liu, M. D. Lan, P. Klavins, and R. N. Shelton  
University of California - Davis, USA

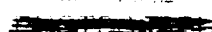
5:15 Growth of Large Size Single Crystals and Whiskers of  $Bi_2Sr_2CaCu_2O_8$  by  
Step Cooling Method  
R. Jayavel, C. Sekar, P. Murugakoothan, C. R. Venkateswara Rao, C.  
Subramanian, and P. Ramasamy  
Anna University, India

\* Indicates Invited Speaker

## TUESDAY EVENING - AUGUST 18, 1992

#### **Exhibit Hall**

8:00 Poster Sessions # 1 and # 2

ORIGINAL PAGE  
COLOR 

## WEDNESDAY MORNING - AUGUST 19, 1992

### SESSION 5

8:00 \* **Grand Ballroom**  
Session Chairperson - A. Jordan, USA

Towards Understanding the Growth Mechanism of III-V Semiconductors on an Atomic Scale  
T. Nishinaga and T. Suzuki, University of Tokyo, Japan

8:45 **BREAK**

#### **Session 5 A - Cuyamaca Room**

##### CONVECTION AND CONVECTIVE INSTABILITIES

Session Chairpersons - S. Coriell, USA and  
G. Muller, Germany

9:00 \* The Effect of Gravitational Modulation on Thermosolutal Convection  
During Crystal Growth  
S. R. Coriell, B. T. Murray, B. V. Saunders, G. B. McFadden,  
and A. A. Wheeler  
National Institute of Standards and Technology, USA

9:30 Control of Marangoni Convection for FZ Crystal Growth  
T. Carlberg and M. Levenstam  
Univ. of Sundvall and Royal Institute of Technology, Sweden

9:45 Convective Instability During Directional Solidification  
of Pseudo-Binary Systems  
J. C. Han and S. Motakef, USA  
Massachusetts Institute of Technology, USA

10:00 **COFFEE BREAK**

10:15 Flow Mode Transitions during Crystal Growth in a Centrifuge  
W. A. Arnold, W. R. Wilcox, F. Carlson, L. L. Regel, and A. Chait  
Clarkson University, Internation Center for Gravity Science and  
Applications and NASA Lewis Research Center, USA

10:30 Directional Solidification with ACRT  
J. Zhou, M. Larrousse and W. R. Wilcox  
Clarkson University, USA

10:45 Convection and Segregation During Growth of Ge and InSb Crystals  
by the Submerged Heater Method  
A. G. Ostrogorsky, H. J. Sell, S. Scharl, and G. Muller  
Columbia University, USA and Universitat Erlangen-Nurnberg, Germany

11:00 Heat Transfer Analysis and Structural Perfection of Shaped  
Semi-Transparent Crystals  
I. Nicoara, D. Nicoara and D. Vizman  
University of Timisoara, Romania

11:15 Growth of 2" Ge:Ga Crystals by the Dynamical VGF Process and its  
Numerical Modelling Including Transient Segregation  
D. Hofmann, T. Jung and G. Muller  
Universitat Erlangen-Nurnberg, Germany

11:30 Numerical Study of Czochralski Silicon Full Process Thermokinetics  
A. Virzi  
MEMC Electronic Materials, Italy

11:45 Modelling of Heat and Mass Transport under Low Frequency Vibrations  
of Crystal in Directed Solidification Technique  
G. A. Dolgikh, E. V. Zharikov, A. Z. Myaldun, N. R. Storozhev,  
N. K. Tolochko, and A. I. Feonychev  
Russian Academy of Sciences, Russia

#### **Session 5 B - Laguna Room**

##### LASER CRYSTALS II (OXIDES AND GARNETS)

Session Chairpersons - B.H.T. Chai, and  
R.E. Fahey, USA

9:00 Disordered Oxide Crystal Hosts for Diode Pumped Lasers  
M. H. Randles, J. E. Creamer, R.F. Belt, G.J. Quarles, and  
L. Esterowitz  
Litton Airtron and Naval Research Laboratories, USA

9:15 Growth and Characterization of Calcium Niobium Gallium Garnet (CNGG)  
Single Crystals for Laser Applications  
K. Shimamura, M. Timoshenckin, T. Sasaki, K. Hoshikawa  
and T. Fukuda  
Tohoku University and Osaka University, Japan

9:30 Si and Mg Doped GGG Single Crystals  
M. Gobbel, S. Kimura, K. Langer, and E. Woermann  
RWTH Aachen, Institute for Mineralogie und Kristallographie, Germany  
and National Institute for Research in Inorganic Materials, Japan

9:45 The Behavior of Chromium Ions in Forsterite  
Y. Yamaguchi, K. Yamagishi and Y. Nobe  
Mitsui Mining & Smelting LTD, Japan

10:00 Czochralski Growth of Rare Earth Oxyorthosilicate Single Crystals  
C. L. Melcher, R. A. Manenete, C. A. Peterson, and J. S. Schweitzer  
Schlumberger-Doll Research, USA

10:15 **COFFEE BREAK**

10:30 Physical Properties of a  $Y_3Al_5O_{12}$  Melt  
V. J. Fratello and C. D. Brande  
AT&T Bell Labs, USA

10:45 Metastable Crystallization of  $Nd_3Ga_5O_{12}$  and  $Gd_3Ga_5O_{12}$  Garnet Melts  
S. A. Markgraf, M. Gobbel and S. Kimura  
National Institute for Research in Inorganic Materials, Japan

11:00 Top-Seeded Solution Growth of Vanadate Garnets  
B. A. Wechsler and C. C. Nelson  
Hughes Research Laboratories, USA

11:15 Theoretical Growth Forms of Natural Garnets  
M. M. R. Boutz and C. F. Woensdregt  
Institute of Earth Sciences Utrecht, The Netherlands

11:30 Crystal Growth and Characterization of New Laser Materials  
R. Collongues, A.M. Lejus, J. Thery and D. Vivien  
Laboratoire de Chimie Applique de l'Etat Solide, France

11:45 Crystal Growth of  $YVO_4$  Using the LHPG Technique  
S. Erdle and F. W. Ainger  
Pennsylvania State University, USA

ORIGINAL PAGE

COLOR 

## WEDNESDAY MORNING - AUGUST 19, 1992

### SESSION 5

#### **Grand Ballroom**

Session Chairperson - A. Jordan, USA

8:00 Towards Understanding the Growth Mechanism of III-V Semiconductors on an Atomic Scale  
T. Nishinaga and T. Suzuki, University of Tokyo, Japan

8:45 BREAK

#### **Session 5 C - Palomar Room**

##### III-V EPITAXIAL GROWTH II

Session Chairpersons - T. F. Keuch and  
T. Nishinaga, Japan

9:00 \* Two Dimensional Carrier Confinement in GaAlAs Quantum Arrays  
Grown by MBE  
Pierre Petroff  
University of California Santa Barbara, USA

9:30 Equilibrium Gas-phase Composition and Thermodynamic Properties  
Including Subhydrides in the Pyrolysis of  $\text{AsH}_3$  and  $\text{PH}_3$   
A.S. Jordan and A. Robertson  
AT&T Bell Laboratories and Engineering Research Center, USA

9:45 Monte Carlo Simulation of  $\text{Li}_{1-x}$ -Type Ordering Due to Surface Step  
Migration in the Epitaxial Growth of III-V Semiconductor Alloys  
M. Ishimaru, S. Matsumura, N. Kuwano, and K. Oki  
Kyushu University, Japan

10:00 COFFEE BREAK

10:15 Growth Kinetics by MBE on Flat and Stepped Surfaces  
T. Uchida, T. Uchida and K. Wada  
Hokkaido University, Japan

10:30 A Study of Group-V Desorption from InP, InAs, GaP, and GaAs by  
Reflection High-Energy Electron Diffraction During Gas-Source  
Molecular-Beam Epitaxy  
B. W. Liang and C. W. Tu  
University of California, San Diego, USA

10:45 Highly Carbon-Doped p-Type  $\text{Ga}_{0.5}\text{In}_{0.5}\text{As}$  By Carbon Tetrachloride in  
Gas-Source Molecular Beam Epitaxy  
T. P. Chin, P. D. Kirchner, G. D. Pittit, C. Lin, J. M. Woodall  
and C. W. Tu  
IBM T.J. Watson Research Center and University of California San Diego,  
USA

11:00 Growth of Semiconductors by LPE  
E. Bauser and H.P. Strunk  
MPI für Festkörperforschung, Germany

11:30 Structure of the Growth Surface of GaAs Grown on (001) GaAs by  
Liquid Phase Epitaxy  
H. P. Strunk and T. Marek  
Universität Erlangen-Nürnberg, Germany

#### **Session 5 D - "White Wines" Room**

##### SUPERCONDUCTORS III

Session Chairpersons - M. Schleber, Israel and  
I. Matsubara, Japan

9:00 \* Crystallization of Oxide Superconductors from Molten Hydroxide  
Ann M. Stacy  
University of California-Berkeley, USA

9:30 High Oxygen Pressure ( $P_{\text{O}_2} \approx 3000$  bar) P-T-x Phase Diagram of the  
Y-Be-Cu-O System  
E. Kaldus, J. Karpinski, S. Rusiecki, and E. Jilek  
ETH - Zurich, Switzerland

9:45 Phase Diagram and Crystal Growth of  $(\text{Y}_{1-x}\text{Pr}_x)\text{Ba}_2\text{Cu}_3\text{O}_{6-y}$   
C. Chen, B. M. Wanklyn, H. Yongle, A. K. Pradham, J. W. Hodby, S.  
Hazell, F. R. Wondre, and A. Boothroyd  
University of Oxford, and University of Warwick, UK

10:00 Crystal Growth Mechanism of  $\text{YBa}_2\text{Cu}_3\text{O}_6$  Superconductors With Peritectic  
Reaction  
T. Izumi, Y. Nakamura, and Y. Shiohara  
Internat'l Superconductivity Tech Center, Japan

10:15 COFFEE BREAK

10:30 CZ Growth of  $\text{YBa}_2\text{Cu}_3\text{O}_6$  Single Crystals  
C. T. Lin, E. Schonherr, H. Bender, and W. Y. Liang  
University of Cambridge, UK and Max-Planck-Institute, Germany

10:45 On the Role of Electron and Optical Microscopy in the Study of Pregrowth  
and Postgrowth History of Some Cuprate Crystals  
A. J. S. Chowdhury and B. M. Wanklyn  
University of Oxford, UK

11:00 Surface Analysis of  $\text{Ln}_{2-x}\text{Ce}_x\text{CuO}_4$  (Ln=Pr and Nd) Single Crystals Grown  
by the Top Seeded Solution Method  
L. C. Sengupta and S. Sengupta  
U.S. Army Materials Tech. Laboratory and Massachusetts Institute of  
Technology, USA

11:15 Real Structure of  $\text{La}_{2-x}\text{Sr}_x\text{CuO}_4$  Single Crystals  
K. V. Gamayunov  
General Physics Institute, Russia

11:30 Technological Parameters Influence on the Morphology and the  
Temperature of Superconducting Transition in  $\text{La}_{2-x}\text{Sr}_x\text{CuO}_4$  Single  
Crystals  
V. V. Voronkov, K. V. Gamayunov, V. I. Zorya, A. L. Ivanov, V. V. Osiko,  
V. O. Tatarintsev, A. I. Chernov, and Yu. P. Yakovets  
General Physics Institute, Russia

\* Indicates Invited Speaker

CRIMINAL PAGE  
COLOR PHOTOGRAPH

## THURSDAY MORNING - AUGUST 20, 1992

### SESSION 6

#### Grand Ballroom

Session Chairperson - D.T.J. Hurle, UK

8:00 \* IOCGR FRANK PRIZE LECTURE, Role of Instabilities in Determination of the Shapes of Growing Crystals,  
Robert F. Sekerka, Carnegie Mellon University, USA

8:45 BREAK

#### Session 6 A - Cuyamaca Room

##### MORPHOLOGICAL STABILITY

Session Chairperson - R. F. Sekerka, USA and  
V. V. Voronkov, Russia

9:00 \* Growth Morphologies in Diffusion Field  
Y. Saito, M. Uwaha and T. Sakiyama  
Keio University, Japan

9:30 \* Simulation of Microscopic Growth Morphologies in Binary Systems  
R. Xiao, J. Iwan Alexander, F. Rosenberger and N-b. Ming  
Univ. of Alabama, Huntsville, USA

10:00 COFFEE BREAK

10:15 Monte Carlo Simulation of Morphological Instability in Step Flow Growth  
C. C. Hsu  
The Chinese University of Hong Kong, Hong Kong

10:30 Fluctuation of Steps in Surface Diffusion Field  
M. Uwaha and Y. Saito  
Tohoku University, Japan

10:45 \* Stability of Vicinal Faces; Growth Kinetics  
A. A. Chernov  
Institute of Crystallography, Russia

11:15 Nonlinear Analysis in Rapid Solidification  
R. J. Braun, G. J. Merchant, K. Brattkus, and S. H. Davis  
National Institute of Standards and Technology, Stanford University,  
California Institute of Technology and Northwestern University, USA

11:30 Thermal Effects in Rapid Directional Solidification  
D. A. Huntley and S. H. Davis  
Northwestern University, USA

11:45 Cellular Solidification with Anisotropic Diffusion  
D. A. Kurtze  
North Dakota State University, USA

#### Session 6 B - Laguna Room

##### OXIDE CRYSTAL GROWTH

Session Chairpersons - J. Wenckus, USA and  
F. Ainger, USA

9:00 Crystal Growth of  $\text{FeBO}_3$  by Top Seed Solution Method  
D. Ni and D. Shen  
Research Institute of Synthetic Crystals, PR China

9:15 Crystal Growth of  $\text{PbTiO}_3$  by a Self-flux Technique  
B. N. Sun, Y. Huang and D. A. Payne  
University of Illinois, USA

9:30 The Growth of Barium-Strontium Titanate ( $\text{Ba}_{1-x}\text{Sr}_x\text{TiO}_3$ ) Single Crystals by the FZ Method  
H. Kojima, M. Watanabe and I. Tanaka  
Yamanashi University, Japan

9:45 Hydrothermal Growth of Bismuth Silicate  
J. J. Larkin, M. T. Harris, J. E. Cormier, R. N. Brown, and A. F. Armington  
Rome Laboratories and Parke Mathematical Laboratory, USA

10:00 Solid-Liquid Interface in the Growth of Sillenite-Type Crystals  
J. Martinez-Lopez, M. A. Caballero, M. T. Santos, L. Arizmendi, and E. Dieguez  
Universidad Autonoma de Madrid and Universidad de Cadiz, Spain

10:15 COFFEE BREAK

10:30 Modelling of Directional Solidification of BSO  
C. Lin and S. Motakef  
Massachusetts Institute of Technology, USA

10:45 Twinning and Dislocation in the Bridgman-Grown  $\text{Li}_2\text{B}_4\text{O}_7$  Crystals  
R.-Y. Sun, S.-J. Fan and Y.-B. Xu  
Shanghai Institute of Ceramics, PR China

11:00 Crystal Growth and Magnetic Characterization of  $\text{Zn}_{1-x}\text{Mn}_x\text{Cr}_2\text{O}_4$  Single Crystals  
F. Leccabue, B. E. Watts, G. Calestani, D. Fiorani and V. Sagredo  
MASPEC Institute, Italy and Universidad de Los Andes, Venezuela

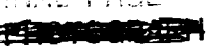
11:15 A Gas Phase Supported Liquid Phase Sintering Process Applied to the Growth of Large Homogeneous EuO Single Crystals  
K. J. Fischer, U. Kobler, B. Stroka, K. Bickmann, and H. Wenzl  
Forschungszentrum Jülich, IFF and Universität Karlsruhe, Germany

11:30 Growth of  $\text{TiO}_2$  Ribbon Crystals by Edge-Defined Film-Fed Growth Method  
H. Machida, K. Hoshikawa and T. Fukuda  
Tohoku University, Japan

11:45 The Growth of Dome-Shaped Sapphire Crystals by the GSM  
A. Horowitz, S. Bilderman, D. Gantz, Y. Einav, G. Ben Amar and M. Weiss  
Nuclear Research Center, Negev, Israel

12:00 Hydrothermal Synthesis and Morphology of  $\text{Li}_2\text{B}_4\text{O}_7$  Crystals  
K. Byrappa and K. V. K. Shekar  
University of Mysore, India

\* Indicates Invited Speaker

ORIGINAL PAGE  
COLOR 

## THURSDAY MORNING - AUGUST 20, 1992

### SESSION 6

#### Grand Ballroom

Session Chairperson - D.T.J. Hurie, UK

8:00 \* IOCGB FRANK PRIZE LECTURE, Role of Instabilities in Determination of the Shapes of Growing Crystals,  
Robert F. Sekerka, Carnegie Mellon University, USA

8:45 BREAK

#### Session 6 C - Palomar Room

##### WIDE BANDGAP MATERIALS I (GaN, SiC, REFRACTORIES, ETC.)

Session Chairpersons - R. H. Hopkins, USA and  
I. Akasaki, Japan

9:00 \* Growth of GaN and AlGaN for UV/Blue p-n Junction Diodes  
I. Akasaki, H. Amano and H. Murakami  
Nagoya University, Japan

9:30 \* Morphological Properties of CVD AlN Films  
R. Rodriguez-Clemente  
Institut de Ciencia de Materiales, Spain and ISGMP-CNRS Laboratoire de  
Physicochimie des Matériaux, France

10:00 COFFEE BREAK

10:15 SiC-AlN Solution Growth by Metalorganic Chemical Vapor Deposition  
V. A. Dmitriev, K. G. Irvine, I. Jenkins, X. Tang, and M. G. Spencer  
Howard University, USA

10:30 Growth of Large SiC Single Crystals  
D. L. Barrett, R. C. Seldensticker, J. P. McHugh, H. M. Hobgood,  
R. H. Hopkins, and W. J. Choyke  
Westinghouse Electric Company and University of Pittsburgh, USA

10:45 Blue Photoluminescence at Room Temperature in Zn-Doped Single  
Crystals of Cu Al S<sub>2</sub>  
K. Sato  
Tokyo University of Agriculture and Technology, Japan

11:00 Floating Zone Growth of Monochromator Grade Crystals of YB<sub>65</sub>  
Y. Kamimura, T. Tanaka, S. Otani, Y. Ishizawa, Z. Rek, and J. Wong  
National Institute for Research, Japan, Stanford University and Lawrence  
Livermore National Laboratory, USA

11:15 Preparation of Boundary-Free LaB<sub>6</sub> Single Crystals by the Traveling  
Solvent Floating Zone Method  
S. Otani, S. Honma, T. Tanaka, and Y. Ishizawa  
National Institute for Research in Inorganic Materials, Japan

11:30 Use of the Bridgman Method for Growth of Peritectic Compounds  
T. Calliat, J.P. Fleurial and A. Borschhevsky  
California Institute of Technology Jet Propulsion Laboratory, USA

11:45 Electrodeposition of Molybdenum onto the Best Single Crystal  
Molybdenum Substrates from Molten Salts  
N. O. Esina, A. N. Baraboshkin, V. O. Esin, Z. I. Valeev, L. M. Minchenko,  
A. A. Pankratov, and D. M. Tagirova  
Institute of Electrochemistry, Russia

#### Session 6 D - "White Wings" Room

##### AQUEOUS SOLUTION GROWTH I (BIO-MATERIALS)

Session Chairpersons - A. McPherson, USA and  
R. Giege, France

9:00 \* Towards an Understanding of the Precrystallization and Early Stages of  
Growth of Biological Macromolecules: The Influence of Macromolecular  
Homogeneity  
R. Giege, B. Lorber, M. S. Kouri, J. P. Munch and S. Candau  
Inst. of Bio. Molec & Cell, CNRS, France

9:30 \* Growth and Dissolution Kinetics of Lysozyme Crystals  
F. Rosenberger, L.A. Monaco, and N.-b. Ming  
University of Alabama, Huntsville, USA

10:00 Nucleation Phenomena in Crystallization of Satellite Tobacco Mosaic  
Virus (STMV)  
A. J. Malkin and A. McPherson  
University of California Davis, USA

10:15 COFFEE BREAK

10:30 Thermal Methods in Protein Crystallization  
R. C. DeMattel and R. S. Feigelson  
Stanford University, USA

10:45 Crystallisation of Nortriptyline Hydrochloride, A Tricyclic Antidepressant  
M. L. MacCalman and K. J. Roberts  
University of Strathclyde, UK

11:00 Growth and Morphology of Cholesterol in Model Biles  
F. C. Voigt, R. M. Geertman, H. Meekes, and B. Groen  
University of Nijmegen, The Netherlands

11:15 On the Morphological and Chemical Stability of Vitamin C Crystals  
S. Halasz and B. Bodor  
Research Institute for Technical Chemistry, Hungary

11:30 Factors Affecting the Morphology of Isoctrate Lyase Crystals  
R. C. DeMattel, R. S. Feigelson and P. Weber  
Stanford University and DuPont Merck Pharmaceutical Co., USA

\* Indicates Invited Speaker

CONFIDENTIAL  
EXCERPT

THURSDAY AFTERNOON - AUGUST 20, 1992

SESSION 7

Grand Ballroom

Session Chairperson - R. A. Laudise

1:30 ICG LAUDISE PRIZE LECTURE I, Development of Skull Melting and Crystallization, Partially Stabilized Zirconia  
V. V. Osiko, Russian Academy of Sciences, Russia

2:15 BREAK

2:30 ICG LAUDISE PRIZE LECTURE II, Mass Production of Refractory Oxide Crystals: Cubic Zirconia,  
Joseph F. Wenckus, Ceres Corporation, USA

Exhibit Hall

3:15 Poster Sessions # 3 and # 4

ORIGINAL PAGE  
COLOR [REDACTED]

## FRIDAY MORNING - AUGUST 21, 1992

Grand Ballroom  
Session Chairperson - A. A. Chernov, Russia

### SESSION 8

8:00 \* Non-linear Effects in Impurity Incorporation in Semiconductor Melt Growth, V.V. Voronkov, Institute of Rare Metals, Russia  
8:45 BREAK

#### Session 8 A - Cuyamaca Room

##### DENDRITIC GROWTH AND PATTERNS

Session Chairpersons - M. Glicksman, USA and Y. Saito, Japan

9:00 \* Formation of Patterns during Growth of Snow Crystals  
Etsuro Yokoyama  
Kyushu Inst. of Technology, Japan

9:30 Capillary Effects at Dynamic Crystal/Melt Interfaces  
M. E. Glicksman and S. P. Marsh  
Rensselaer Polytechnic Institute and Naval Research Laboratories, USA

9:45 Surface Tension Anisotropy and Cell-like Structure Formation  
In Free Solidification  
V. Pines, M. Zletkowski and A. Chait  
NASA Lewis Space Research Center, USA

10:00 COFFEE BREAK

10:15 Three-Dimensional Pattern Formations at Growth of Ice Dendrites  
Y. Furukawa and W. Shimada  
Hokkaido University, Japan

10:30 Dendritic Growth of Cyclohexane  
R. M. Geertman, E. P. G. van den Berg and P. Bennema  
University of Nijmegen, The Netherlands

10:45 Effects of High Magnetic Fields on Fractal Growth of Lead Metal-Leaves  
I. Mogi, S. Okubo and Y. Nakagawa  
Tohoku University, Japan

11:00 Experimental Studies on the Pattern Formation in Aqueous Solution Film System  
M. Wang and N.-b. Ming  
Nanjing University, PR China

11:15 Thermal Evolution of Equilibrium Crystal Shape of  $\alpha$ -Ag<sub>3</sub>S  
T. Ochiai and I. Taniguchi  
Doshisha University, Japan

11:30 The Finiteness Effect on Crystal Equilibrium Shape  
D. Agullano, R. Kern and M. Rubbo  
Universita Degli Studi di Torino, Italy and CRMC2- CNRS Luminy, France

11:45 Vacancy Diffusion in Mercury Cadmium Telluride  
M. Neubert, F. M. Diessling, and K. Jacobs  
Humboldt University of Berlin, Institute of Crystallography and Material Science, Germany

12:00 TEM Investigation of Precipitates in Hg<sub>0.9</sub>Cd<sub>0.1</sub>Te Grown by THM  
F.-M. Klessing and H. S. Leipner  
Humboldt University of Berlin and Martin Luther University of Halle, Germany

Session Chairpersons - J. B. Mullin, UK and M. Brown, USA

9:00 Vapor Growth and Characterization of CdTe Bulk Single Crystals  
H. Wiedemeier and G. H. Wu  
Rensselaer Polytechnic Institute, USA

9:15 Condition for Growing Single and Twinned Crystals in CdTe Vapor Phase Epitaxy  
M. Kasuga, L. Li and Y. Yoshioka  
Yamanashi University, Japan

9:30 Characterization of Large-Diameter Single-Crystal CdTe Grown by the Vertical Bridgman Method  
L. G. Casagrande, D. DiMarzio, D. J. Larson, Jr., M. Dudley and T. Fanning  
Grumman Corporation and Stony Stoneybrook, USA

9:45 Large (Cd,Zn) Te Single Crystals Grown by the Horizontal Bridgman Technique  
P. K. Liao  
Texas Instruments, Inc., USA

10:00 State and Distribution of Point Defects in Doped and Undoped Bridgman-Grown CdTe Single Crystals  
K. W. Benz, D. Sinerius, C. Elche, B. K. Meyer, D. M. Hofmann, C. Albers, R. Bohn, P. Rudolph, and H. Zimmermann  
Albert-Ludwigs-Universität Freiburg, Technical University of Munich and Humboldt University of Berlin, Germany

10:15 COFFEE BREAK

10:30 Defects in CdTe Bridgman Monocrystals Caused by Nonstoichiometric Growth Conditions  
P. Rudolph, M. Neubert and M. Muhler  
Humboldt University of Berlin and Institute Crystallography and Material Science, Germany

10:45 Photoluminescence (PL) Spectra of Cd<sub>1-x</sub>Zn<sub>x</sub>Te Substrates, Correlated to the Free Charge Carriers of Hg<sub>x</sub>Cd<sub>1-x</sub>Te Epitaxial Layers  
M. Azoulay, R. Tenne and H. Feldstein  
Soreq Nuclear Research Center, Israel

11:00 Microgravity Crystal Growth Experiments of CdTe on the Soviet PHOTON 7 Mission  
M. Salk, B. Lexow, K. W. Benz, D. G. Matioukhin, J. M. Gel'fgat, M. Z. Sorkin, A. S. Senchenkov, A. V. Egorov, I. V. Barmin, P. Sickinger, P. Hofmann, R. Klett  
Albert-Ludwigs University Freiburg, Kayser-Threde GmbH Germany, Riga Scientific Research Institute for Radioscope Apparatus, Institute of Physics, Latvia and SPLAV Technical Center, Russia

11:15 Crystal Growth of Semimagnetic-Semiconductors in Very High Magnetic Fields  
G. Kido, N. Adachi, and M. Inoue  
Tohoku University, Japan

11:30 Seedless Seeding and Zero Tellurium Precipitates in Vertical Bridgman Grown CdZnTe (3-5%)  
A. J. Socha Sr.  
Johnson-Matthey Electronics, Inc., USA

\* Indicates Invited Speaker

ORIGINAL PAGE  
COLOR ~~RECORDED~~

**THURSDAY AFTERNOON - AUGUST 20, 1992**

## SESSION 7

### **Grand Ballroom**

**Session Chairperson - R. A. Laudise**

1:30	IOCG LAUDISE PRIZE LECTURE I, Development of Skull Melting and Crystallization, Partially Stabilized Zirconia V. V. Osiko, Russian Academy of Sciences, Russia
2:15	BREAK
2:30	IOCG LAUDISE PRIZE LECTURE II, Mass Production of Refractory Oxide Crystals: Cubic Zirconia, Joseph F. Wenckus, Ceres Corporation, USA
	<b>Exhibit Hall</b>
3:15	Poster Sessions # 3 and # 4

Exhibit H

3:15 **Poster Sessions #3 and #4**

ORIGINAL PAGE  
COLOR [REDACTED]

## FRIDAY MORNING - AUGUST 21, 1992

### SESSION 8

#### Grand Ballroom

Seslon Chairperson - A. A. Chernov, Russia

8:00 \* Non-linear Effects in Impurity Incorporation in Semiconductor Melt Growth, V.V. Voronkov, Institute of Rare Metals

8:45 BREAK

#### Session 8 C - Palomar Room

##### WIDE BANDGAP MATERIALS II (DIAMOND)

Session Chairpersons - I. Sunagawa, Japan and  
B. Spitsyn, Russia

9:00 \* Diamond Films from Vapor Phase  
Boris Spitsyn  
Institute of Physical Chemistry, Russia

9:30 Growth of Diamond by Sequential Deposition and Etching Process  
Using Hot Filament CVD  
J. Wei and Y. Tzeng  
Auburn University, USA

9:45 Selective Area Growth of Diamond Film using Ion Implantation  
K. Kobayashi, S. Karasawa, T. Watanabe, and F. Toghasi  
Industrial Research Institute of Kanagawa and Science University of Tokyo, Japan

10:00 COFFEE BREAK

10:15 The Influence of Growth Parameters on the Formation of a Textured Surface Morphology  
H. Walcher, Ch. Wild, W. Muller-Sebert, N. Herres, T. Eckermann  
Fraunhofer-Gesellschaft Institute, Germany

10:30 Characterization of Thin Film Diamond Growth by Scattering of Light and Surface Reflectance Spectroscopy  
A. M. Bonnot, T. Lopez-Rios, B. Mathis, L. Magaud and F. Cyrot-Lackmann  
Centre Nat'l de la Recherche Scientifique, France

10:45 \* Crystal Growth In the Mineral Kingdom  
Ichiro Sunagawa  
Tohoku University, Japan

11:15 The Separation of Natural From Synthetic GEM-Quality Diamonds on the Basis of Crystal Growth Criteria  
E. Fritsch and J. E. Shigley  
Gemological Institute of America, USA

11:30 Who First Grew Diamond: "The Dog That Did Nothing"  
K. Nassau  
Nassau Consultants, USA

\* Indicates Invited Speaker

#### Session 8 D - "White Wines" Room

##### AQUEOUS SOLUTION GROWTH II (ORGANICS AND PHOSPHATES)

Session Chairpersons - G. Lollacono, USA and  
K. J. Roberts, UK

9:00 \* Effect of Impurities on Crystal Growth  
K. Sangwal  
Technical University of Lublin, Poland

9:30 Molecular Dynamics Simulations of Interfaces Between Crystalline Urea and Aqueous Urea Solutions  
E. S. Boek, W. J. Briels, J. van Eerden, and D. Fell  
University of Twente, The Netherlands

9:45 Bundling Crystallization of Aspartame from Stagnant Aqueous Solutions  
N. Kubota and T. Mori  
Iwate University and Ajinomoto Co. Ltd., Japan

10:00 Growth Kinetics of Sodium Chlorate Crystals Grown From Pure and Sodium Dithionite Doped Solution  
R. I. Ristic, B. Shekunov and J. N. Sherwood  
University of Strathclyde, UK

10:15 COFFEE BREAK

10:30 Studies of the Nature of Diffusion Layer Near KDP Crystal Growing In Solution  
M. J. Krasinski  
Technical University, Poland

10:45 The Influence of Crystal Perfection on the Growth Kinetics of Potash Alum Single Crystals  
H. L. Bhat, R. I. Ristic, J. N. Sherwood, and T. Shripathi  
University of Strathclyde, UK

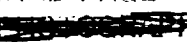
11:00 The Study of the Growth Mechanism of Potash Alum Crystals  
R. I. Ristic, B. Shekunov and J. N. Sherwood  
University of Strathclyde, UK

11:15 Crystal Growth and Characterization of  $MgHPO_4 \cdot 3H_2O$   
B. C. Sales, B. C. Chakourakos, L. A. Boatner, and J. O. Ramey  
Oak Ridge National Lab, USA

11:30 Growth Morphology of Berlinite Crystals Obtained under Hydrothermal Conditions  
J. Gomez-Morales, R. Rodriguez, J. Durand, and L. Cot  
Institut de Ciencia de Materiales, Spain

11:45 Crystal Growth, Morphology, Structure and Properties of Some Superionic Pyrophosphates  
K. Byrappa, B. V. Umesh Dutt, G. S. Gopalakrishna and S. Gall  
University of Mysore, India and Universidad Barcelona, Spain

12:00 Hydrothermal Synthesis of New Potassium Neodymium Silicates  
S. M. Halle, B. J. Wuensch, T. Siegrist, and R. A. Laudise  
Massachusetts Institute of Technology and AT&T Bell Laboratories, USA

ORIGINAL PAGE  
COLOR 

FRIDAY AFTERNOON - AUGUST 21, 1992

SESSION 9

Session 9 A - Cuyamaca Room

SURFACE ROUGHENING AND PARTICLE FORMATION

Session Chairpersons - N.-b. Ming, PR China and  
J. P. van der Eerden, The Netherlands

1:30 Microscopic Condensation Processes of Niobium Microclusters in Sputtering  
K. Obara  
Kagoshima University, Japan

1:45 Optical Absorption Spectra of  $Au_2$  and  $Cu_2$  in Gas Evaporation Technique  
T. Okazaki and Y. Saito  
Meijo University, Japan

2:00 Structure of Alloy and Oxide Particles Produced by the Reaction Between Ultrafine Particles and Films  
Y. Saito, K. Ohtsuka, T. Watanabe, and C. Kaito  
Kyoto Institute of Technology, Japan

2:15 A New Experimental Study on the Production of Clusters Due to Chemical Reaction of Copper Ultrafine Particles  
C. Kaito, T. Watanabe, K. Ohtsuka, H. Chin, and Y. Saito  
Kyoto Institute of Technology, Japan

2:30 Fundamental Criterion for Surface Melting  
J. P. van der Eerden, T. H. M. van de Berg, J. Hulink and  
H. J. F. Knops  
University of Utrecht, The Netherlands

2:45 Electron Microscopy Study of Growth and Aggregation of Microclusters of  $AgI$  and  $HgI_2$   
M. Abdulkader and K. C. George  
Mahatma Ghandi University, India

BREAK

3:15 CLOSING CEREMONY - Grand Ballroom  
B. Cockayne, UK

Session 9 B - Laguna Room

II-VI GROWTH II (TERNARY SEMICONDUCTORS)

Session Chairpersons - T. Ciszek, USA and  
K. Sato, Japan

1:30 Self-Limiting Monolayer Epitaxy (SME): A New Approach to the Growth of Wide Gap II-VI Heterostructures  
W. Faschinger, P. Juza, S. Ferreira, and H. Sitter  
University of Linz, Austria

1:45 Growth of Zinc Selenide Crystals by the Liquid Encapsulated Vertical Bridgman Technique  
Y. Okano, K. Hoshikawa, T. Fukuda, H. Unuma, and K. Tono-Oka  
Tohoku University and GID Laboratories, Japan

2:00 The Growth and Characterization of Cadmium Selenide and Zinc Cadmium Selenide Epilayers by MOCVD  
P. J. Parbrook, A. Kanata and T. Uemoto  
Toshiba Corporation, Japan

2:15 Epitaxial Growth of High Quality ZnSe and ZnSe/ZnS Superlattices for Optical Processing  
C.-D. Pong, R. C. DeMattel and R. S. Fegelson  
Stanford University, USA

2:30 Large-Grained  $CuInSe_2$  Crystal Growth Using Computer-Controlled, High-Pressure LEDS Furnaces  
C. R. Schwerdtfeger and T. F. Ciszek  
National Renewable Energy Lab, USA

2:45 Method of Selenizing Liquid Cu-In Alloy in Growing  $CuInSe_2$  Single Crystal  
S. Nomura and T. Takizawa  
Nihon University, Japan

3:00 Characterization of  $CuInSe_2$  Single Crystals with Various Deviations from Stoichiometry  
H. Nakanishi, A. Tamai, S. Ando, S. Endo, and T. Irie  
Science University of Tokyo, Japan

3:15 BREAK

ORIGINAL PAGE  
COLOR ~~REPRODUCED~~

FRIDAY AFTERNOON - AUGUST 21, 1992

SESSION 9

Session 9 C - Palomar Room

SPECIAL TECHNIQUES

Session Chairperson - W. R. Wilcox, USA and E. I. Givargizov, Russia	Session Chairpersons - R.J. Davy, UK and R. C. DeMattie, USA
1:30 * The Application of X-ray Techniques to Problems in Crystal Science K. F. Roberts University of Strathclyde and SERC Daresbury Laboratory, UK	1:30 Investigations of the Effects of some Additives on the Crystallization of Tetrahydrate Sodium Perborate C. Francis, B. Biscans, <u>N. Gabes</u> , and C. Laguerie National Polytechnique Institute, France
	1:45 Growth of Gypsum III, Influence of Trivalent Ions <u>G. J. Witkamp</u> , C. H. DeVreugd and G. M. van Rosmalen Delft University of Techology, The Netherlands
2:00 Real-time Observation of Stress-Induced Defect Formation and Movement in Si, GaAs and CdTe Single Crystals R. Balasubramanian, W. R. Wilcox and G. Long Clarkson University and National Institute of Standards and Technology, USA	2:00 Characterizing the Effect of Growth Conditions and Crystal Habit on the Distribution of Imperfections Amongst Populations of Crystals C. J. Price AEA Technology, UK
2:15 A Common Orienting Action of Electrical Field and Substrate Patterning In Artificial Epitaxy (Graphoepitaxy) E. I. Givargizov, A. I. Pankashov and L. A. Zadorozhny Institute of Crystallography, Russia	2:15 Adsorption Behavior of Polyelectrolytes in Relation to Their Growth Inhibiting Performance <u>M. C. van der Leeden</u> and G. M. van Rosmalen Delft University of Technology, The Netherlands
2:30 Formation of $Ge_{1-x}Si_x$ Solid Solution by Powder Metallurgy J. Schilz and M. Langerbach German Aerospace Research Est (DLR), Germany	2:30 Crystal Growth Modifiers for Barite and Gypsum, Binding Motifs at Crystal Surfaces S. N. Black, L. A. Bromley, D. Cottler, <u>R. J. Davey</u> , B. Dobbs and J. E. Rout ICI Chemicals & Polymers, Ltd., UK
2:45 A New Development of Laser-Heated Pedestal Growth Technique <u>S. Ja. Rusanov</u> , I. A. Shcherbakov, E. V. Zharikov, G. R. Grigorjan and I. N. Sisakian Central Bureau for Unique Instrumentation, Russia	2:45 The Study of Transport Phenomena in Zeolite Crystal Growth S. Ostrach, Y. Kamotani, and <u>H. Zhang</u> Case Western Reserve University, USA
3:00 The Influence of $Pb^{2+}$ Ions on the Radiation Resistance of $BaF_2$ Crystals G. Chen, S. X. Ren, H. Xiao, S. Q. Man and J. Q. Zhang Beijing Glass Research Institute, PR China	
3:15 BREAK	3:15 BREAK
* Indicates Invited Speaker	
3:30 CLOSING CEREMONY - Grand Ballroom B. Cockayne, UK	

Session 9 D - "White Wines" Room

AQUEOUS SOLUTION GROWTH III (INDUSTRIAL)

ORIGINAL PAGE  
COLOR ~~REPRODUCED~~



## SESSION 1

### DYNAMICS, STABILITY AND CONTROL OF CZOOCKRALSKI CRYSTAL GROWTH

*D.T.J. Hurle and H.H. Wills*

Physics Laboratory, University of Bristol  
Tyndall Avenue, Bristol BS8 1TL, England

Initially crystal pulling equipment was designed purely empirically but, as the industry has grown in importance and the size of crystals has increased, consideration has been given to the optimisation and control of the process. This has led to basic research into the fundamentals together with a large number of computer simulations of its elements.

In this paper, the underlying science which determines the system dynamics is elucidated and methods for achieving stable, robust automatic control described. The linear response of a crystal to temperature and pulling speed variations is derived. Non-linear response is also briefly considered. Recent developments in control strategy are outlined.



## SESSION 1A

### MOLECULAR DYNAMICS SIMULATIONS OF CRYSTAL GROWTH FROM THE VAPOR

*George H. Gilmer*

AT&T Bell Laboratories, Murray Hill, NJ 07974, USA

We have simulated semiconductor surfaces under equilibrium conditions, and during growth. The atomic trajectories were calculated using classical molecular dynamics methods. The Stillinger-Weber interatomic potential was used for silicon-silicon interactions, and potentials with a similar analytical form represented impurities and heteroepitaxial systems.

The influence of surface mobility on the structure of the film was studied by depositing films at different substrate temperatures. The evolution of the latent heat of vaporization when atoms from the beam collide with the substrate is found to have important effects, both on the crystallization process and on the mobility of the atoms at the surface. A transition from amorphous to crystalline deposits was found to occur at about 500°K on the (100) face and 800°K on (111) when a thermal beam was simulated. Columnar structures were observed under conditions of low substrate temperatures and for grazing incidence beams. The latent heat enhanced mobility has a domi-

nant influence on the morphology. The effect of temperature on the column sizes is consistent with results obtained by molecular beam epitaxy.

We have simulated defect generation and strain relaxation in heteroepitaxial systems with appreciable misfit. The stability of uniform films against islanding (the formation of three dimensional clusters) was also studied. In some cases strain in the film leads to a hill and valley structure which evolves into clusters as more material is deposited.

The deposition of clusters of energies from 0.5eV to 10eV per atom was studied. Low energy clusters tend to produce amorphous films and columnar structures, whereas those with higher energies result in uniform crystalline films, and diffuse film-substrate interfaces. We discuss the use of ion and cluster beams to inhibit the segregation of impurities to the surface during molecular beam epitaxy.

---

### DEFECT MECHANISMS OF CRYSTAL GROWTH AND THEIR KINETICS

*Nai-Ben Ming*

National Laboratory of Solid State Microstructures  
Nanjing University, Nanjing 210008, P.R. of China

Dislocations that intersect a growing interface lead to the formation of a self-perpetuating step. It has been demonstrated that this occurs independently of whether the dislocations are of pure edge, pure screw or mixed type.

Similarly, stacking faults that intersect a {111} growth surface of an fcc crystal lead to the formation of a substep (i.e. a step of less than atomic height) along their emergence line. An analysis of the atomic configurations of such substeps show that they can also act as self-perpetuating steps. We have analyzed the growth kinetics at substeps under low and high supersaturation conditions. We found that irrespective of supersaturation, both 2-D heterogeneous mono-nuclear and birth-and-spread nucleation along substeps should provide a growth rate exceeding that of a 2D nucleation mechanism (2D-NM). Furthermore, the stacking fault mechanism (SFM), 2D-NM and screw dislocation mechanism (SDM) were compared with Monte Carlo simulations. These results suggest that at low supersaturation the growth rate for the SFM is always higher

than that for the 2D-NM and less than that for the SDM. At high supersaturation the SFM growth rate is always higher.

On the other hand, {111} growth surfaces that intersect a twin lamella composed of a sequence of parallel stacking faults in fcc crystals possess an atomic configuration corresponding to a rough {100} surface. Therefore, with the vanishing of a nucleation barrier, two types of twinned growth shapes with different growth mechanism can appear: (a) In an isotropic growth system, the combined effects of the rough twinned areas and the re-entrant corners results in a plate-like crystal. (b) In a unidirectional growth system, the twinned, rough and, thus, rapidly growing area should grow out normal to the growth surface and form an "outcrop". This, in turn, can act as a source of growth-steps. The growth of a {111} surface with a twin lamella outcrop was simulated with a Monte Carlo model. The results suggest that the growth activity of a twin lamella mechanism is always larger than that of the 2D-NM and the SFM, but is less than that of the SDM at low supersaturation.

## MODELS FOR THE EARLY STAGES OF NUCLEATION

*H. Riveros, E. Cabrera, M. Gally, C. Ruiz-Mejia and J. Fujioka*

Instituto de Fisica, UNAM, Apdo, Postal 20-364 Mexico DF 01000

The interactions in two-dimensional arrays of ions and dipoles, and the nucleation of two-dimensional clusters, are numerically simulated. Equilibrium configurations with non-lattice symmetries are obtained, in addition to the usual symmetries allowed in macroscopic crystals. The computer program reproduces the movements of the ions or dipoles, and calculates the energy of any configuration. The interaction

between dipoles can be seen using magnets floating on water. It is found that for small clusters of particles (ions or dipoles) the addition of a single particle may produce the rearrangement of the whole cluster, and therefore, in those cases, it would be better to speak of a 'nucleation' process, instead of a 'growth' process.

---

## NUCLEATION AND GROWTH OF FINE CRYSTALS FROM SUPERCRITICAL FLUIDS

*E.M. Berends, O.S.L. Bruinsma and G.M. van Rosmalen*

Delft University of Technology, Laboratory for Process Equipment  
Leeghwaterstraat 44, 2628 CA Delft, The Netherlands

Supercritical fluids well above their critical pressure and temperature can act as adequate solvents for solutes with a low vapour pressure. Upon pressure release the solubility decreases and crystals are formed. If decompression occurs very rapidly as over a nozzle, very high supersaturations are reached almost instantaneously. This leads to an outburst of nuclei followed by their fast growth and thus to the formation of a narrow size distribution of very tiny crystals.

The size and shape of the crystals as well as their size distribution seem to be influenced by parameters such as, (i) the concentration of the solute before the nozzle, (ii) the pressure and temperature before and after the nozzle, (iii) the geometry of the nozzle and (iv) the type of solute.

The aim of this study is to verify and quantify the effects of these parameters for benzoic acid as a model compound crystallizing from supercritical carbon dioxide and to relate them to the prevailing supersaturation profiles. Attempts have been made to model the supersaturation profiles in and after the nozzle. The temperature and pressure profiles had to be calcu-

lated from the estimated hydrodynamic flow pattern. The corresponding equilibrium solubilities were calculated with an appropriate equation of state.

The supercritical solutions were obtained by extracting a bed of benzoic acid crystals with supercritical carbon dioxide at pressures of 150-400 bar and temperatures of 35-75°C. The saturated fluid was afterheated electrically prior to its expansion to atmospheric conditions to prevent solute recrystallisation due to solvent condensation. The nozzle is a small capillary with a diameter of 30-80  $\mu\text{m}$  and a length of 200  $\mu\text{m}$ . The crystals are collected on a paper filter and crystal size distribution, morphology and crystallinity are investigated.

The developed crystals were approximately 0.20  $\mu\text{m}$  in size. A higher pre-expansion pressure and concentration seem to give smaller particles with a narrower size distribution. X-ray diffraction showed a good crystallinity. In spite of their rapid growth the crystals are mostly faceted and also free of solvent inclusions. Attempts will be made to confirm this with phenanthrene and anthracene.

## CRYSTALLIZATION OF AMORPHOUS GERMANIUM ON METAL FILM

Toshio Okabe, Shigeru Saito and Toshiaki Wada

Department of Physics, Toyama University, Toyama 930, Japan

Electron microscopic investigations have been carried out on the crystallization behavior of amorphous Ge films on single crystalline films of Ag and Al. The specimen films were prepared by vacuum deposition, as evaporating germanium thermally on  $<111>$  oriented single crystalline films previously formed by deposition on heated NaCl cleavage plane. The wet-stripped films were heated up at the rate of  $\sim 100^\circ\text{C}/\text{h}$  in an electron microscope by in situ observation. The amorphous Ge on Ag crystallizes at  $\sim 330^\circ\text{C}$  with a distinct orientation relationship:  $(211)_{\text{Ge}} // (211)_{\text{Ag}}$  and  $[\bar{1}11]_{\text{Ge}} // [\bar{1}11]_{\text{Ag}}$  as shown in fig. 1. On the other hand, the amorphous Ge on Al does not

crystallize until  $500^\circ\text{C}$  above the eutectic temperature of this alloy system. On some grains with a  $\alpha$  orientation melting begins as seen in fig. 2 and is followed by crystallization of Ge with some orientation relationships:  $(111)_{\text{Ge}} // (111)_{\text{Al}}$  // and  $[110]_{\text{Ge}} // [312]_{\text{Al}}$  or  $(111)_{\text{Ge}} // (111)_{\text{Al}}$  and  $[400]_{\text{Ge}} // [220]_{\text{Al}}$ . The same situation can be also achieved by the reaction at lower temperature without melting for longer annealing time.

The behavior of amorphous Ge in contact with a metal film will be discussed based on the way of dissolution of Ge into the metal film and the arrangement of atoms on its interface. The behavior of amorphous Ge in contact with a metal film will be discussed based on the way of dissolution of Ge into the metal film and the arrangement of atoms on its interface, comparing with that of amorphous Ge-Al and Ge-Ag evaporated films.

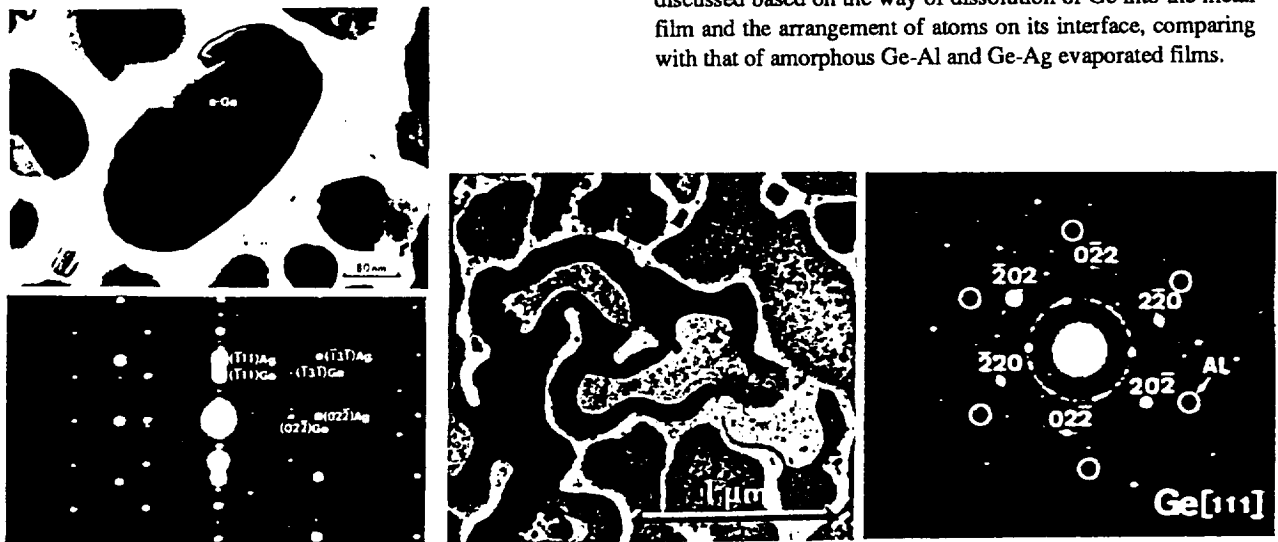


Figure 1. TEM image and electron diffraction of Ge crystal on Ag single particles.

Figure 2. TEM image of melting and electron diffraction of Ge crystal on  $<111>$  Al.

**VISUALIZATION OF SUB-CRITICAL CRYSTALLINE PARTICLES  
THEIR BEHAVIORS IN GROWTH OF KDP CRYSTAL IN AQUEOUS SOLUTION**

*Li Lian, Lu Taigin\*, Kazufumi Sakai, Tomoya Ogawa and Ichiro Sunagawa\*\**

Department of Physics, Gakushuin University, 1-3-1 Mejiro

Toshima-ku, Tokyo 171 Japan

\*The Institute of Physical and Chemical Research (RIKEN),

Hirisawa 2-1, Wako-shi, Saitama, 351-01 Japan

\*\*Yamanashi Institute of Gemmology and Jewelry Arts, Tokoji-machi

1955-1, Kofu, Yamanashi, 400 Japan

By applying a newly developed laser light scattering ultra-microscopy, it was possible to visualize the presence of tiny particles to investigate their behaviors in aqueous solution of KDP in the absence and presence of a growing crystal. The density of the particle increased as increasing supersaturation. Through a series of experiment, it was ascertained that they are neither impurities nor dusts, but in fact sub-critical crystalline particles of KDP. In the bulk solution apart from a growing crystal, their movement is slow, but as soon as they reach a finite distance, which may correlate to the thickness of a diffusion boundary layer, the particles are rapidly sucked to the crystal. The thickness is about 150  $\mu\text{m}$  in [010], as the growth

velocity was 560  $\text{\AA/sec}$ . On the crystal surface, they migrate for a short distance or shake themselves for a while, and then the scattered images disappeared (Fig. 1). Number of particles increases as supersaturation increasing, particularly in the diffusion layer, and relates almost linearly to the growth velocity as indicated in Fig. 2.

All these results suggest that sub-critical crystalline particles are formed in KDP solution, and act as a part of growth unit in the crystallization of the KDP crystals.

Similar phenomenon has been also obtained in other aqueous solution systems such as KCl.

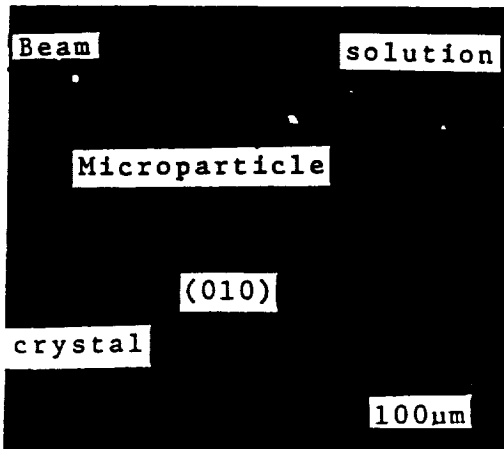


Figure 1. Microparticles existing and interaction with growing crystal.

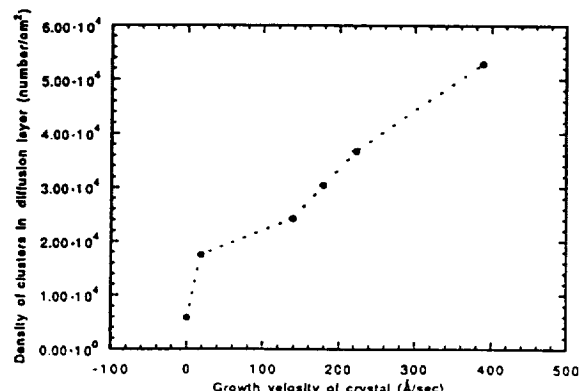


Figure 2. Relationship between growth velocity of crystal and density of microparticles in diffusion boundary layer.

## METASTABLE STATE RELAXATION NEAR THE BINODAL LINE

Allan S. Myerson and Alexander F. Izmailov

Department of Chemical Engineering, Polytechnic University  
333 Jay Street Brooklyn, NY 11201

It is suggested to describe the metastable state relaxation (MSR) in terms of the time-dependent Ginzburg-Landau (TDGL) formalism developed for the kinetics of the first order phase transitions. It seems at present that this approach is the only reasonable one since it does not deal with the numerous assumptions of classical nucleation theory which can not usually be verified experimentally. Thus, the TDGL free energy functional which governs the MSR is constructed for slightly supersaturated solutions far from the critical point. Such solutions, for example, aqueous solutions of glycine, citric acid etc. are of great practical use and at present are under intensive experimental investigation. The obtained non-linear partial differential equation for the MSR near the binodal line was analyzed and solved. Its solution has enabled us to restore for the first time an expression for the induction time in the explicit form for such a relaxation process.

We have succeeded in the theoretical part of our work to find the first correlation functions for the MSR near the binodal line. These functions acquire a special meaning in the vicinity of the nucleation point at which solute density fluctuations become strong and highly correlated. It is well-known that the pair correlation function is the Fourier image of the structure factor which has been measured in our nucleation experiments by light scattering. Taking into account this fact we have verified our theoretical conclusions concerning induction time and time characteristics of the nucleation process. In addition, we have developed the same approach for the microgravity case and in this way some interesting theoretical predictions about nucleation experiments in microgravity environment have been obtained.

---

## SELF-AGGREGATES EN ROUTE TO CRYSTAL FORMATION

M. Lahav and L. Leiserowitz

Department of Materials & Interfaces  
Weizmann Institute of Science, Rehovot 76100, Israel

The understanding of the dynamics of the phase transformation from a supersaturated solution into a crystalline solid requires the knowledge of the structure of the supersaturated solution at the onset of crystallization. In particular, it is of great interest to delineate the role played by structures embryonic aggregates as intermediates in crystal nucleation.

In the present lecture we shall discuss a stereochemical approach on the structure, dynamics growth and dissolution of 2-D self-aggregates formed at the air/solution interface. The packing arrangement and the orientation of the molecules within some of the clusters, which are nucleation transients have been determined and monitored using the methods of grazing incidence X-ray diffraction (GIXD)<sup>1</sup> and second harmonic generation (SHG)<sup>2</sup>.

The role of these clusters in inducing 3-D single crystals will be illustrated for several systems including induced freezing of supercooled water into hexagonal ice by amphiphilic

alcohols.<sup>3</sup> The present stereochemical approach was instrumental for the design of polymers as additives to control crystal polymorphism,<sup>4</sup> crystal twinning<sup>5</sup> and the resolution of enantiomers by crystallization.

1. D. Jacquemain, S. Grayer Wolf, F. Leveiller, M. Duetsch, K. Kjaer, J. Als-Neilsen, M. Lahav and L. Leiserowitz, *Angew. Chem. Int. Ed. Engl.* **31**, 130 (1992).
2. I. Weissbuch, G. Berkovic, L. Leiserowitz and M. Lahav, in "Organic Materials for Non-linear Optics II," Ed. R.A. Hann and D. Bloor, 1991, pp. 82-88.
3. M. Gavish, R. Popovitz-Biro, M. Lahav and L. Leiserowitz, *Science*, **250**, 973-975 (1990).
4. E. Staab, L. Addadi, L. Leiserowitz and M. Lahav, *Adv. Mater.* **1**, 40 (1990).
5. M. Zait, M. Vaida, I. Weissbuch, L. Leiserowitz and M. Lahav, in preparation.



## SESSION 1B

### GROWTH, DEFECTS AND PROPERTIES OF NONLINEAR OPTICAL OXIDE CRYSTALS

*P.A. Morris*

DuPont Company, Experimental Station, Wilmington, DE 19880

The properties of interest for applications of crystalline nonlinear optical oxides are often determined by the defect structures introduced in the materials as a result of the processing procedures used to produce crystals of these materials. Applications of these types of materials, having high second order nonlinear optical susceptibilities ( $\chi^{(2)}$ ), include frequency convertors, electro-optic modulators and switches, and holographic and phase conjugate optics. Several applications require the fabrication of waveguides in the materials. The properties of importance for both bulk and waveguide devices include:  $\chi^{(2)}$ , optical transparency, birefringence and dispersion, ionic and electrical conductivity, optical damage susceptibility, photorefractivity and homogeneity. The defect structures referred to include the intrinsic atomistic defects (e.g. non-stoichiometry), impurities and domains. The growth, defects and resulting properties of several of these materials (e.g.  $\text{KTiOPO}_4$ ,  $\text{KTiOAsO}_4$ ,  $\text{LiNbO}_3$ ,  $\text{BaTiO}_3$ ,  $\beta\text{-BaB}_2\text{O}_4$ ,  $\text{LiB}_3\text{O}_5$ ) are discussed.

The results of studies on these materials indicate that further understanding of the effects of the growth conditions on the resulting defects and properties of bulk nonlinear optical oxide crystals is necessary. Problems still exist regarding the proper-

ties of crystals of traditional nonlinear optical oxides ( $\text{LiNbO}_3$ ,  $\text{BaTiO}_3$ ) which result from the defects introduced by their preferred growth techniques. Many of the problems concerning the growth of the traditional materials with perovskite and tungsten-bronze type structures are inherent due to the tolerance and degree of nonstoichiometry in these structures and the nature of the bulk growth techniques used. The growth conditions and techniques to obtain the highest quality crystals of the more recently developed nonlinear optical oxides ( $\text{KTiOPO}_4$ ,  $\text{KTiOAsO}_4$ ,  $\beta\text{-BaB}_2\text{O}_4$ ,  $\text{LiB}_3\text{O}_5$ ) are not well understood at this time.

Post-growth processing procedures have been used to improve the properties of as-grown crystals, but modification of the defects and properties during growth is obviously preferred. Thin films are attractive for many waveguide devices and future integrated optical applications, however the techniques to produce thin films of these materials are currently being developed and little is known about their defects and properties at this time. The growth-defect-property relationships in nonlinear optical oxides are an important consideration in determining the processing procedures to be used in the development of these materials.

---

### HYDROTHERMAL GROWTH OF POTASSIUM TITANYL ARSENATE (KTA) IN LARGE AUTOCLAVES\*

*Roger F. Belt and John B. Ings*

Airtron Division of Litton Systems Inc.

200 E. Hanover Ave, Morris Plains, NJ 07950 USA

The nonlinear optical crystal KTA is potentially more favorable than its phosphate analog KTP for several applications. The solubility and phase relations were investigated for selected K/As ratios in  $\text{KH}_2\text{AsO}_4$ -KOH solutions over a temperature range of 300-600°C and 10-30000 psi. All initial data were obtained with 0.20 inch diameter x 2.50 inch long platinum capsules in Tem-Pres type autoclaves. The most favorable results were repeated in Morey type autoclaves of 0.875 inch diameter. The P-V-T data were generated and extrapolated for use in gold liners and Rene'41 autoclaves with a pressure balancing method. A direct scale-up was transferred to the 1.5 inch diameter x 18 inch long autoclaves with gold liners. For the latter system, both nutrient and larger seed crystals were grown from a  $\text{K}_2\text{WO}_4$ - $\text{LiWO}_4$  flux. The internal and external

degrees of fill were adjusted to obtain a near balance a near pressure of 25000 psi at a temperature of 560°C. Initial growth runs were made for 1-2 weeks under a growth gradient of 30°C with a 4 molar  $\text{KH}_2\text{AsO}_4$  mineralizer. Three natural seeds were employed while later runs utilized (011) cut and polished seeds. We present data on growth rates, crystal quality, domain behavior, and measured physical properties. Our results are intended for application to production autoclaves for commercial growth of KTA.

---

1. P.A. Morris, et. al., this conference, 1992.

\*This work was supported under contract N00014-90-C-0238.

**GROWTH OF  $\text{KTiOAsO}_4$  (KTA) AND  $\text{CsTiOAsO}_4$  (CTA) CRYSTALS FROM  
NEW MOLTEN-SALT SYSTEM**

*Luo Chuhua, Gu Kaihui, Li Jun, Zheng Chongzhong, Xie Qiuixiang and Luo Fei*  
Southwest Institute of Technical Physics  
P.O. Box 238, Chengdu, China, 610015

Potassium titanyl phosphate referred to as KTP is well-known to possess superior properties for use as a non-linear optical material. Its high damage threshold, good mechanical and thermal stability, large optical nonlinearity, and broad temperature bandwidth have made it arguably the best material for frequency doubling and parametric devices in the visible and near infrared range.

KTP also shows great promise in electro-optic applications due to its low dielectric constants and large electro-optic-coefficients.

KTP is only one member of the family of materials with the formula  $\text{MTiOXO}_4$  where M is K, Rb, Tl or Cs, and X is P or As.

In the past decade, although development has concentrated on KTP for researching the family materials, but the other family members also have large second-order optical nonlinearities. As-substituted analogue  $\text{KTiOAsO}_4$  (KTA) and Cs-Substituted  $\text{CsTiOAsO}_4$  (CTA) have a slightly higher second-order susceptibility than KTP. Because of the larger polarization of Cs and As ions compared to K and P ions.

We have carried out investigations on the growth of single crystals of KTA in new molten-salt system in which  $\text{TiO}_2\text{-KAsO}_3$  is solute and  $\text{K}_4\text{As}_2\text{O}_7\text{-K}_2\text{WO}_4\text{-As}_2\text{O}_5$  is solvent. The new melt with very fluid nonglass forming and little volatility is suitable for a flux or molten solution process. Single crystals of KTA were grown by using a seed crystal. These crystals are clear, transparent, and up to  $12 \times 11 \times 8$  mm in size. But they showed ferroelectric domains which decrease the efficiency of nonlinear optical conversion. The multi-domains of KTA must be eliminated by annealing. Only single domain KTA crystal has higher optical and dielectric properties than KTP crystal.

Single crystals of cesium titanyl arsenate (CTA) have been grown from new molten-salt system in which  $\text{TiO}_2\text{-CsAsO}_3$  is solute and  $\text{Cs}_4\text{As}_2\text{O}_7\text{-Cs}_2\text{WO}_4\text{-As}_2\text{O}_5$  is solvent. Small single crystals of CTA have been grown from new melt by spontaneous crystallization. The results of powder second harmonic generation have proved good, and high-temperature solution using seed crystals is being hired to prepare large single crystals.

---

**GROWTH AND PROPERTIES OF THE NONLINEAR OPTICAL CRYSTAL  $\text{CsTiOAsO}_4$**

*L.K. Cheng\*, L.T. Cheng, A.A. Ballman and E.M. McCarron, III*  
Science and Engineering Laboratory, E.I DuPont de Nemour & Co.  
P.O. Box 80306, Experimental Station, Wilmington, DE 19880-0306

$\text{KTiOPO}_4$  (KTP) is an excellent nonlinear optical crystal particularly suitable for frequency conversion applications. Protas and coworkers<sup>1</sup> have reported that  $\text{CsTiOAsO}_4$  (CTA) is isostructural with KTP and have similarly large optical nonlinearity. Yet, unlike KTP, the crystal growth properties of CTA differ significantly from those of KTP and related isomorphs. We have investigated the growth of CTA crystals using the tungstate-flux, the molybdate-flux and the various self fluxes. A detail understanding of the phase stability regions and of the crystal chemistry of CTA have allowed us to routinely grow large ( $\sim 10 \times 22 \times 32$  mm<sup>3</sup>) inclusion-free crystals of  $\text{CsTiOAsO}_4$ .

$\text{CsTiOAsO}_4$ . Preliminary measurement of the linear and nonlinear optical properties of these crystals reveals that  $\text{CsTiOAsO}_4$  possesses interesting properties which nicely complement that of KTP, thus making CTA of commercial interest. In this talk, both the crystal growth of  $\text{CsTiOAsO}_4$  and its properties are discussed.

*\*Corresponding author.*

<sup>1</sup>Protas, Marnier, Boulanger and Menaert, *Acta Cryst.* (1989), C45, 1123-1125.

**INVESTIGATIONS OF THE FLUX CRYSTALLIZATION PROCESSES AND  
PROPERTIES of  $\text{KTiOPO}_4$  and  $\text{LiB}_3\text{O}_5$**

*V.A. Maslov, L.A. Olkhovaya, V.V. Osiko and E.A. Shcherbakov*

General Physics Institute, 38 Vavilov Str., 117942 Moscow, USSR

In the recent years  $\text{KTiOPO}_4$  and  $\text{LiB}_3\text{O}_5$  crystals are widely used in nonlinear optics [1]. However, the problem of growing of large high-quality crystals, which fit for producing optical elements with high stable characteristics, is not decided up to now.

Morphological and structural characteristics, of KTP and LBO crystals have been described. We have also determined the crystals solubility and metastable region width in the different fluxes. Because of high viscosity, the growth rate do not exceed 1-3mm/day, so total crystallization process continues about 3-4 weeks. For receiving the large optical quality crystals the top- seeded method was used. As a result, the KTP and LBO crystal is were grown with the size of up to 80 cm<sup>3</sup> and 6 cm<sup>3</sup> correspondingly. Habit of grown crystals depends on seeds orientation, flux compositions and some dopant elements. The transmission spectra for clear and Fe-group and Al activative elements are investigated. Using chemical etching, optical and electron microscopes, the real structure of both crystals have been studied. It was established that "grey

tracks," which was arrised in KTP crystals under laser radiation existed due to different dopants elements, in particular Al one. When using especially pure components, the optical damage threshold of the crystals has been increased.

As compared with the  $\text{LiNbO}_3$  substrate the KTP crystal provides new possibilities for integration of active and passive elements required in optical information processing. Some of the integrated optical elements based on the KTP were designed and investigated [2]. For example, the method of fabrication of 2-D structures of optical waveguides in the KTP was presented.

1. J.D. Bierlein, H. Vanherzele, *J. Opt. Soc. Am.B* 6, 622 (1989).
2. E.M. Dianov, V.A. Maslov, A.M. Prokhorov, E.A. Shcherbakov. Conference on Laser and Electro Optics, 1991 (Optical Society of America, Washington, D.C. 1991), pp. 54-56.

---

**SURFACE STABILITY OF LITHIUM TRIBORATE CRYSTALS  
GROWN FROM EXCESS BORIC OXIDE SOLUTIONS**

*E. Brück, R.J. Raymakers, R.K. Route and R.S. Feigelson*

Center for Materials Research  
Stanford University, Stanford, CA 94305

In varying degrees, lithium triborate ( $\text{LiB}_3\text{O}_5$ , LBO) crystals that are exposed to an ambient air atmosphere, either during high temperature processing, or during growth from the melt, exhibit surface decomposition. A thin polycrystalline layer consisting of the lithium-rich phase,  $\text{Li}_4\text{B}_{10}\text{O}_{17}$ , and sometimes other Li-rich phases, forms on the crystal surfaces within a few hours at high temperatures. This is a serious problem because, upon cooling, the underlying LBO crystal always fractures, presumably due to stresses resulting from differential thermal expansion between the crystal and the surface layer. A technique has been developed to prevent surface decomposition of LBO crystals during growth and annealing at elevated temperatures. Crystals grown using this method remain water-clear on the surface during 3-4 week long growth cycles, and have shown no tendency to crack during cooling.

This is in contrast to crystals grown in the same furnaces under normal conditions which almost always exhibit significant amounts of decomposition-related cracking.

The thermal decomposition process appears to be of a catalytic nature, and while the kinetics of the reaction have been studied, an unambiguous determination of its exact chemical pathway is difficult due to challenges in detecting the various reaction products that are produced. The results from spectral and microchemical analysis of the thermal decomposition products, and the chemical decomposition reactions will be presented.

---

This research was supported by the Defense Advanced Research Projects Agency.

**$\beta$ -BaB<sub>2</sub>O<sub>4</sub> SINGLE CRYSTAL GROWTH BY CZOCHRALSKI METHOD  
USING AN  $\alpha$ -BaB<sub>2</sub>O<sub>4</sub>, AND A  $\beta$ -BaB<sub>2</sub>O<sub>4</sub> SINGLE CRYSTAL  
AS STARTING MATERIALS**

*H. Kouta, S. Imoto and Y. Kuwano*

Material Development Center NEC Corporation, Kawasaki, 216, Japan

$\beta$ -BaB<sub>2</sub>O<sub>4</sub> single crystal growth by the Czochralski method[1,2] requires two important factors: 1.  $\beta$ -form (low temperature form) is nucleated from a BaB<sub>2</sub>O<sub>4</sub> melt before  $\alpha$ -form nucleation (high temperature form) on the platinum rod, which is used as a cold finger for first seeding, instead of a seed crystal. 2. Suitable heat transfer conditions are maintained, as a high quality  $\beta$ -form crystal is subsequently grown from the BaB<sub>2</sub>O<sub>4</sub> melt. The reason why the  $\beta$ -form was nucleated from a BaB<sub>2</sub>O<sub>4</sub> melt was explained with the theoretical consideration on the interfacial energy ( $\sigma$ ) with regard to a certain melt structure[2]. In this report, crystal growths using  $\alpha$ -BaB<sub>2</sub>O<sub>4</sub> and  $\beta$ -BaB<sub>2</sub>O<sub>4</sub> single crystal as starting materials were carried out to clarify the effect on these two important factors.

$\alpha$  and  $\beta$ -BaB<sub>2</sub>O<sub>4</sub> single crystals were prepared as starting materials with the Czochralski method, using a  $\beta$ -form powder, which was made of BaB<sub>2</sub>O<sub>4</sub>·4H<sub>2</sub>O. The Czochralski method experiments were implemented using these respective materials with IRE heating. When the starting material was melted, the platinum rod contacted the melt surface at 1050°C. Then the polycrystalline seed was nucleated on the platinum rod tip. As the seed was pulled up, one single crystal, having a specific orientation, was preferentially grown. Then, crystal diameter gradually increased to about 10 mm.

Using  $\alpha$ -form single crystal as a starting material, only  $\alpha$ -form polycrystalline was nucleated just after melting and after keeping melt conditions constant for 3 hours. However,  $\beta$ -form polycrystalline was nucleated after keeping the conditions constant for 4 hours. On the other hand, using  $\beta$ -form single crystal as a starting material,  $\beta$ -form polycrystalline was always nucleated. Especially, just after melting, high quality  $\beta$ -form single crystal was obtained.

It is considered from these experimental facts that the BaB<sub>2</sub>O<sub>4</sub>, just after melting, maintains a specific starting material structure. This structure gradually breaks down with time[3]. This consideration is summarized in Table I. Based on nucleation theory[2], the  $\alpha$ -form melt maintains a specific  $\alpha$ -form structure. Then, the  $\alpha$ -form is nucleated, probably due to  $\sigma_\alpha < \sigma_\beta$ . After this  $\alpha$ -like structure breaks down,  $\beta$ -form is nucleated, probably due to  $\sigma_\alpha < \sigma_\beta$ . Similar consideration on relationship on the interfacial energy may hold for  $\beta$ -form melt, because the  $\beta$ -form melt maintains a specific  $\beta$ -form structure, so the  $\beta$ -form is nucleated and a high quality  $\beta$ -form single crystal can be grown. These  $\sigma$  values would be able to be

*Table I. Relationship between melt structure and nucleated form.*

Starting material	Just after melting	After relaxation time
$\alpha$ -BaB <sub>2</sub> O <sub>4</sub> single crystal	$\alpha$ -like melt $\rightarrow$ $\alpha$ nucleation ( $\sigma_\alpha < \sigma_\beta$ )	Normal melt $\rightarrow$ $\beta$ nucleation ( $\sigma_\alpha > \sigma_\beta$ )
$\beta$ -BaB <sub>2</sub> O <sub>4</sub> single crystal	$\beta$ -like melt $\rightarrow$ $\beta$ nucleation ( $\sigma_\alpha > \sigma_\beta$ )	Normal melt $\rightarrow$ $\beta$ nucleation ( $\sigma_\alpha > \sigma_\beta$ )

estimated, using experimental data for latent heat and degree of supercooling.

[1] K. Ito, F. Marumo and Y. Kuwano, *J. Crystal Growth* 106 (1990) 728.  
[2] H. Kouta, Y. Kuwano, K. Ito and F. Marumo, *J. Crystal Growth*, to be published.  
[3] S. Imoto, S. Kimura, Y. Anzai and Y. Kuwano, The 39th spring meeting (1992); The Japan Society of Applied Physics.

**GROWTH AND PROPERTIES OF NEW TB TYPE PHOTOREFRACTIVE CRYSTALS**

*Huanchu Chen, Daliang Sun, Quanzhong Jiang and Yongyuan Song*

Institute of Crystal Materials, Shandong University 250100, P.R. China

Photorefractive (PR) crystals are extremely interesting materials from the point of view of fundamental studies as well as variety of applications. The most current applications of the PR effect in single crystals involve hologram memory and optical phase conjugation. In this paper, we report a new kind of tungsten bronze crystals with "A sites" unfull-filled and doped with Cu<sup>++</sup> ions. The composition of the crystals were

designed. The crystals with size as large as 35x35x35mm<sup>3</sup> have been obtained by CZ pulling. The crystals showed large gain  $\Gamma$  up to 20cm<sup>-1</sup>, high self-pumped phase conjugation reflectivity around 65% high PR sensitivity in the order of 10<sup>-3</sup>cm<sup>2</sup>/J and high output image quality. Crystal growth conditions and growth habits were discussed.

## SESSION 1C

### POINT DEFECT, CARBON AND OXYGEN COMPLEXING IN POLYCRYSTALLINE SILICON

*J.P. Kalejs*

Mobil Solar Energy Corporation  
4 Suburban Park Drive, Billerica, MA 01821, USA

The importance of native point defects on silicon crystal defect development during melt growth processes and on material electronic properties has become increasingly more recognized since the seminal work of Foell et al (1). Silicon self-interstitials and vacancies together with their interactions with carbon and oxygen need to be examined in formulating models for precipitate and microdefect formation processes during the growth process.

Polycrystalline silicon crystals grown by directional solidification or casting techniques, and by sheet formation methods, present a challenging situation to analyze in terms of point defect influence on material properties. Dislocation densities and grain boundaries are inhomogeneously distributed, and carbon levels are higher. These materials often exhibit different responses in electronic quality changes in subsequent processing, and there is increasing evidence that this response is governed by point defect availability and proceeds via mechanisms similar to those in single crystals.

This paper discusses extensions of point defect models for one polycrystalline silicon material - silicon sheet produced by the Edge-defined Film-fed Growth (EFG) technique - being grown for photovoltaic applications. EFG imposes unique conditions on defect formation, with crystal thicknesses of 300 microns, high interface temperature gradients (1000°C/cm) and cooling rates, and a supersaturated carbon melt. Interstitial oxygen levels can be varied from below detection to the order of  $1 \times 10^{17}/\text{cm}^3$ . Point defect manifestations are deduced from a study of material properties using analysis techniques such as IR spectroscopy, SIMS, and microscopy. New results which help identify important roles for point defects in carbon and oxygen complex development, and self-interstitial and vacancy impacts on defect formation processes are presented.

---

(1) H. Foell, U. Goesele and B.O. Kolbesen, *J. Crystal Growth*  
52 (1981) 907.

## CHARACTERIZATION OF INTERSTITIAL OXYGEN STRIATIONS IN SILICON SINGLE CRYSTALS

*I. Fusegawa, H. Yamagishi, H. Takayama, E. Iino and K. Takano*  
Isobe R&D Center, Shin-Etsu Handotai Co., Ltd.  
Isobe 2-13-1, Annaka, Gunma, Japan

It is well known that striations are formed during Czochralski single crystal growth. Especially, interstitial oxygen (O<sub>i</sub>) impurities are precipitated during LSI fabrication process and formed ununiform O<sub>i</sub> precipitation along those striations. If those striations are accompanied by crystal defects, O<sub>i</sub> impurities are heterogeneously precipitated, which may reduce the yield of LSI device fabrication. In order to evaluate those striations, we developed a micro-FTIR mapping system[1]. This system is effective for measuring the micro distribution of O<sub>i</sub> impurities along striations quantitatively. In this paper, we investigated the relation between the micro distribution of O<sub>i</sub> impurities along striations and CZ growth conditions. And also, those micro precipitation phenomena were investigated whether homogeneous or heterogeneous due to accompanied crystal defects.

In the experiments, several CZ silicon single crystals were grown. The diameters of quartz - crucibles were 30cm, 45cm and 61cm. The diameters of silicon single crystals grown from each crucible were 10cm, 15cm and 20cm, respectively. A magnetic field perpendicular to the growth - axis were applied in the strength up to 0.4T <001> oriented wafers of 2mm thickness were taken from those crystals, sliced parallel to the <100> growth axis. The micro distributions of O<sub>i</sub> concentration ([O<sub>i</sub>]) were measured with a micro-FTIR mapping system of JIR-6500. Its aperture size was 0.1mm (in growth direction) x 0.2mm (in radial direction). The interval of the measuring

step was 0.1mm along the growth direction. Those wafers were treated by striation etching techniques and their optical micro-photographs were taken. In order to measure the precipitated [O<sub>i</sub>], those wafers were treated by an annealing process (at 1073K for 4hrs and at 1273K for 16hrs).

In the results, the micro distribution of O<sub>i</sub> impurities had an interval of about 0.8mm with or without a magnetic field. The peak to valley [O<sub>i</sub>] for each crystal without a magnetic field were as follows;  $0.3 \times 10^{17}/\text{cm}^3$  (Old ASTM) for the crystal of 20cm diameter,  $0.3 \times 10^{17}/\text{cm}^3$  for the one of 15cm diameter and  $0.7 \times 10^{17}/\text{cm}^3$  for the one of 10cm diameter. Those deviation values were higher for small crucible diameter than for large diameter. When a horizontal magnetic field was applied in the strength of 0.4T, the peak to valley [O<sub>i</sub>] was  $0.2 \times 10^{17}/\text{cm}^3$  for intermediate [O<sub>i</sub>] range and  $0.1 \times 10^{17}/\text{cm}^3$  for low [O<sub>i</sub>] one. This result showed that the peak to valley [O<sub>i</sub>] can be reduced only when mean [O<sub>i</sub>] is extremely lowered. An almost linear relation was obtained when the precipitated [O<sub>i</sub>] and initial [O<sub>i</sub>] were plotted. Therefore, the precipitation behavior of the O<sub>i</sub> maximum region is not much different from the other region. We considered that O<sub>i</sub> striations were not accompanied by crystal defects because O<sub>i</sub> precipitation didn't take a place heterogeneously.

---

[1] I. Fusegawa and H. Yamagishi:DRIP4 in England (1991)  
Paper No. P-15.

## DETECTION OF MICRODEFECTS NEAR SURFACE AND INSIDE OF ULTRA-THIN SEMICONDUCTOR CRYSTALS BY LIGHT SCATTERING AND INTERFERENCE METHODS

*Lu Taijing, Koichi Toyoda, Li Lian\*, Nobuhito Nango\*\* and Tomoya Ogawa\**

Laser Science Group, Institute of Physical and Chemical Research, Wako, 351-01 Japan

\*Department of Physics, Gakushuin University, Mejiro, Tokyo 171 Japan

\*\*Ratoc System Engineering Co., Ltd, Nishishinjuku 7-7-33, Tokyo, 160 Japan

By urgent requirement of ULSI technology, non-destructive detection of microdefects near surface of semiconductor crystals and inside of ultra-thin epitaxially grown layers on them become more and more important and necessary. Here, we report two new methods to detect the microdefects and to characterize interfaces in semiconductor crystals, particularly, in the region near the surfaces.

To detect the microdefects and/or microprecipitates located near or just under surfaces, Brewster angle illumination mode of laser light scattering tomography was developed, since the p-component of the illumination completely enters into the wafer and then makes scattering from the defects, where the other s-component reflected by the wafer surface deviates far from an objective lens.

Since the wavelength of incident light is adjusted to control the penetration depth of laser beam, three-dimensional distribution of the microdefects is detected even near the surface of a crystal. The microprecipitates in denuded zone of Si wafers

were clearly detected and characterized by Brewster angle illumination.

To detect the existence of interfaces and its imperfection we developed successfully a new method called new interference fringes method. Interference fringes generated by ultra-thin crystalline layers or thin films were observed by epitaxial layers, SIMOX wafers, and amorphous thin films grown on crystalline substrate, by which the perfection of film and interface between the film and substrate were characterized. It was found that the quality and visibility of the fringes were strongly depended upon the nature of the interfaces such as the microroughness of the interface, refractive indices difference at the interface and the quality of the layer. These fringes are well explained by interference between light reflected from a top surface of the layer and the light scattered from the interface inside of a crystal.

Therefore, the two new methods mentioned above are very effective for thin film crystal characterization and improvement of many processes of ULSI and epitaxial growth.

---

## DEVELOPMENT OF A NONDESTRUCTIVE BULK MICRO-DEFECT ANALYZER FOR SILICON WAFERS

*Kazuo Moriya, Hideo Wada and Katsuyuki Hirai*

R&D Center, Mitsui Mining & Smelting Co., Ltd.

1333-2, Haraichi, Ageo-shi Saitama 362 Japan

Non-destructive laser scattering tomography was developed for measuring the defects in Si wafers. With the conventional laser scattering tomography (destructive), we can obtain the scattering image near the surface of Si wafer, however it is very difficult to measure the subsurface defects, or the defects on the boundary in the ion implanted multilayer wafer.

In this new system, incident laser beam is introduced from the polished surface of the wafer and scattered light from defects is also detected from the surface side. To avoid the influence of surface reflection, the angle of incident laser beam is set near the Brewster angle, and observation angle is set near the perpendicular to the wafer.

Defect image in the wafer can be constructed by scanning the laser beam. The resolution and detectability of observation are almost even with conventional laser scattering tomography<sup>1</sup>. Observable samples range from as-grown, to

SOI(SIMOX etc.), to IG(intrinsic Gettering) treated, to epitaxial wafers.

To obtain the information of the defects in wafer, the following three kinds of measurement mode are applied:

- 1) horizontal cross section image for estimating subsurface defects;
- 2) horizontal layer by layer cross section images for measuring depth profile of defects;
- 3) vertical cross sectional image from the surface to 300 m in depth for estimating Denuded Zone of IG wafer.

By this method and measurement modes, the defects from the surface to the inside were nondestructively estimated, and the surface dust and subsurface defects were also distinguish.

<sup>1</sup>K. Moriya, K. Hirai, K. Kashima and Shin'Takasu, *Appl. Phys.* 66(1989)5267.

**CHARACTERISTICS OF A CRYSTAL TEMPERATURE IN A CZ-PULLER**  
**- COMPARISON BETWEEN SIMULATION AND EXPERIMENT -**  
*T. Fujiwara, S. Inami, S. Miyahara, S. Kobayashi, T. Kubo and H. Fujiwara*  
Advanced Technology Research Labs., Sumitomo Metal Ind. Ltd.  
1-8 Fuso-Cho, Amagasaki, 660 Japan

The authors already developed a mathematical model for a Czochralski crystal growth [1-3]. The model; (1) includes a global radiative heat exchange based on a diffuse-gray radiation and multiple reflection, (2) is a transient model, (3) treats the moving curvature of the crystal-melt interface by the Stefan condition, and (4) permits fast calculation of the view factors by employing an analytical method. The model was applied to 2 and 6"φ Si-CZ crystals. As a result of the calculations, the crystal temperature had the following characteristics: the crystal temperature was determined by the distance from the melt surface and almost independent of the length and the position in the crystal [2,3,4].

In order to investigate the characteristics, the experiments were performed with a 2"φ crystal under stationary condition in the following cases; (1) the crystal is dipped to the melt and the length of the crystal is changed by melting and (2) the crystal is

detached from the melt and the distance between the crystal and the melt surface is changed.

The calculations were also done for the both cases. The experiments and calculations coincided with each other very well for the both cases concerning the crystal temperature. This fact tells that under stationary condition the model can estimate the crystal temperature when the crystal is dipped and detached. Since the transient effect on the crystal temperature is considered to be small because of low pull-rate, the characteristics is also supported by the calculation.

- [1] S. Miyahara et.al; *J. Crystal Growth*, 99, 696(1990)
- [2] S. Miyahara et.al; *Semiconductor Silicon 1990*, 94(1990)
- [3] S. Miyahara et.al; *Computer Aided Innovation of New Materials*, 561(1991)
- [4] S. Shinoyama et.al; *Oyo Buturi*, 60, 766(1991)

IN-SITU OBSERVATION OF SURFACE TENSION DRIVEN FLOW  
ON THE MOLTEN SILICON SURFACE

Koichi Kakimoto, Masahito Watanabe, Minoru Eguchi and Taketoshi Hibiya  
Fundamental Research Laboratories, NEC Corporation  
34, Miyukigaoka, Tsukuba 305, Japan

Oxygen concentration which plays an important role in gettering of contaminants in CZ silicon single crystals may be affected by surface tension driven flow of molten silicon. However, we have not been able to identify main driving force of the flow (temperature gradient or impurity concentration gradient), whereas bulk flow is mainly attributed to temperature distribution in the melt. Therefore, if we can observe both the surface and bulk flows simultaneously, the origin of the surface tension driven flow can be extracted by subtracting the temperature gradient effect.

We have succeeded in the *in-situ* observation of surface tension driven flow using an X-ray radiography system. The simultaneously observed top views of the particle paths in the

melt and on the surface are shown in Figs. 1(a) and 1(b), respectively. We can identify that lower temperature melt exists at point A in Fig. 1(a), because the particle sinks at that point. If the surface tension driven flow is mainly attributed to the temperature gradient on the surface, the particle should move from point B to C in Fig. 1(b), because the thermocapillary force acts in the direction from higher to lower temperature area on the surface. However, as shown by an arrow in Fig. 1(b), the particle moved from C to B. Consequently, we can suggest that the origin of the surface tension driven flow in the CZ system is not mainly temperature gradient but impurity concentration gradient.

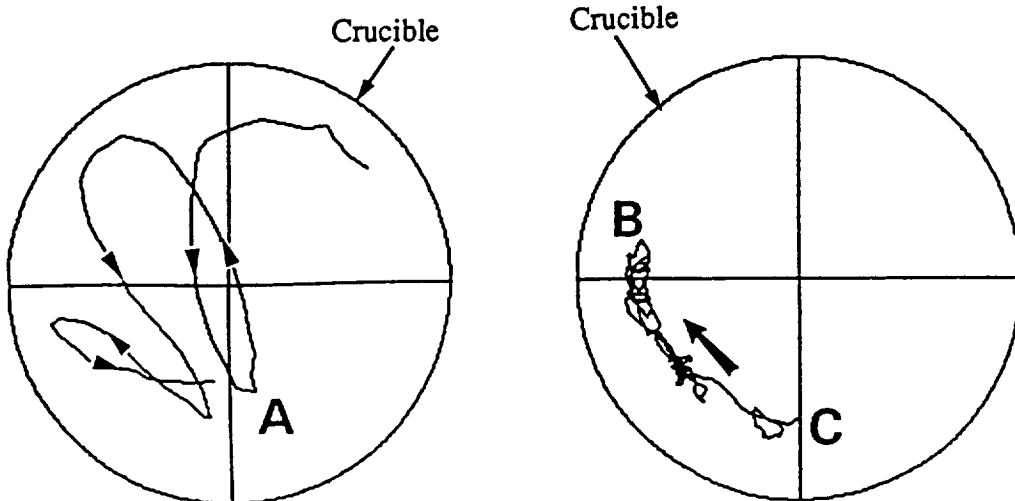


Figure 1. Top view of simultaneously observed particle paths: (a) in the bulk melt and (b) on the surface.

**IN-SITU OBSERVATION OF THE CONVECTION ON THE  
SURFACE OF SILICON MELT**

*H. Yamagishi, I. Fusegawa, E. Iino and K. Takano*  
Isobe R&D Center, Shin-Etsu Handotai Co., Ltd.  
Isobe 2-13-1, Annaka, Gunma, Japan

Convection on the surface of silicon melt in a quartz crucible has great effect on CZ silicon single crystallization. However, it is very difficult to visualize its motion. We developed directly observing method from the top of the surface and investigated the behavior of the motion of silicon melt.

In the experiments, we prepared two types of furnace. The one was cusp MCZ with a quartz crucible of 12" diameter. This furnace was equipped with cusp type magnetic field of 0.1T. The other one was HMCZ with a quartz crucible of 18" diameter. Its maximum magnetic field perpendicular to the growth axis could be applied in the strength of 0.43T. The melt surface without a silicon crystal was observed from the top of surface by a visicon or CCD camera with a silicon wafer mirror of 8" diameter. The image was recorded on video tapes and their motion was analyzed after an enhancing treatment by an image processor.

In the results, irregularly shaped black band images were observed on the silicon melt. They showed complicated motions according to the increasing of the crucible rotation rate. In the case of crucible rotation rate of 0rpm, those black bands seemed to flow towards one direction in the crucible. When the cusp magnetic field was applied and its strength was gradually increased, several black bands were observed but seemed to stand still. When a horizontal magnetic field was applied in the strength of 0.05T, their motion was almost

stopped. This band stretched in the direction perpendicular to the horizontal magnetic field. Those images couldn't be observed in the magnetic field over 0.2T. In the case of increasing the crucible rotation rate, those bands were split into many ones and formed irregularly shaped network both with or without magnetic fields. The temperature at the black band was about 10K lower than the other part by an IR radiation thermometer. The mean temperature of the melt decreased according to the increasing of the crucible rotation rate, which was in good agreement with the enhancement of black band images. In order to investigate the motion of the melt on the surface, granular poly silicon of about 1mm diameter was dropped into the melt and their motions were investigated by changing the crucible rotation rate. When the crucible rotation rate was 0.5rpm, a black band was stretched perpendicular to the horizontal magnetic field of 0.05T as mentioned before. The dropped granular poly silicons were attracted to the band and melted down within a few seconds. Its velocity was about 13.7mm/sec. When the crucible rotation was increased to 8rpm without the magnetic field, all the dropped granular poly silicons were attracted to the developed network. In the case of the applied magnetic field of 0.4T, no black band image was observed. The dropped granular poly silicon stood almost still. In conclusion, the motion of those black bands were related to the convection at the surface of silicon melt.

## GRAVITY EFFECT ON LIQUID PHASE EPITAXY OF SILICON

H. Kanai, S. Motoyama\*, M. Kimura, A. Tanaka and T. Sukegawa

Research Institute of Electronics, Shizuoka University,

Johoku 3-5-1, Hamamatsu 432, Japan

\*Advanced Technology Center, New Japan Radio Ltd.,

Kamifukuoka 2-1-1, Kamifukuoka 356, JAPAN

The principal effect of gravity on dissolution and growth from solution is the generation of convection as a result of density gradients [1,2]. In this paper, the effect of gravity on mass transport during growth will be discussed.

We have examined the epitaxial growth of silicon using horizontal substrate-solution-substrate "sandwich" system under isothermal condition. The epitaxial layers were grown on (111) oriented, n-type silicon substrate by ramp cooling using tin solvent. The epitaxial growth was initiated at 994°C and the temperature was lowered to 974°C at a constant cooling rate of 0.33°C/min. After the growth period, tin solution was removed from both substrates. In all these experiments, no initial melt supersaturation was used and the solution thickness was ranged from 2mm to 7mm. The epitaxial layer thickness of the upper and lower substrates was measured as a function of both solution thickness and growth time. The difference in layer thickness between both substrates provides important information about the gravity effect of crystal growth.

When the solution thickness was thin (2mm), there was little difference in the grown thickness of silicon layers between both substrates. This means normal diffusion-limited growth occurs. In the case of thick tin solution (7mm), however, growth on the upper substrate was larger than that on the lower substrate. Further the ratio of the layer thickness on the upper substrate to that on the lower one was increasing with increase of solution thickness. These results suggest that solute convection occurs in the solution and it enhances the solute transport upwards. The origin of convection is density gradient caused by growth process itself.

[1] T. Sukegawa, M. Kimura and A. Tanaka, *J. Crystal Growth*, 92 (1988) 46-52.

[2] M. Kimura, A. Tanaka and T. Sukegawa, *J. Crystal Growth*, 109 (1991) 181-185.

---

## GROWTH OF THIN CRYSTALLINE SILICON LAYERS FOR PHOTOVOLTAIC DEVICE USE

T.F. Ciszek, R. Burrows and T.H. Wang

National Renewable Energy Laboratory

Golden, Colorado, 80401 USA

The limited optical absorption of silicon necessitates a thickness on the order of 100 $\mu$ m or greater for efficient photovoltaic device operation. However, with suitable light trapping and back reflection designs, it may be possible to substantially reduce the physical thickness while maintaining an optical path length near 100 $\mu$ m. Thus there is current interest in thin-layer (10-50 $\mu$ m) silicon for this application. We have grown thin silicon layers on single-crystal silicon substrates from a variety

of metal solvents, both doping and non-doping. The growth temperature varied with the particular solvent but was always less than 1100°C. The conditions of growth, morphology, solvent incorporation characteristics, and electrical properties of the solution grown layers will be presented and discussed. Thin layers with suitable impurity characteristics and grain size for photovoltaic use were obtained.

## MISFIT DISLOCATION FORMATION AND INTERACTION IN Ge ON (001) Si

*M. Albrecht and H.P. Strunk*

Institut für Werkstoffwissenschaften VII, Universität Erlangen,  
Haberstr. 2, DW-8520 Erlangen, Germany

The heteroepitaxial system Ge on Si is currently of considerable technological interest; also, it serves as a appreciated model system to study the defect processes that may occur to accommodate misfit stresses.

Nucleation and formation of misfit dislocations may, in addition to the misfit stresses, be controlled by the actually occurring growth processes at the growing surface. Some work on these topics is available in the literature, mostly on specimens grown by molecular beam epitaxy (MBE). This growth procedure causes high supersaturations on the growing surface and thus growth occurs appreciably far off the thermodynamical equilibrium.

In order to avoid complications in the interpretation of observations we analyze the misfit dislocation structure in Ge grown by liquid phase epitaxy (Ge solution in Bi liquid) on (001) Si; the Bi is deposited at the saturation temperature of 800°C, i.e. the thermodynamical driving force is almost zero.

The Stranski-Krastanov growth mode is observed. First a pseudomorphic Ge layer of 1.2 nm thickness forms, then islands in the form of truncated tetrahedra, bounded by {111} planes grow pseudomorphically up to a height of 30 nm. It is only then, at a thickness of  $\approx$  25 times the one given by the mechanical equilibrium model, when the first dislocations appear. Transmission electron microscopy reveals, that in a first, obviously transient, stage dislocation segments are nucleated at the corners of the islands. A later stage consists of a combination of perfect and partial dislocations at the interface, whose configuration is analyzed. It can easiest be explained by the assumption of an initial glide process on a {110} plane. This assumption is corroborated by the observation that the misfit dislocations, once a continuous epilayer is formed, lie along <010> directions at the interface instead of <110> directions as expected when {111} glide is activated.

---

## INTRINSIC AND IMPURITY POINT DEFECT AGGREGATION IN SI CRYSTAL PULLING

*V.V. Voronkov*

Institute of Rare Metals, Moscow, Russia

The modern dislocation-free silicon crystals are known to contain grown-in microdefects of different types. At low enough growth rate  $V$  or high enough axial temperature gradient  $G$  the so called swirl defects (A- and B-swirls) are formed. These microdefects disappear at high enough ratio  $V/G$  and quite different type of microdefects appears instead. This feature is common for pure float zone silicon and for Czochralski-grown crystals containing large amount of oxygen impurity, though the concentration and size of microdefects are different for the two growth techniques. This phenomenon as well as many other peculiar features of microdefect formation can be explained by the model of selfinterstitials and vacancies coexisting in equilibrium relation at high temperature close to crystallization point. The annihilation, diffusion and thermal drift of the two kinds of intrinsic point defects result in survival of only one kind, the kind and concentration of the survived defects being the function of  $V/G$  only. The self-interstitials

survive if  $V/G$  is less than some threshold ratio, and vacancies otherwise. The subsequent aggregation of survived point defects can be strongly influenced by impurities, and still is critically dependent on the kind of intrinsic defects. Particularly for vacancy mode of crystal growth the vacancy aggregation in very pure crystals should proceed in the form of voids. However even small concentration of fast diffusing impurity or high enough concentration of slowly diffusing impurity (oxygen) would change the mode of aggregation to formation of joint aggregates of vacancies and impurity atoms. The aggregates (microdefects) should be in fact the small particles of impurity phase (dioxide for Czochralski grown crystals). The joint vacancy impurity aggregation is stimulated by the relatively low interface energy for silicon-particle boundary as compared to silicon-void boundary. The estimates of microdefect concentration both for selfinterstitial and vacancy modes of growth are in accordance with observed values.

## SESSION 1D

### RECENT ADVANCES IN BULK CRYSTAL GROWTH FROM THE VAPOUR

*E. Kaldis and M. Piechocka*

Laboratorium für Festkörperphysik ETH, CH-8093 Zürich, Switzerland

Large single crystals grown from the vapour are important as substrates of thin layers of compounds which melt incongruently, decompose or have phase transitions at temperatures lower than their melting point. A good candidate for substrates of IR-sensitive layers seems CdTe which grown from the vapour showed already many years ago superior physical properties. Also for compounds with very complex properties (chemical, physical or mechanical) for which it is very difficult to grow thin layers, vapour growth of large single crystals is very attractive. Good examples are  $\alpha$ -HgI<sub>2</sub>, a very promising material for x- and  $\gamma$ -ray room temperature detectors, as well as II-VI compounds. As we will discuss, all these crystals have been grown recently in unexpectedly large dimensions and masses (HgI<sub>2</sub>: EG&G and ETC > 500g; CdS: ELMA, Russia up to 1200g).

A systematic investigation of the vapour growth mechanism of large single crystals of  $\alpha$ -HgI<sub>2</sub> and their characterization has been performed recently in our laboratory and will be discussed in detail. Some of the highlights result from the high anisotropy of this layer structure, which leads to five times higher thermal conductivity in the a-planes than in the vertical direction (|| c-axis). With increasing size of the crystals the

heat conduction (strongly dependent on the orientation of the nucleus on the glass substrate) decreases and, therefore, the actual supersaturation on the vapour-solid interface also decreases. This effect leads to decrease of the supersaturation with time. However, we have found that for large crystals at zero growth rate still an apparent undercooling of  $\Delta T \approx 10$  K is necessary although no heat of condensation is evolved. This induced the idea that radiative heat transport takes place from the hot parts of the furnace to the growing crystal. Consideration of small heat conduction and radiative heating led to the theoretical estimation of the conditions for growth stop (A.A. Chernov et al.). This effect has been studied in detail also by numerical modeling of the thermal field of the furnace (A. Roux et al.). A consequence of the above growth stop is the need of a "continuous" increase of supersaturation in order to grow large crystals. With digital technology temperature controllers this is, however only stepwise possible. With steps  $\geq 0.1^\circ\text{C}$  striations are formed.  $0.01^\circ\text{C}$  steps are currently investigated. The formation of striations and other extended defects decrease the lifetime of holes and, therefore, the quality of the detectors. The characterization of such defects will be discussed.

---

### PURIFICATION AND GROWTH OF BaFBr AND IDENTIFICATION OF RADIATION-PRODUCED ELECTRON AND HOLE CENTERS IN OXYGEN-CONTAINING BaFBr

*Raymond S. Eachus, W. Gordon McDugle, Robert H.D. Nuttall and Myra T. Olm*

Corporate Research Laboratories, Eastman Kodak Company

Rochester, New York 14650-2021 USA

*F.K. Koschnick, Th. Hangleiter and J.-M. Spaeth*

University of Paderborn, Fachbereich Physik

Warburger Str. 100, 4790 Paderborn, Federal Republic of Germany

Oxide impurities are pervasive in alkali and alkaline earth halides and mediate radiation damage in these materials. Oxide may substitute for halide or may be incorporated interstitially and function as a coulomb trap for excitons or mobile H or V<sub>K</sub> centers. Oxide centers in BaFBr may be effectively removed by treating molten BaFBr with ultrapure Br<sub>2</sub> gas and selectively reintroduced by doping with anhydrous BaO. The O<sup>+</sup> center formed by the reaction of O<sup>2-</sup> with mobile Br<sub>2</sub>-V<sub>K</sub> centers in x-irradiated BaFBr is long lived at room temperature and has been detected by EPR below 30 K and unambiguously

identified using Ba<sup>17</sup>O. The formation of F(Br<sup>-</sup>) centers at charge compensating bromide ion vacancies accompanies the radiation-induced production of O<sup>+</sup>. BaFBr is a wide band gap solid (8.7 eV). The oxide impurity introduces a mid-gap state having a new optical absorption at about 250 nm. Irradiation with uv light photoionizes O<sup>2-</sup> and the charge compensating Br<sup>-</sup> vacancies trap the photoelectrons producing stable F(Br<sup>-</sup>) centers. An ENDOR study of Bridgman grown doped single crystals has further identified the O<sup>+</sup> center as O<sub>F</sub><sup>-</sup>, an oxide anion substituted at a fluoride site.

THE GROWTH OF Ag DOPED  $PbBr_2$  CRYSTALS USING COUPLED  
VIBRATIONAL STIRRING

R.C. De Mattei and R.S. Feigelson

Center for Materials Research, 105 McCullough Building  
Stanford University, Stanford, CA 94305-4045

The Coupled Vibrational Stirring (CVS) technique was developed for stirring melts during crystal growth in sealed crucibles; particularly those used in the vertical Bridgman and gradient freeze techniques<sup>[1]</sup>. The stirring is accomplished by moving the vertical axis of the crucible around a circular path without rotating the crucible and mixing in the melt is accomplished in much shorter times than is possible with other techniques such as accelerated crucible rotation (ACRT). CVS was recently applied to the growth of lead bromide doped with silver.

Lead bromide is an potentially important material for applications in acousto-optic and opto-electronic devices.<sup>[2-4]</sup>  $PbBr_2$  possesses a number of favorable acousto-optic properties including optical transmission range, photo-elastic coefficient, acousto-optic figure of merit, acoustic velocity and acoustic attenuation. Its mechanical properties allow lead bromide to be easily fabricated into devices. On the negative side,  $PbBr_2$  single crystals are difficult to grow due to cracking caused by a phase transition below the melting point. The addition of dopants such as silver can eliminate the cracking due to this transition, but such dopants can lead to optical inhomogeneity due to inhomogeneous incorporation of the dopant. These dopant inhomogeneities can arise due thermal-solutal convection.

CVS with its strong mixing action can provide well stirred melts with uniform dopant concentrations which will eliminate any effects from thermal-solutal convection. In systems with a distribution coefficient of less than 1, the dopant concentration will increase along the length of the crystal. However, with CVS, this will be a smooth and predictable increase and, in the case of lead bromide, will yield useful optical material.

Results from the growth of Ag doped  $PbBr_2$  crystals will be presented comparing the effect of CVS on the temperature gradient during growth, the growth rate, the crystal quality and the dopant distribution to those obtained without CVS. Comparisons will be made with the expected results.

1. W.-S. Liu, M.F. Wolf, D. Elwell and R.S. Feigelson, *J. Crystal Growth*, 82 (1987) 589.
2. N.B. Singh and M.E. Glicksman, *Mat. Letters*, 5 (1987) 453.
3. N.B. Singh, M. Gottlieb, R. Hopkins and R. Mazelsky, *J. Crystal Growth*, 87 (1988) 113.
4. N.B. Singh et al., ACCG-8, Vail, CO 1990.

This work was supported by the National Science Foundation (DMR-9008399-A1) and the NSF-MRL program.

PRECISE MEASUREMENTS OF THE MASS TRANSPORT RATE OF MERCURIC  
IODIDE IN THE VAPOUR PHASE

M. Piechotka and E. Kaldis

Laboratorium für Festkörperphysik, ETH Hönggerberg  
CH-8093 Zurich, Switzerland.

Precise measurements of the transport rate are important in vapour growth of crystals for several reasons: (a) to check the theoretical models of the vapour transport, (b) to assess possible convective contributions, especially in the systems, in which they can be neither predicted nor excluded by the theory, (c) to evaluate the kinetic behaviour of various starting materials for crystal growth. All the methods used up to now suffered from an unsatisfactory accuracy and a low time resolution (measurements of transients not possible). The new method, which we have developed, does not have these disadvantages. In this method, the velocity of an evaporating interface is measured with a high resolution linear CCD array. The continuous monitoring of the interface allows for quick *in situ* measurements of the changes in the transport rate upon temperature so that a complete relationship between the flux and undercooling can be automatically measured for a given material within a couple of days.

Based on this method, an apparatus for a microgravity experiment aboard the Space Shuttle has been built by Oerlikon-Contraves AG, Switzerland. The following performance characteristics have been achieved: (a) temperature control of 1450.0:3 K in all of the four separately controlled heating zones, (b) resolution of the linear CCD array  $\pm 1\mu m$  within the view field of 15 mm. Measurements with mercuric iodide showed a strong dependence of the transport rate on the purity and stoichiometry of the material (differences up to order of magnitude). Small differences in the transport rate also occur upon changing the position of the ampoule with respect to the gravity vector indicating for the first time, that even in the systems under low pressure (estimated below 1 Torr) convection might contribute to the overall mass transport rate. These results will be discussed in detail.

**THERMO-CONVECTIVE EFFECTS DURING VAPOR-PHASE GROWTH OF  
MERCUROUS CHLORIDE CRYSTALS**  
*M.E. Glicksman, C.T. Kim, O.C. Jones and I.T. Lin*  
Materials Science and Engineering  
Rensselaer Polytechnic Institute, Troy, New York 12180

Mercurous chloride ( $Hg_2Cl_2$ ) has gained considerable interest as an acousto-optic material, - one used as model system for the study of thermo-convective effects during vapor-crystal growth. Thermal convection occurs because single crystals of mercurous chloride are grown by PVT (physical vapor transport) in closed ampoules in a two-zone furnace. The convection flow pattern, caused by the temperature gradients, must be

fully understood for optimal design and improvement of the crystal growth reactors. In this study, a reliable and accurate LDV (laser Doppler velocimetry) technique is employed to obtain detailed information on the vapor-phase fluid dynamics during crystal growth. The relation between the fluid dynamics and crystal growth kinetics will also be discussed.

---

**MORPHOLOGY AND CHARACTERIZATION OF SOLUTION GROWN  
MERCURIC IODIDE CRYSTALS**

*K. Baskar and P. Ramasamy*  
Crystal Growth Centre, Anna University, Madras, India

Mercuric iodide is a wide bandgap semiconductor having high atomic number. These properties enable the material to operate at room temperature as a nuclear detector. The single crystals of mercuric iodide could be grown from solution and vapour techniques. In the present investigation the authors have grown single crystals of mercuric iodide from solution using a protic-aprotic mixed system; dimethyle sulphoxide and water as solvent. Plate like, prismatic and octahedral crystals are obtained depending on the weight fractions of  $DMSO-H_2O$ . The Hartman's theory of periodic bond chain is applied to understand the morphology. The existence of geometrical resemblance between  $5H_2O$  and  $HgI_4$  tetrahedra and its influence over the morphology are discussed.

The photoconductivity measurements over the wavelength range 400 - 700nm under d.c voltage are carried out. The high energy region 3.09 to 2.34eV, peak region 2.34 to 2.07eV and weakly absorbed region 2.07 to 1.77eV independent of applied voltage are explained by the generation and trapping of charge carriers. The photoconductivity and photoluminescence have revealed the trapping of impurities in crystal lattice of mercuric iodide during crystallisation from solution. The stoichiometry of mercuric iodide crystals is estimated by wet chemical analysis. The chemical etching shows that dislocation density of mercuric iodide crystals varies from  $10^3 - 10^7 cm^2$ . The hardness, anisotropy of hardness and creeping in mercuric iodide crystals are explained in terms of bond strengths.

## CHARACTERIZATION OF TRAPPING LEVELS IN SOLUTION GROWN AND PCG MERCURIC IODIDE SINGLE CRYSTALS

T. Pal, S.L. Sharma, H.N. Acharya  
Department of Physics, I.I.T. Kharagpur-721302, India

Red mercuric iodide is one of the most suitable detector materials for x- and  $\gamma$ -ray spectroscopy. The performance of this material as a detector is, however, limited by carrier trapping. Efforts are on to characterize the concerned trapping levels by various optoelectronic measurements. Being the most simple, thermally stimulated current (TSC) investigations are preferred to other measurements. Recently, Mohammed-Brahim [1] carried out TSC measurements on  $\alpha$ -HgI<sub>2</sub> crystals and concluded that the peak at 170K holds a direct bond with the improvement in the performance of  $\alpha$ -HgI<sub>2</sub> detectors. Present work aims at determining the trapping levels in  $\alpha$ -HgI<sub>2</sub> crystals grown in our laboratory from (a) DMSO-MeOH - HgI<sub>2</sub> solution, (b) Tetrahydrofuran - HgI<sub>2</sub> solution and (c) polymer controlled growth (PCG) in vapour phase. Commercial grade  $\alpha$ -HgI<sub>2</sub> was purified through-repeated sublimation to get the starting materials in each crystal growing process. The band gap energy, obtained from photoconductivity and optical absorption studies, is 2.15 eV for PCG crystals and 2.13 eV for solution grown crystals. TSC spectra were recorded for all the three types of crystals. The solution grown crystals exhibit six

to eight peaks with no highly dominating peak. The PCG crystals, however, show a very strong peak at 170K along with three other weak peaks. Clearly, PCG crystals are of much superior quality than the solution grown crystals for detector fabrication. Our values of energies, cross-sections and the densities of the trapping levels agree well with those of Mohammed-Brahim [1] and Whited et al. [2]. Relative low peak height at 170K for solution grown crystals may be due to pre-treatments (cleaving, etching, polishing etc.) of these crystals. The peaks at 253K and 271 are similar to the observation of Mohammed-Brahim [1] which may be due to the lack of iodine. Efforts are being made to further investigate the effects of various parameters on the trapping levels. Photon stimulated current (PSC) studies are also being carried out on these crystals to confirm the PSC results.

[1] T. Mohammed-Brahim et al. *Phys. Stat. Sol.*(a) 79 (1983) 71.  
[2] R.C. Whited et al. *IEEE Trans. Nucl. Sci.* NS-24 (1977) 165.

## CHARACTERIZATION OF MODIFIED PYROCHLORES CsMFeF<sub>6</sub> (M=Mn,Co,Zn)

K.S. Raju and B.M. Wanklyn\*  
Department of Crystallography and Biophysics  
University of Madras, Guindy Campus, Madras 600 025, India  
\*Clarendon Laboratory, University of Oxford, Oxford, England

The flux grown single crystals of pyrochlores (CsMnFeF<sub>6</sub>, CsCoFeF<sub>6</sub>, CsZnFeF<sub>6</sub>) have been characterized employing powder x-ray diffraction, Infra-red absorption, Energy dispersive x-ray analysis (EDAX) studies reveal that and Mossbauer studies. X-ray diffraction CsMnFeF<sub>6</sub>, CsCoFeF<sub>6</sub> and CsZnFeF<sub>6</sub> are iso-structural, belonging to face centred cubic, having lattice parameters,  $a$ , 10.542(3), 10.429(4) and 10.409(7) Å respectively. This variation in cell dimensions indicates that these mainly occur due to atomic size factor (Mn=0.91 Å, Co=0.82 Å and Zn=0.83 Å). The characteristic absorption peaks relating to (FeF<sub>6</sub>)<sup>3-</sup> are evidenced by the presence of peaks at

253, 374 and around 500 cm<sup>-1</sup> in the IR absorption spectra of CsMnFeF<sub>6</sub>, CsCoFeF<sub>6</sub> and CsZnFeF<sub>6</sub> samples. The EDAX studies establish the presence of the elemental constituents (Cs, Mn, Co, Zn, Fe) in their respective samples and the atomic weight percentages of Cs:Mn:Fe, Cs:Co:Fe and Cs:Zn:Fe are found to be approximately 1:1:1. The room temperature Mossbauer spectra of powdered samples exhibit almost the same isomer and quadrupole shifts meaning almost identical environment for the iron state and that iron ions are in high-spin ferric state, in paramagnetic phase.

## GROWTH OF SOME V-VI-VII GROUP COMPOUNDS FROM VAPOUR

*R. Ganesh, D. Arivuoli and P. Ramasamy*

Crystal Growth Centre, Anna University, Madras 600 025 India

The discovery of ferroelectricity in SbSI has stimulated large interest. Though there are many reports on SbSI and its type compounds, less attention has been devoted to the growth and characterisation of oxyhalides of antimony, bismuth and arsenic. Crystals of SbOI, BiOS, BiOCl and AsOI have been successfully grown from vapour. These crystals show platelet morphology at low supersaturation. The SbOI crystals belong to the very rare class of pure ferroelastic crystals, while the BiOCl and BiOI crystalline platelets are strongly anisotropic semiconductors with bandgap 3.455 eV and 1.89 eV respectively. The BiOCl platelets are highly transparent while BiOI platelets exhibit mirror like faces with metallic lustre. The interesting morphological features of these crystals are studied by optical and scanning electron microscopy. The layered structure observed plays an important role in deciding their characteristic physical properties. The complex growth spiral observed throws light on the growth mechanism by screw dislocation. The optical interferogram studies reveal that the steps

are not monoatomic but are multiples of Burger's vector. Large size (25mm x 15mm x 8mm crystals of BiSeI have been grown from vapour. The platelets usually show (110) faces. Chemical etchants revealed pyramidal etch pits and the shape of the etch pits depends on the etchant used. Surface features have been analysed using scanning electron microscopy.

Dielectric studies of BiSeI showed a new phase transition at 410 K. The crystals have been further characterised by XPS, DSC and TGA. From the XPS analysis the chemical shifts of the constituent elements in all the compounds have been calculated by estimating the percentage ionicity of the chemical bonds using the Pauling's electronegativity data. From the DSC data, the change of enthalpies of  $\Delta H$  of the observed phase transitions have been calculated. The variation of specific heat with temperature is discussed. The dissociation schemes of the compounds have been proposed using the TGA data.

---

## AUTOMATED PULLING FROM THE MELT - THE EFFECTIVE METHOD OF GROWING LARGE ALKALI HALIDE SINGLE CRYSTALS FOR OPTICAL AND SCINTILLATION APPLICATIONS

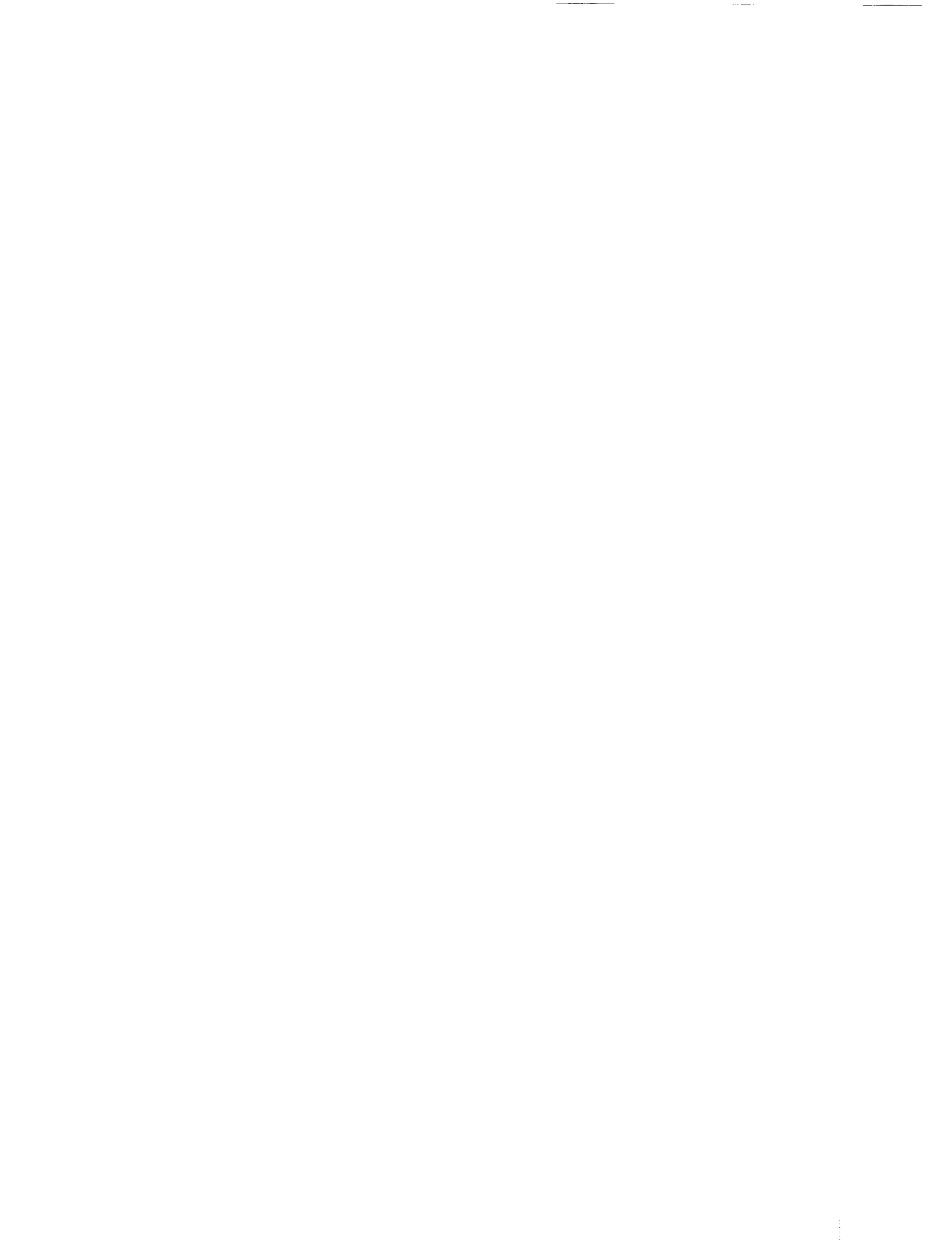
*L.G. Eidelman, V.I. Goriletsky, V.G. Protsenko, A.V. Radkevich and V.V. Trofimenko*

Institute for Single Crystals, Kharkov, Ukraine

Successful development of the automated pulling method (Crystal Res. and Technol., 20 (1985) 167) made it possible to pull from melt large alkali halide single crystals up to 600 mm in diameter and over 400 kg. Previously such size crystals could be grown only by Stockbarger technique which has some disadvantages as compared to the pulling method. Automation of the method under consideration is ensured by the heater temperature control in response to the signal from the electric contact melt-level sensor. In fact this sensor allows to measure either the deviation of the mass growth rate from a preset value or the area of the crystal cross section (i.e. the crystal diameter) on the level of the melt surface. In the former case with a constant pulling rate slight deviations of the growing crystal diameter from a preset value can take place due to the changes in the solid-liquid interface shape. In the latter case better stability of the growing crystal diameter can be achieved, precise crystal diameter values being obtained by means of periodic fast lifting of the growing crystal on a certain small

distance (e.g. 1 mm) with subsequent measurement of the corresponding value of the melt level drop.

The developed growth furnace allows to perform two types of growth: with simultaneous feeding of starting material into the melt (the crystal diameter being maximum 500 mm) and without feeding (maximum dia. - 600 mm). In terms of the impurity distribution in the growing crystal the first type is similar to zone melting, therefore a uniform distribution of the dopant in this type can be easily achieved using the methods applied for zone melting [this is especially important for large scintillators made of doped crystals like NaI(Tl), CsI(Tl) and CsI(Na)]. The second type allows to carry out an additional purification of raw material directly prior to the growth process i.e. to promote an intensive evaporation of impurities from large area of the superheated melt surface by pumping out the growth furnace (with this method used, highly IR transparent large optical KCl single crystals have been obtained).



## SESSION 2

### CONVECTIVE INSTABILITIES IN MELT GROWTH CONFIGURATIONS

*Georg Müller*

Institut für Werkstoffwissenschaften, Universität Erlangen-Nürnberg (FRG)

One of the most important goals in the growth of bulk crystals is to achieve uniform material properties (both electronic, optical and mechanical), i.e. uniform composition. Stable growth conditions especially with respect to the growth rate are an unalterable prerequisite for that. In melt growth this requirement means a steady heat transport to and away from the interface, as the growth rate is generally controlled by heat transfer.

From the above we can deduce that any convective instability in melt growth configurations is deleterious for the growth of semiconductor crystals, oxides, etc. It creates so-called "growth-striations," a term which is generally used for any compositional fluctuations of a crystal in the microscale.

A profound knowledge of the origins of convective instability in the various melt growth configurations is necessary, in order to avoid its occurrence during the growth process.

In this work we study the hydrodynamic phenomena causing convective instability and its relation to the formation of striations by experimental means and theoretical analysis of the moving growth interface.

The evidence of convective instability in melt growth configurations is treated in more detail. Different methods for the

detection of unsteady flows are discussed and illustrated by various examples.

Visual observation of flow instabilities is possible in transparent melts and by X-rays with intransparent ones. The analysis of convection-induced temperature fluctuations in the melt gives special insight into turbulent flow states.

A new method is presented which allows for the detection of unsteady flows in semiconductor and metal melts by means of a magnetohydrodynamic effect. A static magnetic field of certain strength is used to induce a weak magnetic field being strongly correlated to the flow. This induced field is detected by magnetometer probes outside the melt.

Finally it is discussed how the occurrence of convective instability can be avoided in the various melt growth configurations. The dependance of the transition to flow instability from geometrical and thermal boundary conditions is studied experimentally and by numerical modelling, as well as the influence of gravity. The most extensive discussion is devoted to the application of static magnetic fields to damp unsteady flows in electrically conducting melts. Examples of experimental results and numerical modelling are given for the most important melt growth configurations - Bridgman, Zone Melting, Czochralski, LEC and floating zone techniques.



## SESSION 2A

### IN SITU OBSERVATION OF INTERFACE KINETICS AND FLOW DYNAMICS

Katsuo Tsukamoto

Faculty of Science, Tohoku University  
Aramaki Aoba, Sendai 980, Japan

Since crystal growth/dissolution involves many unknown processes, it is necessary to investigate from different aspects and in different environments. The tool which we have chosen for the experimental investigation is *in situ* observation by optical methods. This is because the solution and crystals are mostly transparent to visible light.

Among varieties of interesting topics, we have first selected the kinetics of growth steps on crystals grown in aqueous solution. The monomolecular growth steps can be visualized by phase sensitive microscopy. The growth rate from individual growth hillocks can be measured in less than ten seconds by means of interferometry. It was found that the activity of growth hillocks depends on the solution flow speed, supersaturation and the character of dislocations. The growth and dissolution surfaces of dislocation-free  $\text{Ba}(\text{NO}_3)_2$  crystals were also investigated. There are two types of nucleation, one of which is probably due to microdefects generated from tiny crystals or impurities which are transported from the bulk solution to the crystal surface. This nucleation takes place at very low supersaturation and is largely influenced by flow dynamics.

So far it was assumed that the environment is time stationary when the crystal growth mechanism is analyzed. However, the environment is always fluctuating, mainly because of con-

vection. In the case of solution growth the solutal convection plays a more dominant role than thermal convection. In order to understand the effect of flow on the surface kinetics, the flow dynamics around a crystal was investigated by interferometry or by other *in situ* methods. It was found that the fluctuation of solutal convection is responsible for the growth rate fluctuation even in the regime of surface-controlled kinetics.

In order to obtain an extreme condition in which convection could be suppressed, and thus reducing the fluctuation in environment, *in situ* observation of crystal growth in microgravity was performed using a Japanese TR-1A rocket. Because of an accidentally introduced small gas bubble (1.5mm, diameter), Marangoni convection developed around the bubble which was situated very close to the seed crystal. The interaction between the concentration field around the crystal and the Marangoni convection was first visualized, leading to instability in the Marangoni convection. It was also found that the growth rate in microgravity in the presence of a small gas bubble is very close to the growth rate in gravity and is much larger than the value when diffusion controlled growth is assumed.

PRECEDING PAGE BLANK NOT FILMED

## NON-EQUILIBRIUM PHASE TRANSFORMATIONS IN TWO COMPONENT SYSTEMS

*Kenneth A. Jackson*

University of Arizona

*George H. Gilmer*

AT&T Bell Laboratories

*Dmitri E. Temkin*

Research Institute of Ferrous Metallurgy, Moscow

We have been performing computer simulations of the growth process in two component systems. In our model, which is formally in the spin-1 Ising universality class, an interface moves though an array containing a random distribution of two different species of atom. Transition probabilities at the interface are based on bond energies which are calculated from the thermodynamic properties of the system. The growth process is simulated using Monte Carlo methods in which the atoms jump onto and off the crystal depending on their local bond configuration. The atoms in the liquid can also interchange sites.

When the diffusion jump rate is fast compared to the growth rate, we find that the phase transformation is governed by the difference between the chemical potentials of the components in the two phases, so that, as the system approaches equilibrium its behavior is described by classical thermodynamics. However, in the diffusionless limit, when the atoms can jump on and off the crystal but cannot interchange positions, we find that equilibrium occurs when the total free energies of the two phases are equal. In this limit, there is no segregation associated with the passage of the interface. We find that the  $k$ -value in the transition between these two regimes depends on the dimensionless parameter  $av^2/Dv^+$ , where  $a$  is the interatomic distance,  $v$  is the growth rate,  $D$  is

the diffusion coefficient, and  $v^+$  is the rate at which atoms join the crystal at a repeatable step site. This dependence of the  $k$ -value in the transition region was previously reported by D.E. Temkin [1].

We have been able to reproduce the spatial distribution of bismuth atoms in silicon which has been observed following laser melting of bismuth-ion-implanted silicon [2]. In these experiments, the interfacial  $k$ -value was two orders of magnitude greater than the equilibrium  $k$ -value. The velocity dependence of the  $k$ -value found in these experiments is in accord with the velocity dependence described above which we found in our simulations. These simulations permit us to explore a regime, which has previously been identified experimentally, in which the crystallization behavior of a two component system is significantly different from classical behavior based on equilibrium thermodynamics.

1. D.E. Temkin, *Sov. Phys. - Crystallography*, **17** (1972) 405.
2. P. Baeri, J.M. Poate, S.U. Campisano, G. Foti, E. Rimini and A.G. Cullis, *Appl. Phys. Lett.* **37** (1980) 912.
3. C.W. White, S.R. Wilson, B.R. Appleton and F.W. Young, Jr., *J. Appl. Phys.* **51** (1980) 738.

# A NEW MODEL OF EFFECTIVE SEGREGATION COEFFICIENT\*

A.G. Ostrogorsky

Columbia University, New York, N.Y. 10027, USA

G. Müller

Werkstoffwissenschaften VI, Universität Erlangen-Nürnberg, Germany

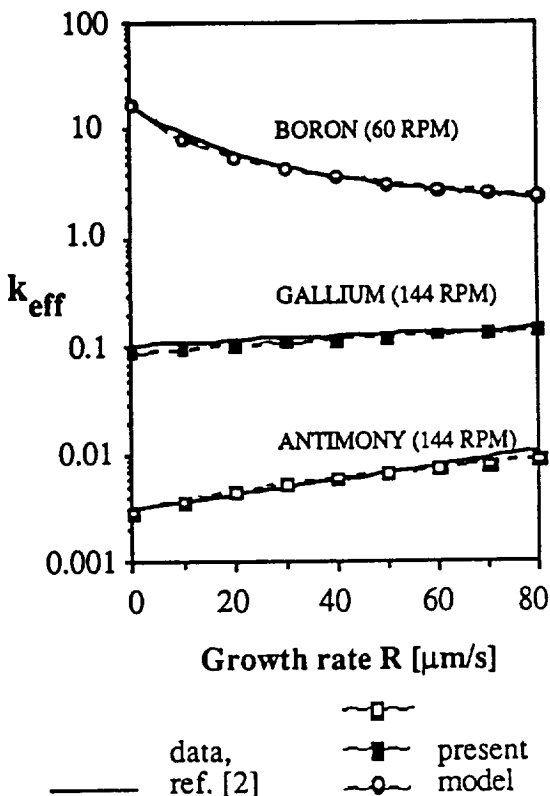
A model of the effective segregation coefficient  $k_{\text{eff}}$  accounting for convective mass transport at the growth interface is presented. The model provides a simple relation between the effective segregation coefficient  $k_{\text{eff}}$  and: i) the real physical thickness of the solute layer  $\delta_D$ , ii) the convective velocity  $V_D$  relevant for removing the solute from the region of the advancing interface, iii) material parameters and iv) growth rate  $R$ .

Using the established analytical results of boundary layer analysis,  $\delta_D$  and  $V_D$  were determined for several important crystal growth configurations. For crystal growth by the Czochralski method, a good agreement is obtained between the model and the data in the literature. Without any parameter adjustment, the model predictions agree well with the data obtained by Burton et al. [1] in the classical experiments used to fit the Burton, Prim and Slichter (BPS) model by the trial and error procedure. The agreement is even better with the data obtained by Bridgers [2], both for  $k < 1$  and  $k > 1$ , (see the fig.)

The model provides a criterion for the maximum convective velocity in the solute layer, which allows diffusion-controlled segregation. The criterion is used to explain some of the segregation data obtained in microgravity, which were not well understood in terms of the existing models.

[1] J.A. Burton, E.D. Kolb, W.P. Slichter and J.D. Struthers, *J. Chemical Physics* 21 (1953) 1991-1996.  
 [2] H.E. Bridgers, *J. Applied Physics* 27, (1956) 686.

\*Supported by the Alexander von Humboldt Foundation.



## RELEVANCE OF SURFACE ROUGHENING AND MELTING FOR CRYSTAL GROWTH

*J.P. van der Eerden*

Laboratory of Interfaces and Thermodynamics  
Padualaan 8, 3584CH Utrecht, The Netherlands

In the last several years a lot of progress has been made in our fundamental understanding of surface roughening and surface melting. It has been established that surface roughening is determined by the vanishing of the edge free energy above the roughening temperature and surface melting by the vanishing of the surface shear modulus above the surface melting temperature.

By now there exist a large number of atomic models in which these phenomena can be demonstrated and calculated. Surface roughening has been introduced in the Kossel model, which is (as a simple cubic lattice model with nearest neighbor interactions only) quite inaccurate for the description of a real crystal. Surface melting has been established for a Lennard-Jones crystal model, which is a reasonable model for noble gas crystals and other crystals with effectively spherical building units (e.g.  $C\ Cl_4$  and  $C_{60}$  above their critical temperature for free molecular rotation in the crystal). A problem with the L-J model is that surface roughening and surface melting occur as coupled transitions.

Also in experimental systems phenomena related to surface phase transitions have been observed in many cases. Just below the melting point surface disorder has been observed on metal surfaces by ion or small angle X-ray scattering and enhanced surface mobility by inelastic neutron scattering. Such experiments are interpreted as indications for surface melting.

Morphological observations are used to detect surface roughening.

In my contribution I will show that these fundamental notions do have impact on practical crystal growth situations. At low temperatures pure crystals are faceted, grow slowly, are very sensitive to traces of impurities (growth is easily blocked and macrosteps formed) and gradients in the mother phase (hydrodynamics and temperature gradients) have relatively little influence on the growth mode.

Surface roughening changes e.g. the growth form (decrease of anisotropy), the growth rate (increase of kinetic coefficients), the sensitivity for impurities (smaller decrease in growth rate but more incorporation) and the morphological instability (easier transition to dendritic and cellular growth modes).

If surface melting occurs at temperatures above the roughening point then it enhances the effects of roughening. If it occurs below the proper roughening point then it may induce surface roughening. In such a case roughening may appear as a first order phase transition and the roughening effects mentioned above occur in a narrow temperature interval. And if surface melting does not induce surface roughening then still the kinetic coefficients are expected to increase considerably and the blocking effects of some trace impurities will decrease.

---

## KINETICAL ROUGHENING AND ROUGHENING TRANSITION IN ODD-NUMBERED NORMAL ALKANES

*Xiang-Yang Liu and P. Bennema*

Laboratory of Solid State Chemistry University of Nijmegen  
The Netherlands

A way to estimate the critical supersaturation  $\beta^c$  of the kinetical roughening in connection with thermal roughening will be described. To that extent, the step free energy and its critical behaviour around the roughening transition for the {110} faces of odd-numbered paraffin crystals will be explored. We have to consider the shape of the two dimensional nuclei. The relation between  $\beta^c$  and  $\gamma (= \gamma kT/l)$  is adapted with a shape and anisotropy factor for the interaction of the building units. This relation is applied to the growth of {110} faces of  $n-C_{21}H_{44}$  and other  $n$ -paraffins growing from  $\eta$ -hexane solutions. In doing so, a newly found "rough-flat-rough" transition and besides the bulk supersaturation, also the mass and heat transfer are taken into account. Thus the edge free energy  $\gamma$ , the order parameter, is deduced from the experimental results. We find that  $\gamma$  does not depend on the tempera-

ture  $T$  when  $T < T^r$  ( $T^r$  the roughening transition temperature), and suddenly vanishes at  $T^r$  and that the edge free energies, which are almost equal to the edge energies, give values which are four to five times smaller than expected from the equivalent wetting condition. These results suggest that the steps on the surfaces are very straight. The {110} faces at the critical point behave much more similar to a first order phase transition than to the infinite order roughening transition, suggesting a coupling between roughening and surface melting. We find that ordering of fluid units at the interface plays a substantial role in the interaction between solid and fluid phase.

Finally, the relation between the critical supersaturation  $\beta^c$  turns out, in agreement with our experimental results, to be weakly dependent on the carbon number  $n$  for large  $n$ .

## COMPUTER SIMULATION OF MOLECULAR LIQUIDS ON CRYSTAL SURFACES

T.A. Cherepanova and A.V. Stekolnikov

Centre of Microelectronics, Latvian Academy of Sciences  
19 Turgenev Street, Riga, Latvian Republic

We present the survey of statistical mechanical theories of the surface phenomena such as wetting and pre-wetting, phase transitions in liquids on crystal surfaces, in absorbed films, particularly, in surfactant films. These can play an essential role for the problems of crystal morphology and kinetics of crystal growth. We shall focus our attention on molecular liquids (from dimer to chain molecules) to understand, among others, the influence of chain-molecule flexibility on the effects under consideration. Another important point is the relief of crystal faces to atomic scale and the peculiarity of the above mentioned phenomena on such surfaces. The long and short-range order parameter functions at the crystal-vapour and crystal-liquid interfaces will be analyzed, which give a variety of ordered structures.

Crystal-vapour interface, (i) In-plane translational ordering (herringbone structure, etc.); (ii) orientational freezing of molecules end-grafted to the crystal surface; (iii) localized-mobile monolayer transitions.

Crystal-melt interface, (i) Complete wetting by nematic phase, so that the thickness of nematic film between the crystal and isotropic liquid increases logarithmically when the temperature tends to the bulk nematic-isotropic liquid transition temperature, (ii) Incomplete wetting by smectic phase. Only the finite number of smectic molecular layers appears on the crystal surface when the temperature tends to the bulk isotropic liquid-smectic phase transition temperature. Layering transitions are discontinuous. (iii) Orientational effect induced by corrugation of crystal surfaces on the adjacent liquid layers and equivalent wetting conditions.

Surfactants at the crystal-vapour and crystal-liquid interfaces. The formation of surfactant films even in the case of extremely low surfactant concentration in bulk phases. (i) Conformational and orientational transitions in liquid surfactant films. (ii) Layering transitions in surfactant films and formation of multilayer patterns. (iii) The role of crystal surface as a heterogeneous catalisator of amphiphilic aggregation.

---

## MAPPING OF CRYSTAL GROWTH ONTO THE 6-VERTEX MODEL: GROWTH MODE AND SURFACE ROUGHNESS

Miroslav Kotrla and Andrea C. Levi

Università di Genova, Dipartimento di Fisica, Viale Dodecaneso 33  
16146 Genova, Italy

Two models of crystal growth are developed and solved using the 6-vertex model of statistical mechanics, onto which two different mappings are considered. One mapping establishes a direct correspondence between surface steps and the lines occurring in the *line representation* of the vertex model; the other mapping is that of van Beijeren. These two mappings correspond to two different physical situations: a vicinal surface near the (100) surface of a simple cubic crystal, and the (100) surface of a bcc crystal (together with its vicinal surfaces) respectively. Master equations are written for finite-size versions of the models, and solved either analytically (for extremely small sizes), or by Monte Carlo simulation, using Glauber's rules for the probabilities of the various processes relevant for growth, evaporation and diffusion.

In the case of the first model, the approach of finite-size samples to the thermodynamic limit is accompanied by a characteristic change of the growth rate, which approaches its  $N \rightarrow \infty$  value as  $N^2$ : the significance of this behaviour is discussed.

The second model, on the other hand, depends explicitly on temperature  $T$  and supersaturation  $\Delta\mu$ : as a function of these parameters, the growth mode changes. Moreover, the structure of the surface also depends on  $T$  and  $\Delta\mu$ . It is shown that, contrary to the equilibrium case, the surface is rough at all temperatures. However the nature of the roughness also changes: in particular, at high temperatures, the roughness is logarithmic if  $\Delta\mu$  is small, but a cross over takes place to a power-law behaviour when  $\Delta\mu$  increases. The significance of these different kinds of roughness is discussed in terms of stochastic differential equations.



## SESSION 2B

### GROWTH OF LARGE SIZE KNbO<sub>3</sub> CRYSTALS AND EPITAXIAL LAYERS OF KTa<sub>1-x</sub>Nb<sub>x</sub>O<sub>3</sub>

J. Hulliger, R. Gutmann and H. Wüest

Institute of Quantum Electronics, ETH-Hönggerberg, CH-8093 Zürich

Potassium niobate (KNbO<sub>3</sub>) is one of today's most promising nonlinear optical, electro-optical and photorefractive oxide crystals. Growth of quality bulk material uses an [110] oriented seed and pulling along [110] will result in a morphology showing flat (100) faces and a non-faceted, arbitrarily shaped bounds perpendicular to them. Non-optimized growth attempts produce preferentially a plate-like morphology. Growth of large size samples became now possible and resulted in a first 100 g crack-free crystal (Fig. 1) of the typical morphology, but 20 mm thick along the [100] direction.

One thin layer technology for KNbO<sub>3</sub> based on He<sup>+</sup> implantation resulted in 2-d as well as 1-d optical waveguides [1,2]. Similarly, liquid phase epitaxy (LPE) of the solid solution KTa<sub>1-x</sub>Nb<sub>x</sub>O<sub>3</sub> (KTN) produced  $\mu\text{m}$  thick waveguiding layers (m3m, mm4) [3] (Fig. 2). LPE of pure KNbO<sub>3</sub> (mm2) on e.g. KTaO<sub>3</sub> (m3m) is prohibitive because of a serious lattice

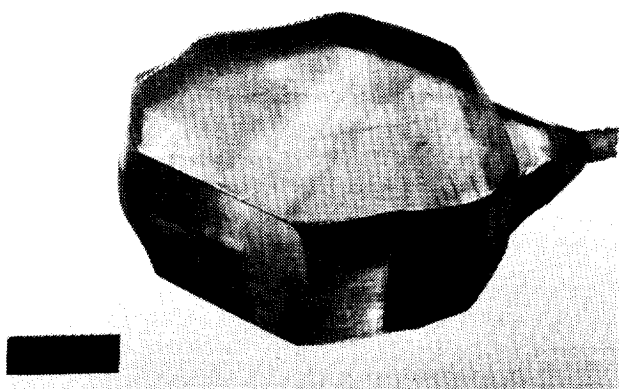


Figure 1. A first 100 g KNbO<sub>3</sub> single cristal (thickness: 20 mm).

mismatch. Even the growth of a KTN mm4 phase on KTaO<sub>3</sub> showed lattice relaxation defects that could be reduced to a minimum by LPE of K<sub>1-y</sub>Na<sub>y</sub>Ta<sub>1-x</sub>Nb<sub>x</sub>O<sub>3</sub> [4].

The lecture will shortly summarize the state of the art of KNbO<sub>3</sub> bulk growth, review general work on ABO<sub>3</sub> epitaxy, but concentrate on KTN growth of lattice matched layers and their characterization.

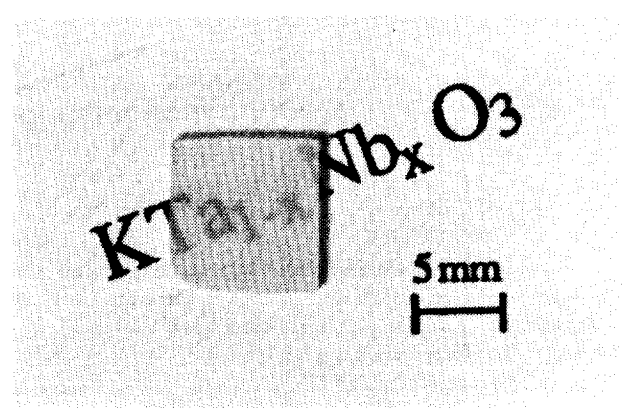


Figure 2. Ferroelectric KTN ( $x = 0.46$ ) layer grown on a (100) KTaO<sub>3</sub> substrate (layer thickness 38  $\mu\text{m}$ ).

1. T. Bremer, E. Krätzig et al., *Ferroelectrics Lett.*, 9 (1988) II.
2. D. Fluck, P. Günter, R. Irmscher and Ch. Buchal, *Appl. Phys. Lett.*, 59(25) (1991) 3213.
3. R. Gutmann and I. Hulliger, *Cryst. Prop. Prep.* 32 (1991) 117.
4. R. Gutmann, I. Hulliger and E. Reusser, *J. Cryst. Growth* (to be submitted).

PRECEDING PAGE BLANK NOT FILMED

DEFECT STRUCTURE IN TRANSITION METAL IONS DOPED  
PHOTOREFRACTIVE  $\text{KNbO}_3$  CRYSTALS  
*Xiaoyan Ma and Dezhong Shen*  
Research Institute of Synthetic Crystals  
P.O. Box 733, Beijing 100018, P.R. China

The exact nature of the microscopic centers in  $\text{KNbO}_3$  crystal responsible for the photorefractive effect, is not very clear. The defects introduced by doping with transition metal ions in the crystal, play an important role in the photorefractive effect.

$\text{KNbO}_3$  single crystals doped with Fe, Co, Ni, Cu, V, Cr were grown by top-seeded solution growth. In order to understand the nature (charge state, local symmetry, and electronic structure) of the defects/impurities present in these crystals, we have carried out electron paramagnetic resonance (EPR), photo-EPR, and optical absorption measurements on a variety of  $\text{KNbO}_3$  samples doped with transition metal ions. Extensive

EPR measurements as a function of temperature on single crystal and polycrystal samples are given. We describe our EPR results for various oxidation-reduction conditions. From these measurements, we are able to establish a relative energy scale for the positions of the various charge states of the transition metal dopants in the bandgap of  $\text{KNbO}_3$ . In the photo-EPR measurements, the change in the charge state of a paramagnetic dopant under illumination is monitored. Measurements of the steady-state photo-EPR response as a function of wavelength, intensity, and temperature have also been carried out.

---

ELECTRIC FIELD POLING OF POTASSIUM NIOBATE CRYSTALS

*Richard H. Jarman and Barry C. Johnson*  
Amoco Technology Company  
P.O. Box 3011, Naperville, IL 60563

A critical step in the fabrication of potassium niobate crystals for nonlinear optical applications is the removal of the ferroelectric domains that are introduced during cooling through the phase transitions after growth. Typically this is performed by application of a large electric field at a temperature somewhat below the orthorhombic - tetragonal phase transition at 225°C. We report on several aspects of this process, paying particular attention to the electrical properties of the material. We find that the electrical conductivity of potassium niobate exhibits complex dependencies on time and applied

field as well as temperature. Different portions of the same crystal can also display widely different behavior; which we attribute, at least in part, to the significant role that impurity ions play in determining the electrical properties. We find that, to a large degree, the electrical conductivity of the material is diagnostic of the optical quality of the poled piece. We also address the issue of incomplete domain removal, i.e., situations in which domain boundaries appear to be immobile under the applied field, which can severely affect the yield of optical quality material.

**GROWTH AND CHARACTERIZATION OF OFF-CONGRUENT  $\text{LiNbO}_3$  SINGLE CRYSTALS GROWN BY DOUBLE CRUCIBLE METHOD**

*Yasunori Furukawa, Masayoshi Sato, Kenji Kitamura\*, Fumio Nitanda and Kohei Ito*

Magnetic and Electronic Materials Research Laboratory,  
Hitachi Metals, Ltd., Mikajiri Kumagaya, Saitama 360 Japan

\*National Institute for Research in Inorganic Materials,  
Namiki, Tsukuba, Ibaragi 305 Japan

$\text{LiNbO}_3$  single crystals available commercially are grown from the melt of the congruent composition by the conventional Czochralski technique. They generally have good optical quality and uniform birefringence, although they contain many Li vacancies. The stoichiometric composition is expected to be superior because its greater birefringence and fewer non-stoichiometric defects by decreasing the Li vacancies. Recently it was reported that lithium-rich  $\text{LiNbO}_3$  fabricated by vapor transport equilibration has high optical quality [1]. It has been reported that either  $\text{MgO}$  doping or reducing the amount of transition metals in the crystal improves the optical damage threshold [2], but it is not certain whether the Li vacancies will influence the optical damage.

In this study, we grew off-congruent  $\text{LiNbO}_3$  single crystals by the double crucible method in order to control the composition variations of crystal, and to investigate the optical damage properties.

The crystal compositions were characterized by the measurement of the non critical phase matching temperature of

SHG from  $1.064\mu\text{m}$ . The phase matching temperature increases linearly with the Li/Nb ratio and the slope is  $173^\circ\text{C/mol\%}$ . The composition variation throughout the crystal grown by the double crucible method was measured to be within  $0.035\text{ mol\%}$ . Further improvement is expected for better control of the starting composition.

No remarkable improvement has been observed in the optical damage threshold by varying the Li/Nb ratio. Moreover, the optical damage threshold of the stoichiometric crystal is unexpectedly lower than that of the congruent composition. However, at this stage, we can't conclude that there is a relationship between the optical damage threshold and nonstoichiometric defects. The microscopic crystal line defects in off-congruent crystals have been observed by the X-ray topography and rocking curves.

---

- 1) D.H. Jundt et al., *IEEE J. Quantum Electron.* 26 (1990) 135.
- 2) Y. Furukawa et al., *J. Crystal Growth* 99 (1990) 832.

STOICHIOMETRIC  $\text{LiNbO}_3$  SINGLE CRYSTAL GROWTH BY DOUBLE CRUCIBLE  
CZOCHRALSKI METHOD USING AUTOMATIC POWDER SUPPLY SYSTEM

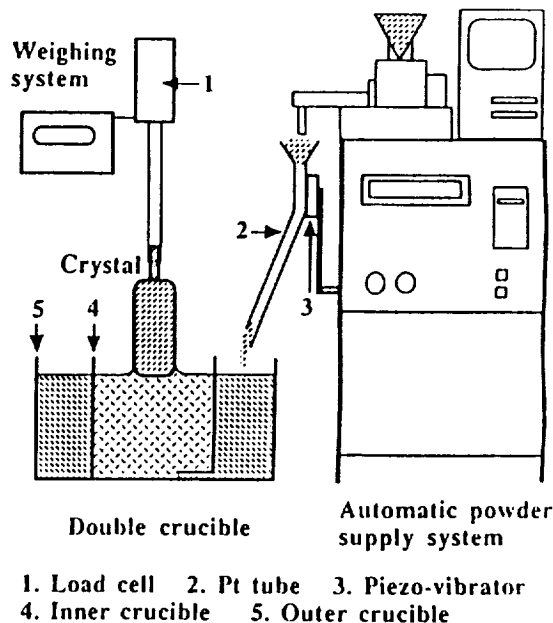
K. Kitamura, J.K. Yamamoto, N. Iyi and S. Kimura  
National Institute for Research in Inorganic Materials

1-1, Namiki, Tsukuba, Ibaraki, 305 Japan

T. Hayashi

ASGAL Co. Ltd., 5-5 Tokodai, Tsukuba, Ibaraki, 305 Japan

Stoichiometric  $\text{LiNbO}_3$  single crystals above 2 inches in diameter and 100 mm in length were grown by the Czochralski method using a double crucible and automatic powder supply system as shown by a right figure. The crystals were grown from a Li-rich melt ( $\text{Li}_2\text{O}$  60 mol %) in the inner crucible, and the stoichiometric  $\text{LiNbO}_3$  powder was supplied smoothly and continuously to the outer melt. The powder supply rate could be controlled within a range of 1 g/hr to 40 g/hr. The accuracy of the supply rate depended on the powder conditions. In this study, coarse grained powder of the stoichiometric LN, obtained by enhanced grain growth, produced the best result. From the lattice parameter and Curie temperature measurements, the chemical composition (Li/Nb ratio) through the grown crystal was found to be close to the stoichiometric composition. The as-grown crystals were of single domain except at the periphery. From a comparison of the transmittance between stoichiometric and congruent  $\text{LiNbO}_3$  single crystals, the absorption edge wavelength of the stoichiometric crystal was found to be 10 nm shorter than the congruent crystal. The congruent composition, normally used by the ordinary Czochralski method, does not always exhibit the suitable properties for the applications. Depending on the application, some crystals may require growth under stoichiometry control conditions. It is expected that this double crucible Czochralski method can be effectively applied to control crystal stoichiometry during growth and to produce uniformly doped single crystals of various oxide compositions.



1. Load cell 2. Pt tube 3. Piezo-vibrator  
4. Inner crucible 5. Outer crucible

# LiNbO<sub>3</sub> SINGLE CRYSTAL GROWTH FROM Li-RICH MELTS BY THE CONTINUOUS CHARGING AND DOUBLE CRUCIBLE CZOCHRALSKI METHODS

M. Sakamoto\*, S. Kan\*\*, Y. Okano, K. Hoshikawa and T. Fukuda

Institute for Materials Research

Tohoku Univ., Sendai, 980, Japan

Ltd., Toda-shi, Saitama, 335, Japan

Although a LiNbO<sub>3</sub> (LN) single crystal with a congruent composition is widely used for surface acoustic devices, optical properties of LN crystals with incongruent compositions such as a stoichiometric one are interested. However, it is difficult to grow uniform LN with incongruent compositions by the conventional Czochralski method, because the crystal composition changes along the crystal growth direction when the melt composition is different from congruent one. From the view point of the Li/Nb ratio control, the continuous charging Czochralski (CC-CZ) method<sup>1)</sup> and the double crucible Czochralski (DC-CZ) method were investigated in this study. In order to keep the melt composition constant, LN powder with the same composition and amount as the grown crystal was fed to the melt in the CC-CZ method, and the corresponding melt was introduced to the inner crucible from the outer crucible in the DC-CZ method. Crystals were grown by an RF-heating Czochralski furnace with a Pt crucible 60 mm in

diameter in both methods. Diameter of a Pt partition cylinder in the CC-CZ method and a Pt inner crucible in the DC-CZ method were 40 mm. The pulling rate was 1.0 mm/h, and the crystal rotation rate was 10 rpm. LN crystals, 1 inch in diameter, were successfully grown from Li-rich (55.0 ~ 60.0 mol% Li<sub>2</sub>O) melts (Fig. 1). Measurements of the extraordinary refractive index,  $n_e$ , by the prism coupling method (Fig. 2) and the SHG phase matching temperature indicated compositional uniformity of the crystals. It is noted that LN crystals with compositional uniformity along the growth direction were obtained by these methods.

1) S. Kan, M. Sakamoto, Y. Okano, K. Hoshikawa and T. Fukuda, submitted to *J. Crystal Growth*.

\*Present address: Nippon Mining Co., Ltd., Toda-shi, Saitama, 335, Japan.

\*\*Present address: Daiso Co., Ltd., Amagasaki-shi, Hyogo, 660, Japan.

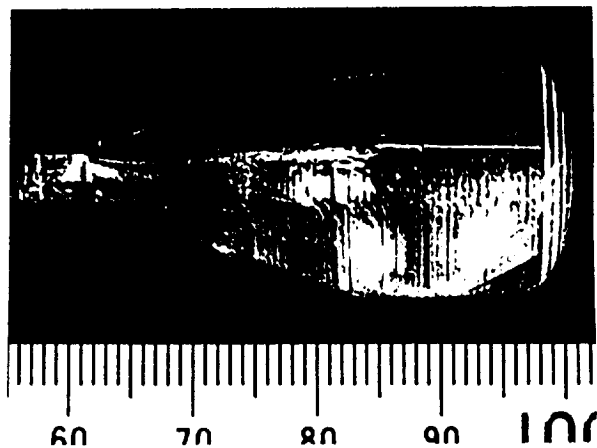


Figure 1. LN crystal grown from 55 mol% Li<sub>2</sub>O.

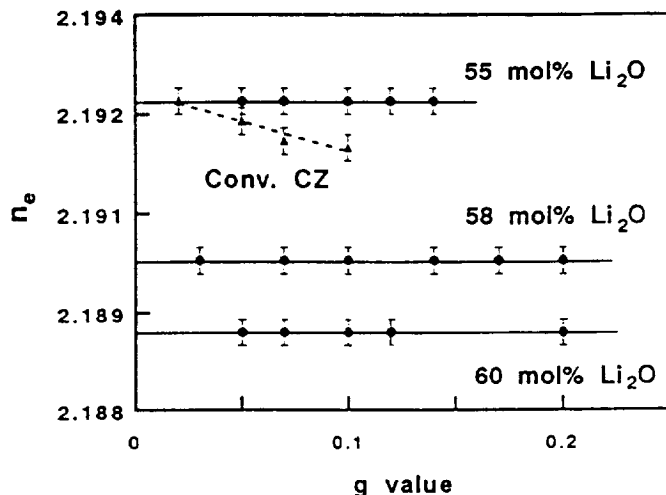


Figure 2. Extraordinary refractive index,  $n_e$ , along the growth direction (632.8 nm, 292 K).

# PHYSICAL PROPERTY VARIATION OF MOLTEN LITHIUM NIOBATE BY

## DOPING WITH MAGNESIUM OXIDE

Eiji Tokizaki, Kazutaka Terashima and Shigeyuki Kimura

KIMURA METAMELT Project

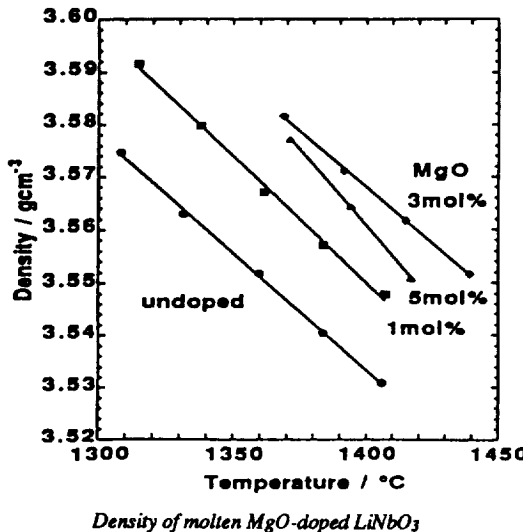
ERATO, Research Development Corporation of Japan

Tsukuba Research Consortium, Tokodai 5-9-9, Tsukuba, Ibaraki, 300-26, Japan

$\text{LiNbO}_3$  single crystals are the most promising materials for the use in optical devices because of its excellent photorefractive and electro-optical properties. The large diameter crystals of  $\text{LiNbO}_3$  can be grown by the Czochralski technique without domains and subgrain boundaries. It is, however, damaged by laser light to change its refractive index. This tendency is detrimental to application in optical devices. The doping  $\text{MgO}$  to molten  $\text{LiNbO}_3$  at the growing process was reported to improve the optical properties such as refractive index variation by exposing to high power laser<sup>1,2)</sup>. But the doped  $\text{MgO}$  inhomogeneously distributes in the boules<sup>3)</sup>.

The crystal qualities are closely related to the melt properties which influence the convection in the vicinity of the crystal-melt interface. To investigate physical properties of the melt is very important to understand the crystal quality variation. Many papers reported on the melt properties of pure  $\text{LiNbO}_3$ <sup>4,5,6)</sup>. But there is no paper on that of  $\text{MgO}$ -doped  $\text{LiNbO}_3$ . We have recognized that the properties of molten state is closely related to the crystal qualities and then measured the properties of molten  $\text{LiNbO}_3$  doped with  $\text{MgO}$ . It was found that the physical properties, such as the density, the surface tension and the viscosity, widely varied by doping with  $\text{MgO}$  to  $\text{LiNbO}_3$  melt. The densities of  $\text{MgO}$ -doped  $\text{LiNbO}_3$  melts are shown in figure with that of undoped  $\text{LiNbO}_3$  melt.

This paper reports the density, surface tension and viscosity of molten  $\text{LiNbO}_3$  doped with  $\text{MgO}$  up to 5 mol% at the temperature from 1300°C to 1450°C measured by hydrostatic weighing method, ring method and on the basis of the Stokes' Law, respectively<sup>5)</sup>. The  $\text{MgO}$ -doping effect to molten  $\text{LiNbO}_3$  will be discussed.



Density of molten  $\text{MgO}$ -doped  $\text{LiNbO}_3$

- 1) Gi-Guo Zhong, Jin Jian and Zhong-Kang Wu: 11th International Quantum Electronics Conference, IEEE cat No. 80 GH1561-0 (1980) 631.
- 2) D.A. Bryan, R. Gerson and H.E. Tomachke: *Appl. Phys. Letters* 44 (1984) 847.
- 3) Y. Furukawa, M. Sato, F. Nitanda and K. Ito: *J. Crystal Growth* 99 (1990) 832.
- 4) J.A.S. Ikeda, V.J. Fratello and C.D. Brandle: *J. Crystal Growth* 92 (1988) 271.
- 5) K. Shigematsu, Y. Anzai, S. Morita, M. Yamada, H. Yokoyama: *Japanese J. Applied Phys.* 26 (1987), 1988.
- 6) S. Hara, N. Ikemiya, K. Ogino: *J. Japan Inst. Metals*, 53 (1989), 1148.

## SESSION 2C

### ADVANCES IN PREPARATION OF GaAs AND InP CRYSTALS BY LEC METHOD

*R. Fornari*

MASPEC-CNR Institute, Via Chiavari 18/A, 43100 Parma, Italy

The quality of bulk III-V compounds has been greatly improved in the last years. This essentially depends on the fact that much research has been focused on the understanding of the generation mechanisms of the most common crystallographic defects, i.e. dislocations, microprecipitates, grain boundaries as well as on the doping/composition homogeneity and electrical properties of the crystals. These efforts have led to the identification of some crucial growth parameters which play an important role in generation of crystallographic defects. The crystal growers have understood that melt stoichiometry, thermal gradients and thermal instabilities in the growth chamber are of paramount importance. Consequently, the growth processes have been modified in order to control accurately the temperature stability and melt composition. For the liquid encapsulation Czochralski (LEC) technique, this has meant the application of magnetic fields, multizone heaters and double-chamber systems with controlled atmosphere. This double-chamber version of the Czochralski puller is particu-

larly attractive since it allows the growth of GaAs without the use of the encapsulant and gives the opportunity of changing the melt composition during growth. In the case of InP the encapsulant has been maintained but the controlled atmosphere (containing P vapor) of the inner chamber has allowed the pulling under very low thermal gradients without the usual degradation of the crystal surface.

This presentation reviews the progress made in crystal growth of large-diameter III-V crystals. Some emphasis will also be placed on pre- and post-growth treatments; in the former case these essentially consist of a higher degree of purification of the raw elements, which has made the production of semi-insulating crystals, either undoped (GaAs) or lightly doped (InP), possible. The post-growth treatments include, for example, thermal annealing, which is now routinely carried out on SI GaAs in order to homogenize the deep level distribution and the sheet resistance across the ingots.

---

### MLEK CRYSTAL GROWTH OF (100) INDIUM PHOSPHIDE

*David F. Bliss and Robert M. Hilton*

Rome Laboratory, Hanscom Air Force Base, Mass., 01731

*Joseph A. Adamski*

Parke Mathematical Laboratories, Carlisle, Mass., 01741

Indium Phosphide bulk crystal growth methods have been improved recently by the use of magnetic field stabilization of the melt and a flat-top shaping technique to reduce the incidence of twinning. These processing improvements affect the crystal properties such as dopant distribution and stress-induced dislocation density. The magnetically stabilized liquid encapsulated Kyropoulos (MLEK) method for growth of InP in the (100) direction creates a highly stable environment: for crystal growth by reducing turbulence in the melt. Combining MLEK with magnetic liquid encapsulated Czochralski (MLEK), the crystal is grown with a flat top roughly three inches in diameter, and then slowly pulled as a cylinder 70 mm in length. Controlling the shape of the growing crystal (defined by its aspect ratio) is a major factor in preventing twin formation. There are several advantages for MLEK growth of twin-free InP crystals. (1) With magnetic stabilization, it is possible

to control the shape of the solid-liquid interface. Twin nucleation is less likely when a convex interface is maintained, and it appears that an aspect ratio of 1.6 is sufficient to reduce the probability of twinning, although this may not be the optimized growth condition. (2) The MLEK growth environment induces a smaller amount of thermal stress than non-magnetic LEC. Since the growing crystal is held below the encapsulating layer during the first phase of growth, the axial temperature gradient in the crystal is low. Controlling the thermal environment during crystal growth is critical to the success of the MLEK process. The axial magnetic field causes an increase in the radial temperature gradient, and increased viscosity in the melt. The authors have investigated the effect of applied magnetic field on dopant distribution and dislocation density. The results show that the MLEK growth environment favors both a uniform dopant distribution as well as uniform dislocation density.

**A THERMAL STRESS THEORY OF DISLOCATION REDUCTION IN THE VERTICAL  
GRADIENT FREEZE (VGF) GROWTH OF GaAs**  
*A.S. Jordan<sup>1</sup>, E.M. Monberg<sup>1</sup> and J.E. Clemans<sup>2</sup>*  
<sup>1</sup>AT&T Bell Laboratories, Murray Hill, NJ 07974  
<sup>2</sup>Engineering Research Center Princeton, NJ 08540

An important requirement in the growth of semi-insulating (SI) GaAs boules, for high-speed electronic device and circuit applications, is the reduction of the dislocation density. An advanced method to produce 2 and 3 inch diameter undoped SI wafers with low defect density is the VGF technique. We have formulated a tractable model of the VGF process providing dislocation density contour lines in terms of geometrical and physical parameters. First, the temperature distribution in a cylindrical boule has been determined in closed form (modified Bessel functions of the first kind, order zero ( $I_0$ ) in the radial and sine functions in the axial coordinate) by solving the quasi-steady state partial differential equation for heat conduction subject to suitable boundary conditions. Similar to our treatment of liquid-encapsulated Czochralski (LEC) growth, the principal thermoelastic stress components have been evaluated and then resolved in the  $\{111\}$ ,  $\langle1\bar{1}0\rangle$  slip system. Whenever the resolved shear stress components exceed the critical resolved shear (CRSS) dislocations are introduced by slip.

We present dislocation density contour maps for 2 and 3 inch diameter undoped (100) GaAs grown by VGF under a variety of linear thermal gradients ( $v$ ) imposed on the periphery of the boule. We show that for large  $v$  the dislocation distribution is similar to that observed in LEC material. By lowering  $v$ ,

dislocation generation is suppressed and the density at the base of the crystal is insensitive to its length. Although larger diameter crystals contain more dislocations at the periphery than smaller ones (in agreement with etchpit density (EPD) data) at  $v = 2\text{K/cm}$  both 2 and 3 inch diameter wafers become virtually dislocation-free.

Finally, we compare dislocation elimination in VGF and LEC grown GaAs on the 3 inch scale employing the recent CRSS data of Guruswamy et al. obtained at elevated temperatures on undoped VGF and In-doped LEC specimens. We show that the approximately three-fold increase in CRSS with In inhibits defect formation in (100) LEC wafers, grown in a high ambient temperature gradient, across  $\sim 75\%$  of the diameter, in accord with the EPD data. At  $v = 5\text{K/cm}$  the theoretical results for undoped GaAs grown by VGF track the low EPD in both the  $\langle100\rangle$  and  $\langle110\rangle$  directions. However, the fact that in some locations the thermal stress theory predicts no dislocations while  $\sim 1000 \text{ cm}^{-2}$  are counted suggests a secondary mechanism of generation which may be vacancy condensation into dislocation loops. Therefore, we recommend the addition of a moderate amount of In ( $\sim 2 \times 10^{19} \text{ cm}^{-3}$ ) in VGF to fill vacant Ga sites and thus prevent condensation into loops.

## LEC GROWTH OF LARGE GaAs SINGLE CRYSTALS

*M. Shibata, T. Suzuki, T. Inada and S. Kuma*

Advanced Research Center, Hitachi Cable, Ltd.

5-1-1 Hitaka-cho, Hitachi-city, Ibaraki 319-14, Japan

Length of LEC GaAs crystals has been limited by polycrystallization during growth. It is traditionally said growth of a single crystal is difficult when the shape of solid/liquid interface becomes concave toward the melt.

From close observation of dislocations in the crystals, existence of dislocations succeeding perpendicular to the solid/liquid interface was recognized. These perpendicular succeeding dislocations will develop toward the center of the curvature of the concave interface and accumulate there. The accumulation will finally lead to polygonization shown in Fig. 1. However, we cannot avoid the concave shape, because the interface usually tends to be sigmoidal shape that is partially concave in real growth.

Considering that a simple fact that dislocations cannot exist out of crystal, the position of the accumulation is more important; in the crystal or out of the crystal. If the center of the curvature locates out of the crystal, the dislocations must stop developing at the surface of the crystal before accumulation.

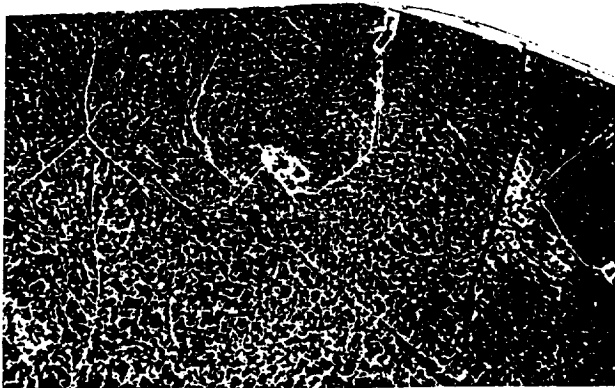


Figure 1. Polygonization area in a (001) KOH etched wafer.

This consideration leads to a new index D shown in Fig. 2; the distance from the crystal surface to the curvature center. The index value D should be large during growth for a single crystal. The technology to bring a sufficient interface for the large index value have been built up by the adjustment of the heatflow from the melt to the crystal in a three zone furnace. Using this technology, 4 inch single crystals with 320 mm length and 6 inch single crystals with 170 mm length have been obtained.

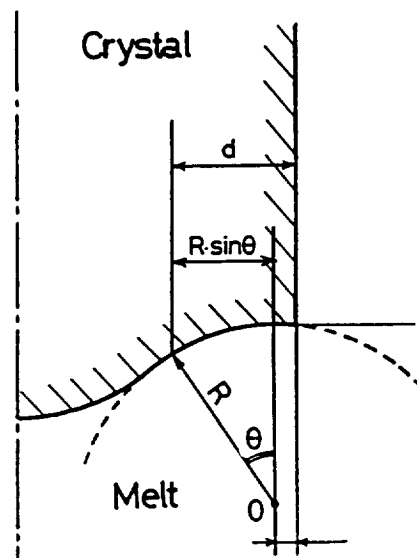


Figure 2. Definition of the index D.

## HEAT TRANSFER DURING GaAs GROWTH OF BULK SINGLE CRYSTAL BY THE

### LIQUID ENCAPSULATED VERTICAL BRIDGMAN TECHNIQUE

*Tomonari Suzuki, Yasunori Okano, Keigo Hoshikawa and Tsuguo Fukuda*

IMR, Tohoku University, Sendai 980, Japan

The liquid encapsulated vertical bridgman (LE-VB) technique is one of the attractive techniques for growth of high quality semi-insulating GaAs crystals with low dislocation density<sup>1)</sup>.

In order to establish the optimum furnace design and growth condition, the heat transfer in melt, crystal and thermal shields during single crystal growth of GaAs by the LE-VB technique was analyzed by the finite element method. As thermal boundary conditions, temperature values near the crucible monitored by thermocouples in an actual growth system were used. A growth rate and a latent heat of solidification were considered in the boundary condition along the crystal/melt interface. In the analysis, thermal conductivity dependence on crucible materials (quartz and carbon) and thermal conductivity anisotropy in case of pBN crucible were considered.

In this analysis, parameters affecting the crystal/melt interface shape which is one of the most important factors determining quality of the grown crystal such as dislocation density are discussed. It was pointed out that the thermal conductivity of the crucible including anisotropy significantly affected the interface shape. Especially, heat flow behavior around conical part of the pBN was different from those of the quartz and carbon crucibles because of the anisotropy.

In order to control the interface shape, effects of temperature gradient near the interface, which could be controlled by change of thermal shield materials around the crucible, and growth rate on the interface shape were analyzed. The results obtained by the numerical analysis were compared with the results by experiments.

1) K. Hoshikawa et al.. *J. Crystal Growth*, 94(1989) 643.

**CONSECUTIVE THERMAL COOLING CYCLE EFFECT OF LIQUID-ENCAPSULATED-CZOCHRALSKI  
GaAs CRYSTAL GROWTH ON THE CRYSTALLOGRAPHIC UNIFORMITY**

Yasuyuki Saito

Microelectronics Center in Tarnagawa Works Toshiba Corp.  
1, Komukai Toshiba-cho, Saiwai-ku, Kawasaki 210, Japan

We have investigated the crystallographic origin of the ununiformity related to the threshold voltage ( $V_{th}$ ) scattering origin of Si-implanted metal-semi-conductor field-effect-transistors (MESFETs) on GaAs liquid-encapsulated Czochralski-technique (LEC) substrates. Thus, we investigated consecutive cooling thermal cycle effect of LEC GaAs crystal growth on the  $V_{th}$  scatterings of Si-implanted MESFETs by using different furnace structures as shown in Fig. 1.[1,2]

If the free-electron carrier-depth profile of the MESFET channel conductive layer is constant, the  $V_{th}$  of the profile is related to resultant occupation ratio of Ga-site Si atom concentration  $[Si_{Ga}]$  to As-site Si atom concentration  $[Si_{As}]$  for the implanted Si atoms of the profile in a semi-insulating (SI) GaAs crystal. The occupation ratio  $[Si_{Ga}]/[Si_{As}]$  is sensitive to bond length (Si-Ga, Si-As, Ga-As) of a neighboring GaAs crystal cell on the implanted-Si atom under the thermal equilibrium condition of annealing for the Si-implanted GaAs crystal.

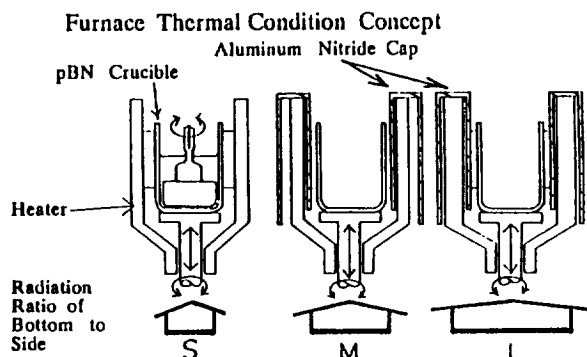


Figure 1

For example, it was shown [3] that the occupation ratio  $[Si_{Ga}]/[Si_{As}]$  for the expanded bond of the GaAs crystal by thermal strain for cap annealing is lower than that of the non-expanded bond by the carrier-concentration-depth-profile comparison by the capacitance-voltage method such as shown in Fig. 2. Thus, the crystal uniformity or crystal structural characteristics depending on the consecutive cooling thermal cycle together with the melt composition has been analyzed. We will present the experimental procedure and the analyzed result.

[1] Y. Saito, K. Fukuda, S. Yasuami, J. Nishio, S. Yashiro, S. Washizuka, M. Watanabe, M. Hirose, Y. Kitaura and N. Uchitomi, Jpn. J. Appl. Phys. 30, (1991) 2432.  
[2] Y. Saito and S. Washizuka, Jpn. PAT. Application Kokai S61-242995.  
[3] Y. Saito, submitted to J. Appl. Phys (R0550, 1991).

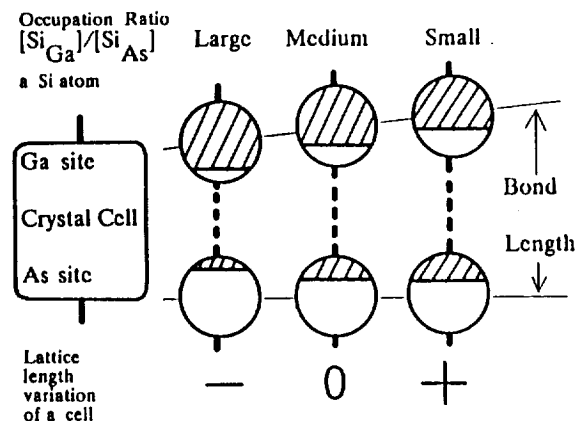


Figure 2

**GaAs AND CdTe CRYSTAL GROWTH BY THE VZM TECHNIQUE**

R.L. Henry, P.E.R. Nordquist and R.J. Gorman  
Naval Research Laboratory, Washington, DC 20375-5000

The Vertical Zone Melt (VZM) technique has been applied to the single crystal growth of both GaAs and CdTe. For both compounds, a pyrolytic boron nitride crucible and a (100) oriented seed were used along with liquid encapsulation by boric oxide. In the case of GaAs, the ampoule was pressurized with either argon or arsenic vapor from elemental arsenic at pressures ranging from 1 to 2 atmospheres. A molten zone length of 22 mm gave a growth interface which is nearly flat and resulted in routine single crystal growth. Temperature gradients of  $4^{\circ}\text{C}/\text{cm}$ . and  $9^{\circ}\text{C}/\text{cm}$ . have produced dislocation densities of  $<1000/\text{cm}^2$  and  $2000-5000/\text{cm}^2$  respectively for 34 mm dia-

ter GaAs. Post growth cooling rates for GaAs have been 50, 160 and  $500^{\circ}\text{C}/\text{hr}$ . The cooling rate affects the number and size of arsenic precipitates and the EL2 concentration in the GaAs crystal. In the case of CdTe, the ampoule was pressurized to 1 atmosphere using argon. The thermal spike necessary to create and sustain a molten zone 22mm in length for CdTe is very different from the thermal spike necessary to accomplish a molten zone of the same size in GaAs. As a result, the temperature gradient imposed on the solid is larger for CdTe. Growth conditions and results for CdTe are discussed and compared to those for GaAs.



## SESSION 2D

### GROWTH OF PERFECT QUASICRYSTALS; FROM CURIOSITY TO REALITY

*A. Refik Kortan*

AT&T Bell Laboratories, 600 Mountain Ave.  
Murray Hill, NJ 07972-0636

Ideal quasicrystalline form of matter is defined by an atomic structure that exhibits a perfect orientational long range order, a non-periodic perfect long range translational order, and a non-crystallographic point group symmetry. In view of these exotic structural properties, perhaps not so surprisingly "quasicrystals" were also called as "impossible crystals". If you imagine tiling your floor using pentagonal tiles it will very soon come to your attention that it is almost impossible to maintain any long range order in the process. Understandably, carrying out a similar space filling in three dimensions with non-crystallographic building blocks becomes even more complicated. Such exotic structures do exist in nature and were first

discovered in 1984 in an Al-Mn alloy. This particular alloy had a grain size of few hundred angstroms, and was thermodynamically metastable. In eight short years, and after the discovery of many other quasicrystalline compounds the quasicrystalline single grain size we could grow increased from a fraction of a micron to few centimeters. Today, we can grow nearly defect free and stable two and three dimensional quasicrystals with macroscopic dimensions. All quasicrystals discovered to date exhibit a universal non-congruent melting property which we exploit in our crystal growth techniques. This lecture will review the progress made in understanding quasicrystals, growing single grains, and the present day status of the field.

---

### ON THE MORPHOLOGY OF AlCuFe QUASICRYSTALS AND RELATED PHASES

*K. Balzuweit and H. Meekes*

Laboratory of Solid State Chemistry University of Nijmegen  
The Netherlands

The icosahedral phase of AlCuFe was first observed to be stable by Tsai, Inoue and Masumoto [1]. As a consequence of that stability and the availability of relatively large single crystals, AlCuFe offers an attractive system to study quasi crystals; many investigations have been reported. There seem to be many different compositions which present the icosahedral phase, the degree of perfection of these phases often being explained by phason strain.

The aim of our investigation was to grow single crystals with the icosahedral phase with two main goals. First of all to produce large crystals for characterisation of different physical properties and secondly to study the growth of quasi crystals in the light of normal growth theories.

Various samples with different start compositions were prepared. All the samples were molten and well homogenized in

an argon arc furnace. Some of the resulting pellets were then annealed at different temperatures. The samples were characterised using scanning electron microscopy and microprobe, interference optical microscopy, scanning tunnelling microscopy and x-ray powder diffraction.

The morphology of the as-grown phases, icosahedral and crystalline, of the different samples (annealed and as-cast) is discussed in relation to both initial and final composition. A simple growth model and the presence of classical growth phenomena such as step, spiral-like patterns, dendritical and cellular growth is also discussed.

[1] A.P. Tsai, A. Inoue and T. Masumoto, *Jpn. J. Appl. Phys.*  
26(1987)L1505.

PRECEDING PAGE BLANK NOT FILMED

## GENERALISATION OF MORPHOLOGICAL HARTMAN PERDOK THEORY TO MODULATED AND QUASI CRYSTALS

*P. Bennema, K. Balzuweit, J.P. van der Eerden, M. Kremers,*

*H. Meekes, M.A. Verheijen and L.J.P. Vogels*

Laboratory of Solid State Chemistry University of Nijmegen  
The Netherlands

In a recent survey paper it was shown that on modulated crystals forms of facets to be indexed with four integral integers  $\{hklm\}$  occur [1]. These facets were discovered on two types of totally different modulated crystals:

- i) Crystals with an average  $\beta\text{-K}_2\text{SO}_4$  structure grown from an aqueous solution, like  $\text{Rb}_2\text{ZnBr}_4$ ,  $(\text{N}(\text{CH}_3)_4)_2\text{ZnCl}_4$ , etc.
- ii) Crystals of the mineral Calaverite ( $\text{Au}_{1-x}\text{Ag}_x\text{Te}_2$ ).

Furthermore, it has been shown that faces  $\{hklmno\}$  occurring on quasi crystals can be understood in terms of a generalised Hartman Perdok theory. The main aim of this contribution is to show how in the more-than-three dimensional (superspace) crystallography of de Wolff, Janner and Janssen -where modulated (and quasi crystals) are considered as three dimensional cuts of a translational invariant super space- the

Hartman Perdok theory can be generalised to explain the occurrence of  $\{hklm(n)\}$  faces on modulated and quasi crystals. In order to identify generalised nets  $\{hklm(n)\}$  parallel to F-faces, showing a roughening transition, the concepts of bond and bond energy have to be generalised. To this end a bond is considered as a continuum of slightly varying bonds suspended between two 'worldlines' in superspace. Using this concept, the crystal connected-net-theory is generalised by checking whether slabs corresponding to three dimensional crystal cuts with a thickness  $d_{hklmno}$  are connected and calculating the corresponding slice energies.

[1] P. Bennema, K. Balzuweit, B. dam, H. Meekes, M.A. Verheijen and L.J.P. Vogels, *I. Phys. D: Applied Phys.* 24(1991)186.

---

## NEW RELEVANCE FOR RESIDUAL CRYSTAL AND MELT ANALYSIS

*B. Cockayne*

DRA Electronics Division, RSRE Malvern

St Andrews Road, Malvern, Worcs WR14 3PS, UK

It is well recognised that analysis of the last portions of single crystals to solidify during growth from the melt has helped to interpret many phenomena associated with the segregation of impurities, including the development of cellular structures due to constitutional supercooling and precipitation phenomena. However, severe impairment of crystalline perfection induced by such defects prevents such material being of practical use in device structures and it is frequently discarded.

In this review, it will be shown that information derived from both structural and chemical analysis of such imperfect

crystal regions and associated melt residues can be used to gain a wide variety of additional information pertinent to improving and understanding crystal properties and to developing new materials. Particular examples will include: a) lattice hardening in relation to the growth of dislocation-free III-V semiconducting compounds, b) the identification of phase relationships relevant to the formation of scattering particles in laser materials, c) an improvement in crucible lifetime for the growth of garnets, and d) the discovery of a new family of iron-based ferromagnetic compounds.

TEMPERATURE DIFFERENCE IN RADIAL DIRECTION OF  
CZOCHRALSKI COPPER CRYSTAL

*Y. Imashimizu and J. Watanabé*

Department of Materials Engineering and Applied Chemistry  
Mining College, Akita University, Akita 010, Japan

It was attempted to measure the temperature difference in radial direction and the axial temperature gradient of a bottle-neck shaped copper specimen 10 mm diameter under pulling in a stream of argon gas, and the role of radial temperature gradient in the dislocation formation of Czochralski copper crystal was examined.

For the measurement of the temperature difference in radial direction, a differential thermocouple of Pt-13%Rh/Pt/Pt-13Rh wires 0.1 mm in diameter was attached to a diametrical hole perforated at a position of main body of the specimens in such a way that one of the junctions was located at the center and the other at the side surface near the hole. The temperature difference between the center and the side surface of the specimen were measured by recording thermo-electromotive force of the differential thermocouple during the pulling process. In order to determine the axial temperature gradient of the pulling cop-

per specimen, a Pt/Pt-13%Rh thermocouple was attached to a diametrical hole of the specimen, and the temperature variation with pulling of the specimen was measured.

The temperature difference between the center and the side surface was about 5 K independent of the distance from the melt but showed an oscillation with a small amplitude which may be resulted from temperature oscillation of convective gas around the pulling specimen. The axial temperature gradient was about  $2.3 \times 10^3 \text{ K/m}$ .

The dislocation density of the copper crystal pulled under a similar condition to this experiment is larger than the estimated value from the above radial temperature difference. Therefore it is inferred that thermal stress arising from the temperature difference in radial direction is not the main factor for the formation of dislocations in Czochralski copper crystal.

---

FUNDAMENTAL ASPECTS OF PARTICLE ENGULFMENT  
BY A SOLIDIFYING FRONT

*M. Yemou and M.A. Azouni*

Laboratoire d'Aérothermique din CNRS  
4ter route des Gardes, 92190 Meudon (France)  
*G. Pétré*  
Chem. Phys. E.P. Dept., CP 165, ULB  
50 av. F.D. Roosevelt, 1050 Bruxelles (Belgique)

The engulfment or rejection of solid particles by advancing solidification is important in metallurgy, materials science, cryobiology, cryoconcentration, soil mechanics and many other processes.

In a previous paper [1], we experimentally determined the critical velocity (the value of the rate of the ice-water interface at which both the repulsion and the capture of a foreign particle are possible) for polyamide particle sizes ranging from  $10^{-1}$  to 1 cm.

Using the same set-up and procedure, we extended our investigation to steel beads (diameter of 0.6 cm) in order to

elucidate the mechanism of engulfment of particles of different thermal conductivities (see the following table).

In particular, what governs the shape of the interface, since the particle touches the interface until encapsulation ? Hydrodynamic forces ? Capillary forces ? Thermal effects ?

The theoretical analysis of these parameters, and the examination of all subsequent stages of trapping (evolution of the meniscus, contact angle determination) make evident that the thermal effects are of prime importance in the interface shape when large particles are considered.

[1] M.A. Azouni, W. Kalita, M. Yemou - *J. Crystal Growth*, 99(1990), p. 201.

	water	polyamide	steel	ice
Thermal conductivity, erg/cm°C	$56.10^3$	$23.10^3$	$46.10^5$	$221.10^3$

## MECHANISM OF GROWTH OF ORGANIC HOURGLASS INCLUSIONS: OLD MATERIALS WITH PHOTONIC APPLICATIONS

Bart Kahr, Marianne Nyman and Jason K. Chow

Department of Chemistry, Purdue University, West Lafayette, IN 47907-1393

Organic hourglass inclusions are simple ionic salts containing oriented organic dyes adsorbed through specific crystal faces. These materials, first described more than 100 years ago but subsequently abandoned as curiosities, have characteristics that address scientific and technological issues not foreseen: [1] Aromatic molecules trapped in ordered ionic matrices test the spectroscopic consequences of "salting" organic molecules; [2] Oriented chromophores sealed in robust ionic matrices are promising second order nonlinear optical devices. We are elucidating the recognition processes upon which the growth of

hourglass inclusions depend. The extensive literature on habit modification of simple salts by organic dyes is correlated with dye structure. Tailor-made dyes are synthesized to probe growth active surface sites systematically. Semi-empirical molecular orbital calculations of dye ground state geometries are determined in order to fit guests onto host surface structures predicted using simple models. The combined studies are essential for designing new hourglass inclusions with optimized optical properties.

## PROPERTIES AND SURFACE MORPHOLOGY OF INDIUM TIN OXIDE FILMS PREPARED BY ELECTRON SHOWER METHOD

H. Yumoto, J. Hatano, T. Watanabe, K. Fujikawa and H. Sato\*

Faculty of Industrial Science and Technology  
The Science University of Tokyo, Noda, Chiba 278, Japan

\*Sato Seigyo Co., Ltd., Yokohama 244, Japan

Indium tin oxide (ITO) films have been investigated for applications such as transparent electrodes, and heat reflecting films for heat insulation. Most ITO films have been prepared by the sputtering technique. Authors have developed a new method to produce thin solid films: electron shower method. The purpose of this study is to make ITO films by this method and to characterize them.

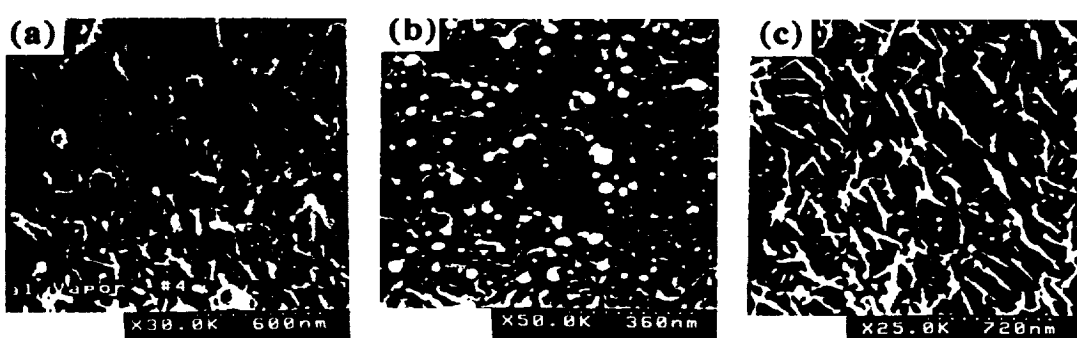
The electron shower was made by accelerating thermal electrons with 500 V, which were emitted from a heated tungsten filament. The pellets of ITO ( $\text{SnO}_2$ =5wt.%) were used as the source material for evaporation from an electron gun with a discharge power of about 0.6 kW. The ITO molecules evaporated by electron beam was activated by passing through the electron shower and deposited on the substrates. The substrates used were glass plates and copper microgrids coated with carbon. The properties of these ITO films prepared by electron shower (E.S.) was compared with ones formed by electron beam (E.B.). The pressure in the vacuum chamber was  $2 \times 10^{-5}$  Torr. and oxygen gas was not flowed through the chamber.

The electron resistivity of ITO films prepared by electron shower was  $4 \times 10^{-4} \Omega \text{ cm}$  and was one or two orders in magnitude smaller than that prepared by electron beam. The favor-

able orientations of the films made by E.B. were (222) and (400), and the orientation of one formed by electron shower was (622). As the amount of the crystallization was higher in the case of the electron shower, the grain size of the film affected the electron resistivity.

Photographs show that surface morphology of the ITO films was changed by the growth condition: (a) VLS whiskers (E.B. with 6.5 kV, 0.1A), (b) two-dimensional VLS whiskers (E.B. with 6 kV, 0.1A plus E.S. with 0.02A), and (c) lawn-like crystals (E.B. with 6.7 kV, 0.1 A plus E.S. with 0.05A). The concentration of Sn in the tip droplet of the VLS whiskers was 40-60 w.%. The two-dimensional VLS growth was due to the surface diffusion, because the growth rate of the film of (b) was 25 Å/min. and was one order of magnitude less than those of (a) and (c), and the most ITO molecules were supplied to the tip of the whiskers by the surface diffusion and not directly from the vapor phase.

Dendrite crystals also grew at the edges of holes of the copper microgrids. As there was holes, few crystals could grow only at the edges. Therefore, the supersaturation of the vapor at the holes became higher than that of other places.



## SESSION 3

### STUDIES ON CRYSTAL GROWTH AND THIN LAYER FORMATION

BY TEAS AND STM

*Boyan Mutafitschiev*

Laboratoire de Minéralogie-Cristallographie, Universités de Paris VI et VII  
F-75252 Paris Cedex 05, France

The continuously increasing requirement of microelectronics for thin layers, multilayer structures, and quantum wires with well defined surfaces or interfaces, triggered the recent development of powerful techniques for structural and morphological surface analysis on atomic scale. Most of them, however, based on conventional or high resolution transmission electron microscopy, are suitable either for *ex situ* observations, or make necessary heavy and sophisticated equipment, for *in situ* experiments. Same can be said for X-ray diffraction methods using synchrotron radiation.

Two relatively light and very complementary techniques emerged during the last decade, allowing *in situ*, studies of the topmost lattice plane of a crystal surface, and hence, of the dynamics of two-dimensional (2D) phase transformations, including crystal growth and thin filter formation.

The scanning tunneling microscopy (STM) permits the direct imaging, in the real space, of surface morphology, down to atomic features, thus providing information about the density and shape of 2D islands during growth or evaporation, the interaction between islands and moving growth lamellae, the structure of reconstructed surfaces or 2D layers on foreign substrate, etc. It is sometimes used to check the validity of results obtained by the less direct diffraction methods.

The impossibility of STM to look at the overall growth or nucleation processes on large surface areas, as well as the presumed damages, induced by the high current density at the tip on the surface of more frame substances, are only two

points on which is based the strength of the Thermal Energy Atom Scattering (TEAS) of supersonic quasi-monokinetic helium beams.

As by other diffraction methods, the measured spectra, diffracted intensity vs incident angle, are integrated over sample areas of several square millimeters. However, the very low kinetic energies of the helium atoms, of the order of 10 to 100 meV, make of the TEAS the most unperturbing method for surface analysis. Thanks these low energies, the measurement of energy lost (or gain) spectra, due to inelastic scattering, can be a precious tool for the characterization of 2D phases and their transformations.

Furthermore, the long range interaction potential between helium and target, provides for the isolated atoms, adsorbed on the target surface, effective scattering cross sections, of the order of  $100 \text{ \AA}^2$ . The subsequent attenuation of the reflected beam intensity thus enables measurements of extremely low adsorption coverages. Accordingly, surface occupancy laws, issued from different theoretical models, can be checked in the entire coverage interval from  $10^{-3}$  to 1. The method can be successfully used for studying the types of 2D phase transitions, surface disordering and 2D critical phenomena.

The talk is a review of some more significant results on surface growth and evaporation morphology obtained by the two techniques. At the end are presented our own TEAS studies on the formation of monomolecular overlayers of Pb on Cu(110).



## SESSION 3A

### GROWTH MECHANISMS AND MORPHOLOGY OF CRYSTALS

P. Bennema

RIM Laboratory of Solid State Chemistry  
Faculty of Science, University of Nijmegen  
Toernooiveld, 6525 ED NIJMEGEN  
The Netherlands

In the talk first of all a short survey will be given of modern theories on morphology of crystals. These theories consist of a logical integration of the Hartman-Perdok theory and statistical mechanical theories on thermal roughening and kinetical roughening. In passing recent examples of observed thermal roughening and kinetical roughening of paraffin crystals growing from an hexane solution will be discussed.

Next a brief survey will be given of theories which go beyond surface theories mentioned above, concerning the structure of the first layers of the mother phase, adjacent to the crystalline surface. Three types of theories can be distinguished:

- (1) functional density theories,
- (2) molecular dynamical models,
- (3) regular solution like theories.

It will be shown how from observed roughening temperatures and kinetical roughening of paraffin crystals growing from an hexane solution, actual bond energies occurring at the surface due to the structuring of fluid mentioned above can be calculated. It will also be shown how growth mechanisms are influenced by the structuring mentioned above.

Finally it will be shown briefly, how the occurrence of a new type of faces to be described by four integers (hklm): occurring on modulated crystals can be interpreted by a kind of generalisation of the Hartman-Perdok theory, by generalising the concept of chemical bond. Bonds are spread out as a continuum of bonds using an extra dimension and higher than three dimensional crystallography according to the crystallographic theory of de Wolff, Janner and Jansen.

Implication for crystal growth mechanisms on faces (hklm) will be discussed briefly.

---

### FACE STATISTICS ON THE DISSOLUTION FORMS OF GARNET CRYSTALS

E. Hartmann<sup>(a)</sup> and E. Beregi<sup>(b)</sup>

<sup>(a)</sup>Research Laboratory for Crystal Physics, Budapest, Hungary  
<sup>(b)</sup>Research Institute for Telecommunications, Budapest, Hungary

The crystal forms observed on natural garnets were collected by Goldschmidt [1]. On this basis Rinne and Kulaszewski [2] made a face statistics according to which the relative proportion of the faces {110} and {211} is about 75% on natural garnets. Bennema et al. [3] theoretically studied the morphology of garnets. It was shown by them that the relative morphological importance is given by a series {211}, {220}, {400}.

The dissolution forms of garnets crystals were investigated earlier very rarely [2,4,5]. In the last decade we have investigated systematically the dissolution forms of garnet crystals ( $R_3A_{(5-x)}B_xO_{12}$ , where R=Lu, Yb, Er, Ho, Y, Gd, Sm, Ca and Bi, A,B=Fe, Ga, Al, Sc, Ge, In and V,  $0 \leq x \leq 5$ ). Our first paper was published in 1983 [6]. The polished crystal spheres with a diameter of 0.6-0.8 mm were dissolved in various acids at different temperatures. The dissolution forms were investigated by a Jeol-JSM-35 scanning electron microscope.

Octahedron and tetrakisheptahedron faces occurred most frequently on the dissolution forms obtained by us. In the lecture we will report about the face statistics on dissolution forms of garnet crystals based on our results and those found in the literature.

---

- [1] V. Goldschmidt, *Atlas der Kristalformen* (C.F. Winter, sche Buchdruckerei, Heidelberg, 1918).
- [2] F. Rinne and L. Kulaszewski, *Tschermaks Mineral. Petrog. Mitt.* (NF) 38 (1925) 376.
- [3] P. Bennema, E.A. Giess and J.E. Weidenborner, *J. Crystal Growth* 62 (1983) 41.
- [4] R.B. Heimann, Auflösung von Kristallen, in *Applied Mineralogy*, Vol. 8. (Springer, Vienna, 1975).
- [5] R.B. Heimann and W. Tolksdorf, *J. Crystal Growth* 65 (1983) 562.
- [6] E. Beregi, E. Hartmann, J. Labar, E. Sterk and F. Tanos, *J. Crystal Growth*, 65 (1983) 562.

## ELEMENTARY PROCESSES OF DISSOLUTION; (101) ADP FACE

P.G. Vekilov

Institute of Physical Chemistry, Sofia 1040, Bulgaria

Yu.G. Kuznetsov and A.A. Chernov

Institute of Crystallography, USSR Academy of Sciences, Moscow 117333, USSR

X-ray topography and in situ laser Michelson interferometry combined with a two thermostat interswitchable growth system were applied to study the (101) ADP face during dissolution in undersaturated solutions as compared to growth. The movement of existing step patterns proved to be symmetrical with respect to growth and dissolution. Consequently, the two-dimensional anisotropy of the step pattern in case of dissolution is inversely symmetrical to the growth anisotropy. Uncontrolled impurities were inactive to growth at the conditions of the experiment. The limiting under-saturation for the appearance of the dislocation etchpit ( $\sigma^* \approx 0.5\%$ ) allowed us to estimate the Burgers vector/effective free surface energy ratio for one of the dislocation sources -  $b/\alpha = 5.3 \times 10^{-8} \text{ J}^{-1} \text{ m}^3$ . Hence, the most probable value of the effective free surface energy of the step riser on the studied face  $\alpha = 29 \text{ erg/cm}^2$  which

confirms the value determined in growth experiments. The dependence of the etchpit slope on the undersaturation gave the dimensionless rotation frequency of the spiral in undersaturated solutions  $\omega = 1.19$ . Etching of micro-defects and colloid size particles present in the crystal was observed. Mutual retardation of steps during dissolution and regeneration of the crystal edges and in the dislocation etchpits indicates a strong step (most probably surface) diffusion field overlap. The (100) ADP face dissolves in a slightly supersaturated solution presumably due to excess stress. Etching of vicinal boundaries was observed and the existence of limiting supersaturation for it helped us to propose a new model of vicinal sectorial boundaries - accumulated impurities there lead to elastic stress, observed by X-Ray topography.

## INTERSTEP INTERACTION IN SOLUTION GROWTH (101) ADP FACE

P.G. Vekilov, Yu.G. Kuznetsov and A.A. Chernov

Institute of Crystallography, Academy of Sciences of the USSR

Leninskii pr, 59, Moscow 117333, USSR

Michelson interferometry was applied to study dependences of the tangential velocity  $v$  of the growth steps on supersaturation for various dislocation sources.

It is experimentally shown that the tangential velocity increases with supersaturation weaker than linearly and  $v(\sigma)$  curve lies the lower the stronger the dislocation source.

To check whether the  $v(\sigma)$  nonlinearity comes from the step density, i.e. of hillock slope  $p$  only the slope and supersaturation have been changed independently one from another. For that, a new setup with two rapidly ( $\approx 10$  s) interchangeable tracts in which solutions with two different supersaturations were circulated was used. At  $p=\text{const}$ , the  $v(\sigma)$  dependence turns out to be linear. The slope of this  $v(\sigma)$  line decreases when  $p$  increases. The effect is not sensitive to the solution flow rate, i.e. is determined by processes on or at the interface.

Contrary to the prismatic face, the obtained results have been interpreted in terms of surface diffusion in which case anisotropy of vicinals appeared during growth and dissolution

is attributed to the anisotropy of surface diffusion length,  $\lambda_s$ . The latter was determined experimentally from the average interstep distance for the minimal slope at which the nonlinearity of  $v(\sigma)$  starts. The  $\lambda_s$  values for the 3 azimuthal directions normal to the triangular hillock slope were found. These values turns out to be proportional to the minimal interatomic distances in the atomic structure of the (101) face. Temperature dependence of  $v(\sigma)$  gives activation energies for  $\lambda_s \approx (31.0 \pm 1 \text{ kJ/mol})$  and step propagation (65 kJ/mol for  $T < 40^\circ\text{C}$  and 47 kJ/mol for  $T > 40^\circ\text{C}$ ). These dependences suggest that preferentially triple and double steps move at  $29 < T < 40^\circ\text{C}$  and single steps at  $40 < T < 67^\circ\text{C}$ . Entropy repulsion of steps at elevated temperature might be one of the reasons.

Since conventional surface diffusion model seems to be problematic for solution growth a possibility of partly ordered subsurface layer several intermolecular spacing this is discussed.

IN SITU OBSERVATION OF PROTEIN CRYSTAL GROWTH BY  
ATOMIC FORCE MICROSCOPY

Stephen D. Durbin and Warren E. Carlson

Department of Physics and Astronomy, Carleton College, Northfield, MN 55057

We have used atomic force microscopy (AFM) to observe growing crystals of the protein lysozyme in their mother liquor.<sup>1</sup> To date we have not resolved individual protein molecules, but we have clearly seen the edges of layers that are one or two molecules high. Images of the crystal surface show the time course of nucleation, spreading, and merging of two-dimensional islands to form successive layers of the crystal. From these images we obtained step velocities and rates of two-dimensional nucleation of new islands. As deduced previously from electron microscopic observations of surface step patterns,<sup>2</sup> the step velocities are anisotropic. Both step velocities and nucleation rates increase rapidly with supersaturation.

We have frequently observed both small and large macrosteps (5-100 closely spaced, unit height steps) on crystals growing at relatively low supersaturation. In the cases studied so far, the macrosteps move at the same velocity as the unit height steps. This implies that two-dimensional diffusion of molecules over terraces to attachment sites at steps is not a rate-limiting factor under these conditions.

Most of the surfaces observed have been lacking in visible defects (though there may be unresolved ones). On such surfaces, the nucleation of new islands appeared to occur at random sites on successive layers, i.e. there was little or no repeated nucleation such as might be expected from certain types of lattice defect. We have also observed other surfaces possessing obvious defects or clusters of defects. As successive layers grew on the crystal, these defect centers were sometimes healed over, sometimes maintained unchanged from layer to layer, and sometimes became active sources of new islands. By rapid and repeated formation of new islands, the defect centers could produce macrosteps.

The AFM technique offers not only a means of viewing a growing crystal surface, but also the possibility of making modifications to the surface and monitoring the response of the system. For example, we have removed portions of a layer by scanning with a high force between tip and sample, then watched regrowth when the force was lowered.

---

1. S.D. Durbin and W.E. Carlson, *J. Crystal Growth*, in press.
2. S.D. Durbin and G. Feher, *J. Mol. Biol.* **212** (1990) 763.

**GROWTH MECHANISM OF LONG CHAIN MOLECULAR CRYSTALS  
ON KCL SUBSTRATE DUE TO ANNEALING**

*Mikihiro Yamanaka, Kohji Minura, Kiyoshi Yase and Kiyotaka Sato*

Faculty of Applied Biological Science, Hiroshima University

1-4-4 Kagamiyama, Higashi-Hiroshima 724, Japan

*Kimio Inaoka*

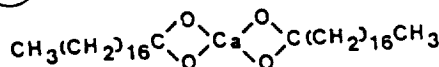
Yuge Merchantile Marine College, Yuge-cho, Ohchi-gun, Ehime 794-25, Japan

It has been found that a long chain compound, calcium stearate ( $(CH_3(CH_2)_{16}COO)_2Ca$ : fig. 1), grew epitaxially and arranged parallel to the substrate surface, when it was evaporated onto KCl kept at 25°C, as shown in fig. 2 [1-3]. After annealing at 30-115°C, the deposited crystals grew in length and the molecular orientation converted from parallel to normal as shown in fig. 3 [4,5]. The molecular dynamics on the surface was investigated by electron microscopic observation to be made clear as follows: at moderate temperatures of substrate below 60°C, the molecules removed from the original slender crystals, migrated on the substrate surface, and were absorbed onto more stable crystals, which elongated with increasing the annealing temperature and time. By contrast, above 60°C of annealing temperature, the nuclei having molecular orientation normal to the substrate were created, and pla-

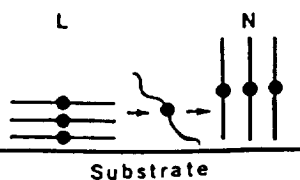
nar thin crystals grew. The activation energies for growing the slender crystals and converting the molecular orientations were evaluated ca.43 and 33 kJ/mol, respectively.

- [1] T. Miki, K. Inaoka, K. Sato & M. Okada, *Jpn. J. App. Phys.* 24(1985)L672.
- [2] K. Inaoka, K. Yase & M. Okada, *Appl. Surface Sci.* 33/34(1988)1293.
- [3] K. Yase, T. Inoue, K. Inaoka & M. Okada, *Jpn. J. Appl. Phys.* 287(1989)872.
- [4] M. Yamanaka, K. Yase, K. Inaoka & K. Sato, submitted to *J. Cryst. Growth*.
- [5] K. Yase, M. Yamanaka & K. Sato, *Appl. Surface Sci.*(1992) in press.

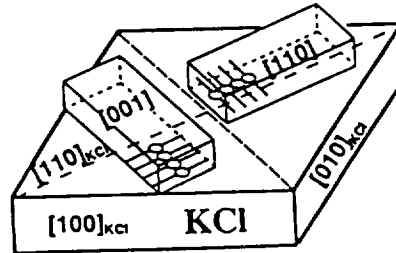
①



③



②



**IN-SITU X-RAY TOPOGRAPHY AND INTERFEROMETRY TO STUDY  
SOLUTION GROWTH MECHANISMS**

*Yu.G. Kuznetsov*

Institute of Crystallography, Academy of Sciences of Russia  
Leninskii Pr. 59, Moscow 117333, Russia

The optic and ex-situ X-ray topography studies showed the dislocations were the growth step sources. The progress in the in-situ X-ray topography and the interferometry enables to get not only qualitative estimations but and the quantitative ones of the growth process characteristics.

Due to these methods some phenomenon occurred during crystal growth from aqueous solution was understood and the quantitative values of some growth parameters were received:

- growth kinetic of each crystal face is bound up with the dislocation structure of the crystal and depends on the structure of the complex dislocation sources which are changed during crystal growth;
- on the crystal faces having the azimuthal anisotropy of the growth step motion the edges of the dislocation growth hillock form the flat vicinal sectorial boundaries

into the crystal body due to the different capacities of the growth steps to capture the impurities;

- the complex dislocation source model enabled to determine the total Burger's vector of the source and free surface energy of the growth step riser;

- the growth step kinetic on (101) ADP face is described in terms of the surface diffusion model and the elementary jumps of the absorbed particles along the surface set the kinetic coefficients in defined by the face crystallography;

- The step structure of the growth hillock changes with the temperature. The average height of the growth steps depends on the Burger's vector of the dislocation source. At  $T < 40^\circ\text{C}$  the average height decreases with the increasing of the temperature and at  $T > 40^\circ\text{C}$  one is constant and has the height equal to the lattice parameter.



## SESSION 3B

### DEFECT STRUCTURES IN $\text{LiNbO}_3$ WITH DIFFERENT COMPOSITION

*N. Iyi, K. Kitamura, F. Izumi, J.K. Yamamoto, H. Hayashi\*, H. Asano\*\* and S. Kimura*

National Institute for Research in Inorganic Materials, Namiki 1-1, Tsukuba-shi, Ibaraki 305, Japan

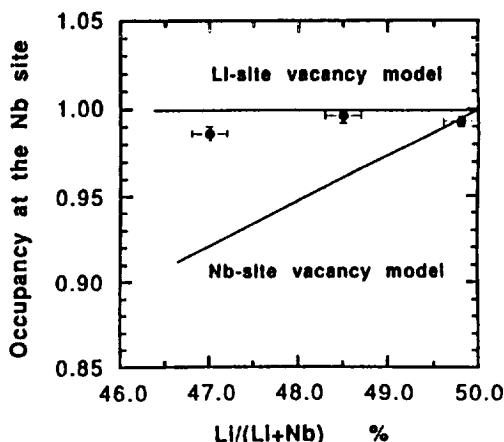
\*Tsukuba Asgal Co., Ltd Tokaidai 5-5, Tsukuba-shi, Ibaraki 300-26, Japan

Institute of Materials Science, University of Tsukuba, Tsukuba-shi, Ibaraki 305, Japan

The structure refinement was conducted on  $\text{LiNbO}_3$  crystals with 4 different composition by the X-ray single crystal diffraction method and the TOF neutron powder diffraction (KEK, Japan) method to clarify the major defect mechanism of  $\text{LiNbO}_3$  governing its nonstoichiometry. The composition covers from near-stoichiometry ( $\text{Li}/(\text{Li}+\text{Nb}) = 0.498$ ) to high nonstoichiometry ( $\text{Li}/(\text{Li}+\text{Nb}) = 0.470$ ). The specimens were taken from the single crystals grown by the floating zone and Czochralski methods, whose composition had been characterized by the chemical analysis, lattice parameters and the Curie temperature.

So far three defect models were proposed for  $\text{LiNbO}_3$ . On the basis of density data, two "cation substitution model" - "Li-site vacancy model" and "Nb-site vacancy model" - were chosen and examined in the refinements. The former is expressed in chemical formula as  $[\text{Li}_{1-5x}\text{Nb}_x\square_{4x}][\text{Nb}]\text{O}_3$  and the latter  $[\text{Li}_{1-5x}]\text{Nb}_{5x}[\text{Nb}_{1-4x}\square_{4x}]\text{O}_3$ , where  $\square$  stands for vacancy. At present, the "Nb-site vacancy model" is the generally accepted  $\text{LiNbO}_3$  defect model. The present refinement results revealed that the amount of Nb occupancy was composition-independent (See Figure) and indicated that  $\text{Li}^{++}$  ions were replaced by the  $\text{Nb}^{5+}$  ions creating vacancies at the Li site. For example, the final anisotropic refinement under the compositional constraint resulted in  $[\text{Li}_{0.948(3)}\text{Nb}_{0.011(3)}\square_{0.041(3)}][\text{Nb}_{0.996(4)}]\text{O}_3$  for the congruent

$\text{LN} (\text{Li}/(\text{Li}+\text{Nb}) = 0.485)$  with  $R=1.03\%$  and  $wR=1.24\%$ . When the "Li-site vacancy model" was assumed in the Rietveld analysis of the neutron diffraction data, reasonable results were obtained; on the other hand, the "Nb-site vacancy model" yielded worse R-factors and negative temperature parameters at the Li site for nonstoichiometric  $\text{LiNbO}_3$  specimens. These results are consistent with the "Li-site vacancy model."



PARTITIONING OF INTRINSIC SPECIES DURING PHASE EQUILIBRIA AND  
CRYSTALLIZATION OF  $\text{LiNbO}_3$  MELTS

Satoshi Uda and William A. Tiller

Department of Materials Science and Engineering  
Stanford University Stanford, CA 94305-2205, USA

Lithium niobate melts contain seven intrinsic species created by dissociation and ionization reactions[1]. These species are  $\text{LiNbO}_3$ ,  $\text{LiNbO}_3$ ,  $\text{Nb}_2\text{O}_5$ ,  $\text{Li}^+$ ,  $\text{OL}^-$ ,  $\text{Nb}_2\text{O}_4\text{V}_0^{2+}$  and  $\text{O}^{2-}$ . In this report, phase diagram solute partition coefficients,  $k_0$  and partial liquidus slopes,  $m_L$  for these intrinsic species are calculated over a 30°C range immediately below the congruent liquid liquidus point by using the population data of intrinsic species in the  $\text{LiNbO}_3$  melt along the liquidus line (Fig 1 for the Nb-rich side)[1] combined with the published phase diagram, ionic conductivity and diffusivity data for  $\text{Li}^+$  and  $\text{O}^{2-}$  in crystalline  $\text{LiNbO}_3$ . The constraints used for solving for the seven values of ( $k_0$ ,  $m_L$ ) are; (1) two constraints for the phase diagram collective results for  $\text{Li}_2\text{O}$  and  $\text{Nb}_2\text{O}_5$  using the pub-

lished phase diagram, (2) two constraints for effective stoichiometry in the solid for  $\text{Li}_2\text{O}$  and  $\text{Nb}_2\text{O}_5$  and they are equivalent to the charge neutrality constraints, (3) the concentrations of two ionic species,  $n^{\text{Li}^+}$  and  $n^{\text{O}^{2-}}$  in the crystal are calculated via the Nernst-Einstein equation using the published ionic conductivity data and diffusivity data for these ions, and (4) we assume  $k_0\text{LiNbO}_3 = 1$  since it is the solvent. One of our results is illustrated in Fig 2 showing the variation of  $K_0$  along the Nb-rich liquidus line around the congruent liquid point.

[1] S. Uda, W.A. Tiller, Submitted to *J. Crystal Growth*.

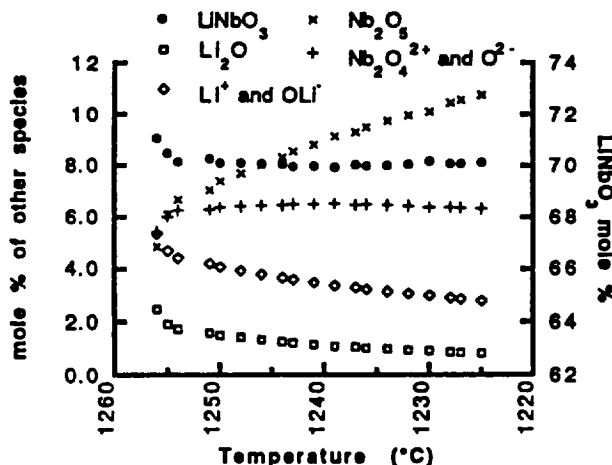


Figure 1

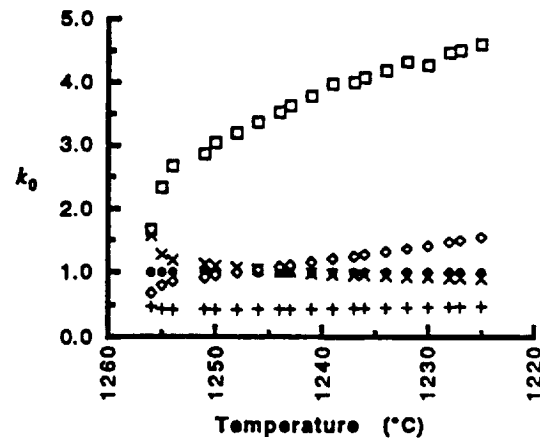


Figure 2

## CONTROL OF CRYSTAL-MELT INTERFACE SHAPE DURING GROWTH OF

### LITHIUM NIOBATE SINGLE CRYSTAL

*A. Hirata, M. Tachibana and T. Sugimoto*

Department of Chemical Engineering, Waseda University

3-4-1 Ohkubo, Shinjuku-ku, Tokyo 169, Japan

*Y. Okano and T. Fukuda*

Institute for Materials Research, Tohoku University

2-1-1 Katahira, Aoba-ku, Sendai 980, Japan

Convective phenomena during CZ growth of single crystal affect crystal-melt interface shape, that is quality of grown single crystal. In this study, in order to control crystal-melt interface shape, the effect of convective phenomena on crystal-melt interface shape during growth of single crystal were studied experimentally.

Single crystals of lithium niobate were grown using a RF heated CZ puller with 50 mm diameter crucible. During growth of crystals, temperature distributions along the crucible wall were measured using thermocouples and the weights of grown crystals were measured using load cell.

The critical crystal rotation rate where inversion of crystal-melt interface occurred were evaluated from the weight change of grown single crystal. Melt depth almost did not affect the

critical crystal rotation rates. Increasing the crystal radius, critical crystal rotation rate decreased. The authors have theoretically studied about the control of crystal-melt interface shape and proposed the correlated equations about critical crystal rotation rate under various conditions[1]. In this study, critical crystal rotation rate was depend on the Marangoni number and there was good agreement between the proposed equation under Marangoni convection dominant condition and experimental results. This suggested that Marangoni convection was dominant in the melt and it can be said that it is possible to control crystal-melt interface shape according to this results.

[1] Y. Okano et al., *J. Chem. Eng. Japan* **22** (1989) 389.

---

## ORGANIC-ON-INORGANIC SEMICONDUCTOR MOLECULAR BEAM EPITAXY

*Norbert Karl*

3. Physikalisches Institut der Universität Stuttgart, Germany

Organic materials, in contrast to inorganic materials, possess the potential of tremendous structural variability, as Nature has clearly demonstrated in living beings. Motivated therefrom synthetic chemistry has developed methods of creating nearly any imaginable molecular structure that does not contradict elementary physical principles.

Thus it has been possible to gradually increase the conductivity of organic crystals from photoconduction over dark-semiconduction to high quasi-metallic conduction, and even organic superconductors were found, with a slope of the  $T_c$  versus (calendar) time curve much steeper than for any other class of superconductors. There are now organic ferroelectric and ferromagnetic materials, and crystals exhibiting optical nonlinearities that by far exceed all previously known values. Highly selective organic electrochemical and electrophysical sensors are conceivable. Besides liquid crystal displays and dispersed electrophotography composites, cheap organic materials may soon conquer such fields as thin film field effect transistors, solar cells, environmental sensors, electrooptical and photochromic optical switch and memory structures.

This contribution will trace out that such ideas are no longer the progeny of science fiction but are gradually shaping up while progress is evolving in small but firm steps.

Molecular beam epitaxy, in combination with ultra-high vacuum and with the surface and thin film analytical techniques possible therein (e.g. low energy electron diffraction, LEED, thermal desorption spectroscopy, TDS), appears to become one of the most important techniques for basic research as well as for application-oriented development in this field. Subsequent further characterization of the produced thin films by X-ray diffraction and X-ray absorption (NEXAFS), by high energy electron microscopy and diffraction, as well as by scanning tunneling microscopy (STM) proves extremely helpful.

Specifically, fundamental aspects of organic epitaxial thin film formation on inorganic substrates like silicon, graphite,  $\text{MoS}_2$ ,  $\text{GeS}$  and mica will be discussed, and results with substances such as coronene, ovalene, hexa-peri-benzocoronene, perylene-3,4,9,10-tetracarboxylic-dianhydride ("PTCDA") and palladium-phthalocyanine: iodine will be presented.

## GROWTH OF A FIRST ORGANIC PHOTOREFRACTIVE CRYSTAL

J. Hulliger and Y. Schumacher

Institute of Quantum Electronics

Swiss Federal Institute of Technology, 8093 Zürich, Switzerland

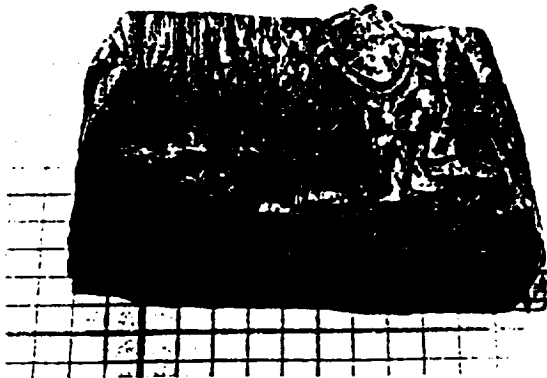
Space charge induced photorefractive effects of inorganic crystals (e.g.  $\text{LiNbO}_3$ ,  $\text{BaTiO}_3$ ,  $\text{KNbO}_3$ ,  $\text{GaAs}$ ) are known for more than 20 years. Recent growth of 2-cyclooctylamino-5-nitropyridine (COANP) doped by derivatives of the electron acceptor 7,7,8,8-tetracyanoquinodimethane (TCNQ) produced a first organic photorefractive single crystal [1,2]. Optical quality crystals of pure and doped COANP were obtained either by seeded (dipped or pulled) growth from a supercooled melt [3,4] as well as by solution growth using a temperature lowering procedure assisted by a laminar flow of nutrient directed toward the seed.

Dissolution of TCNQ at 80°C in a superheated COANP melt resulted in a dark green nutrient, containing  $\sim 1000$  ppm of  $[\text{TCNQ}]_2^{-2}$  after some time. Seeded growth at supercoolings of 0.5 - 1.5 °C yielded transparent olive-green crystals showing an extra optical absorption band at 650 nm typical for  $[\text{TCNQ}]_2^{-2}$ .

In contrast to solution grown pure COANP and melt grown pure and doped COANP, solution growth using acetonitrile and

TCNQ produced habit-modified (showing (0 1 l) facets) doped COANP crystals of a brownish-orange colour. For various growth media COANP typically shows faceting only for (h 0 l) faces and fast growth proceeds along the c-axis. Pyroelectric measurements revealed that COANP and several similar polar crystals (classes mm2 and 2) of amino-nitro-pyridine/benzene systems propagate preferentially along the electrically negative end of the polar axis.

- [1] K. Sutter, J. Hulliger, and P. Günter, *Solid State Commun.* 74, 867-870 (1990).
- [2] K. Sutter and P. Günter, *J. Opt Soc. Am. B* 7, 2274-2278 (1990).
- [3] J. Hulliger, Y. Schumacher, K. Sutter, O. Bezina, and H. Ammann, *Mat. Res. Bull.* 26, 887-891 (1991).
- [4] J. Hulliger, O. Brezina, and M. Ehrensperger, *J. Cryst. Growth* 106, 605-610 (1990).



As grown (olive-green) transparent doped COANP crystals: dipped and rotated in a supercooled melt (left, 6 x 8 x 14 mm), pulled from a supercooled melt (right, 8 x 8 x 12 mm).

## HIGH EFFICIENCY AGILE LASER MATERIALS: BINARY ORGANIC CRYSTALS

*N.B. Singh, T. Henningsen, R. Hamacher, E.P. Supertzi, R.H. Hopkins and R. Mazelsky*

Westinghouse Science and Technology Center, Pittsburgh, PA 15235

*F.K. Hopkins and D.E. Zelmon*

Materials Directorate, Wright Research Laboratories, Wright-Patterson, AFB, OH 45433

Organic crystals have shown a very large magnitude of high order polarizabilities. This offers great potential for their application as the second harmonic and higher order harmonic frequency converters in the short wavelength region. For these applications, organic crystals with a low optical absorption, high threshold to laser power damage, a high homogeneity in refractive index and low thermal and mechanical strain are required.

We have carried out detailed experiments on the purification, crystal growth and characterization of pure and binary substituted nitroanilines. Crystals grow by the Bridgman method showed both good optical quality and a high damage

threshold. For example when tested up to  $100 \text{ MW/cm}^2$  the crystals showed no sign of any deterioration. The SHG efficiency of CNA-m.NA alloy crystal was several times larger than pure compounds. The measured values project an efficiency over 75% for a 1 cm crystal operated at energy densities below the damage threshold power. These results will be compared with those for existing commercial crystals applied to the conversion of 1.06 micrometer wavelength.

We are grateful to Ms. Debbie Todd for preparing the subject matter. The financial supported by Materials Directorate, Wright Laboratories at Wright-Patterson AFB, Ohio is gratefully acknowledged.

---

## THE GROWTH, STRUCTURAL AND OPTICAL CHARACTERISATION OF LARGE AREA, SINGLE CRYSTALLINE THIN FILMS OF 3-NITROANILINE (mNA)

*J.N. Sherwood and G.S. Simpson*

Department of Pure and Applied Chemistry  
University of Strathclyde, Glasgow G1 1XL

The use of organic materials in opto-electronic device systems will be more readily achieved if the organic material can be prepared in the form of single crystalline thin films or single crystal cored fibres. The classical organic non-linear optical material 3-nitroaniline (mNA) has been used as a model compound to study the growth of such materials in thin, single crystalline films.

We have used the excellent melt stability of mNA to grow from the melt phase (under ideal conditions) large area ( $1 \times 6 \text{ cm}^2$ ) films which vary in thickness from 5-20  $\mu\text{m}$ .

The use of the Laue X-ray technique has allowed the identification of the in-plane film orientation. The structural perfection of the films was assessed using glancing angle X-ray topography.

The optical characterisation of such films using a Maker fringe experiment has allowed a value for the  $d_{31}$  coefficient to be measured.

CRYSTAL GROWTH AND CHARACTERISATION OF THE ELECTRO-OPTIC MATERIAL,  
3-(1,1-DICYANOETHENYL)-1-PHENYL-4,5-DIHYDRO-1H-PYRAZOLE

*P. Halfpenny and J.N. Sherwood*

Department of Pure and Applied Chemistry, University of Strathclyde, Glasgow, UK

*S.N. Black, R.J. Davey and P.R. Morley*

ICI Chemicals and Polymers Limited, Research and Technology Department

The Heath, Runcorn, Cheshire, UK

There is currently considerable interest in the development of organic non-linear optic materials which, compared to their inorganic counterparts, have greater non-linearities and the prospect of higher optical damage thresholds. The title compound has recently been the subject of an extensive study (1) including molecular design, crystal structure, and electro-optic characterisation. The material crystallises in the non-centric space group Cc and exhibits a polar morphology which in common with many other organic crystals varies with growth solvent (2). This contribution deals with the growth kinetics and morphology of this material grown from ethyl acetate and

toluene solutions. Morphological predictions have been made using molecular mechanics calculations and the effect of solvent on growth along the polar axis has been used to make an absolute assignment. Characterisation of seed and as grown crystals has been made by selected volume Laue diffraction and X-ray section topography.

---

1. S. Allen, et al *J Appl Phys* **64** (1988) 2583.
2. R.J. Davey, *Current Topics in Materials Science* **8** (1982) 428.

---

**ZnGeP<sub>2</sub> CRYSTAL GROWTH STUDIES USING THE HORIZONTAL  
GRADIENT FREEZE TECHNIQUE**

*P.G. Schunemann and T.M. Pollak*

Lockheed Sanders, Inc.

MER15-1813, P.O. Box 868, Nashua, NH 03061-0868

Large, high optical quality ZnGeP<sub>2</sub> crystals have been successfully grown using the horizontal gradient freeze technique. Crack-free boules up to 19mm in diameter by 140mm in length exhibited superior optical uniformity and lower mid-infrared losses than the best results reported to date, allowing optical parametric oscillation to be demonstrated for the first time in this material. Further improvements in the reproducibility of the growth process are required, however, in order to make ZnGeP<sub>2</sub> readily available for tunable mid-infrared laser applications.

Crystal growth of ZnGeP<sub>2</sub> is complicated by a number of factors. Thermal expansion coefficients along the a- and c-axes differ by nearly a factor of two, and this anisotropy often leads to severe cracking, particularly in twinned or polycrystalline boules. Cracking can be minimized if low thermal gradients are used, but these conditions not only make seeding difficult but also tend to favor a concave solid/liquid interface, which allows secondary grains nucleated at the container wall to grow

in toward the center of the boule. Low thermal gradients also simplify stoichiometry control, which is vital to the final optical properties, by minimizing vapor transport of the volatile components (zinc and phosphorus).

The above trade-offs were evaluated by studying the effects of longitudinal and radial temperature gradients, growth rate, and boat material and geometry on the shape of the solid/liquid interface and the incidence of secondary nucleation. Solid/liquid interface shapes were determined by quenching experiments as well as by *in situ* observations using a transparent furnace. The results of this investigation, and their implications for the growth of ZnGeP<sub>2</sub> and related compounds, will be discussed.

---

Work supported by Wright Laboratory Materials Directorate (WL/MLPO), Wright Patterson AFB, Contract No. F33615-88-C-5438.

## NEW APPROACHES TO NONLINEAR OPTICAL MATERIALS

*Martin Fejer*

Stanford University

The development of media useful for nonlinear optical frequency conversion of moderate power solid state pump sources has been driven by continuing improvements in diode laser technology. Interactions such as waveguide second harmonic generation of blue light and resonant bulk devices put strict requirements on nonlinear crystals that are often difficult to meet with conventional media. The factor that limits the range of applicability of a given material is generally the combination of dispersion and birefringence necessary for phasematching. A method for circumventing this phasematching requirement is thus of considerable practical interest.

Quasi-phasematching (QPM) entails the use of periodic modulation of the nonlinear susceptibility to compensate for the velocity difference due to dispersion, and hence can be applied independent of the birefringence of the medium. Essentially any interaction in the transparency range of the medium can be phasematched by this means, using any of the components of the nonlinear susceptibility tensor (including the large diagonal components inaccessible to birefringent phasematching). The difficulty in applying QPM is the short spatial scale (typically several microns) needed for the modulation of the nonlinear susceptibility, which in most cases pre-

cludes the conceptually simplest implementation, slicing a crystal into thin plates and rotating every other plate by 180°.

Practical QPM requires a monolithic technique for patterning the nonlinear susceptibility of the medium. Over the past three years, rapid progress has been made by several groups in the use of ferroelectric crystals with periodically reversed domains for QPM in both waveguide and bulk interactions. In this talk, techniques for patterning the ferroelectric domains  $\text{LiNbO}_3$ ,  $\text{LiTaO}_3$ , and KTP are reviewed, along with results for visible and IR generation in waveguides, including recent reports of milliwatts of blue light by second harmonic generation (SHG) and tunable 2  $\mu\text{m}$  generation by differencing near infrared sources. Bulk periodically poled crystals, and their application to generation of as much as 2 watts of visible radiation by SHG will also be described. Other media with patternable nonlinear susceptibilities including polymer and semiconductor films, will also be discussed.

These media are "generic" in the sense that standard processing techniques applied to an available material allows it to be efficiently applied to a broad range of interactions. It is likely that a few such media will be able to satisfy the requirements for most nonlinear devices.



## SESSION 3C

### THM GROWTH OF BINARY AND TERNARY III-V SEMICONDUCTOR SINGLE CRYSTALS

*K.W. Benz*

Kristallographisches Institut, Universität  
D-7800 Freiburg, Germany

The Travelling Heater Method uses a liquid zone between a substrate crystal and a polycrystalline feed. III-V-Semiconductor single crystals can be grown by taking a metallic solution zone of group III elements.

Binary crystals e.g. GaSb, InP, GaAs have been grown at temperatures ranging from 500°C (GaSb) up to 950° (GaAs) with growth rates of about 2 mm d<sup>-1</sup>. Undoped crystals up to 25 mm diameter and several cm in length exhibit the quality of liquid phase epitaxial layers. Highly doped crystals like InP:S or GaAs:Zn were used to study the behaviour of the formation of kinetic type II-striations, which is strongly governed by the off-orientation of the phase boundary solid/liquid, the tempera-

ture gradient at the interface and the growth velocity. The striations type I due to time dependent convection in the solution zone were analysed to study the influence of an axial magnetic field up to 0,44 Tesla on thermal and solutal flow phenomena in the liquid zone.

Bulk ternary III-V's like  $Al_xGa_{1-x}Sb$  were successfully grown with a diameter of 25 mm and a length of more than 25 mm and a AlSb solid composition x in the range of 0,1 to 0,8. Results will be given on the structure and composition of the ternary feed material as well as on growth parameters and the axial and radial Al-concentration in the grown crystals.

---

### GROWTH OF $Al_xGa_{1-x}Sb$ AND GaSb BULK CRYSTALS WITH LIQUID PHASE ELECTRO EPITAXY (LPEE)

*G. Bischofink and K.W. Benz*

Kristallographisches Institut und  
Freiburger Material-Forschungszentrum, Universität Freiburg  
Hebelstraße 25, D-7800 Freiburg, Fed. Rep. of Germany

In liquid phase electro epitaxy (LPEE), the material transport of the diluted compounds in the metallic solution zone is initiated and sustained by passing a direct electrical current across the solution zone and the substrate-solution interface. The growth temperature of the whole system is constant during growth. The mechanism of material transport bases on Peltier cooling at the substrate-solution interface and on electromigration of the dissolved compounds in the solution zone. The growth is mainly governed by electromigration, whereas Peltier cooling produces an appreciable part of the growth velocity at the beginning of growth.

We report the growth of bulk  $Al_xGa_{1-x}Sb$  and GaSb crystals with a layer thickness of more than 3 mm with LPEE from a mathematical description which bases on the time dependent transport equation including electromigration.

A growth cell configuration was developed which allows growth of bulk crystals by using GaSb or  $(Al,Ga)Sb$  feed mate-

rial. The LPEE apparatus has a vertical setup to avoid thermal non symmetries in axial and radial direction. The crystals were grown with a Ga rich solution zone at temperatures of 500 and 550°C, the current density ranged from 2 to 15 A/cm<sup>2</sup>. The growth velocity (0.1 to 1.0 mm/day) depends in a linear way from the current density. GaSb substrates were used with (111)B and (100) orientation and diameter of 15 mm. The substrates had a thickness of 5 mm to establish a homogeneous current density through the substrate-solution interface caused by an inhomogeneous electrical resistivity distribution inside the substrate. The grown crystals were characterized with x-ray microprobe analysis, spatially resolved photoluminescence and by Hall measurements. The  $Al_xGa_{1-x}Sb$  crystals had a constant AlSb solid composition in axial and radial direction. Detailed information about the layer surface morphology, measurement results and growth parameters will be given.

## InGaAs MIXED CRYSTALS GROWN BY GRADIENT FREEZE, AND ROTARY BRIDGMAN METHODS

*Y. Hayakawa, M. Ando, T. Ozawa, T.J. Anderson\*, P.H. Holloway\*, B. Pathaney\* and M. Kumagawa*

Research Institute of Electronics, Shizuoka University,

Johoku 3-5-1, Hamamatsu-shi, Shizuoka 432, Japan

\*University of Florida, Gainesville, FL 32611, USA

ZnSe is a semiconductor with a wide direct energy gap (2.7 eV) at room temperature and is suitable for blue light emitting diodes, lasers and other opto-electronic devices. GaAs has been mainly used as a substrate for ZnSe, but there exists a 0.27% lattice mismatch between them. As this mismatch causes the generation of many dislocations and defects, the quality of ZnSe layers becomes poor.  $In_xGa_{1-x}As$  can be adjusted its lattice constant to that of a ZnSe layer by controlling the In composition ratio (x). However, it is very difficult to obtain large mixed crystals in a single crystalline state, because the constitutional supercooling is easy to occur ahead of a growth interface.

This paper describes growth morphologies and In composition profiles in  $In_xGa_{1-x}As$  mixed crystals grown by three methods. One method is a Gradient Freeze method (GFM). The temperature of the furnace was kept constant. The solute is

transported toward the interface under the temperature gradient, and the crystal is grown. Second method is a Vertical Bridgman Method (VBM). The crystal growth is made under the supersaturation by lowering the growth temperature. Third method is a Rotary Bridgman Method (RBM) which has been developed by us for the first time. A growth ampoule is rotated at high speed and then the growth is made by temperature region.

In conclusion, the In composition profile was uniform in crystals grown by GFM. In cases of VBM and RBM, the In compositions were gradually lowered as the crystal grew. The In composition gradient with respect to the grown distance was 0.02/mm for the VBM, and was 0.009/mm for the RBM. The high rotation of the growth ampoule improved the inhomogeneity of the crystal.

## GROWTH AND CHARACTERIZATION OF GaSb SINGLE CRYSTALS

*Frantisek Moravec*

Institute of Physics, Czechoslovak Academy of Sciences  
Cukrovarnická 10, 162 00 Prague - 6, Czechoslovakia

The GaSb single crystals are very important material as substrates for semiconductor lasers and detectors working in the long wavelengths infraregion ( $\lambda \geq 1.5 \mu\text{m}$ ). A comparative study on the growth of GaSb single crystals resulted in a conclusion that the most advantageous method seems to be the Czochralski method with hydrogen atmosphere. The influence of different orientation of seed on the Czochralski crystal growth of GaSb was investigated and was concluded that the tendency to polycrystalline growth and twinning increase in the following manner:  $<111>$ ,  $<112>$  and  $<100>$ .

The GaSb single crystals are of high chemical purity. The GaSb samples were measured by means of spark source mass spectroscopy. The concentration of all elements contained in crystals with the exception of oxygen and nitrogen is under 1 ppm. Dislocations in the  $<111>$  GaSb crystals were examined by chemical etching. It has been found that the dislocation density is not spread uniformly on the surface of the samples.

There were places on GaSb wafers where no etch pits were found, but some dislocations were usually observed near the edge of the wafers where agglomerations of dislocations were formed. The average etch pit density is under  $100 \text{ cm}^{-2}$  for all grown  $<111>$  GaSb single crystals.

Crystals grown from nearly stoichiometric melts yield the constant hole concentration  $1 - 3 \times 10^{17} \text{ cm}^{-3}$  whereas Sb-rich melt growth reduces the concentration from  $1 \times 10^{17} \text{ cm}^{-3}$  to  $3 \times 10^{16} \text{ cm}^{-3}$ . Indium and nitrogen as isovalent dopants does not affect substantially the concentration of natural acceptors which are the main source of the room temperature hole conduction in GaSb crystals. The electrical and optical methods support the conclusion that the residual acceptors in GaSb have a more complicated structure based on  $V_{\text{Ga}}\text{GaSb}$  complex. Finally, some potentially useful techniques for the modification of residual concentration of natural acceptors will be presented.

## NON-INVASIVE BULK CHARACTERIZATION OF GaAs AND Si WAFERS

A.F. Witt

Department of Materials Science & Engineering  
Massachusetts Institute of Technology  
Cambridge, MA 02139

Recent results are reported on non-invasive, macro- and micro-scale bulk defect analyses of GaAs and Si wafers. The characterization is based on NIR transmission microscopy (bright field, dark field and phase contrast) in conjunction with computational image analysis. The properties being investigated include, micro and macro-segregation of dopant (quantitative), residual stress dislocations (in doped and semi-insulating material), precipitates, surface damage, anneal-

ing effects and ion implantation effects. Time requirement for an analysis is in the fractional second range. Transmission data are digitally stored and can be used for correlation analyses with defects introduced during early device processing stages and ultimately through comparison with device performance and yield for the determination of application based property requirements. Approaches to the implementation of this analysis in a fab-line environment are discussed.

## DISLOCATION DISTRIBUTION ON X-RAY TOPOGRAPHS: RESIDUAL STRAIN AND COMPOSITION AND IMPURITY EFFECT IN LEC GaAs CRYSTALS ON THRESHOLD VOLTAGE SCATTERING ON THE SUBSTRATES

Yasuyuki Saito

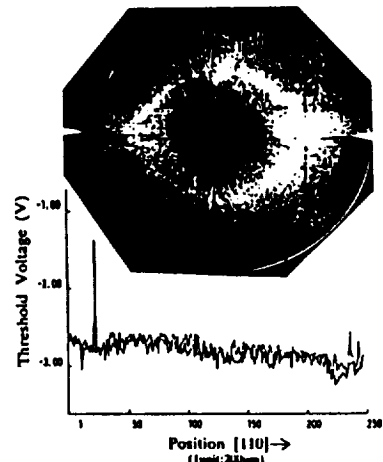
Microelectronics Center in Tamagawa Works, Toshiba Corp.  
1, Komukai Toshiba-cho, Saiwai-ku, Kawasaki 210, Japan

We have analyzed dislocation effect in liquid-encapsulated-Czochralski-technique (LEC) grown crystal boules on threshold voltage ( $V_{th}$ ) of Si-implanted metal-semiconductor-field-effect-transistors (MESFETs). The interesting contrasts of the dislocation distributions on the X-ray Lang topographs with the  $V_{th}$  scatterings across [110] direction have been obtained though there were some contrasts of noncorrelation between the dislocation distributions and the  $V_{th}$  scattering distributions [1,2,3,4]. For example, one of the topographs shows a four-fold-symmetrical pattern such as shown in the previous report.[5] The interesting contrasts have been analyzed as follows.

$V_{th}$  variation means the variation of implanted-Si-atom occupation ratio of Ga-site Si atom concentration  $[Si_{Ga}]$  to As-site Si atom  $[Si_{As}]$  in the GaAs crystals of conductive channel layers of the Si-implanted MESFETs. The occupation ratio  $[Si_{Ga}][Si_{As}]^{-1}$  depends on the structures of neighboring GaAs crystal cells on the implanted Si atoms through the bond length of a cell as the representative parameter of the GaAs crystal on the thermal equilibrium condition for thermal annealing.[6] Therefore,  $V_{th}$  distribution reflects GaAs crystal cell structure variation rather than impurity, such as carbon, distribution if the impurity concentration is low. The distribution of the cell structure variation depends on residual strain distribution involving composition distribution and impurity. We found that As-rich non-stoichiometry effect in As-rich-melt LEC-grown crystals pins residual strain distribution effect of dislocation on  $V_{th}$  scattering distribution as shown in Fig. 1.

We will present the contrasts of the dislocation distributions with the  $V_{th}$  distributions and the analyzed results for the interesting contrasts from viewpoints of induced residual strain involving composition and impurity during LEC boule growth.

SA-7-T



- [1] Y. Saito, K. Fukuda and S. Yasuami, the Extended Abstracts (The 52nd Autumn Meeting, 1991); Japan Society of Applied Physics, JSAP Catalog Num. AP-911125-01, page 266.
- [2] Y. Saito, submitted to *J. Appl. Phys.* (R2167), 1991.
- [3] Y. Saito, K. Fukuda, S. Yasuami, T. Fujii and M. Watanabe, submitted to *Jpn. J. Appl. Phys.* (1S0309, 1991).
- [4] Y. Saito, K. Fukuda, S. Yasuami, T. Fujii and M. Watanabe, the same abstracts as [1], page 267.
- [5] A.S. Jordan R. Caruso and A.V. Von Neida, *Bell Syst. Tech. J.* 59, 593 (1980).
- [6] Y. Saito, submitted to *J. Appl. Phys.* (R0550, 1991).

## NOVEL APPROACHES TO CRYSTAL GROWTH OF BULK TERNARY SOLID SOLUTIONS

J.J. Venkrbec<sup>1</sup>, Z. Cecil<sup>1</sup>, V. Rosicka<sup>2</sup>, J. Kohout<sup>2</sup>, J. Sedlacek<sup>1</sup>,  
Z. Kodejs<sup>3</sup> and P. Pacak<sup>3</sup>

<sup>1</sup>Czech Technical University in Prague, Fac. Electr. Eng., 16627 Prague 6

<sup>2</sup>Inst. of Radioelectronics

<sup>3</sup>Inst. of Inorganic Chem. - both Prague, Czechoslovak Acad Sci.

This work can partially contribute to the direct growth of bulk substrate crystals of TSS (Ternary Solid Solutions) - (Ga,In)Sb - with a lattice parameter "a" constant throughout the significant part of the ingot length. The combination of our original methods CAM-S (A Crystallization Method Providing Composition Autocontrol in Situ) and COM-S (Calculation

Method of Optimal Molten-Solution Composition) with a vibrational stirring enables to grow crystalline ingots with "a" apriori chosen and calculated - having the deviation from its constancy less than 0.033 % (0.2 ppm) on the 75 mm of a length. Crystals possess mosaic structure, at this stage.

---

## MATHEMATICAL MODELLING AND CONTROL SYSTEM DESIGN OF THE CZOCHRALSKI AND LEC PROCESS

G.A. Satunkin and A.G. Leonov  
USSR

In the work is preposed a new digital control system design based on a low order mathematical model (LOM) of CZ and LEC growth and weighing measurements [1].

Theoretical analysis of heat conditions in the meniscus and crystal part, and their changes during the deviation from stationary growth using asymptotic expansion make it possible to get the variation of the overage axial temperature gradients near the crystallization front. Take into consideration also the presence of a variable buoyancy force component in the output weighing signal we get the generalized non-stationary LOM by LEC with weighing control.

The control system for CZ process make full use of LOM and realized the more complicated criterion of controlling quality - limitation of crystallization rate variation. In the case was used optimal parametric (PID) multi-channel regulators [2].

For LEC process has been explain the difficulty using of PID regulators and preposed a new control system based on the identification of state variable vector wit a help of observers, and adjustment in optimal state regulator class. Also was investigated the question of full observability and controllability in the close state take into account the delayed components in output weighing signal. Heat inertia means corrections of control object and determination of variable delay time in observation signals have been completed the digital system design for LEC process with weighing measurement only.

---

1. G.A. Satunkin, A.G. Leonov, *J. Crystal Growth* 102 (1990) 592.
2. G.A. Satunkin, S.N. Rossolenko, *Cryst. Res. Technol.* 21 (1986) 1125.

## SESSION 3D

### SUBSTRATES FOR HIGH-T<sub>c</sub> SUPERCONDUCTORS

*Hans J. Scheel*

Crystal Growth Group, Institute of Micro- and Optoelectronics  
Swiss Federal Institute of Technology  
Chemin de Bellerive 34, CH-1007 Lausanne, Switzerland

Epitaxial layers of high-temperature superconductors (HTSC) and multilayer structures are required for numerous potential applications and for fundamental physical investigations of HTSC phenomena. Although HTSC layers with high T<sub>c</sub> and with remarkable critical current densities have been achieved, really single-crystalline epitaxial layers with required surface flatness could not be obtained so far[1]. For once, there are limitations in the experimental conditions of the mostly preferred physical deposition techniques like sputtering, laser ablation, MBE. Another limiting factor are the substrates: no substrate material is available which would allow layer-by-layer growth (as required for achieving quasi atomically flat surfaces), which has a misfit of less than 0.1% and a tolerable thermal expansion coefficient. Other requirements for HTSC substrates[2] are 1) no twinning due to structural phase transitions, 2) chemical interface stability during epitaxial growth, 3) congruent melting between 1600° and 2100°C for Czochralski growth, and 4) specific dielectric properties/microwave losses dependent on the application. The combination of these requirements, especially however the misfit conditions, make search for optimized substrates quite difficult.

Perovskite-type compound, ABO<sub>3</sub> offer the flexibility of mixed cations on the B-site[3], of doping on the A-site[4], and of complex solid solutions on both sites[5]. Drawbacks from these approaches arise from the complexity of the compositions and from the difficulty of economic growth of sufficiently homogeneous crystals. Another approach is growth of simple perovskite crystals like LaGaO<sub>3</sub>, NdGaO<sub>3</sub>, PrGaO<sub>3</sub>[2] and to solve the twinning problem (leading to surface corrugations

and deterioration of HTSC properties[6]) by a de-twinning procedure[7]. So far, PrGaO<sub>3</sub> could not be grown to good quality[8].

As nearly all perovskites show structural phase transitions, the potential of non-perovskite structure families should be explored for finding optimized substrates. For example, the K<sub>2</sub>NiF<sub>4</sub> and the gehlenite (ABC<sub>3</sub>O<sub>7</sub>) structures have been studied[2] by crystal chemical (theoretical) considerations and by experimental syntheses and lattice-parameter determinations. More efforts are still required to solve the substrate and the buffer layer problems for HTSC epitaxy and for a combined HTSC-semiconductor technology.

1. H.J. Scheel, M. Berkowski and B. Chabot, Proceedings 7th Intern. Conf. on Vapour Growth and Epitaxy (Nagoya, July 1991) and *J. Crystal Growth* 115 (1991) 19-30.
2. H.J. Scheel, M. Berkowski and B. Chabot, *Physica C* 185-189 (1991) 2095-2096.
3. C.D. Brandle and V.J. Fratello, *J. Mater. Res.* 5 (1990) 2160.
4. G. Koren, A. Gupta, E.A. Giess, A. Segmüller and R.B. Laibowitz, *Appl. Phys. Lett.* 54 (1989) 1054.
5. D. Mateika, H. Kohler, H. Laudan and E. Völkel, *J. Crystal Growth* 109 (1991) 447.
6. S. Miyazawa, *Appl. Phys. Lett.* 55 (1989) 2230.
7. M. Berkowski, M. Maamouri and H.J. Scheel, in preparation.
8. S. Miyazawa, private communication (July 1991).

---

### CONGRUENT COMPOSITION FOR GROWTH OF LANTHANUM ALUMINATE

*G.W. Berkstresser, A.J. Valentino and C.D. Brandle*

AT&T Bell Laboratories, Murray Hill, NJ

Single crystals of lanthanum aluminate have application as a substrate for deposition of thin films of the high temperature superconductors. Initial trials at Czochralski growth of this material revealed that only a small fraction of a stoichiometric melt may be crystalized before the onset of inclusions or voids at the growth interface. The composition of lanthanum aluminate

Czochralski grown crystals was analyzed using X-ray fluorescence with a special procedure for sample preparation. The crystal composition was found to be non-stoichiometric, with 0.987 gmoles of La per gmole of Al. Crystal growth from melts covering this composition range have confirmed that the greatest yield of good material comes with the above composition.

## VERTICAL GRADIENT-FREEZE GROWTH OF ALUMINATE CRYSTALS TO PROVIDE SUBSTRATES FOR HIGH-TEMPERATURE SUPERCONDUCTING FILMS

R.E. Fahey, A.J. Strauss and A.C. Anderson

Lincoln Laboratory, Massachusetts Institute of Technology  
Lexington, Massachusetts 02173-9108

With the objective of developing improved substrates for the deposition of thin films of  $YBa_2Cu_3O_x$  (YBCO) other high- $T_c$  superconductors, we have been investigating the use of the vertical gradient-freeze (VGF) method for growing crystals of two types of aluminates: (1) the rare earth orthoaluminates  $LaAlO_3$ ,  $NdAlO_3$  and  $DyAlO_3$ , and (2) the mixed aluminates  $SrAl_{0.5}O_3Ta_{0.5}O_3$  (SAT) and  $SrAl_{0.5}Nb_{0.5}O_3$  (SAN), which are cubic perovskite analogs of  $SrTiO_3$  in which half the  $Ti^{4+}$  ions are replaced by  $Al^{3+}$  ions and the other half by  $Ti^{5+}$  or  $Nb^{5+}$  ions. Single crystals of  $LaAlO_3$  and  $DyAlO_3$  up to 3 cm in diameter and  $NdAlO_3$  up to 5 cm in diameter have been grown by the VGF method in sealed tungsten crucibles. Melt growth of  $NdAlO_3$  and  $DyAlO_3$  crystals has not been reported previously. The growth charges are prepared by melting stoichiometric mixtures of  $Al_2O_3$  and the rare earth oxide in molybdenum crucibles. Initially, we used the VGF method for  $LaAlO_3$  with the goal of avoiding the extensive twinning that occurs in Czochralski-grown crystals as a consequence of the transition that occurs at  $\sim 500^\circ C$  from the high-temperature cubic form to the rhombohedral form that is stable at room temperature. The VGF crystals are water white, not yellowish or brownish like most Czochralski-grown  $LaAlO_3$  crystals, but are still heavily twinned. The VGF crystals  $NdAlO_3$ , from which the cubic-to-rhombohedral transition occurs at  $\sim 1500^\circ C$ , are also heavily twinned. In contrast, the  $DyAlO_3$  crystals are not twinned, because  $DyAlO_3$  (like  $NdGaO_3$ ) is orthorhombic at all temperatures. Thin films of YBCO with  $T_c$  of 90 K and low values of normal-state resistivity have been grown by off-axis magnetron sputtering on substrates cut from crystals of all three orthoaluminates. From experiments on a stripline resonator fabricated with YBCO/ $NdAlO_3$  components, the dielectric

constant of  $NdAlO_3$  was found to be 17.5, compared with 23 for  $LaAlO_3$ , but the loss tangent is much higher for  $NdAlO_3$ , probably because of magnetic transitions of the  $Nd^{3+}$  ions. We also plan to measure the dielectric properties of  $DyAlO_3$  by means of the resonator method.

The compounds SAT and SAN, which were first reported in 1990 [1], have recently been obtained in single-crystal form by pulling fibers from melts produced by laser heating [2]. To prepare charges for VGF growth of these materials, stoichiometric mixtures of  $SrCO_3$ ,  $Al_2O_3$ , and either  $Ta_2O_5$  or  $Nb_2O_5$  are fired in air at  $\sim 1500^\circ C$  in alundum crucibles, then melted under argon in molybdenum crucibles. Two unseeded growth runs, one on each compound, have been made to date. Both yielded large-grained polycrystalline boules. X-ray diffraction data for these slowly cooled boules indicate that the  $Al^{3+}$  and  $Ta^{5+}$  ions in SAT are strongly ordered, while the  $Al^{3+}$  and  $Nb^{5+}$  ions in SAN are only weakly ordered. We anticipate no major difficulty in growing single crystals with dimensions large enough to permit evaluation of these compounds as substrate materials for high- $T_c$  films.

This work was conducted under the auspices of the Consortium for Superconducting Electronic with support by the Defense Advanced Research Projects Agency (Contract MDA972-90-C-0021).

[1] C.D. Brandle and V.J. Fratello, *J. Mater. Res.* 5, 2160 (1990).

[2] L.E. Cross and R. Ray, Third Annual DARPA Workshop on High-Temperature Superconductivity, Seattle, WA, September 30 - October 2, 1991.

## MICROANALYTICAL CHARACTERIZATION OF FLUX GROWN

### $LaAlO_3$ SINGLE CRYSTALS

Ashok K. Razdan and P.N. Kotru

Department of Physics, University of Jammu  
Jammu Tawi, 180 001 India

B.M. Wanklyn

Department of Physics, Clarendon Laboratory  
University of Oxford, Oxford, OX1 3PU England

Results of scanning electron microscopic and energy dispersive X-ray analytical studies conducted on some microstructures displayed by the virgin (as-grown) and polished surfaces of single crystals of  $LaAlO_3$  are described. The crystals are grown from a  $PbO-PbF_2$  flux. Some irregular microelevations suffering elemental-compositional changes are noticed on the virgin surfaces. A few specific microregions are found to be deficient in rare earth ion; its replacement by lead gives rise to the secondary crystallization of lead compounds.

Also evinced is the deposition of platinum, and its traces are, albeit, accompanied by solidified flux. The microareas of polished surfaces also vindicate the formation of lead compounds, and thereby results in their trapping in the crystal as inclusions. The depositions of lead compounds and platinum on the virgin surface and the formation of former on the polished surface during the flux growth, and their implications on the crystal perfection are discussed.

## ANOMALIES IN CRYSTAL GROWTH BY CZOCHRALSKI TECHNIQUE

*A. Pajaczkowska<sup>a,b</sup> and P. Byszewski<sup>a</sup>*

<sup>a</sup>Institute of Physics, Polish Academy of Sciences, 02-668 Warsaw, Poland

<sup>b</sup>Institute of Electronic Materials Technology, 01-919 Warsaw, Poland

In the Czochralski technique the flat crystal/melt interface is used in growth the best quality single crystals. In our case the interface of grown crystals is strongly convex formed by crystallographic (101) planes, because the flat interface is unstable in the investigated crystals.

The considered crystals  $\text{CaNdAlO}_4$  (CNA) and  $\text{SrLaAlO}_4$  (SLA) belong to the group compounds with general formula  $\text{ABCO}_4$ , where  $\text{A} = \text{Sr, Ca}$ ;  $\text{B} = \text{Y or rare earth elements}$  and  $\text{C} = \text{Al, Ga}$  and which crystallize in the tetragonal structure of  $\text{K}_2\text{NiF}_4$ , where  $a=b$  and  $c=3a$ . Some of these compounds e.g. CNA and SLA melt congruently. The results of our investigations show the strong anisotropic behaviour reflected in thermal expansion coefficients vs temperature along  $\langle 100 \rangle$  and  $\langle 001 \rangle$  directions and by anisotropic dielectric properties. The measurements of the thermal expansion coefficient proved nonlinear  $a(T)$  dependence. These effects are explained in

terms of the phase transition observed also in DSC experiments.

The stability of  $\text{ABCO}_4$  structure is limited by ionic radius of all ions which form the crystal planes and we suppose that the effects may be explained by ions reordering in  $\text{ABCO}_4$  structure.

We found that the melt of  $\text{ABCO}_4$  polycomponent compounds is unstable and sensitive to initial stoichiometry and the crystal growth is strongly anisotropic, however, all crystals were pulled out without cracking and opaque inclusions and their cross section was size up to 300 mm<sup>2</sup>.

$\text{ABCO}_4$  single crystals are interesting as substrates for high  $T_c$  superconductors from the stand point of lattice matching and their dielectric properties.

---

## FLUX GROWTH OF SINGLE CRYSTALS OF $\text{Nd}_y\text{Pr}_{1-y}\text{GaO}_3$ SOLID SOLUTIONS

*H. Dabkowski, A. Dabkowski and J.E. Greidan*

Institute for Materials Research, McMaster University  
1280 Main Street West, Hamilton, Ontario, Canada. L8S 4M1

Single crystals of solid solutions between  $\text{NdGaO}_3$  and  $\text{PrGaO}_3$  have been obtained from  $\text{PbO-PbF}_2\text{-MoO}_3$  flux. The flux method allowed to grow single crystals up to 4.5x4x2 mm (from 20 ccm crucible) at temperature range 1260-1080°C.

The aim was to avoid the cubic to orthorhombic phase transition, usually causing twinning in this pseudoperovskite material. The chemical composition, its dependence on crystal growth conditions and the impurities level have been established by EPMA and by EDAX. Strong influence of chemical composition on the crystal quality has been observed.

The high resolution Guinier camera powder patterns have been used to determine lattice parameters and their changes with crystallization conditions. Because the lattice parameters, depending on composition, are in the range  $a=5.42\text{-}5.45$ ,  $b=5.50\text{-}5.52$ ,  $c=7.72$ , such solid solutions can be regarded as potential materials for substrates for thin films of  $\text{YBa}_2\text{Cu}_3\text{O}_x$  or  $\text{Pb}_2\text{Sr}_2(\text{Y,Ca})\text{Cu}_3\text{O}_x$  (and related Bi-based and Tl-based systems) superconductors.

## INVESTIGATION OF THE GROWTH OF NEIGHBORITE, $\text{NaMgF}_3$

S. Sengupta, A. Cassanho and H.P. Janssen

Laboratory for Advanced Solid State Laser Materials

Center for Materials Science and Engineering

Massachusetts Institute of Technology, Cambridge, MA 02139

The search for suitable crystals that can be used as substrates for high temperature superconductor films has led us to study the naturally occurring neighborite,  $\text{NaMgF}_3$ . Neighborite is a perovskite structured crystal, with low dielectric constant and lattice constants well matching the ones for the high  $T_c$  materials. The crystal undergoes two high temperature phase transitions<sup>(1)</sup>, first cubic to tetragonal (920C) and second tetragonal to orthorhombic (760C). The lattice constants are  $a=5.363\text{\AA}$ ,  $b=7.676\text{\AA}$  and  $c=5.503\text{\AA}$ . The mined crystal presents severe twinning<sup>(1)</sup> believed to be due to the phase transitions.

When we pulled the crystal from a stoichiometric melt it was initially clear, but became opaque when it underwent the first phase transition. Subsequent growth runs with NaF excess

in the melt resulted in clear crystals at room temperature. The best results were attained with a melt composition of 65% NaF. Crystals as large as 13 mm in diameter and 25 mm long were obtained. Polarized optical spectroscopy and X-ray analysis both reveal twinning due to the tetragonal to orthorhombic phase transition. The nature and orientation of the twin planes are currently under study and will be reported on.

(1) Chao et al., *The American Mineralogist* 46(1961)379.

This work was conducted under the auspices of the Consortium for Superconducting Electronics with full support by the Defence Advanced Research Projects Agency (Contract MDA972-90-C-0021).

## SINGLE CRYSTAL GROWTH OF RARE-EARTH GALLATES AND EPITACTIC GROWTH NATURE OF HIGH- $T_c$ SUPERCONDUCTING YBCO THIN FILMS ON THEM

S. Miyazawa, M. Sasaura and M. Mukaida

NTT LSI Laboratories, 3-1, Morinosato Wakamiya, Kanagawa 243-01, Japan

Epitaxial thin film of high  $T_c$  superconducting  $\text{YBa}_2\text{Cu}_3\text{O}_x$  (YBCO) is of current interest in both basic studies on superconducting behaviors and electronic device applications. A smooth surface of the as-grown film is strictly required to device applications such as an SIS junction. Then, the development of new substrate materials lattice-matched with YBCO is needed from the viewpoint of "epitaxial" film growth. In this paper, we present the single crystal growth of rare-earth gallates as substrates lattice-matched with YBCO, and early growth stages of YBCO ultrathin film on the substrates are demonstrated with AFM (Atomic Force Microscope) observations.

The gallate single crystals of  $\text{NdGaO}_3$  and  $\text{PrGaO}_3$  were grown by conventional rf-heating Czochralski pulling.  $\text{NdGaO}_3$  was twin-free, and single crystallinity showed as good as 25" of FWHM on an X-ray double-crystal rocking curve, while  $\text{PrGaO}_3$  still included twins and subgrains, resulting in 220" of FWHM. The twinning in  $\text{PrGaO}_3$  may be due to phase transitions just below the melting temperature. On these substrates, YBCO thin films were deposited by an ArF laser ablation. Single crystallinity of the film on  $\text{NdGaO}_3$  showed as good as 12" of FWHM, which is about one half that on an

usual  $\text{SrTiO}_3$ , while that on  $\text{PrGaO}_3$  was 24" of FWHM, due to poor crystallinity of the  $\text{PrGaO}_3$  substrate.

To investigate the early growth stages of the film, YBCO ultrathin film of about 20 $\text{\AA}$  in nominal thickness was deposited on the substrates. AFM observations revealed that the early growth stage of the film on lattice-mismatched  $\text{SrTiO}_3$  ( $\Delta d=1.06\%$ ) was of three-dimensional granular growth mode. This picture strongly suggests the growth mode of Volmer-Waber type. This mode resulted in irregular surface morphology on the final film of about 2000 $\text{\AA}$ , revealed by a field-emission type SEM. On the other hand, the early growth stage on the lattice-matched  $\text{NdGaO}_3$  ( $\Delta d=0.3\%$ ) and  $\text{PrGaO}_3$  ( $\Delta d=0.03\%$ ) substrates was verified to be of two-dimensional island formation. The islands had a height of 12 $\text{\AA}$  with a rectangular shape corresponding to the basal plane of orthorhombic/tetragonal YBCO lattice. The growth mode was of Stranski-Krastanov type. The as-grown surface morphology on the final film was certified to be very smooth by the SEM.

It can be concluded that new gallate substrates lattice-matched with YBCO are promising for two-dimensional epitaxial growth of YBCO. Nucleation-and-growth nature of YBCO thin films will be discussed.

## LPE OF HIGH-T<sub>c</sub> SUPERCONDUCTORS

C. Klemenz and H.J. Scheel

Crystal Growth Group, Institute of Micro- and Optoelectronics

Swiss Federal Institute of Technology

Chemin de Bellerive 34, CH-1007 Lausanne, Switzerland

Layers of high-temperature superconductors (HTSC) are mostly prepared by physical vapour deposition techniques including sputtering, laser ablation and MBE. These HTSC layers show high critical current densities  $J_c$  due to numerous defects. In contrast, LPE has the potential for structurally more perfect layers with atomically flat surfaces[1] as required for low- $J_c$  applications and for fundamental studies of HTSC phenomena.

However, a number of obstacles had to be overcome before LPE of  $\text{YBa}_2\text{Cu}_3\text{O}_{7-x}$  (YBCO) and related 123-HTSC could be achieved. The determination of the eutectic of the solvent system  $\text{BaCuO}_2\text{-CuO}$ [2] and the establishment of the primary crystallization field of YBCO[3] allowed to obtain the required composition/temperature/supersaturation conditions. The corrosion mechanism of commercial crucibles[4] showed that new crucibles had to be developed[5]. Another problem are the substrates, especially in LPE, where near thermodynamic equilibrium a very low misfit, of less than 0.2%, at the growth temperature is required to achieve layer-by-layer growth at tolerable (low) supersaturation[6]. Such low supersaturation is also required for the stable growth regime and for preventing spontaneous nucleation at the crucible walls.

With these prerequisites partially established, thick grain-boundary-free HTSC-123 layers up to presently 12 mm<sup>2</sup> could

be achieved for the first time. Nomarski interference contrast microscopy shows growth steps over macroscopic dimensions, whereas step structures on PVD-grown HTSC layers (islands) extend only over typically 200 nm[7,8].

Further systematic LPE work and substrate development are required to obtain large-area growth with controlled step heights on crack-free HTSC layers.

1. H.J. Scheel, G. Binnig and H. Rohrer, *J. Crystal Growth* **60** (1982) 199.
2. F. Licci, H.J. Scheel and P. Tissot, *J. Crystal Growth* **112** (1991) 600.
3. H.J. Scheel and P. Holba, *J. Crystal Growth*, submitted.
4. H.J. Scheel, W. Sadowski and I. Schellenberg, *Superconductor Science & Technol.*, **2** (1989) 17.
5. P. Bowen, M. Berkowski, T. Liechti and H.J. Scheel, *J. Amer. Ceram. Soc.*, accepted.
6. H.J. Scheel, M. Berkowski and B. Chabot, Proceedings of 7th Internat. Conf. Vapour Growth and Epitaxy, Nagoya 14-17 July 1991, and *J. Crystal Growth* **115** (1991) 19.
7. C. Gerber, D. Anselmetti, J.G. Bednorz, J. Mannhart, D.G. Schlom. *Nature* **350** (1991) 277.
8. M. Hawley, I.D. Raistrick, I.G. Beery, R.J. Houlton. *Science* **251** (1991) 1587.



## SESSION 4

### IN-SITU ANALYSIS OF ORGANOMETALLIC VAPOR PHASE EPITAXY USING GRAZING INCIDENCE X-RAY SCATTERING

*D.W. Kisker and G.B. Stephenson*

IBM Research Division, Yorktown Heights, NY 10598

*P.H. Fuoss, F.J. Lameiras and P. Imperatori*

AT&T Bell Labs, Murray Hill, NJ 07974

*S. Brennan*

Stanford Synchrotron Radiation Lab, Menlo Park, CA 94035

Despite the importance of chemical vapor deposition (CVD) as a critical process for semiconductor materials preparation, little is known about the detailed reactions and surface processes which occur. Unlike UHV techniques such as molecular beam epitaxy which make wide use of the electron based analytical tools such as Auger and RHEED, CVD techniques have in general been studied after the fact. Generally, films are deposited or grown, and then post-growth characterization is performed to try to understand what happened. Obviously, this approach is not likely to answer all the relevant questions regarding this important technology.

In this work, we have for the first time used x-ray scattering to begin to understand the detailed nature of chemical vapor deposition of compound semiconductors using organometallic sources: OMCVD. We have developed a purpose built reactor which incorporates a pair of beryllium windows which allows real-time x-ray scattering measurements during growth of GaAs and related compounds. Using this technique, we have made the first direct observation of these surfaces as this non-UHV process proceeds.

Our results indicate that although the surface reconstruction in a steady-state arsenic-containing environment is similar to MBE (i.e. c(4x4)), when growth is initiated, the surface changes dramatically with the reconstruction being completely

disrupted, perhaps by the presence of large amounts of organic by-products present during OMCVD. Despite this surface disruption, we have been able to establish conditions under which layer-by-layer growth occurs, as indicated by the observation of intensity oscillations which occur due to the cyclic nucleation and completion of single layers of material. In addition, we have observed a transition to step-flow growth at temperatures around 625°C. By analysis of the diffuse scattering of x-rays around the crystal truncation rod position at (110), we have made estimates of the maximum island size at the point where the oscillatory scattering is a minimum—where islands are beginning to coalesce. As the temperature of growth is increased, this maximum island size increases, until at the crossover to step-flow growth, no more oscillations occur, and the island size is comparable to the terrace width.

Equipped with such a tool for the in-situ monitoring of growth processes, we have also begun to do detailed characterization of the OMCVD process kinetics. We find that using this highly accurate growth rate probe for example, we can quickly establish the range of conditions where the process is limited by surface kinetics, for example. We will report the details of these and related experiments directed toward the understanding of the microscopic details of OMCVD.



## SESSION 4A

### THE BOUNDARY LAYER CONCEPT: A KEY TO SEGREGATION PHENOMENA IN CRYSTAL GROWTH FROM THE MELT

*J.J. Favier, J.P. Garandet and D. Camel*

CEA/DTA/CEREM/DEM, Section d'Etudes de la Solidification & de la Cristallogénèse  
Centre d'Etudes Nucléaires, 85 X, 38041 Grenoble Cedex

On the basis of existing experimental and numerical data, we first bring evidence of the existence of a solute boundary layer in front of the growth front during solidification. A general method is proposed to estimate its thickness  $\delta$  when the flow field in the vicinity of the interface is known. We then

show that  $\delta$  governs segregation phenomena in melt growth experiments. Finally, applications of this boundary layer concept are proposed in the fields of both macro- (axial and radial) and micro-segregation.

---

### ANALYSIS OF THE BRIDGMAN GROWTH OF SEMITRSPARENT CRYSTALS

*S. Brandon and J.J. Derby*

Department of Chemical Engineering and Materials Science  
University of Minnesota, Minneapolis, MN 55455

High-quality single crystals of materials such as neodymium-doped yttrium aluminum garnet (Nd:YAG) are required for the fabrication of high-average power, solid-state lasers. The production of crystals of sufficient size and quality is limited by an incomplete understanding of the growth process, especially the complicating effects of internal radiative energy transport, i.e. the radiative transport of energy through participating, condensed phases. A fundamental understanding of these effects is a prerequisite for improving the growth processes employed to produce these crystals.

We have developed a Galerkin finite element method to solve for heat transport via internal radiation, conduction, and convection in axisymmetric geometries. We will present a quasi-steady state model for the vertical Bridgman growth of semitransparent crystals [1,2]. The integro-differential equation describing combined radiation and conduction heat transfer is applied in the crystal, while combined convective and conductive heat transfer is assumed to dominate in the melt. Heat is also conducted through the ampoule walls, whose outer surface exchanges energy with the furnace via combined natural convection and enclosure radiation. The position of the melt/crystal interface is determined self-consistently by the isotherm method.

The vertical Bridgman growth of an oxide crystal with properties chosen to resemble those of yttrium aluminum gar-

net (YAG) is investigated. Results indicate that heat transfer through the system is strongly affected by the optical absorption coefficient of the crystal and that convective heat transfer through the melt is unimportant for this small-scale system. Coupling of internal radiation through the crystal with conduction through the ampoule walls promotes melt/crystal interface shapes which are highly deflected near the ampoule wall. This radiative interface effect is much more pronounced than that observed in the Bridgman growth of opaque crystals, where the interface deflection at the ampoule wall is attributed to the thermal conductivity mismatch between ampoule and charge [3]. Calculations demonstrate that a flatter overall interface shape can be achieved through optimization of ampoule material properties and furnace temperature profiles.

- [1] S. Brandon and J.J. Derby, "Internal radiative transport in the vertical Bridgman growth of semitransparent crystals," *J. Crystal Growth* **110**, 481-500 (1991).
- [2] S. Brandon and J.J. Derby, "Heat transfer in vertical Bridgman growth of oxides: Effects of conduction, convection, and internal radiation," *J. Crystal Growth*, submitted (1991).
- [3] T. Jasinski and A.F. Witt, "On control of the interface shape during growth in vertical Bridgman configuration," *J. Crystal Growth* **71** (1985) 295.

## RADIAL SEGREGATION IN FLOATING-ZONE CRYSTAL GROWTH

C.W. Lan and S. Kou

Department of Materials Science and Engineering  
and  
Center of Excellence in Solidification Processing  
Technologies of Engineering Materials  
University of Wisconsin  
Madison, WI 53706-1595

Radial segregation in floating-zone crystal growth under the steady-state condition was studied. A computer model was developed, considering heat transfer, fluid flow and mass transfer. Three different driving forces for flow were included, i.e., the buoyancy force, the surface-tension gradient and the cen-

trifugal force. The effects of these driving forces on radial segregation were investigated. Floating-zone growth of doped  $\text{NaNO}_3$  single crystals was conducted, and the measured radial segregation was used to check the computer model.

---

## FLUID PATTERNS IN THE DIFFUSIVE FIELD SURROUNDING A GROWING CRYSTAL

Juan Manuel García-Ruiz and Fermín Otálora  
Instituto Andaluz de Geología Mediterránea  
CSIC-Universidad de Granada

Revealing the concentration patterns in the solution surrounding a growing crystal (using several interferometric techniques) has been the object of many studies in the past because of its important role in the phenomena taking place on the crystal-solution interface. We use a crystal growth simulation program<sup>1</sup> designed to allow a fine tuning of the crystal morphology in the range between disordered dendrites to single crystals, to study the complex coupling between a diffusive field and a crystal growing from it. Our model is a modified multiparticle DLA in which, diffusional transport is simulated by random walking particles.

The concentration patterns we obtain from simulations show that the concentration gradients at the normal to any point on the crystal surface are similar in the case of single crystals but, for dendritic crystals, the main branches of the crystals cut the isotones as they penetrate into the regions of the solution at higher concentration. Therefore, the program led

one to clearly observe the Berg effect. We also observe the formation of a cellular arrangement in the diffusive field around the crystals. This pattern appears clearly when morphological instabilities are forming. The apparition of the cellular patterns linked to the existence of morphological instabilities and to Berg's effect let us to suspect that the last ones produce the break-out of the radial diffusive field and the formation of preferred flow lines. This cross-interaction between the crystal interface and its surrounding solution creates a convective flux. Once the morphological instability appears, the formation of this cellular structures reenforce the morphological pattern. Numerical simulations as the one presented here may help to evaluate the role of such fluid patterns in the control of crystal morphology. The limitations and possible enhancements of the simulations are discussed in the text.

1. Garcí-Ruiz & F. Otálora. *Physica A* 178 (1991) 415-420.

CHARACTERIZATION OF THE ONSET OF TURBULENCE IN LIQUID  
TIN IN A BRIDGMAN CONFIGURATION

*David J. Knuteson<sup>1</sup>, Archibald L. Fripp, William J. Debnam, Jr., and Glenn A. Woodell*

NASA-Langley Research Center

*Ranga Narayanan*

University of Florida

It has been shown that crystals directionally solidified from a thermally time-dependent melt have a larger defect density and increased occurrence of compositional striations. Thus, it is important to better understand the different convection flow regimes and flow patterns that occur under various furnace conditions. Thermocouple measurements from a Bridgman ampoule will be presented for the case when the molten tin inside changes from a simple oscillatory flow regime to turbulence. Although not the normal Bridgman orientation, the ampoule is heated from below to facilitate the study of unsteady convection. The cell wall is instrumented with thermocouples at various vertical positions and azimuthal angles.

Phase relationships of temperature oscillations from the thermocouples will be used to obtain data on convection flow cells. Fast Fourier transforms (FFTs) of temperature measurements will be used to clarify the mechanism of the transition to turbulence. There are currently three major scenarios for the onset of turbulence, and the FFT data will reveal which mechanism applies to this system. The FFT measurements are designed to enable high resolution at the low frequencies that are characteristic of thermal oscillations in liquid metals.

1. Department of Materials Science, University of Virginia.

---

EFFECT OF TURBULENCE MODELLING ON THE PREDICTIONS OF AN INTEGRATED  
THERMAL-CAPILLARY MODEL FOR CZOCHRALSKI CRYSTAL GROWTH

*Thomas A. Kinney and Robert A. Brown*

Department of Chemical Engineering

Massachusetts Institute of Technology, Cambridge, MA 02139

Convection in large-scale Czochralski (CZ) systems for the growth of silicon and other optoelectronic materials is at least chaotic and three-dimensional. The computation of this flow and its effect on the temperature and composition fields in the melt and crystal is beyond current simulation capabilities, especially when models account for the complexity of radiation and coupled heat transfer between the elements of the furnace. The purpose of this work is to examine the potential for using turbulence models, in conjunction with an integrated thermal-capillary model for the CZ system, to describe heat transfer and solute redistribution. Turbulent convection is accounted for by the Reynolds equations for momentum and energy transport and ke-model for turbulent fluxes, which includes coupled balance equations for the scalar kinetic energy and energy dissipation in the melt. These equations are solved simultaneously with the equations that describe energy and mass transport in the melt, crystal and the parts of the CZ system and diffuse-gray radiation between components of the enclosure. The melt/crystal interface, the melt meniscus, and the radius of the crystal are computed as part of the solution.

The entire set of equations is solved simultaneously by Newton's method.

Simulations for a prototype system for growth of 5" diameter silicon crystals demonstrate the feasibility of analysis of large-scale systems and the importance of convective heat and mass transport. Interesting effects are seen that are explained by turbulent interactions. The temperature difference across the melt is small without any obvious internal layer structure in the melt. Also, increasing crucible rotation increases convection in the melt, contrary to predictions of laminar flow calculations, where the increased Coriolis force would be expected to damp convection. The increased convection seen with turbulence is caused by kinetic energy generation due to the interaction between the azimuthal flow driven by crucible rotation and the meridional motion driven by buoyancy differences. The increase in convection with crucible rotation and the meridional motion driven by buoyancy differences. The increase in convection with crucible rotation has been seen experimentally.

**CONTROL OF RADIATIVE-CONDUCTIVE HEAT TRANSFER IN SHAPED  
SEMI-TRANSPARENT CRYSTALS BEING PULLED FROM THE MELT**

*V.S. Yuferev, M.G. Vasil'ev, E.N. Kolesnikova and L.A. Stefanova*  
A.F. Ioffe Phisical - Technical Institute

When solving heat transfer problem in crystal growth it is usually considered that external conditions are given and that the temperature field in the crystal has to be found. Yet from the viewpoint of practice the following inverse problem is of special interest: what temperature fields in crystals are desirable and how this fields can be really produced. The latter means to find and dispose such heaters and thermal screens that the resultant temperature distribution would be as close to the prescribed one as possible.

The paper deals with the heat transfer problem in the system consisting of a cylindrical crystal, a set of parallel plane screens normal to the growth direction and an outer heater. Such system is often used if the shaped sapphire crystals are grown. Here parallel screens help to localyze the thermal influence of the heater on the crystal. Along with a number of

control parameters the size of the screens, the distance between them, their emissivity and etc.) it gives possibility to control the temperature field in the crystal over wide limits. In order to reduce the computational difficulties the semi-empirical formulae were derived to describe the radiative transfer in gaps between screen plates. It is shown that solutions of the direct problem are in good agreement with experimental data. Solution of the inverse problem shows that it is really possible to generate in crystal such thermal field that at fixed pulling rate thermal stresses prove to be minimal. The problem of crystal growth stability is also solved. The novelty of the present approach is in consideration of the space periodical perturbations of the crystal surface and taking into account radiative heat transfer.

## SESSION 4B

### RECENT DEVELOPMENT OF NEW LASER CRYSTALS

*Bruce H.T. Chai*

Center for Research in Electro-Optics and Lasers  
University of Central Florida  
12424 Research Parkway, Orlando, FL 32826

In a recent presentation (1) the work "renaissance" was used to describe the renew interest and the rapid advances in solid state lasers. This is because of the combination of the development of high-power laser diodes, new solid state laser materials and new nonlinear optical materials. They hold the promise of more efficient, compact, reliable and versatile lasers. Combination of new wavelengths and efficient nonlinear conversions, these lasers can deliver more power and have broader lasing wavelengths. The message here is very clear that it is the development of new "materials" which holds the key for these advances.

The development of new laser materials has followed very closely to the basic requirement of diode pumpable. Current high power laser diodes are available in three wavelengths – 670, 800 and 960 nm. Because of the small thermal loading and great reduction of crystal size in the diode pumping scheme, the material strength requirement is greatly relaxed. Moreover, congruent melting is no longer a requirement. This opens great opportunity to look for materials with unique lasing properties. Sensitization also becomes a key consideration for efficient diode pumping.

The specific research areas of interest will include:

- (1) Cr<sup>3+</sup> doped fluorides, such as LiCaAlF<sub>6</sub>(LiCAF) and LiSrAlF<sub>6</sub>(LiSAF),
- (2) rare earth doped fluorides, such as high Nd concentration fluorides, up-conversion lasers,
- (3) transitional metal doped oxides, such as Cr<sup>4+</sup>, Mn<sup>5+</sup> in Y<sub>2</sub>SiO<sub>5</sub>, Ca<sub>5</sub>(PO<sub>4</sub>)<sub>3</sub>F, etc.,
- (4) rare earth doped oxides, such as Tm in YAlO<sub>3</sub>, ND in Y<sub>2</sub>SiO<sub>5</sub>, Yb in Ca<sub>5</sub>(PO<sub>4</sub>)<sub>3</sub>F,
- (5) transitional metal sensitizing of rare earth doped oxides, such as Cr<sup>4+</sup>, Er<sup>3+</sup> in Y<sub>2</sub>SiO<sub>5</sub> and Ca<sub>5</sub>(PO<sub>4</sub>)<sub>3</sub>F,
- (6) wave guide structures in oxides and fluorides, such as YAG, YLF, LiCAF and LiSAF.

One of the key factors to make these works feasible is the perfection of crystal growth in a peritectic melt using crystal weighing feed back control. Examples will be presented to illustrate the technique. This technique will become more important in the search of new laser materials.

---

(1) Peter F. Moulton, "Solid state lasers: the renaissance continues" (R.V. Pole Memorial Plenary Lectures), CLEO/QELS '92, Anaheim, CA, May 11, 1992.

## CaClF:Sm<sup>2+</sup> CRYSTAL GROWTH AND SPECTROSCOPY

J.P. Chaminade<sup>1</sup>, A. Garcia<sup>1</sup>, A. Oppenländer<sup>2</sup>, J.C. Vial<sup>2</sup> and R.M. Macfarlane<sup>3</sup>

<sup>1</sup>Laboratoire de Chimie du Solide du CNRS, 351, cours de la Libération, 33405 Talence Cedex, France

<sup>2</sup>Laboratoire de Spectrométrie Physique (associé au CNRS) BP 87, 38402 Saint-Martin d'Hères, France

<sup>3</sup>Permanent address: IBM Almaden Research Center, 650 Harry Rd, San José, Ca 95120, USA

A variety of interesting phenomena have recently been demonstrated in AXF fluorohalide crystals (where A = Ba, Sr and X = Br, Cl) containing divalent rare earth ions. These properties depend on the possibility of photo ionizing the divalent rare earths, a process which is optical reversible. Photon gated spectral hole burning was demonstrated in BaClF:Sm<sup>2+</sup> and SrClF:Sm<sup>2+</sup>. In order to investigate the influence of the ionic radius of the A cation, a previous study on BaClF:Sm<sup>2+</sup> and SrClF:Sm<sup>2+</sup> was extended to the case of CaClF:Sm<sup>2+</sup>, so this material has to be prepared in single crystalline form.

CaClF melts incongruently so these crystals were grown using a flux method. In the CaCl<sub>2</sub>-CaF<sub>2</sub> phase diagram, an eutectic point of 645°C for 18.5 mole CaCl<sub>2</sub> composition has been established and a decomposition temperature of 735°C was found for CaClF. CaCl<sub>2</sub> appears to be a good solvent for the growth of CaClF at temperatures higher than 645°C. CaCl<sub>2</sub>, CaF<sub>2</sub> and SmCl<sub>2</sub> were used as starting materials. All the manipulations were carried out in a dry box filled with dried and deoxygenated Ar, due to the highly hygroscopic nature of CaCl<sub>2</sub> and SmCl<sub>2</sub>. Several steps were involved in the reaction procedure: solid state preparation of a Ca<sub>0.95</sub>Sm<sub>0.05</sub>ClF sam-

ple, dilution to the required amount of Sm<sup>2+</sup> by adding weighted quantities of CaCl<sub>2</sub> and CaF<sub>2</sub>, and the addition of an excess of CaCl<sub>2</sub> as a flux for the crystal growth run. The latter proceeded in cylindrical 30 cm<sup>3</sup> Pt-90/Rh-10 crucibles. The following thermal cycle was used: (i) heating up to the operational temperature (750°C); (ii) slow cooling with a rate of 0.5 of 3°C/h to the temperature of the solidification of the flux (645°C), (iii) a rapid decrease to room temperature. Single crystals were removed ultrasonically in dry acetone and stored in sealed glass tubes containing a few torr of Ar gas.

CaClF:Sm<sup>2+</sup> grew as transparent, optically clear platelets with a maximum size of 10x10x1.5 mm<sup>3</sup>. The crystals have the PbCl layer structure with the c-axis perpendicular to the plane of the plate. The average lattice parameters of the crystals (a=3.894(2) Å, c=6.809(4) Å; tetragonal system, P4/nmm, Z=2) are in good agreement with those published previously.

The nominal concentration of Sm was 0.05% but only a minority of the dopant atoms are in the divalent state. Nevertheless optical and photon gated hole burning spectra of CaClF:Sm<sup>2+</sup> are successfully recorded and discussed.

## NEW FLUORIDE CRYSTALS FOR LASER APPLICATIONS

A. Cassanho and H.P. Janssen

Center for Materials Science and Engineering

Massachusetts Institute of Technology, Cambridge, MA 02139

Fluoride crystals have many desirable properties for use as laser hosts. A well known fluoride laser crystal, LiYF<sub>4</sub> is now commercially available in reasonably good quality. However, other new promising fluoride laser systems are not fully developed due to problems with crystal growth. We will report on our growth experiments of three very promising laser systems BaY<sub>2</sub>F<sub>8</sub>, NaYF<sub>4</sub> and Cr<sup>3+</sup>:LiSrGaF<sub>6</sub>. The first two compounds are good candidates for diode pumped lasers. Cr<sup>3+</sup>:LiSrGaF<sub>6</sub> is a good candidate for flash-lamp pumped laser, with very low passive loss.

BaY<sub>2</sub>F<sub>8</sub> has a tendency to crack due to its strong anisotropic thermal coefficients and it is prone to diffuse scattering. We will present our data on the effects of different growth directions on cracking. According to our results, diffuse scattering can be avoided by careful preparation of the fluoride starting material.

When NaYF<sub>4</sub> is grown by the top-seeded solution method, it has to be pulled from a melt with composition near the eutectic composition to avoid a destructive phase transition. As a result it is difficult to have NaYF<sub>4</sub> single crystals of even 1cm<sup>3</sup>. In our early experiments we obtained only a maximum size of 1cm x 0.5cm x 0.5cm. We are going to report improvements in size and quality of these crystals.

Finally, we will discuss the common factors involved in growth of fluorides for lasers, such as synthesis of oxygen-free starting material, care with the growth atmosphere and temperature control during the growth run. The synthesis of oxide-free fluoride is the most important factor affecting the growth of Cr<sup>3+</sup>:LiSrGaF<sub>6</sub>.

---

Work supported by DARPA/ONR contract No. N00014-90-J-4073.

## THREE-DIMENSIONAL HEAT TRANSFER DURING THE SEEDING OF LiCAF SINGLE CRYSTALS IN A MODIFIED BRIDGMAN SYSTEM\*

*S. Brandon and I.I. Derby*

Department of Chemical Engineering and Materials Science

University of Minnesota, Minneapolis, MN 55455

*J.J. DeYoreo, D.H. Roberts, and L.J. Atherton*

Lawrence Livermore National Laboratory, Livermore, CA 94550

A three-dimensional, steady-state analysis of heat transfer is performed for a prototype Bridgman system designed for the growth of Cr:LiCaAlF<sub>6</sub> (Cr:LiCAF<sub>6</sub>) single crystals. The experimental configuration is similar to that utilized in [1] to grow Cr:LiCAF slabs, but modified to simultaneously growth three cylindrical crystalline rods. It is hoped that this modification will greatly increase production throughput. The seeding geometry of this configuration is quite complicated; all three rods are seeded via channels diverging from a common central seed crystal.

A finite element study of conduction and radiation (using the commercial code FIDAP) has been performed to gain

insight to the heat transfer occurring during seeding of this system. We compare results from this analysis with experimental observations.

[1] L.I. Atherton, J.J. DeYoreo, S.A. Payne, D.H. Roberts, J.F. Cooper, and R.W. Martin, "Growth of Cr:LiCaAlF<sub>6</sub> by the Bridgman and Gradient Freeze Processes," AACG Newsletter 21(2) (1991).

\*Portions of this work were performed under the auspices of the U.S. Department of Energy by Lawrence Livermore National Laboratory under Contract W-7405-Eng-48.

---

## GROWTH OF HIGH-QUALITY Yb-DOPED FLUORO-APATITE FOR ADVANCED LASER APPLICATIONS

*W.L. Kway, S.A. Payne, W.F. Krupke, L.D. DeLoach, L.K. Smith and J.B. Tassano*

University of California

Lawrence Livermore National Laboratory, Livermore, California 94550

Yb-doped calcium fluoro-apatite (Yb:Ca<sub>5</sub>(PO<sub>4</sub>)<sub>3</sub>F or Yb:FAP) has recently been demonstrated to possess outstanding laser properties. For our present laser applications, it is desired to have single crystals grown with high optical quality and Yb substitution only in the 7-coordinated Ca sites.

Yb:FAP melts congruently near 1,700°C. The melt is fairly stable in an argon atmosphere. However, it is not uncommon to obtain crystals grown with poor optical quality and the dopant substituted into multiple Ca sites. The crystal is currently grown by the Czochralski technique with pull rates of 1-3 mm/hr and rotation rates of 30-100 rpm. Since the Yb-doped crystal is colorless, the heat loss through the crystal during growth is enhanced, thereby causing the growth solid-liquid interface to become highly convex even at a fast rotation rate. As a result, crystal defects are developed in the forms of cellu-

lar structure at the core and small particle inclusions at the interface-facets, or in planes along the growth axis for c-axis grown crystals. This problem has been correlated to the melts with noncongruent compositions. In our experiments, the starting material and the growth parameters are varied and optimized to attain growth perfection and high optical quality. These results, together with the interface morphology, will be correlated and discussed. In addition, it has been found that single site Yb substitution can be achieved by the use of a high purity CaHPO<sub>4</sub> as a starting component.

---

This work was performed under the auspices of the U.S. Department of Energy by Lawrence Livermore National Laboratory under Contract No. W-7405-Eng-48.

CHARACTERIZATION OF THE  $\text{LiSrAlF}_6$ - $\text{LiSrCrF}_6$  SOLID-SOLUTION  
FOR Cr-LASER APPLICATIONS

W.L. Kway B. Rupp, S.A. Payne, W.F. Krupke, L.K. Smith, L.D. DeLoach and J.B. Tassano

University of California

Lawrence Livermore National Laboratory, Livermore, California 94550

It has recently been demonstrated in our laboratory that the Cr-doping level in  $\text{LiSrAlF}_6$  can be made as high as 50% without noticeably degrading the laser performance of this system. In fact, the strong light absorption evidenced by the  $\text{LiSrAlF}_6$ - $\text{LiSrCrF}_6$  solid-solution with  $x > 0.2$  has permitted the demonstration of a new wing-pumped laser design.<sup>1</sup> Several samples with  $x = 0, .04, .2, .4, .6, .8$ , and 1 were synthesized by the high-temperature hydrofluorination process. Single crystals of these samples were then grown by the Czochralski technique. In addition to the spectroscopic and laser characterization, various chemical and physical properties were also investigated. Using the single crystal samples, differential thermal analyses and x-ray diffraction patterns were obtained. Some samples were also analyzed by wet-chemical techniques to determine the composition. By analyzing this data, a phase

diagram was plotted in this pseudo-binary region. Additionally, the lattice constants were calculated and plotted from the x-ray data. By combining all this information into a composite plot, it can be shown that  $\text{LiSrAlF}_6$ - $\text{LiSrCrF}_6$  is truly a continuous solid-solution with a very narrow solid-liquid region. These results, together with all the relevant process and growth parameters of interest will be summarized and presented.

This work was performed under the auspices of the U.S. Department of Energy by Lawrence Livermore National Laboratory under Contract No. W-7405-Eng-48.

1. S.A. Payne, W.F. Krupke, L.K. Smith, W.L. Kway, and L.D. DeLoach, *Advanced Solid State Lasers*, Santa Fe, NM (1992).

## SESSION 4C

### NOVEL PRECURSORS FOR ORGANOMETALLIC VAPOR PHASE EPITAXY

*G.B. Stringfellow*

Departments of Materials Science and Engineering  
and Electrical Engineering  
University of Utah, Salt Lake City, Utah 84112

During the development of organometallic vapor phase epitaxy (OMVPE) for the growth of III/V semiconductor materials, the choice of group III and group V source molecules has been limited: 1) only trimethyl- and triethyl-group III and antimony compounds, developed for other applications, were available; 2) the hydrides were the only As and P sources capable of producing device quality material. The hazard posed by the hydride sources, due to their extreme toxicity as well as their storage in high pressure cylinders, was a major motivation for the development of new precursor molecules. This led to the realization that many features of the OMVPE process could

be improved by the development of "designer" source molecules. This paper will emphasize the tertiarybutyl-As, P, and Sb precursors  $C_4H_9AsH_2$ ,  $C_4H_9PH_2$ , and  $C_4H_9Sb(CH_3)_2$ . However, recent results using alternate In precursors, such as triisopropylindium ( $C_3H_7)_3In$ , will be included. The fundamental aspects of the design of source molecules, including pyrolysis routes, will be mentioned; however, the talk will focus on the practical results obtained using these precursors for the OMVPE growth of III/V semiconductors such as GaAs, GaSb, InP, InAs, and InSb.

---

### THE MODELING OF MOVPE GaAs GROWTH FROM $(C_2H_5)_2GaCl$ AND $AsH_3$ ASSUMING THERMODYNAMIC EQUILIBRIUM AT THE GROWTH FRONT

*Matthias Hierlemann and Thomas F. Kuech*

University of Wisconsin  
Department of Chemical Engineering, Madison, WI, 53706 USA

Metal-organic vapor phase epitaxy (MOVPE) of GaAs is carried out in a 'cold-wall' flowing gas reactor. The typical growth reactants are metal organic compounds, such as  $(CH_3)_3Ga$  and  $(CH_3)_3Al$ , that decompose rapidly at the growth front. The modeling of the growth rate and uniformity is often accomplished using the assumption of a very fast surface decomposition reaction rate which leads to the appearance of a mass transport limited growth rate. A quantitative description of the growth from these precursors can be achieved by using this assumption. In previous calculational studies, thermodynamic equilibrium is therefore not invoked at the growth surface. Thermodynamics does play a role in these reactions in providing the driving force for the growth and local thermodynamic equilibrium between the gas ambient and the growth front may determine some materials properties.

Other growth precursors have been used in the MOVPE growth system that provide a difference in the growth characteristics, with respect to the primary system variables such as pressure and temperature, as well as exhibiting new growth habits. We have studied the growth of GaAs and  $Al_xGa_{1-x}As$  from the metal-organic precursors, diethyl gallium (aluminum) chloride,  $(C_2H_5)_2Ga(Al)Cl$ , and arsine ( $AsH_3$ ). This growth chemistry has been successfully used to produce selective area growth over a wide range of growth conditions. The experimentally determined growth rate and composition of GaAs and  $Al_xGa_{1-x}As$  from these chloride-based precursors exhibit a

much stronger dependence on temperature and gas phase composition than with the conventional all organic ligand compounds typically employed in the growth. Previous studies have indicated that calculations based on thermodynamic equilibrium can qualitatively describe this dependence on temperature and gas phase composition. In order to quantitatively model and understand the growth behavior, the assumption of local thermodynamic equilibrium at the growth front must be included within a realistic model of the flowing gas environment.

This present work presents a two-dimensional model of the epitaxial growth of GaAs within a horizontal reactor using  $(C_2H_5)_2GaCl$  and  $AsH_3$ . The velocity, temperature, and concentration fields have been solved for using the Galerkin finite element method. This growth model involves the assumption of thermodynamic equilibrium as a boundary condition at the growth surface. A form of marching solution with dynamic implementation of the reaction boundary condition is used to incorporate the thermodynamic equilibrium assumption. The description of the incorporation of this boundary condition into the calculation will be described since it is a departure from the usually employed boundary conditions within the MOVPE model description. Comparison of the calculated growth rates with experimental data indicates the surface may not be fully described by this assumption and kinetic factors may play an important role in the growth reaction.

## MOVPE GROWTH OF InGaAsP USING EDMIn, TBP AND TBA FOR OPTICAL DEVICES

Matsuyuki Ogasawara and Yoshihiro Imamura

NTT Opto-electronics Laboratories

3-1, Morinosato Wakamiya, Atsugi-shi, Kanagawa, 243-01 Japan

**Introduction:** Ethyldimethylindium(EDMIn)[1] is a liquid In source whose feed rate is stabler than that of solid TMI. Tertiarybutylphosphine(TBP) and tertiarybutylarsine(TBA)[2] are less hazardous group-V sources that can replace toxic PH<sub>3</sub> and AsH<sub>3</sub>. Therefore, from the viewpoint of safety in manufacturing the combination of EDMIn, TBP and TBA is very important to reproducibly obtain high-quality InGaAsP lattice matched to InP. Some anomalous vapor phase reactions were observed, but they did not affect the controllability of InGaAsP composition. DH wafers grown using these new sources were applied to DFB-laser.

**Experiments:** Growth experiments were performed using a horizontal reactor. Purified H<sub>2</sub> was used as a carrier gas. The flow rates of EDMIn and TBP were kept constant, and the flow rates of TEG and TBA were varied to investigate lattice matching conditions. Typical growth conditions are summarized in Table 1.

**Results and Discussion:** The InGaAsP having bandgap wavelength between 1.3  $\mu\text{m}$  and 1.67  $\mu\text{m}$  were successfully grown with good compositional controllability using the new sources. The morphology and PL intensity of DH wafers were comparable to those using conventional sources. Some anomalous phenomena were also observed. First, growth rates were dependent on V/III ratio. Second, the group-III distribution coefficient  $k_{\text{III}}$  became lower as the TBA partial pressure was increased (see Fig.1). The origin of these phenomena is thought to be vapor phase reactions between ethyl radicals of EDMIn and tertiarybutyl radicals of TBP and TBA. DFB-lasers were fabricated from DH wafers grown using new sources and their performance was comparable to DFB-lasers fabricated using conventional sources.

It has been demonstrated that a device-quality InGaAsP can be grown by MOVPE using new sources. This indicates that combination of EDMIn, TBP and TBA is useful for MOVPE growth of InGaAsP for optical devices.

Table 1. Typical Growth Condition

Growth Pressure: 100 torr
Growth Temperature: 570°C
Total Flow Rate (H <sub>2</sub> ): 8 SLM
EDMIn: 5.9 $\times$ 10 <sup>-7</sup> mol/min.
TBP: 6.6 $\times$ 10 <sup>-4</sup> mol/min.
V/III Ratio: 23 - 124

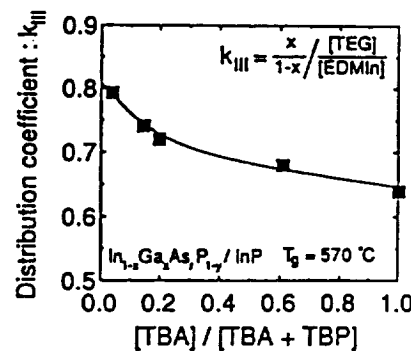


Figure 1.

[1] J. Knauf, et al: *J. Cryst. Growth* 93, (1988) 34.

[2] G.B. Stringfellow: *J. Electron. Mater.* 17, (1988) 327.

## MOCVD GROWTH OF InAs FROM MONOETHYL ARSINE

R.J. Egan, T.L. Tansley and V.W.L. Chin

Semiconductor Science and Technology Laboratories

Physics Department, Macquarie University, NSW 2109, Australia

We have grown InAs and InAsSb on GaAs substrates using a novel chilled monoethyl arsine source by low pressure MOCVD. Conventional trimethyl indium and trimethyl antimony precursors were used to source the other components. The reduced vapour pressure and lower decomposition temperature of the cooled metalorganic arsenic source enabled enhanced compositional control over the alloy. A wide range of conditions of temperature and V/III ratio prove amenable to the growth of specular epilayers of InAs and InAsSb on GaAs, despite the large lattice mismatch. In particular, temperatures as low as 420°C have been employed to grow epilayers of good morphology. Mobilities for InAs prepared at reduced substrate

temperature are only marginally less than those grown from arsine at higher temperatures ( $1000 \text{ cm}^2 \text{V}^{-1} \text{s}^{-1}$  for  $n=2 \times 10^{16} \text{ cm}^{-3}$ ). InAsSb, of high antimony content, exhibits high mobilities ( $20000 \text{ cm}^2 \text{V}^{-1} \text{s}^{-1}$  for  $n=10^{16} \text{ cm}^{-3}$ ), comparable to other reported values. Epilayers were n-type for all conditions considered. A reduction in carrier concentration and enhancement of mobility is observed with increasing substrate temperature. We report a study of growth rate and transport properties as a function of substrate temperature and V/III ratio, complementing a theoretical understanding of the transport properties of the alloy.

## THE GROWTH OF InSb USING ALTERNATE ORGANOMETALLIC Sb SOURCES\*

R.M. Biefeld

Sandia National Laboratories, Albuquerque, NM 87185

Recently, infrared response has been demonstrated for  $InAs_{1-x}Sb_x/InSb$  strained-layer superlattices (SLS's) out to 16  $\mu\text{m}$ . Factors affecting the performance of these devices include background doping and dopant profiles. Alternate organometallic Sb sources are being investigated to improve the materials characteristics of InSb grown by metal-organic chemical vapor deposition (MOCVD). The best InSb grown in this laboratory by MOCVD at 200 Torr, 470 C using trimethylindium (TMIn) and trimethylantimony (TMSb) at a V/III ratio of 35 has a p-type carrier concentration of  $3 \times 10^{15} \text{ cm}^{-3}$  and a mobility of  $9700 \text{ cm}^2/\text{Vs}$ . This material is of better quality than the material previously grown in this laboratory at atmospheric pressure. InSb grown using TMIn and TESb yielded similar quality materials under similar growth conditions. InSb grown using TEIn and TESb under similar growth conditions yielded very poor quality n-type material. Two new organometallic Sb sources, triisopropylantimony (TIPSb) and tertiarybutyldimethylantimony (TBDMsB) are being investigated. The growth of InSb using TIPSb or TBDMsB and TMIn was investigated over a temperature range of 350 to 475 C. The growth of InSb using TMIn and TIPSb resulted in very low growth rates,  $\approx 0.04 \mu\text{m}/\text{h}$ , due to the low vapor pressure of

TIPSb and the high V/III ratios required for growth at 350 C. The InSb grown at 350 C was n-type with a carrier concentration of  $2.3 \times 10^{16} \text{ cm}^{-3}$  and a mobility of  $37,330 \text{ cm}^2/\text{Vs}$ . The majority carrier type changed from n-type to p-type depending on the growth conditions. Low temperature, low pressure and high TMIn flow rates favored n-type growth. The mobilities for the n-type material were similar to those of InSb prepared using TIPSb which are considerably below those in the literature for InSb grown from the liquid as well as those grown with an n-type dopant by MOCVD in this laboratory. The surface morphology of InSb grown using either TIPSb or TBDMsB was very rough for growth temperatures  $\approx 400$  C. This may be due to the complex decomposition mechanisms involved and the presence of methyl groups on the surface. The effects of pressure, temperature, 3/5 ratio and sources on the properties of InSb will be discussed. Work is under way to investigate the use of TEIn with these sources as well as new Sb and In sources as they become available.

\*This work was supported by the US DOE under Contract No. DE-AC04-76DP00789.

---

## STUDY ON INTERFACES OF MOVPE $\text{GaAs}/\text{Al}_x\text{Ga}_{1-x}\text{As}$ QUANTUM HETEROSTRUCTURES

Xiangang Xu, Hongwen Ren, Baibiao Huang, Shiwen Liu and Minhua Jiang

Institute of Crystal Materials, Shandong Univ., Jinan, P.R. China

This paper presents study on the interfaces of Metalorganic Chemical Vapor Epitaxy (MOVPE)  $\text{GaAs}/\text{Al}_x\text{Ga}_{1-x}\text{As}$  quantum heterostructures. Both cross-sectional transmission electron microscopy (TEM) and low temperature photoluminescence (PL) are used to characterize the heterointerfacial structure and the optical properties of the epilayers.

The initial stage of nucleation on the substrate has been clearly verified by examining the undulations of a 30nm GaAs layer sandwiched between the substrate and the superlattice used as buffer layer in high electron mobility transistor (HEMT) devices. Both  $\text{Al}_{0.5}\text{Ga}_{0.5}\text{As}/\text{GaAs}$  and  $\text{AlAs}/\text{GaAs}$  superlattices can smooth out interface roughness caused by contaminations and dislocations on the substrate surface. The smoothing mechanism is mainly due to the migrations of Ga and Al species on the growing surface and the anisotropic growth rate of GaAs on different facets.

Interrupted growth causes additional interface in MOVPE. We have chosen 0, 30, 60, 90 seconds interrupting times in some growths respectively. The quantum wells grown by using 30 seconds interruption at the heterointerface have a weak exciton luminescence measured at 11K. The 90 seconds interruption in the HEMT causes additional interfaces and the device does not possess the desired properties. Double-barrier resonant tunneling diodes (DBRTD18) was grown with interruption at the interface between the barrier and the well. DBRTD69 was grown without any interruption. The ratios of the current peak to valley in the I-V curve for DBRTD18 and DBRTD69 are 0.9 and 1.3, respectively. The (100) cross-sectional TEM image shows that additional interfaces are formed in DBRTD18.

In conclusion, superlattices used as buffer layers can smooth out interface roughness. Interrupting more than 30 second may cause additional interface in MOVPE.

## NOVEL CHARACTERIZATION TECHNIQUES TO OBTAIN BASIC SEMICONDUCTOR PROPERTIES IN EPITAXIAL CRYSTALS AND QUANTUM WELL STRUCTURES

B.K. Meyer, C. Wetzel, P. Omling\* and F. Scholz\*\*

Physikdepartment, E 16, Technical University Munich, 8046 Garching, Germany

\*Department of Solid State Physics, University of Lund, Box 118, Lund, Sweden

\*\*4. Physikalisches Institut, University Stuttgart, Pfaffenwaldring 57, 7000 Stuttgart, Germany

Band gap engineering is a key word for modelling new semiconductors, in composition as well as in doping. This refers to semiconductors such as InGaP as well as to strained InGaAs epitaxial crystals and realizing p-modulation doped Quantum Well (QW) structures in InGaAs. Very often classical characterization techniques (Hall effect, current transport) fail because the inability to make contacts for electrical characterization. However, basic properties such as effective masses, mobilities (scattering times), scattering mechanism and carrier densities in two dimensional systems can be obtained by advanced contactless microwave techniques. We will report on Shubnikov de Haas measurement (carrier density) in doped and undoped InGaAs single QW's using electron spin reso-

nance techniques[1], which show the advantage of this advanced technique. By the application of optically detected cyclotron resonance in the microwave and far-infrared region, scattering times and thus mobilities of high purity epitaxial crystals as well as QW's could be studied. The role of the interface roughness and interface scattering with decreasing QW thickness is discussed by comparing binary and ternary semiconductor QW's.

[1] P. Omling, B.K. Meyer and P. Emanuelsson, *Appl. Phys. Lett.* 58 (1991) 931.

## STABLE STRAINED SUPERLATTICES: FORMATION VIA COHERENT PHASE SEPARATION OF SEMICONDUCTOR ALLOYS

I.P. Ipatova, V.G. Malyshkin, A.Yu. Maslov and V.A. Shchukin

A.F. Ioffe Physical Technical Institute  
194021 St. Petersburg, USSR

The theory of thermodynamical stability of III-V  $A_{1-x}B_x$   $C_{1-y}D_y$ -type quaternary semiconductor alloys is developed with respect to coherent phase separation. It is shown that the "soft mode" providing instability corresponds to the phase separation into a periodic structure of layers with alternating alloy composition (a system of compositional domains, e.g. a strained superlattice with a macroscopic periodicity). The phase separation is governed by the interplay of two terms in the free energy,  $F_{\text{CHEMICAL}}$  and  $F_{\text{ELASTIC}}$ . In alloys with positive formation enthalpy,  $F_{\text{CHEMICAL}}$  provides the tendency to phase separation. The elastic contribution plays the stabilizing role, it hinders the phase separation, and results in the lowering of the phase transition temperature  $T_c$ . It is proven that in the case of coherent phase separation into the layered system, the

stabilizing factor of elastic strains does not prevent completely the phase separation of quaternary alloys.

The layered system is formed along the direction of the lowest stiffness, namely [100] for III-V alloys. The period of the structure is determined by the inhomogeneous part of  $F_{\text{ELASTIC}}$ .

The phase diagrams presenting miscibility limits and regions of absolute instability are numerically calculated for GaAlAsSb and GaInAsP. The periods of corresponding absolutely stable superlattices are found to be of the order of 10-100 nm.

The results are in qualitative agreement with many experimental data on spatially modulated structures observed in epitaxial growth of III-V alloys.

## SESSION 4D

### SOLID SOURCE MOCVD OF OXIDE THIN FILMS

*R. Hiskes and S.A. DiCarolis*

Hewlett Packard Laboratories, 3500 Deer Creek Road

Palo Alto, CA 94303

*Z. Lu and R.S. Feigelson*

Department of Materials Science and Engineering

R.K. Route, Center for Materials Research

Stanford University, Stanford, CA 94305-4045

*J.L. Young*

Department of Materials Science

University of California, Los Angeles, CA 90024

A novel and inexpensive single source metalorganic chemical vapor deposition reactor has been developed at Hewlett Packard Laboratories which permits the controlled and reproducible growth of device quality thin film heterostructures on a variety of substrates, using marginally volatile beta-diketonate powdered solid sources. This reactor has been used to deposit state-of-the-art dielectrics, ferroelectrics and yttrium barium copper oxide high temperature superconducting multilayers on

substrates up to 4" in diameter. The technique is readily applicable to a variety of other oxide and non-oxide material systems. In this talk we will describe the reactor and present recent results for single layers and heterostructures of YBCO, MgO, CeO<sub>2</sub> and other oxides on sapphire and related substrates for superconducting biepitaxial junctions, microwave devices, sensors and ferroelectric applications.

---

### SOLID SOURCE MOCVD FOR EPITAXIAL OXIDE THIN FILM GROWTH

*Z. Lu and R.S. Feigelson*

Department of Materials Science and Engineering

R.K. Route, Center for Materials Research

Stanford University, Stanford, CA 94305-4045

*S.A. DiCarolis, R. Hiskes and R.D. Jacobitz*

Hewlett-Packard Laboratories

3500 Deer Creek Road, Palo Alto, CA 94305

Metal-organic chemical vapor deposition (MOCVD) has been used to grow thin films of CeO<sub>2</sub>, MgO, LiNbO<sub>3</sub> and (Sr<sub>x</sub>Ba<sub>1-x</sub>)Nb<sub>2</sub>O<sub>6</sub> using all solid phase  $\beta$ -diketonate sources and a novel steady-state method for delivering the reactants to the heated substrate. Epitaxial CeO<sub>2</sub> buffer layers (120Å thick) were grown on R-plane sapphire substrates to facilitate the growth of YBCO on sapphire for microwave applications. X-ray diffraction studies have shown that both 100% (100)-oriented and 100% (111)-oriented CeO<sub>2</sub> films can be grown, depending on the growth system parameters. Higher substrate temperatures favor the (111) orientation. Atomic force micro-

scopic (topographic) analysis has revealed average surface roughness in the  $\pm 20\text{Å}$  range, which translates to only a few CeO<sub>2</sub> lattice constants and little more than one YBCO c-axis lattice constant.

MgO buffer layers on SrTiO<sub>3</sub> substrates, which are used for the growth of high T<sub>c</sub> grain boundary Josephson junctions, have been grown with (100) orientation. Micron thick LiNbO<sub>3</sub> films for optical waveguide applications and (Sr<sub>x</sub>Ba<sub>1-x</sub>)Nb<sub>2</sub>O<sub>6</sub> films for holographic storage applications are also under study.

Details of the MOCVD growth method and recent results in thin film growth and property determinations will be presented.

## OMCVD GROWTH OF $\text{YBa}_2\text{Cu}_3\text{O}_{7-\delta}$ THIN FILMS ON $\text{SrTiO}_3$ AND $\text{LaAlO}_3$

William J. DeSisto, R.L. Henry, H.S. Newman, M.S. Osofsky and V.C. Cestone

Naval Research Laboratory, Washington, DC 20375-5000

Thin films of  $\text{YBa}_2\text{Cu}_3\text{O}_{7-\delta}$  have been deposited on (100)  $\text{SrTiO}_3$  and (100)  $\text{LaAlO}_3$  by organometallic chemical vapor deposition. The tetramethylheptanedionates of Y, Ba, and Cu were used as the solid sources for transport. Films were grown under reduced pressure using nitrous oxide as an oxidizing source. Growth temperatures were varied from 700 to 775°C. Film growth rates were between 500 and 1000 Å/hr. The metals ratio in the films were controlled by accurately controlling the source bubbler temperatures to within 0.1°C. Films deposited on both  $\text{LaAlO}_3$  and  $\text{SrTiO}_3$  at 775°C have  $T_c$ 's between 87 and 89 K with  $J_c$ 's of  $1.3 \times 10^6$  Amps/cm<sup>2</sup> (measured at 77

K). At lower growth temperatures (700 - 750°C),  $T_c$  and  $J_c$  of films on  $\text{LaAlO}_3$  degrade more significantly than films on  $\text{SrTiO}_3$ . Microwave surface resistance vs. temperature measurements for thicker films (i.e. 5000 Å) grown at 775°C have been measured in a 36 GHz cavity and show a sharp drop through the transition temperature, indicative of high quality thin films. Calculated  $R_s$  values corresponding to 10 GHz indicate improvements greater than an order of magnitude over copper metal at 77 K. The effect of film stoichiometry and growth conditions on film properties will be discussed.

---

## GROWTH OF EPITAXIAL $\text{Bi}_2\text{Sr}_2\text{Ca}_{n-1}\text{Cu}_n\text{O}_{2n+4}$ FILMS BY PULSED LASER ABLATION

Shen Zhu\*, Douglas H. Lowndes, B. Chakoumakos, R. Feenstra and X.-Y. Zheng\*

Solid State Division, Oak Ridge National Laboratory, Oak Ridge, TN 37831-6056

\*Dept. of Physics and Astronomy, University of Tennessee, Knoxville, TN 37996

Pulsed-laser ablation (PLA) has been widely used to grow epitaxial  $\text{YBa}_2\text{Cu}_3\text{O}_{7-x}$  (YBCO) thin films, as well as multi-layer and superlattice structures based on YBCO. However, there has been much less use of PLA to grow epitaxial films in the  $\text{Bi}_2\text{Sr}_2\text{Ca}_{n-1}\text{Cu}_n\text{O}_{2n+4}$  (BSCCO) system, in part because several competing phases coexist, e.g., stable  $n = 1, 2$  and 3 materials (the last two of which have  $T_c \sim 80$  K and  $\sim 107$  K, respectively), as well as unstable phases with higher  $n$ . To compound the phase-purity problem, the superconducting properties in BSCCO are quite sensitive to oxygen content, and can be modified by low-temperature oxygen post-annealing to obtain optimal doping (probably accompanied by small rearrangements of cations). We are carrying out a systematic study of in situ BSCCO film growth by PLA, starting from stoichiometric polycrystalline targets of the various pure phases. The focal points of the study are (1) to determine the role of substrate temperature and ambient oxygen pressure in controlling BSCCO phase formation and phase purity, and to determine the film growth mechanism(s). We also are studying the effect on superconducting transport properties of oxygen addi-

tion/removal by post-annealing in controlled atmospheres, in order to obtain optimal doping for superconductivity. The primary analytic tools are x-ray diffraction (to determine phase purity), scanning tunneling microscopy and transmission electron microscopy (to study growth mechanisms, at various stages of growth), and superconducting transport measurements (for  $T_c$ , transition width, and  $J_c$ ). Films ranging in thickness from a few unit cells to  $\sim 250$  nm are being grown on  $\text{MgO}$ ,  $\text{SrTiO}_3$ , and  $\text{LaAlO}_3$  substrates for the growth mechanism studies. We find that it is possible to select particular phases by careful control of deposition conditions. For the in situ 2212 films, we find  $T_c(R = 0) \sim 60$  K, but with an onset temperature that varies, depending on the presence of small amounts of other phases.

---

This research was sponsored by the Division of Materials Sciences, U.S. Department of Energy under contract DE-AC05-84OR21400 with Martin Marietta Energy Systems, Inc.

## GROWTH OF SUPERCONDUCTING WHISKERS IN BI SYSTEM

*Ichiro Matsubara, Hiroshi Yamashita and Tomoji Kawai\**

Government Industrial Research Institute, Osaka,

Midorigaoka, Ikeda, Osaka 563, Japan

\*The Institute of Scientific and Industrial Research,

Osaka University, Ibaraki, Osaka 567, Japan

This paper presents growth and properties of  $\text{Bi}_2\text{Sr}_2\text{CaCu}_2\text{O}_x$ (2212) and  $\text{Bi}_2\text{Sr}_2\text{Ca}_2\text{Cu}_3\text{O}_x$ (2223) superconducting whiskers. The 2212 whiskers have been prepared by annealing a melt-quenched glass plate in a stream of  $\text{O}_2$  gas. The whiskers grow up from the surface of the glass plate. Each whisker with the dimensions of 2-10 $\mu\text{m}$  thick, 10-500 $\mu\text{m}$  wide and ~15mm long is composed of several plate-like single crystals which are stacked in a layered structure. The glass state as a precursor is necessary for growing the whisker; no whisker grows from a polycrystalline precursor. Although the reason of the necessity of the glass precursor is not clear, the growth mechanism is considered to be the base end growth, that is, the growing point is a bottom part of the whisker. The critical temperature of this whisker is 77K by susceptibility measurements and a critical current density of  $7.3 \times 10^4 \text{ A/cm}^2$  (66K, 0T) is obtained. One of the most characteristic properties of this whisker is its bending property. The 2212 whiskers are elastically bent up to 0.2mm of the curvature of radius corresponding to a bending strain of 0.5%. A maximum tensile strength

and elastic modulus obtained from stress-strain curve are 930MPa and 97GPa, respectively.

On the other hand, the 2223 whiskers have been prepared by Conversion by Annealing in Powder method (CAP method). Typically the 2212 whiskers are annealed in a Ca and Cu rich Bi-Sr-Ca-Cu-Pb-O calcined powder. When the annealing temperature is appropriate, the whiskers converted to the 2223 phase are removable from the calcined powder. The surface of the CAP treated whisker loses flatness and smoothness compared with the original 2212 whiskers and it has many steps with round edge, suggesting the existence of a liquid phase around the whiskers during the annealing. The appropriate annealing temperature is in the partial melting region of the calcined powder, as determined by DTA analysis. The phase conversion is considered to be brought by diffusion of Ca and Cu into the 2212 whiskers from the liquid phase. The CAP method has been also applied to single crystals prepared by a flux method, resulting in 2223 sheet crystals as large as 1mm<sup>2</sup>.

## DETAILED STUDY ON HIGH $T_c$ PHASE OF $\text{BiSrCaCuO}$ FROM HIGH TEMPERATURE SOLUTIONS

Satoru Miyashita, Hiroshi Komatsu, Tetsuo Inoue, Shigeyuki Hayashi,  
Hiroyuki Horiuchi\* and Shigeho Sueno\*\*

Institute for Materials Research, Tohoku University, Katahira, Sendai 930, Japan

\*Mineralogical Institute, Faculty of Science, University of Tokyo, Hongo, Tokyo 113, Japan

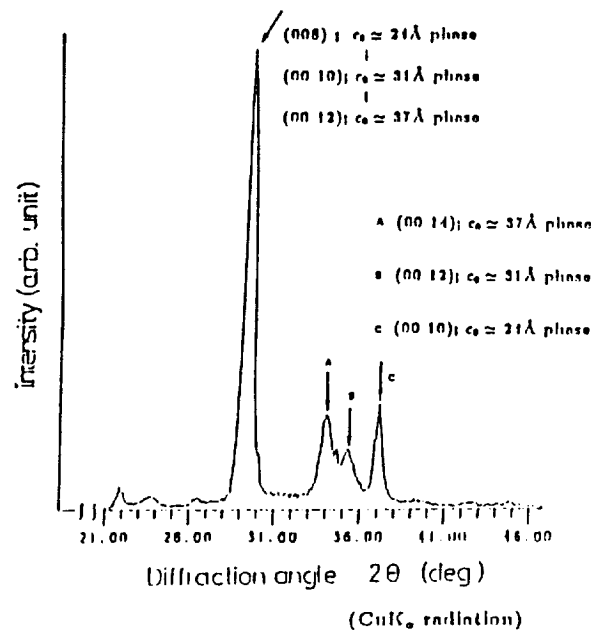
\*\*Institute of Geoscience, University of Tsukuba, Tsukuba-city 305, Japan

Three types of Bi-based oxide superconductors,  $\text{Bi}_2\text{Sr}_2\text{CuO}_6$ ,  $\text{Bi}_2\text{Sr}_2\text{CaCuO}_8$  (low  $T_c$  Phase) and  $\text{Bi}_2\text{Sr}_2\text{Ca}_2\text{Cu}_3\text{O}_{10}$  (high  $T_c$  Phase), are known. We need a reliable phase diagram to grow single crystals of the high  $T_c$  phase from a solution. Shigematsu et al. proposed the  $\text{Bi}_2(\text{Sr,Ca})\text{O}_4$ - $(\text{Sr,Ca})\text{CuO}_2$  pseudo binary phase diagram<sup>[1]</sup>, which shows no liquidus coexisting with the high  $T_c$  phase. However, there are a few reports suggesting that the crystal of the high  $T_c$  phase can be grown from a liquid<sup>[2]</sup>. We carried out experiments using high temperature optical microscopy and differential thermal analysis, and proposed a modified phase diagram<sup>[3]</sup>. There, we suggested the coexistence of a liquid in the narrow temperature range, since it decomposed into the low  $T_c$  phase by a peritectic reaction as temperature was decreased. In this work, we prove the coexistence of the high  $T_c$  phase and the liquid by using x-ray and EDX analysis.

The starting material used was the low  $T_c$  phase crystals grown from the flux ( $\text{Bi}:\text{Sr}:\text{Ca}:\text{Cu}=1.65:1:1:1.35$ ). These samples were heated in air at a rate of 3°C/min under a high temperature optical microscope. As temperature is increased, the low  $T_c$  crystals began to decompose into liquid at 865°C. When we kept the samples at this temperature, needle crystals of  $(\text{Sr,Ca})\text{CuO}_2$  began to grow. Then, two kinds of solids (the needle and the low  $T_c$  phase) and a liquid co-existed for a while. 10 hours later, very thin plate crystals began to grow on the surface of the liquid and grew for 20 hours. We quenched them at a rate of 100°C/s, then annealed at 800°C for 24 hours in oxygen flow in order to oxidize. The annealing temperature being low enough, no phase change occurred. We measured the electric resistance of them, which clearly revealed the existence of the high  $T_c$  phase. It was assumed that the thin plate crystals were the high  $T_c$  phase. The size of these crystals was too small ( $100 \times 100 \times 2/\mu\text{m}^3$ ) for us to identify the high  $T_c$  phase by normal x-ray diffraction. Therefore, a microfocus x-ray diffractometer was used to identify them. The incident beam size was  $50\mu\text{m}$  in diameter. One of their (00l) x-ray profiles is

shown in the figure. Peaks attributed to the high  $T_c$  phase ( $c_0 = 37\text{\AA}$ ) are found and existence of the high  $T_c$  phase is proved. Electron probe x-ray microanalysis was also performed and the results will be discussed.

(00l) diffraction



- 1) K. Shigematsu, H. Takei, I. Higashi, K. Hoshino, H. Takahara and M. Aono: *J. Cryst. Growth* 100 (1990) 661.
- 2) Y. Suzuki, T. Inoue, S. Hayashi and H. Komatsu: *Jpn. J. Appl. Phys.* 29 (1990) L1089.
- 3) H. Komatsu, Y. Kato, S. Miyashita, T. Inoue and S. Hayashi, submitted to *Physica C* 183 (1991).

## CRYSTAL GROWTH AND SUPERCONDUCTIVITY OF $\text{Bi}_{1.7}\text{Pb}_{0.3}\text{Sr}_2\text{CaCu}_2\text{O}_8$ \*

*Lu Zhang, J.Z. Liu, M.D. Lan, P. Klavins and R.N. Shelton*

University of California, Davis, CA 95616

Single crystals of  $\text{Bi}_{1.7}\text{Pb}_{0.3}\text{Sr}_2\text{CaCu}_2\text{O}_8$  were grown by a self flux and local cooling method. The mixture was placed in a Pt crucible and heated in a vertical furnace with a stainless steel rod contacted at the bottom serving as a local cooling center. The crystals have a/b dimensions as large as 5 mm - 10 mm. The sample quality was examined by x-ray diffraction and scanning electron microscopy. Magnetic measurements were performed on a SQUID magnetometer. The magnetic measurements indicate superconducting transition temperatures of 92-96 K with transition widths of 2-4 K. Measurements of long time magnetic relaxations were made over a wide range of

temperatures and magnetic fields. The relaxation rates exhibit strong temperature and field dependence. This behavior reflects that giant flux creep is induced by thermally activated flux motion in the  $\text{Bi}_{1.7}\text{Pb}_{0.3}\text{Sr}_2\text{CaCu}_2\text{O}_8$  system. The experimental data will be compared with both a logarithmic time decay in a conventional theory and a power-law time dependence in a self-organized critical state model.

\*Supported by U.S. DOE under contract No. W-V-7405-ENG-48 and by the National Science Foundation under grant number DMR-90-21029.

## GROWTH OF LARGE SIZE SINGLE CRYSTALS AND WHISKERS OF $\text{Bi}_2\text{Sr}_2\text{CaCu}_2\text{O}_8$ BY STEP COOLING METHOD

*R. Jayavel, C. Sekar, P. Murugakoothan, C.R. Venkateswara Rao,*

*C. Subramanian and P. Ramasamy*

Crystal Growth Centre, Anna University, Madras 600 025, India

The unique properties of superconducting Bi-Sr-Ca-Cu-O system have given rise to many attempts in growing bulk crystals of this material. However the difficulties, mainly due to the large anisotropic nature and intergrowth phenomena, have not yet been overcome. In this study a step cooling process has been adopted to grow  $\text{Bi}_2\text{Sr}_2\text{CaCu}_2\text{O}_8$  single crystals in order to suppress the initial multi nucleation and enhance the growth along one direction with further cooling. The charge with excess CuO flux of appropriate molar ratio was melted up to 980°C and equilibrated at that temperature for 12 hours. Subsequently, a six-step cooling commenced at a rate of 2°C/hr followed by an intermediate soaking of about 2 hours for every 25°C interval up to 855°C and rapidly cooled to room temperature. Single crystals of large surface area (10 x 3 x 0.1 mm<sup>3</sup>)

with terrace-like morphology (Fig. 1) and whiskers of length 5-8 mm (Fig. 2) on the surface of the solidified matrix were obtained.

The grown crystals were subjected to Laue and powder X-ray diffraction studies and found to be tetragonal in structure. Superconductivity studies were made by using a AC susceptometer. The large crystal shows a sharp superconducting transition at 82K. The whiskers which were formed due to the diffusion like transformation of one composition to another during the growth are not superconductive. The anisotropic complex susceptibility, its field and frequency dependence and the higher harmonics of susceptibility (Non-linear behaviour) are discussed.

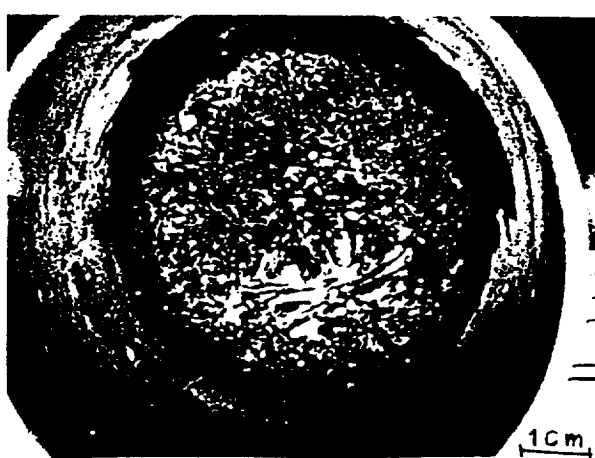


Figure 1



Figure 2



## SESSION 5

### TOWARDS UNDERSTANDING THE GROWTH MECHANISM OF III-V SEMICONDUCTORS IN A ATOMIC SCALE

*T. Nishinaga and T. Suzuki*

Department of Electronic Engineering

The Faculty of Engineering

The University of Tokyo

Present day electronic device technology requires the atomic scale control of crystal growth. To approach this goal one should understand the epitaxial growth of semiconductors in atomic scale.

The epitaxial growth of semiconductor can be classified into two large categories. One is solution growth such as liquid phase epitaxy (LPE) and the other is vapor growth such as molecular beam epitaxy (MBE), metal organic chemical vapor deposition (MOCVD) and vapor growth with hydrides and/or halides sources (HVG). In the present talk, the epitaxial growth mechanism of III-V compound semiconductor so far understood is reviewed. To give the whole view of the understanding of the growth, the mechanisms for both of solution and vapor

growth are discussed, where LPE and MBE are taken respectively as their representatives. The transport of the growth species from the sources to the growth point such as kink of the growth step is divided in several stages. The first one is the diffusion through the bulk phase to the growth surface and the second is the surface diffusion to the step. It is shown that the bulk diffusion directly to the growth step is playing a major role in LPE while in MBE the surface diffusion is the rate limiting process to determine the growth rate.

The topics such as an interface supersaturation and the formation of macrostep in the solution growth, nucleation, surface diffusion and the degree of equilibrium at the step edge in MBE will be discussed in detail.



## SESSION 5A

### THE EFFECT OF GRAVITATIONAL MODULATION ON THERMOSOLUTAL CONVECTION DURING CRYSTAL GROWTH

*S.R. Coriell, B.T. Murray, B.V. Saunders, G.B. McFadden and A.A. Wheeler*  
National Institute of Standards and Technology  
Gaithersburg, MD 20899 USA

During vertical directional solidification of a binary alloy at constant velocity, buoyancy-driven thermosolutal convection may occur due to the temperature and solute gradients associated with the crystal growth process. The effect of time-periodic modulation (vibration) is studied by considering a gravitational acceleration of the form  $g(t) = g_0 + g_1 \cos(\Omega t)$ . The conditions for the onset of instability are obtained numerically, employing two distinct computational procedures based on Floquet theory. Numerical calculations have been carried out for a variety of metallic and semiconductor systems. In general, a stable state can be destabilized by modulation and an unstable state can be stabilized. The flow, temperature and

solute fields show both synchronous and subharmonic temporal response to the driving sinusoidal modulation.

In the limit of high frequency modulation, the method of averaging and a multiple-scale asymptotic analysis allow examination of the dependence of the stability criterion on the processing and materials parameters. In addition, in order to understand possible resonance phenomena, we investigate the effect of gravity modulation on double-diffusive convection in an infinite horizontal fluid layer. In the regime where oscillatory onset occurs in the unmodulated problem, regions of resonant instability occur and exhibit strong coupling with the unmodulated oscillatory frequency.

---

### CONTROL OF MARANGONI CONVECTION FOR FZ CRYSTAL GROWTH

*Torbjörn Carlberg*  
University of Sundsvall, Box 860  
85124 Sundsvall, Sweden  
*Mårten Levenstam*  
Dept. of Hydrodynamics, Royal Inst. of Technology  
10044 Stockholm, Sweden

During FZ crystal growth the surface tension forces usually reach such a level that the so called Marangoni convection dominates the flow (possibly with the exception of cases with RF heating). The surface tension driven flow span from laminar over oscillatory to turbulent, but the parameters controlling the transitions and the nature of the flow are not yet fully known. The objectives with the present study are to increase the knowledge of parameters influencing the Marangoni convection through close interaction between experiments and numerical modelling. As it is likely that the axial distribution of the heat flux, being absorbed at the surface of the liquid zone, is important for the type and magnitude of the convection, a furnace has been developed in which the heat flux profile can be manipulated. The heating system consists of six halogen lamps with ellipsoidal reflectors mounted in a circle. The lamps

can be tilted and the focal plane thus spread out. For example, a double foci arrangement can be obtained, and this is the configuration, which has been studied until now. To obtain the necessary coupling between the experiments and the numerical modelling thermovision has been used to map the surface temperature of the zone. A technique to monitor the heat flux has also been tested. Results from the thermal mapping, and from the first crystals (Si, 8 mm diameter) grown by the double foci arrangement will be presented.

Results from numerical simulations, showing the different flow fields obtained by implementation of single and double foci heat flux profiles, will also be presented. These results clearly shows that manipulation of the heat flux is a powerful tool to influence the Marangoni convection.

CONVECTIVE INSTABILITIES DURING DIRECTIONAL SOLIDIFICATION  
OF PSEUDO-BINARY SYSTEMS

*J.C. Han and S. Motakef*

Massachusetts Institute of Technology, Cambridge, MA 02139

This study is focused on the numerical simulation of buoyancy-induced convection during directional solidification of pseudo-binary systems where the more dense melt component is rejected into the melt at the growth front, e.g., HgCdTe, GaInSb. Time-accurate numerical simulation of transport in these systems have revealed, for the first time, an unstable flow field in the melt driven by the interaction of thermal and solutal buoyancy forces. Numerical results suggest that, under certain conditions, flow in the melt may become turbulent. These

results are surprising in that establishment of an axially stabilizing solutal gradient in the melt generally suggests reduced convection; the mechanisms leading to the flow instabilities will be discussed. Experimental results on growth of HgMnTe, as well as other II-VI systems, indicate axial and radial compositional variations which can be only explained by the present model. Furthermore, magnetic damping of convection in HgMnTe crystals is experimentally found to eliminate radial compositional ondulations associated with the unsteady flow field.

---

FLOW MODE TRANSITIONS DURING CRYSTAL GROWTH IN A CENTRIFUGE

*William A. Arnold, William R. Wilcox and Frederick Carlson*

Clarkson University, Potsdam, New York, 13699 USA

*Liya L. Regel*

International Center for Gravity Science and Applications

Potsdam, New York, 13699 USA

*Arnon Chait*

NASA Lewis Research Center, Cleveland, Ohio 44135 USA

Dopant distribution in semiconductor crystals grown by the Bridgman technique is highly dependant upon the buoyancy driven convective flows. When the crystals are grown in a centrifuge, the resulting flow modes can be determined by the value of a new nondimensional number, Ad.

A fully nonlinear three-dimensional numerical model for the parametric examination of the new nondimensional number, Ad, is presented. In a centrifuge the net acceleration field is not homogeneous due to the centrifugal acceleration being dependant on radial position. The Ad number is the ratio of buoyancy driven flow due to the inhomogeneous part of the acceleration field, to the buoyancy driven flow driven by the average acceleration field. The importance of the inhomogeneous part of the acceleration field (here called the gradient

acceleration) is determined by the value of the Ad number. Results are presented based on both steady-state and fully transient models. Flows result from thermally induced density gradients. In the model the axial and radial temperature gradients are controlled, as is fluid geometry. It is shown that a flow mode transition at  $Ad = O[1]$  occurs and that the value of the Ad number is nearly constant over a wide range of Grashof numbers, hence applies to centrifuges in space as well as terrestrial centrifugation. It is also shown that the transition at  $Ad = O[1]$  is not a function of radial and axial temperature gradients, nor the length or radius of the fluid. Hence, the Ad number is truly an indicator of flow mode regime in the melt during crystal growth in a centrifuge.

## DIRECTIONAL SOLIDIFICATION WITH ACRT

J. Zhou, M. Larrousse and W.R. Wilcox

Center for Crystal Growth in Space

Clarkson University, Potsdam, NY 13699, USA

Two sets of experiments were performed on transport processes in the Bridgman configuration with spin-up/spin-down (ACRT) applied. In one set of experiments mass transfer rates were directly measured during ACRT using electrochemical limiting current density measurements at two different radial positions [1,2]. The mass transfer rate varied significantly during each spin-up/spin-down cycle. The dependence on rotation rate and periodicity was determined, so that conditions can now be specified that minimize fluctuations in transport rate.

In the second set of experiments, doped InSb was directionally solidified with ACRT [3]. Etching revealed rotational striations formed during the time the ampoule was being rotated. Current interface demarcation revealed that the freezing rate varied significantly during each ACRT cycle.

Compositional or doping striations may not always be observed in crystals growth with ACRT because the solid state diffusion may be sufficient for them to disappear before the crystals cool to room temperature [4].

This research was supported by grants from NASA's Microgravity Science and Applications Division.

1. M.F. Larrousse and W.R. Wilcox, *Chem. Eng. Sci.* **45** (1990) 1571-1581.
2. M.F. Larrousse, Ph.D. Thesis, Clarkson University (1987).
3. J. Zhou, M.S. Thesis, Clarkson University (1991).
4. R.T. Gray, M.F. Larrousse and W.R. Wilcox, *J. Crystal Growth* **92** (1988) 530-542.

## CONVECTION AND SEGREGATION DURING GROWTH OF Ge AND InSb CRYSTALS BY THE SUBMERGED HEATER METHOD\*

A.G. Ostrogorsky

Columbia University, New York, N.Y. 10027, USA

H.I. Sell, S. Scharl and G. Müller

Universität Erlangen-Nürnberg, Germany

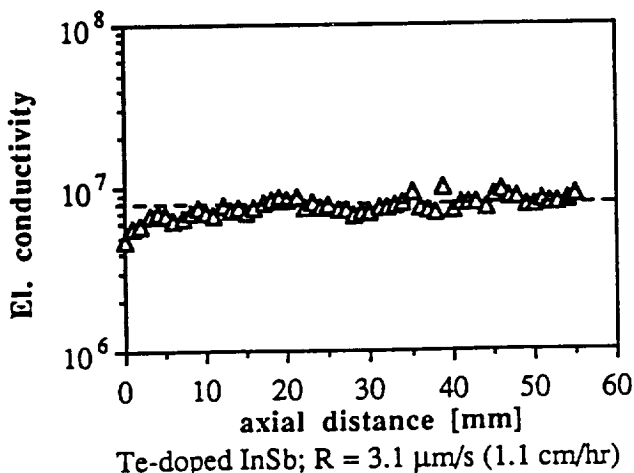
In most methods for bulk crystal growth from the melt (e.g. Czochralski, Bridgman, Zone Melting), solidification occurs inside tube-type furnaces. Because of the heat exchange across the crucible sidewalls, radial temperature gradients must exist in the melt. In the presence of gravity, radial temperature gradients always generate buoyant forces which result in hydrostatic instability and convection.

The Submerged Heater Method (SHM) utilizes an axial disc-shaped heater submerged in the melt. Therefore, it reduces the radial temperature gradients in the melt and at the same time acts as a convection baffle. The Rayleigh number of the melt (i.e., the ratio between buoyancy and viscous forces) is reduced by a factor of  $\sim 10^4$ , compared to the Vertical Bridgman configuration without the submerged heater, a reduction which is compatible to that of decreasing the gravitational acceleration to  $10^{-4}$  of the earth gravity.

Melt convection and segregation was studied numerically and experimentally. We found that, in some melt-dopant systems, SHM reduces the buoyancy driven convection to the level which allows diffusion-controlled solidification. For example, we achieved the ideal diffusion-controlled steady-state segregation of Te-doped InSb (see fig.). The steady-state segregation was achieved  $\sim 0.5$  cm from the seed.

In Ga-doped Ge crystals, diffusion-controlled segregation was not achieved. However, the effective segregation coeffi-

cient varied between  $k_{eff} = 0.3$  and 0.5, depending on the growth rate. However, in contrast to the space-grown crystals, we obtained homogeneous radial segregation. Although highly doped, the crystals were virtually striation free.



\*Partially supported by the Alexander von Humboldt Foundation.

HEAT TRANSFER ANALYSIS AND STRUCTURE PERFECTION  
OF SHAPED SEMI-TRANSPARENT CRYSTALS

*Irina Nicoara, Dumitru Nicoara and Daniel Vizman*

University of Timisoara, Dept. of Physics  
1900 Timisoara, Romania

The influence of heat transfer in Edge-defined Film-fed Growth on melt-solid interface, dopand segregation, crystal perfection and operating limits by finite - element analysis is extensively investigated especially for non-transparent crystals, such as silicon, GaAs, etc.[1,2]. In the case of the EFG process, the heat transfer through the die, melt and crystal and to surroundings determines the meniscus shape and links operating parameters e.g. growth rates and furnace power, to the size and perfection of the crystal and to the stability of the growth process. In this paper the radiative and conductive heat transfer in semi-transparent shaped crystals such as sapphire and fluorite is studied. These crystals have been grown under different conditions[2,3,4] at various pulling speeds and temperature gradients in the growth zone. Structural defects have been studied especially the dislocation distribution, by selective etching method and optical microscopy; surface morphology and void distribution are also described. A model of heat transfer analysis in order to investigate the shaped semi-trans-

parent crystals growth process is developed. The temperature fields in the melt and crystal are calculated by finite - element analysis; the thermal stress distribution in crystals is also studied. The radiative heat transfer in semi-transparent shaped crystals has certain peculiarities associated with the small diameter of the crystals, the larger growth rates and the small height of the melt layer between the crystal and the die. From obtained results we can predict the possibility of radiative supercooling in the melt leading to morphological instability of the crystallization front.

1. Ettouney, H.M., Kalejs, J.P.: *J. Crystal Growth* 1987, 82 17.
2. Nicoara, D., Nicoara, I.: *J. Crystal Growth* 1987, 82 95.
3. Nicoara, I., Nicoara, D., Sofonea, V.: *J. Crystal Growth* 1990, 104 169.
4. Nicoara, I., Nicoara, D., Vizman, D.: 5-th European Conference on Crystal Growth, Budapest, 1991.

## GROWTH OF 2" Ge:Ga CRYSTALS BY THE DYNAMICAL VGF PROCESS AND ITS NUMERICAL MODELLING INCLUDING TRANSIENT SEGREGATION

D. Hofmann, T. Jung and G. Müller

Institut für Werkstoffwissenschaften 6, Kristallabor  
Universität Erlangen-Nürnberg, Martensstr. 7  
D-8520 Erlangen, FRG

Recently there has been an increasing interest in the growth of compound semiconductor crystals by vertical directional solidification with bottom seeding, generally termed as Vertical Bridgman technique (VB). This growth method offers in principle the thermal environment for the preparation of low defect III-V- and II-VI-compounds provided that growth conditions can be controlled carefully. A promising VB variant represents the dynamical Vertical Gradient Freeze (DVGF) technique using multizone furnace technology because temperature profiles can be tailored during the whole growth process. A drawback of the DVGF method is the complexity of the system and the process.

In spite of the potential of DVGF processing there exist only a few theoretical studies about the influence of the thermal field on the shape of the solid liquid interface and the resulting dopant segregation in the crystal [1,2]. Quantitative comparisons of experiments and numerical simulations have only been published for small crystal diameters and using quasi-steady modelling of segregation [3,4]. These analysis are not able to predict quantitatively doping distributions or optimal control parameters for technically interesting 2" configurations because of the transient nature of the DVGF process.

We studied, therefore, a more realistic numerical model of the DVGF growth process considering its transient character as well as details of the heat transfer. Our primary objective is to investigate the correlation of the thermal boundary conditions at the furnace level with the shape of the solid/liquid interface and the dopant segregation in 2" crystals during the whole gradient freeze process. These calculations are compared to experimental results obtained by DVGF growth of Ga doped Ge crystals (2" diameter).

The growth experiments were conducted in a new type of multisegment furnace (23 zones) which was especially

designed to establish thermal profiles of high flexibility for crystal growth of III-V-compounds under high pressure (e.g. InP). The results of 3 typical growth processes applying linear and non linear thermal profiles are shown. Crystals were characterized by revealing the interface shapes by chemical etching and by electrical mapping of the axial and radial dopant distribution.

Depending on the thermal boundary conditions concave, flat and convex interfaces and variations of the radial dopant distribution were found. These experimental results are compared to numerical calculations which were performed on two different levels. The heat transfer in the multizone furnace is evaluated by a commercial code NEKTON [5] (relevant heat transfer coefficients in the DVGF apparatus were determined experimentally). The results give the boundary conditions for numerical simulations with a code which calculates time dependently the convective flow in the melt and dopant distribution in the melt and crystal considering the decreasing melt volume during a DVGF growth run. This code using the finite volume method was developed in collaboration with the Fluid Mechanics Institute at the University Erlangen-Nürnberg.

This comparison of experimental and numerical results and the parameter variations provide the basis for our further work on the improvement of the control of DVGF processing.

---

- [1] M.J. Crochet, F. Dupret, Y. Ryckmans, F.T. Geyling, E.M. Monberg: *J. Crystal Growth* **97** (1989) 173.
- [2] D.H. Kim, R.A. Brown: *J. Crystal Growth* **109** (1991) 66.
- [3] P.M. Adornato, R.A. Brown: *J. Crystal Growth* **80** (1987) 155.
- [4] C.A. Wang: Doctoral Thesis MIT 1984.
- [5] Nectonics Inc., Cambridge MA (USA).

## NUMERICAL STUDY OF CZOCHRALSKI SILICON FULL PROCESS THERMOKINETICS

A. Virzi

MEMC Electronic Materials, 39012 Merano, Italy

The as-grown microdefect density and chemical inhomogeneity of a Czochralski silicon single crystal are basically conditioned by dynamics of heat and mass flows through the coupled nutrient melt and growing boule, thermally interacting with the surrounding puller environment. Moreover, a significant role on bulk defect nucleation and stabilization seems to be played by the post-growth crystal cooling pathway too. Mathematical modelling and computer simulation of CZ transport phenomena stand as effective means for getting exhaustive insight into melt hydrodynamics and heat transfer features, feeding research for linking process state variables kinetics with silicon microdefect formation mechanisms [1].

This paper reports the Finite Element Analysis (FEA) of the global process thermal history for a typical CZ silicon production run, where a 125 mm diameter monocrystal is grown from 25 Kg polysilicon charge and then slowly cooled down to the ambient temperature inside the furnace. Due to the long geometrical time scale of the pulling stage the CZ growth thermal history is fitted from a suitable set of thermal field snapshots as the crystal lengthening proceeds, whose time coordinate is given by integration of the reciprocal pull rate function [1-3]. An axisymmetric, conduction dominated, quasi-steady formulation of the energy balance in the system [4] is solved for each

growth step, with temperature dependent material properties and detailed boundary conditions accounting for gas convection, view factors modulated diffuse-gray radiation and latent heat delivery at the free-shaped silicon phase change interface. The physical consistency of the crystal thermal field predictions is guaranteed by the recursive updating of heater power level so that the solid/liquid/gas tri-junction temperature matches the silicon melting one. The FEA result for the rod tail ending configuration provides the initial conditions of the final fully transient crystal cool-down simulation driven by a self-adapting time step algorithm for an accurate but not redundant scanning of the temperature fall. The numerical study is followed by the discussion of the influence of melt hydrodynamics and gas cooling modelling idealizations on reliability of the computed crystal thermal field, comparing FEA heater power and temperature outputs with homologous experimental data.

- [1] A. Virzi et M. Porrini, E-MRS Conf., Strasbourg (F), June 1992, abs. CVII/P10.
- [2] A. Virzi, *J. Crystal Growth* 97 (1989) 152.
- [3] A. Virzi, EUROMAT'91 Conf. Proc., Cambridge (UK), July 1991, 166.
- [4] A. Virzi, *J. Crystal Growth* 112 (1991) 699.

---

## MODELLING OF HEAT AND MASS TRANSPORT UNDER LOW FREQUENCY VIBRATIONS OF CRYSTAL IN DIRECTED SOLIDIFICATION TECHNIQUE

G.A. Dolgikh\*, E.V. Zharikov, A.Z. Myaldun, N.R. Storozhev, N.K. Tolochko and A.I. Feonychev\*

General Physics Institute, Acad. of Sci., Moscow, USSR

\*Applied Mechanics and Electrodynamics Institute, MAI, Moscow, USSR

The new type of convection exciting from low frequency vibrations of small amplitude [1] is a powerful method to effect the heat and mass transport processes in crystallization. In presented report the melt flows and heat and mass transfer under harmonic oscillations of growing crystal is investigated considering the deformation of liquid free surface, and without deformation also.

The cases of interaction of vibrational, gravitational and thermocapillary convections and also the case of absence of thermogravitational component (i.e. microgravitational conditions) are examined. Vibrations of crystal in last case leads to the deformation of contour of thermocapillary liquid motion and the domination of vibrational motion near the crystal. By means of numerical simulation was shown that hydrodynamic

flow patterns near liquid-solid interface is totally determined by the action of secondary flow of vibrational convection. The flows inversion of vibrational convection in Chochralsky configuration with submerge depth variation of the vibrating body was found.

The crystal vibrations leads to variation of macro- and micro-segregation of impurities and dopants in the crystal.

The numerical modelling results are in a good agreement with experimentally observed pictures of liquid or melt flows under crystal vibrations.

---

- [1] Zharikov E.V., Prihod'ko L.V., Storozhev N.R., Proceeding ICCG-9, pp. 910-914.

## SESSION 5B

### DISORDERED OXIDE CRYSTAL HOSTS FOR DIODE PUMPED LASERS

*Mark H. Randles and John E. Creamer*

Litton Airtron SYNOPTICS, P.O. Box 410168, Charlotte, NC 28241

*Roger F. Belt*

Litton Airtron, 200 East Hanover Avenue, Morris Plains, NJ 07950

*Gregory J. Quarles and Leon Esterowitz*

Naval Research Laboratory, Code 6551, Washington, DC 20375-5000

Diode pumped lasers are efficient, compact sources. However, typical rare earth ions have narrow absorption linewidths in highly ordered crystals like YAG and precise control of the diode wavelength is required for effective pumping. The 808nm absorption line of Nd:YAG has a width of only 1nm compared to a typical laser diode output linewidth of 3nm. Disordered structures provide line broadening and a suitable disordered host will improve performance and reduce cost of the diode pumped laser.

We grew and characterized various disordered host crystals. We selected congruent compositions with sites suitable for rare earth substitution. Data will be presented for  $\text{SrGdGa}_3\text{O}_7$  (SGGM),  $\text{La}_3\text{Ga}_5\text{SiO}_{14}$  (LGS),  $\text{La}_3\text{Ga}_5\text{GeO}_{14}$  (LGG),  $\text{Y}_2\text{SiO}_5$  (YOS) and  $\text{CaLa}_4(\text{SiO}_4)_3\text{O}$  (CaLaSOAP). To compare the hosts, crystals were doped with 2-4 at % Nd, and in some cases

with the smaller rare earths. We discuss crystal growth issues and measurements of lattice parameters and distribution coefficients.

The crystals were characterized by absorption and fluorescence spectroscopy. Measurements include the maximum absorption coefficients at convenient diode pump wavelengths, absorption linewidths, fluorescent lifetimes, and stimulated emission cross-sections. Absorption, excitation and emission spectra will be shown. Initial results look promising. For example, the 808nm Nd absorption linewidth in SGGM is 8nm and the excitation spectrum linewidth is 30nm.

---

Support is gratefully acknowledged from the Office of Naval Research and DARPA.

## GROWTH AND CHARACTERIZATION OF CALCIUM NIOBIUM GALLIUM GARNET

### [CNGG] SINGLE CRYSTALS FOR LASER APPLICATIONS

*K. Shimamura, M. Timoshechkin\*\*, T. Sasaki\*, K. Hoshikawa and T. Fukuda*

Institute for Materials Research, Tohoku University, Sendai, 980, Japan

\*Faculty of Engineering, Osaka University, Japan

We have successfully grown Nd doped calcium niobium gallium garnet (Nd:CNGG single crystal and firstly demonstrated laser diode (LD) pumped Nd:CNGG laser oscillation. Single crystals of various active ions doped CNGG were found to exhibit very interesting spectroscopic properties as new, LD pumped laser and tunable laser in the 1-3 $\mu$ m ranges. In this paper, we report Czochralski growth and characterization of CNGG single crystals. Growth conditions, properties and crystal quality of CNGG for laser applications are discussed.

Single crystals were grown by the Czochralski technique.  $\text{Ca}_3\text{Nb}_{1.6875}\text{Ga}_{3.1875}\text{O}_{12}$  was found to be the congruently melting composition with a melting point around 1470°C. By using Pt or Ir crucibles, CNGG single crystals (22mm $\phi$  x 70mm) were grown along <111> direction under air or  $\text{N}_2+1\%\text{O}_2$  atmosphere at the rate of 4mm/hr without after heater. Nd<sup>3+</sup>,

Tm<sup>3+</sup>, Er<sup>3+</sup>, Ho<sup>3+</sup> and Cr<sup>3+</sup> were selected as dopants. A typical Nd:CNGG as-grown crystal is shown in Fig. 1. The crystal shows smooth surface with a facet of three-fold symmetry. Lattice constants along the growth axis were almost constant (12.51Å). Transparent bubble free Tm:CNGG (Tm<sub>2</sub>O<sub>3</sub>:2.7wt%) crystals were grown at the rate of 3mm/h, whereas for growth of high quality Nd:CNGG (Td<sub>2</sub>O<sub>3</sub>:2.5wt%) crystals to reduce pull rate down to 1.1mm/h was required. The absorption spectra of Nd:CNGG and Tm:CNGG showed nonuniform broadening absorption line compared with those of Nd:YAG and Tm:YAG (see Fig. 2), that is supposed to be based on disordered structure and is very profit for plural LDS pumped laser.

\*\*Permanent address: General Physics Institute, Moscow B-333, USSR

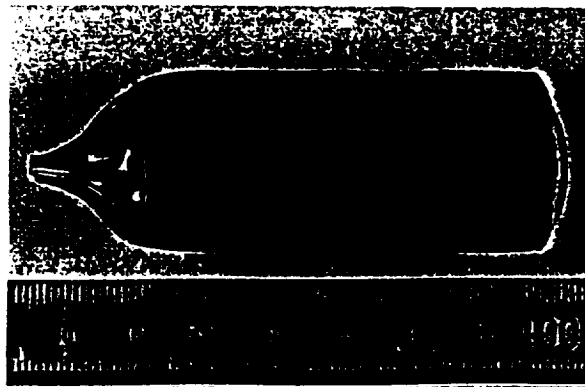


Figure 1. Nd:CNGG single crystal.

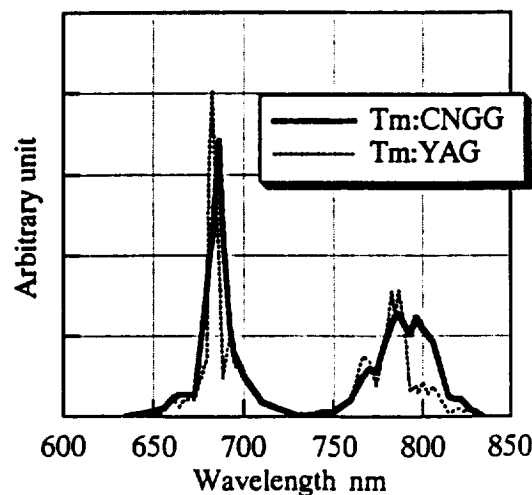


Figure 2. Absorption spectra of Tm:CNGG compared with that of Tm:YAG.

## Si AND Mg DOPED GGG SINGLE CRYSTALS

*M. Göbbels<sup>1</sup>, S. Kimura<sup>2</sup>, K. Langer<sup>3</sup> and E. Woermann<sup>1</sup>*

<sup>1</sup>Institut für Kristallographie, RWTH Aachen, Jägerstraße 17/19, D-5100 Aachen, Germany

<sup>2</sup>National Institute for Research in Inorganic Materials, Namiki 1-1, Tsukuba Ibaraki 305, Japan

<sup>3</sup>Institut für Mineralogie und Kristallographie, TU Berlin, Ernst-Reuter-Platz 1, D-1000 Berlin 12, Germany

There is a wide range of application for GGG ( $Gd_3Ga_5O_{12}$ ) single crystals as laser host materials and substrates for magnetic bubble devices. Due to impurities, especially Si, in the starting oxides color centers are formed in the GGG crystal.

Several GGG single crystals with different doping levels of Si, Mg and Si+Mg were grown by the floating-zone method. The actual doping level was checked by chemical and spectroscopic analysis. The color centers were activated by anneal-

ing at 1673 K in argon, hydrogen or oxygen atmospheres respectively followed by a Xe-lamp irradiation. The transmission spectra of the crystals were measured.

The absorption bands corresponding to the activated color center can be correlated with the respective dopant and the type of activation (Table 1). In case of Si+Mg-doping the Si-color center formation is eliminated.

*Table 1. Color centers and the corresponding activation.*

	Si-doped GGG	Mg-doped GGG
Annealing in $H_2$	Absorption band at 320 nm after additional irradiation	Decrease of absorption at 240-310 nm. Increase of absorption at 240-310 nm due to additional irradiation.
Annealing in $O_2$	Decrease of absorption at 240-310 nm.	Absorption at 240-310 nm increases.
Annealing in Ar	Absorption band at 420 nm.	No influence on the absorption.

## THE BEHAVIOR OF CHROMIUM IONS IN FORSTERITE

*Yasuhide Yamaguchi\*, Kiyoshi Yamagishi and Yukio Nobe*

MITTSUI Mining & Smelting Co., Ltd. (Japan)

The chromium ion doped forsterite( $Cr:Mg_2SiO_4$ ) is the only 1.2m laser crystal known. It is assumed that the activator is tetravalent chromium ions which are substituted at the tetrahedral silicon sites. We have grown forsterite crystals with various chromium concentrations and under different growth atmospheres. The crystals were grown by the Czochralski technique or, when the growth atmosphere was oxygen, the floating zone technique was used. Post growth annealing under both oxidizing and reducing conditions was also done.

The absorption spectra of the crystals were different, depending on the oxygen partial pressure during growth. The absorption is caused by tetravalent, trivalent and divalent chromium ions, and the absorption strength is related to the quantity and stability of each valency of chromium. In heavily doped forsterites, divalent chromium appeared even with growth under oxidizing atmosphere.

We annealed the crystals under different oxygen partial pressures at 1750°C for 10 hours. When crystals grown in oxidizing atmosphere were annealed under low oxygen partial pressure, tetrahedral chromium absorption became weak and divalent chromium absorption appeared. When we re-annealed these crystals under oxygen atmosphere, the absorption

reverted to that observed in the as grown crystals. On the other hand, when crystals that were grown under low oxygen partial pressure were annealed in high partial pressure oxygen, a very small change in the absorption was observed.

We conclude that chromium ions in forsterite can move from tetragonal to octahedral sites. There are many cation vacancies at the magnesium sites because of the required charge compensation for the always present trivalent chromium. Reduced tetragonal chromium ions move to the magnesium site vacancies and back to the tetragonal sites when re-annealed in oxidizing atmosphere. In the crystal grown under low oxygen partial pressure, there are also many magnesium vacancies because of trivalent chromium ions. But there are no silicon vacancies, and tetravalent chromium ions can therefore not move to tetrahedral sites. This explains the difficulty in obtaining tetravalent chromium by annealing in an oxidizing atmosphere.

\*Visiting Scientist, Laboratory for Advanced Solid State Laser Materials, Center for Materials Science and Engineering, Massachusetts Institute of Technology, Cambridge, MA 02139.

## CZOCHRALSKI GROWTH OF RARE EARTH OXYORTHOSILICATE SINGLE CRYSTALS

C.L. Melcher, R.A. Manente, C.A. Peterson and J.S. Schweitzer  
Schlumberger-Doll Research, Ridgefield, CT 06877-4108, USA

The rare earth oxyorthosilicates ( $\text{Ln}_2(\text{SiO}_4)\text{O}$ , where  $\text{Ln} = \text{Sc, Y, La...Lu}$ ) have been studied previously both in powder form and as single crystals<sup>1,2</sup>. They melt congruently at ~1870 - 2070°C and crystallize in either monoclinic C or monoclinic P structures, depending on the size of the rare earth ion.<sup>3</sup> The Gd and Y compounds have been studied for possible applications as lasers, CRT faceplates, and scintillators.<sup>4,5,6</sup>

We used the Czochralski technique to grow single crystals of  $\text{Ln}_2(\text{SiO}_4)\text{O}$  where  $\text{Ln} = \text{Y, Gd, or Lu}$  from Ir crucibles in an atmosphere of either pure  $\text{N}_2$  or  $\text{N}_2 + 0.3\% \text{O}_2$ . Typically the boules were 2 cm diameter and 5-6 cm long. In addition to pure crystals, several crystals of each type were grown with Ce doping at 0.25 - 0.5 atomic to produce scintillators. The distribution coefficient of Ce varied from ~0.2 in  $\text{Y}_2(\text{SiO}_4)\text{O}$  and  $\text{Lu}_2(\text{SiO}_4)\text{O}$  to ~0.6 in  $\text{Gd}_2(\text{SiO}_4)\text{O}$ . The scintillation emission arises from a 5d to 4f transition in the trivalent Ce ions. The wavelength and, to a lesser degree, the decay time of the emission are influenced by the crystal field at the Ce site due to the host lattice. Typically, the emission wavelength is ~400 - 450 nm and the decay time is ~50 ns. Ce-doped boules of  $\text{Y}_2(\text{SiO}_4)\text{O}$  and  $\text{Gd}_2(\text{SiO}_4)\text{O}$  were slightly yellow in color while Ce-doped  $\text{Lu}_2(\text{SiO}_4)\text{O}$  boules were colorless.

We found that the optimum growth conditions varied significantly among the three materials. The extent of defect and void formation in  $\text{Gd}_2(\text{SiO}_4)\text{O}$  was more strongly affected by rotation rate, pulling rate, and thermal gradient compared to

$\text{Y}_2(\text{SiO}_4)\text{O}$  and  $\text{Lu}_2(\text{SiO}_4)\text{O}$ . In addition, the use of seed crystals as opposed to Ir wire was more important for  $\text{Gd}_2(\text{SiO}_4)\text{O}$  due to its relatively poor mechanical strength.

1. G.V. Anan'eva, A.M. Korovkin, T.I. Merkulyaeva, A.M. Morozova, M. V. Petrov, I.R. Savinova, V.R. Startsev, and P.P. Feofilov, Growth of lanthanide oxyorthosilicate single crystals and their structural and optical characteristics, *Izvestiya Akademii Nauk SSSR, Neorganicheskie Materialy*, 17(6), 1037-1042 (1981).
2. P.I. Born, D.S. Robertson, and P.C. Smith, *J. Mat. Sci. Lett.* 4, 497-501 (1985).
3. I. Felsche, The crystal chemistry of the rare-earth silicates, in *Structure and Bonding* V13, Springer-Verlag, 99-197 (1973).
4. R.F. Belt and J.A. Catalano, Growth of cerium-doped rare earth silicates for tunable lasers, in *Tunable Solid-State Lasers II*; Proceedings of the OSA topical meeting, A.B. Budgor, L. Esterowitz, and L.G. DeShazer, eds. (Springer Series in Optical Sciences, V. 52) 94-101 (1986).
5. C.D. Brandl, A.I. Valentino, and G.W. Berkstresser, Czochralski growth of rare-earth orthosilicates ( $\text{Ln}_2\text{SiO}_5$ ), *J. Crystal Growth* 79, 308-315 (1986).
6. K. Takagi and T. Fukazawa, Cerium-activated  $\text{Gd}_2\text{SiO}_5$  single crystal scintillator, *Appl. Phys. Lett.* 42(1) 43-45 (1983).

## PHYSICAL PROPERTIES OF A $\text{Y}_3\text{Al}_5\text{O}_{12}$

V.J. Fratello and C.D. Brandl  
AT&T Bell Laboratories, Murray Hill, NJ

Data on density, surface tension and contact angle (with an Ir wire) were taken in a  $\text{Y}_3\text{Al}_5\text{O}_{12}$  melt from 1970°C (just above the melting point) to 2070°C. Density, as determined by the Archimedean two bob technique, was 3.688 g/cm<sup>3</sup> at the melting point, with a volume coefficient of thermal expansion of only  $1.8 \pm 0.5 \times 10^{-5}$ . The maximum bubble pressure method found the surface tension to be high, 781 dyne/cm at 1970°C,

but also with a very low temperature dependence. Data from these two measurements allowed determination of the contact angle of the melt with the iridium suspension wire to be approximately 113°. These data would account for a lack of convective and surface tension driven fluid flow that makes yttrium aluminum garnet melts appear quiescent.

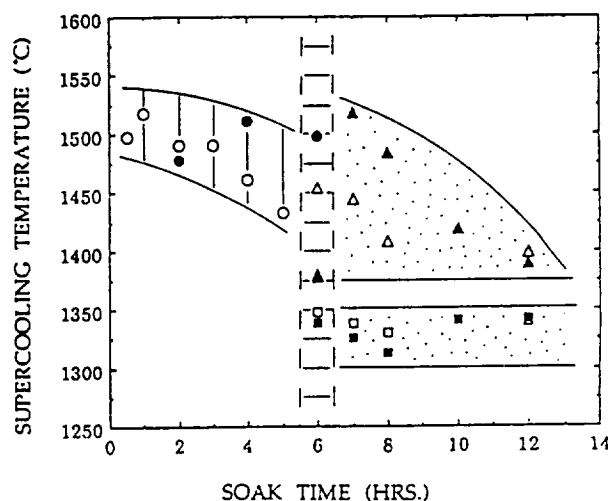
# METASTABLE CRYSTALLIZATION OF $\text{Nd}_3\text{Ga}_5\text{O}_{12}$ AND $\text{Gd}_3\text{Ga}_5\text{O}_{12}$ GARNET MELTS

*S.A. Markgraf\*, M. Göbbels\*\* and S. Kimura  
 National Institute for Research in Inorganic Materials  
 Namiki 1-1, Tsukuba, Ibaraki 305 Japan*

The metastable crystallization of garnet melts has been the subject of numerous investigations. These investigations have centered on the departure from the equilibrium phase diagram during crystallization from a stoichiometric garnet melt. It was observed that either pure garnet phase, or a mixture of perovskite + oxide (metastable condition), can be obtained depending on the degree of superheating. This difference in crystallization behavior was often coupled with large undercooling of the melt.

The concept of a critical temperature has been widely cited concerning the metastable crystallization of garnet melts. Recently it was shown that the time the melt is held above the melting temperature is also important. In this presentation we will introduce the concept of critical time for the case of  $\text{Gd}_3\text{Ga}_5\text{O}_{12}$ , and further examine the characteristics of critical time with studies on the metastable crystallization behavior of  $\text{Nd}_3\text{Ga}_5\text{O}_{12}$  (NdGG). The variables investigated were: the effect of soak time, soak temperature, crucible material, and starting material (crushed single crystal; calcined powder; unfired, stoich. mix of oxides). The use of different crucible material had no effect on the time necessary to produce metastable crystallization. Increasing the soak temperature shortened the critical time, and the critical time was shown to be strongly dependent on the nature of the starting material. The fig. below shows the supercooling temp. as a function of soak time at  $\sim 1570^\circ\text{C}$  for calcined NdGG powder. The vertically-striped region yielded garnet upon crystallization; the horizontally-striped area was either multiphase material or garnet; the

stippled regions indicate metastable crystallization. Filled symbols represent Pt/Rh crucibles; open symbols are from Pt crucibles. We will discuss these results on the basis of competing interactions between embryos of the garnet phase and the perovskite phase.



\*Present Address: Hitachi Metals, Ltd.; Magnetic & Electronic Materials Research Laboratory, 5200 Mikajiri, Kumagaya-shi, Saitama-ken 361, Japan.

\*\*Present Address: Institut für Kristallographie; RWTH Aachen, Jägerstr. 17/19, D-5100 Aachen, Germany.

## TOP-SEEDED SOLUTION GROWTH OF VANADATE GARNETS

Barry A. Wechsler and Charles C. Nelson  
Hughes Research Laboratories, 3011 Malibu Canyon Road  
Malibu, California 90265 USA

Garnets in which the tetrahedral site is occupied by a pentavalent ion include the minerals palenzonite,  $\text{NaCa}_2\text{Mn}_2\text{V}_3\text{O}_{12}$ , and berzeliite,  $\text{NaCa}_2\text{Mn}_2\text{As}_3\text{O}_{12}$ . Many other vanadate, arsenate, and phosphate garnets have been synthesized in powder and single crystal forms. Single crystals of vanadate garnets  $\text{NaCa}_2\text{M}_2\text{V}_3\text{O}_{12}$  ( $\text{M} = \text{Mg, Mn, Co, Ni}$ ) have previously been grown by Czochralski, flux, and top-seeded solution growth (TSSG) methods. The best crystals appear to have been produced by TSSG with lead oxide added to the melt, although incorporation of lead is a problem in that

approach. In this work, we have used TSSG to grow large (up to  $4 \text{ cm}^3$  in a  $30 \text{ cm}^3$  crucible) crystals of  $\text{NaCa}_2\text{Mg}_2\text{V}_3\text{O}_{12}$  and  $\text{NaCa}_2\text{Co}_2\text{V}_3\text{O}_{12}$  (Figure 1). An excess of sodium vanadate was used as the solvent, and growth was driven by slow cooling. This method produces crystals very close to the ideal stoichiometric composition and has the advantage of avoiding contamination by flux atoms such as Pb. Samples free of macroscopic inclusions have been grown on [001], [011], and [111] oriented seeds.

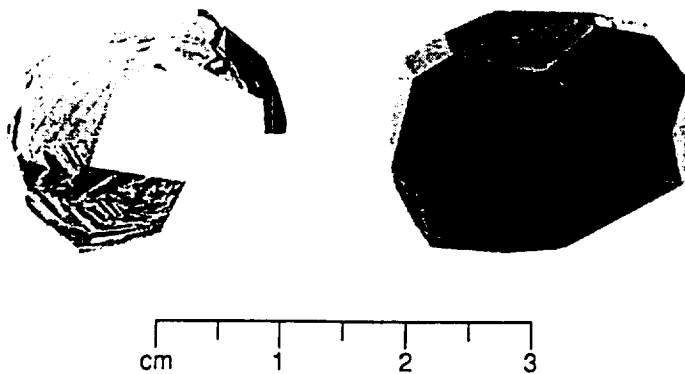


Figure 1. Vanadate garnet crystals,  $\text{NaCa}_2\text{Mg}_2\text{V}_3\text{O}_{12}$  (left) and  $\text{NaCa}_2\text{Co}_2\text{V}_3\text{O}_{12}$  (right).

## THEORETICAL GROWTH FORMS OF NATURAL GARNETS

*M.M.R. Boutz\* and C.F. Woensdregt*

Institute of Sciences Utrecht, Department of Geochemistry, Section of Crystallography  
P.O. Box 80.021, NL-3508 TA Utrecht, the Netherlands

Natural garnets,  $X^{2+}Y^{3+}2(SiO_4)_3$ , where X represents bivalent cations such as  $Fe^{2+}$ ,  $Mg^{2+}$ ,  $Mn^{2+}$  or  $Ca^{2+}$ , and Y trivalent ones such as  $Al^{3+}$ ,  $Fe^{3+}$ , or  $Cr^{3+}$ , form an important group of rockforming minerals. The most important F faces of natural garnets, which grow slowly according to a layer mechanism, are  $\{112\}$ ,  $\{110\}$ ,  $\{123\}$ ,  $\{001\}$ ,  $\{120\}$  and  $\{332\}$ . The crystal structure of pyrope,  $Mg_3Al_2(SiO_4)_3$ , has been selected as representative of the whole garnet group. The surface configurations of the elementary growth layers called slices, are bounded by  $Al$  ions in the case of  $d_{220}$  and  $d_{240}$ . An other boundary configuration can also been chosen for the former one, that by  $Si$  and  $Al$  ions, just as in the case of  $d_{040}$ . For  $d_{112}$  two boundaries are possible, one with  $Al$  and  $Mg$ , and an other one with  $Al$  and  $Si$ . In three different electrostatic point charge models, in which the point charges of the atoms forming the  $Si-O$  tetrahedral bonds vary from the completely ionic model with formal charges,  $[Si^{4+}O^{2-}_4]^{4-}$ , to the covalent one with reduced charges,  $[Si^0O^-_4]^{4-}$ , the attachment energies of the F faces have been calculated. In all models the formal point charges of the  $Al$  and  $Mg$  ions have been used. For F faces these energies are sup-

posed to be directly proportional to their growth rates. The three dimensional Wulff plots of these energies yield the theoretical growth forms. For models with formal charges these growth forms consist only of  $\{112\}$ . However, on the more covalent like models, which have lower effective charges of oxygen  $q_0$ ,  $\{100\}$  and  $\{110\}$  appear, while, at the same time,  $\{112\}$  disappears slowly. If the effective charge of  $q_0 = 1$  the growth form is merely bounded by  $\{110\}$ . Only at high effective point charges on oxygen,  $2 \leq q_0 \leq 1.7$ -ordering of the boundary cations changes substantially the growth forms. They consist of  $\{100\}$  and  $\{110\}$ , but at lower effective charges the growth form is more or less similar to that of the disordered models. If the mineral growth of natural garnets proceeds with isolated silicate tetrahedra as building units, the theoretical growth form would be  $\{112\}$ .

\*Present address: University of Twente, Faculty of Chemical Technology, Laboratory for Inorganic Chemistry, Materials Science and Catalysis, P.O. Box 217, NL-7500 AE Enschede, the Netherlands.

---

## CRYSTAL GROWTH AND CHARACTERIZATION OF NEW LASER MATERIALS

*R. Collongues, A.M. Lejus, I. Théry and D. Vivien*

Laboratoire de Chimie Appliquée de l'Etat Solide

ENSCP, 11 rue P. et M. Curie, 75231 Paris cedex 05, France

During the last ten years, new laser materials were discovered in our laboratory. One of them is the LMA:Nd<sup>3+</sup> (or LNA) (lanthanum neodymium aluminate Nd<sup>3+</sup> doped) which is industrially developed and can lead to applications in nuclear physics and high sensitivity magnetometers.

Another material is the ASN (strontium neodymium aluminate) of which the formula is  $Sr_{1-x}Nd_xMg_xAl_{12-x}O_{19}$ . It belongs to the same structural type as LNA (magnetoplumbite) and exhibits similar optical properties. But, while LNA can be grown only along the "a" crystallographic direction, which does not favor laser action, ASN can be grown along both "a" and "c" direction, the "c" direction being the preferred direction for the laser emission as well as for the cooling of the rod laser (maximum of thermal conductivity perpendicularly to the "c" direction). Furthermore the emission spectrum shows

three tunable humps, one of them being very broad (between approximately 1066 and 1078 nm). Therefore ASN is a promising material for power lasers as well as tunable lasers.

The third material belongs to a very different structural type. It is the gehlenite neodymium doped of which the formula is  $Ca_{2-x}Nd_xAl_{2+x}Si_{1-x}O_7$ . The calcium (or neodymium) crystallographic site is of very low symmetry leading to a strong absorption band around 800 nm which is the emission band of laser diodes used for optical pumping of neodymium lasers. Furthermore  $Al^{3+}$  and  $Si^{4+}$  ions are randomly distributed in the same type of sites which leads to an enlargement of the absorption and emission bands. The broadness of the absorption band is able to cover the drift of the diode during operating and thus to avoid the use of a Peltier element to control the temperature. The Nd<sup>3+</sup> doped gehlenite appeal as a very convenient material for optical pumping by laser diodes.

## CRYSTAL GROWTH OF $\text{YVO}_4$ USING THE LHPG TECHNIQUE

*S. Erdei and F. W. Anger*

Materials Research Laboratory

The Pennsylvania State University, University Park, PA 16802

Some difficulties are encountered in the growth of neodymium doped yttrium vanadate Nd:YVO<sub>4</sub> single crystals which have outstanding laser optical properties. Since vanadium oxide has an exceptionally high vapor pressure at the melting point of YVO<sub>4</sub> [1810°C] [1], it was practical to select a growth method where the whole volume of the substance is not melted, but only a small region at the crystallization front of the melt. Steady-state high temperature solution growth may be achieved using vanadium rich YVO<sub>4</sub> feed rods to compensate for the V<sub>2</sub>O<sub>5</sub> vaporization.

A 50 watt focused CO<sub>2</sub> laser beam was used for the fiber growth experiments. Ceramic rods of YVO<sub>4</sub> with different square cross-sections and different V<sub>2</sub>O<sub>5</sub>-Y<sub>2</sub>O<sub>3</sub> starting compositions were prepared for both seed rods and feed rods. The YVO<sub>4</sub> powder samples were synthesized by two methods: 1) Preparation from aqueous solution and 2) Solid state reaction of Y<sub>2</sub>O<sub>3</sub> and V<sub>2</sub>O<sub>5</sub> oxides. The firing process employed generally led to a change in the starting composition of the YVO<sub>4</sub> due to the vaporization and diffusion of V<sub>2</sub>O<sub>5</sub>.

We have developed a quite sensitive "diffusion-colorization" method to find the YVO<sub>4</sub> "congruency." Our measurements indicate that this congruency is at 49.3 mol% V<sub>2</sub>O<sub>5</sub>-50.7 mol% Y<sub>2</sub>O<sub>3</sub>. The crystal fibers of different V<sub>2</sub>O<sub>5</sub>-Y<sub>2</sub>O<sub>3</sub> starting compositions were composed of a mixture of yellowish-white, light yellow and black crystalline regions, the proportions of which were found to vary with the composition.

The steady-state growth of the light yellow YVO<sub>4</sub> crystals, which were grown with different lengths at the necks of the fibers depend on the vanadium content of the feed rods. The presence of Y<sub>8</sub>V<sub>2</sub>O<sub>17</sub> was detected in the YVO<sub>4</sub> fibers by X-ray powder diffraction for congruent and stoichiometric compositions. The color of Y<sub>8</sub>V<sub>2</sub>O<sub>17</sub> identified by Electron Microprobe Analysis is yellowish-white similar to that of YVO<sub>4</sub>. The single crystal structure of the light yellow YVO<sub>4</sub> crystal fibers which were grown with small cracks was identified by Laue method. The oxygen deficiency which is evident in the black crystals has been interpreted as a YVO<sub>3</sub> formation [2]. The YVO<sub>3</sub> → YVO<sub>4</sub> reoxidation is carried out in the solid phase and requires more time than the LHPG crystal growth process. The melting point of YVO<sub>3</sub> is 1860°C [3]. The most effective method to avoid reduction is to maintain the local zone temperature below 1860°C inside the floating zone. This can be accomplished by decreasing the floating zone length, decreasing the temperature gradient inside the zone and by using ceramic feed rods which have relatively high vanadium concentrations.

The best results were obtained for starting compositions of approximately 55 mol% V<sub>2</sub>O<sub>5</sub>.

1. E. M. Levin, *J. Am. Ceram. Soc.* 50(7), 381 (1967).
2. R. C. Ropp, *Mat. Res. Bull.*, Vol. 10, pp. 271-276 (1975).
3. D. B. Rogers et al., *J. Appl. Phys.* 37 (3) (1967).

## SESSION 5C

### DIRECT GROWTH OF NANOMETER SIZE QUANTUM WIRE SUPERLATTICES

P.M. Petroff

Materials Department University of California  
Santa Barbara, CA 93106

We describe a novel quantum wire superlattice [1] that is grown directly by Molecular Beam Epitaxy. This superlattice is deposited using alternate fractional submonolayers of GaAs and  $Al_xGa_{1-x}As$  on a vicinally oriented surface. The cross section transmission electron micrograph (Figure 1) shows that the interface may be shaped in the form of parabolas. These structures have a build in carrier confinement along the growth direction([001]) and the lateral direction([110]). The scale of the confinement is smaller than 10nm and can be adjusted by varying the interface curvature or the substrate vicinal angle. The 1D quantum wire array formed are called Serpentine Superlattices (SSL) and the apex of the parabolas corresponds to the location of the quantum wires in the SSL. Photoluminescence (Figure 2) and Photoluminescence excitation spectra show polarization effects that are associated with the two dimensional confining potential of the structure. Comparison of the observed polarization with the theoretically computed one[2] indicates that the structures are not perfect and that a certain amount of Al is present in the quantum wire region of the SSL. This amount is estimated to be close to 30% of the amount of the Al content in the barrier regions of the structure. The resulting lateral confinement for a structure with 33% Al in the barrier is found to be around 80meV. The poor segregation

of Al at the step edges and the presence of superkinks at step edges are the probable reasons for the observed intermixing of Al and Ga in the quantum wires. Theory and experiments indicate that for the  $AlGaAs$ - $GaAs$  SSL the holes are confined to a 1D structure while the electrons, because of the weak lateral confinement have a 2D character.

The origin of the large improvement (300%) in the observed Al segregation obtained by growing on (110) vicinal surfaces will be discussed.

Quantum wire structures made of  $AlGaSb$ - $GaSb$ [3] will be described and their structural and optical properties compared to those of the  $AlGaAs$ - $GaAs$  SSL structures.

[1] M.S. Miller, C.E. Pryor, H. Wehman, L.A. Samoska, H. Kroemer, and P.M. Petroff. *J. Crystal Growth* 111, 323(1991); M.S. Miller, H. Weman, C.E. Pryor, M. Krishnamurty, P.M. Petroff, H. Kroemer, and J.L. Merz. *Phys. Rev Lett.* (submitted 1992).  
[2] C. Pryor. *Phys. Rev. B* 44, 12912(1991).  
[3] S. Chalmers, H. Weman, J.C. Yi, H. Kroemer, J.L. Merz, and N. Dagli. *Appl. Phys Lett.* 60, 1676 (1992).

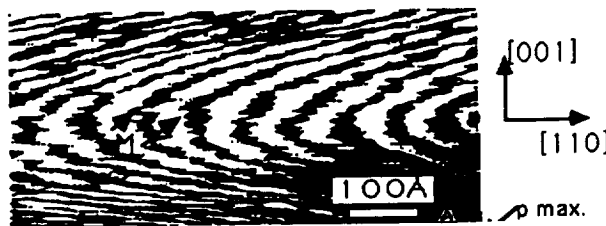


Figure 1. A) Cross section TM micrograph of a single crescent SSL. Black represents areas that are GaAs rich while white region correspond to the Al rich digital alloy barrier layers. Arrows in M indicate a meandering of the interface.

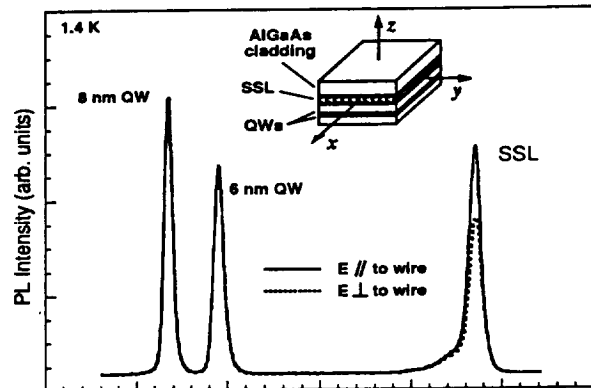


Figure 2. Polarization dependent PL spectra for a single quantum wire SSL. The observation direction is along the z axis as defined in the inset which also shows the SSL position and the quantum wells in the sample. The solid and dashed lines are for light polarized parallel and perpendicular to the quantum wires respectively. The quantum wells emit unpolarized light in this direction while the SSL displays a polarization of -23%.

EQUILIBRIUM GAS-PHASE COMPOSITION AND THERMODYNAMIC PROPERTIES  
INCLUDING SUBHYDRIDES IN THE PYROLYSIS OF  $\text{AsH}_3$  AND  $\text{PH}_3$

A.S. Jordan<sup>1</sup> and A. Robertson<sup>2</sup>

AT&T Bell Laboratories

<sup>1</sup>Murray Hill, New Jersey 07974

<sup>2</sup>Engineering Research Center Princeton, New Jersey 08540

We have determined the gas-phase composition produced by the pyrolysis of  $\text{AsH}_3$  and  $\text{PH}_3$  in chemical equilibrium over a wide range of temperatures (T) and pressures ( $p_{\text{tot}}$ ). The results are directly applicable to the metalorganic MBE (MOMBE or CBE) growth technique for III-V materials and have important implications in low pressure (LP) and atmospheric pressure (AP) MOVPE. As a starting point, the thermodynamic properties of  $\text{AsH}_3$  and its subhydrides  $\text{AsH}$  and  $\text{AsH}_2$  were evaluated from critically assessed or estimated spectroscopic data. The calculation of thermodynamic functions (free-energy function, entropy, enthalpy, and heat capacity) was based on statistical thermodynamics. For the first time, a complete set of these functions has been generated between 0 and 1600K for all three species. In addition, the standard enthalpies of formation of the hydrides were derived from the photoionization mass-spectrometric bond energy values of Berkowitz. Similar data for the three phosphorous hydrides were also calculated, thereby updating corresponding values in the JANAF Tables. Next, using a novel Gibbs free-energy minimization technique we evaluated the equilibrium concentrations of As,  $\text{As}_2$ ,  $\text{As}_4$ ,  $\text{AsH}$ ,  $\text{AsH}_2$ ,  $\text{AsH}_3$ , H and  $\text{H}_2$  resulting from the thermal decomposition of  $\text{AsH}_3$  as a function of  $p_{\text{tot}}$  between 900 and 1500K. The pyrolysis of  $\text{PH}_3$  was separately treated in a similar fashion.

In LP-MOVPE growth ( $T = 900\text{K}$ ,  $10^{-2} < p_{\text{tot}} \text{ (atm)} < 10^{-1}$ ) the dominant species in  $\text{AsH}_3$  pyrolysis (As/H ratio = 1/3) are  $\text{As}_4$  and  $\text{As}_2$ . The subhydrides  $\text{AsH}$  and  $\text{AsH}_2$  are equally prominent, the partial pressure of  $\text{AsH}_2$  reaching  $2.5 \times 10^{-9}$  atm at  $p_{\text{tot}} = 10^{-1}$  atm. Under AP-MOVPE conditions the  $\text{As}_4/\text{As}_2$  ratio further increases and  $\text{AsH}_2$  is the major subhydride. Semi-

quantitatively, the decomposition of  $\text{PH}_3$  is similar to that of  $\text{AsH}_3$  except in this case the PH concentration is significant. The "cross-over" temperature from tetramer to dimer dominance is not only a function of  $p_{\text{tot}}$  but also of T. With increasing  $\text{H}_2$  dilution at a constant  $p_{\text{tot}}$  the input As/H or P/H ratio drops and the cross-over temperature progressively declines. It will be shown that a large separation in cross-over temperatures between  $\text{As}_4/\text{As}_2$  and  $\text{P}_4/\text{P}_2$  adversely effects the T dependence of the [As/P] ratio in the gas phase and hence, the compositional uniformity on group V sites in quaternary InGaAsP films grown by LP-MOVPE.

For a MOMBE cracker, we have derived the steady-state pressure and the surface flux of the important species at the substrate. The major subhydride is  $\text{AsH}$  as its mole fraction reaches  $\sim 10^{-4}$  at a cracker T of 1500K and  $p_{\text{tot}} = 10^{-5}$  atm. Under similar conditions, the concentration of PH is about an order of magnitude lower than that of AsH. We have found that the atomic H concentration rises with temperature; it reaches a mole fraction of  $\sim 3 \times 10^{-4}$  at 1300K which translates to 0.011 monolayers (mL/sec). Similarly, the atomic As concentration increases with temperature and at 1300K it equals that of atomic H. For  $\text{PH}_3$  decomposition the atomic H is about an order of magnitude more abundant than P. In the low pressure regime, the mole fraction of the majority dimeric species is always greater than that of tetramers. At higher T, the dimer/tetramer ratio rapidly increases; but the vapor pressure of dimers is insensitive to T under conditions appropriate for MOMBE crackers. Finally, we discuss the limitations and improvements of equilibrium analysis with regard to LP-MOVPE and MOMBE growth.

MONTE CARLO SIMULATION OF  $L1_1$ -TYPE ORDERING DUE TO SURFACE STEP MIGRATION IN THE EPITAXIAL GROWTH OF III-V SEMICONDUCTOR ALLOYS

Manabu Ishimaru, Syo Matsumura, Noriyuki Kuwano and Kensuke Oki

Department of Materials Science and Technology

Graduate School of Engineering Sciences

Kyushu University-39, Kasuga, Fukuoka 816, Japan

Recently the present authors proposed an Ising model for the layer-by-layer growth including rearrangement of surface atoms [1], and simulated the  $L1_1$ -type ordering in the (001) growth by Monte Carlo method [2]. The results explained quite successfully some of the features, e.g. wavy diffuse streaks appearing in the electron diffraction patterns and their change as a function of growth rate or temperature, which were obtained for OMVPE or MBE grown specimens [2]. In the present study, the model has been modified to be fit for the ordering due to surface-step migration in the epitaxial growth on a slightly inclined substrate. Here, atoms at step-edges on the (001) surface are permitted to exchange their positions with each other, and epitaxial layers are assumed to grow by the step migration. Figure 1 gives an example of (110) Fourier power spectra of the atomic arrangements thus obtained. The step

edges were assumed to be along [110], and have a tendency to form like-atom chains. Superlattice spots at  $\bar{1}/2, 1/2, 1/2$  show that the (T11)-type variant of  $L1_1$  prevails in the epilayer. Note that the spots elongate along [T11], owing to non-conservative antiphase boundaries on (T11) planes. In contrast, the surface steps along [T10] bear two variants of (T11) and (1T1)-types simultaneously, as shown in Fig. 2. Wavy streaks appear along [001] in Fig. 2. The results in Figs. 1 and 2 are in good agreement with the electron diffraction patterns of  $Ge_{1-x}In_xP$  [3].

[1] S. Matsumura et al.: *Jpn. J. Appl. Phys.*, 29(1990), 688.

[2] S. Matsumura et al.: *J. Crystal Growth*, in press.

[3] e.g. P. Bellon et al.: *J. Appl. Phys.*, 66(1989), 2388.

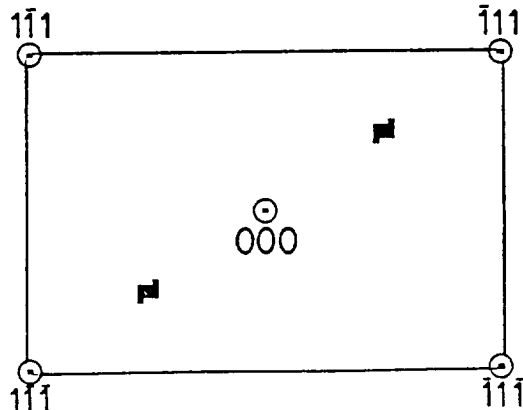


Figure 1. Step // [110].

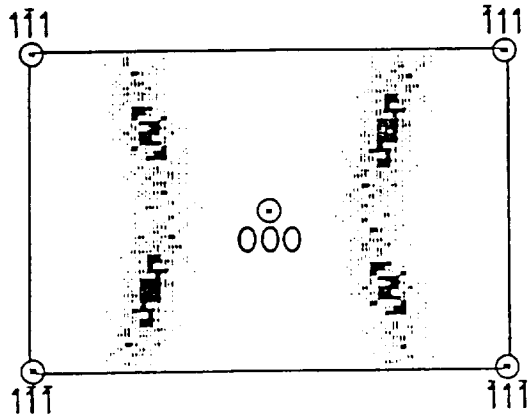


Figure 2. Step // [110].

## GROWTH KINETICS BY MBE ON FLAT AND STEPPED SURFACES

Tetsuya Uchida, Takashi Uchida and Koh Wada

Department of Physics, Faculty of Science  
Hokkaido University, Sapporo 060, Japan

The growth kinetics for III-V compound semiconductor by molecular beam epitaxy(MBE) is studied analytically on flat and stepped surfaces. The kinetic equation which describes the impingement and the diffusion of atoms on the surface is derived on the basis of the solid-on-solid(SOS) model using the path probability method (PPM) [1] introduced by Kikuchi as a method of non-equilibrium statistical mechanics. The time evolution of the surface roughness defined as the average number of lateral atom-vacancy pairs shows qualitatively the same features as those of the observed specular spot intensities in reflection high energy electron diffraction (RHEED) [2], which is used as a typical technique for monitoring crystal growth by MBE. In particular, on a stepped surface the present specular intensity calculation (Fig. 1) shows that the growth mode changes from the layer-by-layer growth mode on terraces to the step propagation mode as the temperature is raised (Fig.1). This result agrees well with that of RHEED intensity on vicinal GaAs surface by Neave et al. We also study the effect of anisotropy on the growth mode, typically observed in growth of Si by the MBE processes.

[1] K. Wada, H. Kaburagi, T. Uchida and R. Kikuchi, *J. Stat. Phys.* 53(1988)1081.

[2] T. Uchida, *Phys. Lett. A*, in printing.

[3] J.H. Neave, P.J. Dobson, B.A. Joyce and J. Zhang, *Appl. Phys. Lett.* 47(1985)100.

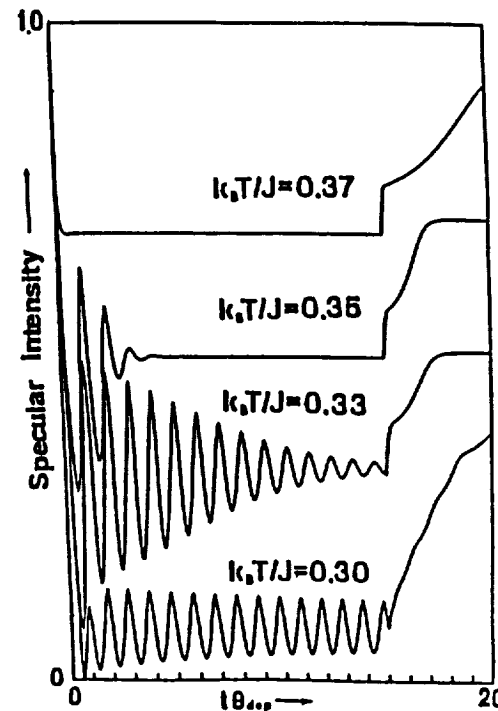


Figure 1. Impingement is off at  $t\theta_{dep}=15$ .

**A STUDY OF GROUP-V DESORPTION FROM InP, InAs, GaP, AND GaAs BY  
REFLECTION HIGH-ENERGY ELECTRON DIFFRACTION DURING  
GAS-SOURCE MOLECULAR-BEAM EPITAXY**

*B.W. Liang and C.W. Tu*

Department of Electrical and Computer Engineering  
University of California at San Diego  
La Jolla, CA 92093-0407

Desorption behaviors of arsenic and phosphorus from InAs and InP surface, respectively, have been studied by the specular-beam intensity transition of reflection high-energy electron diffraction (RHEED) when the group-V-cracker shutter was closed in gas-source molecular-beam epitaxy. The intensity, we found, is an exponential function of time. From the transition time constant, we obtained the desorption rate constant ( $k$ ) for both arsenic on InAs and phosphorus on InP. From an Arrhenius relation between  $k$  and the substrate temperature ( $T_s$ ), we obtained the activation energies for arsenic desorption from InAs and phosphorus from InP. For arsenic on InAs, the relation between  $k$  and  $T_s$  in the high-temperature range is different from that in the low-temperature range. Based on the comparison between the activation energies obtained by RHEED and those from  $As_2$  and  $As_4$  vapor pressure curves, we believe that in the high-temperature range, it is arsenic dimer

that desorbs from the arsenic-rich InAs surface, but in the low-temperature range, it is arsenic tetramer. Compared with arsenic on InAs, phosphorus on InP has a very large desorption rate constant but only one activation energy, which is consistent with that obtained from the  $P_2$  vapor pressure curve. We can use these results to explain why arsenic has a much higher incorporation rate than phosphorus in InAsP ternary layers grown by gas-source molecular-beam epitaxy.

Similar studies were performed for GaP and GaAs. Because of the higher temperature range studied, only  $P_2$  and  $As_2$  desorption was observed. The data were also used to establish a model for the group-V composition in GaAsP under different growth conditions.

---

This work is partially supported by the Office of Naval Research.

---

**HIGHLY CARBON-DOPED p-TYPE  $Ge_{0.05}In_{0.5}As$  BY CARBON TETRACHLORIDE  
IN GAS-SOURCE MOLECULAR BEAM EPITAXY**

*T.P. Chin\*, P.D. Kirchner, G.D. Pettit, C. Lin and J.M. Woodall*  
IBM Research Division, T. J. Watson Research Center  
Yorktown Heights, New York 10598

*C.W. Tu*

Department of Electrical and Computer Engineering, 0407  
University of California, San Diego, La Jolla, California 92093-0407

Carbon has been demonstrated as an important *p*-type dopant in GaAs, AlGaAs, and GaP because of achievable high carrier concentration ( $1 \times 10^{20} \text{ cm}^{-3}$  by MOVPE and  $1 \times 10^{21} \text{ cm}^{-3}$  by MOMB) and low diffusivity (compare to beryllium, magnesium, and zinc). These characteristics of carbon permit thin, highly conducting layers to be used in devices such as the heterojunction bipolar transistor. However, in MBE or MOMB, carbon-doped  $Ge_{0.5}In_{0.5}As$  was usually found to be *n*-type or *p*-type with low carrier concentration, because of either low carbon incorporation or compensation attributed to amphotericity.

In this work, we demonstrated that highly carbon-doped *p*-type  $Ge_{0.5}In_{0.5}As$  can be obtained by using carbon tetrachloride ( $CCl_4$ ) as a doping source in gas-source MBE. Elemental group-III and thermally cracked arsine were used as sources.

$p=3 \times 10^{19} \text{ cm}^{-3}$  was achieved after a post-growth anneal. This is so far the highest reported net carbon acceptor density in this material system. Compared to methyl or elemental carbon in MBE-related growth techniques,  $CCl_4$  was shown to be much more effective for carbon-doped *p*-type  $Ge_{0.5}In_{0.5}As$ . 4K and 300K photoluminescence were also measured. Comparing the growth conditions with those reported by others, we proposed a reversible acceptor hydrogenation to explain the annealing behavior.

C.W. Tu is supported by the Office of Naval Research.

---

\*Permanent address: Department of Electrical and Computer Engineering, 0407, University of California, San Diego, La Jolla, California, 92093-0407.

## GROWTH OF SEMICONDUCTORS BY LIQUID PHASE EPITAXY

*E. Bauser\* and H.P. Strunk\*\**

\*Max-Planck-Institut für Festkörperforschung, Heisenbergstr.1

DW-7000 Stuttgart 80, Germany

\*\*Institut für Werkstoffwissenschaften VII,

Universität Erlangen, Cauerstr.6, DW-8520 Erlangen, Germany

Liquid phase epitaxy of semiconductors is shown to bring into operation unadulteratedly most of the classical crystal growth mechanisms. These growth mechanisms influence crystal properties and offer various possibilities to further evolve specific qualities of crystals. Structural perfection is one of the most widespread quality requests and was strived for in recent experiments with silicon LPE layers. These layers, grown on silicon substrates, are shown to be free of extended defects and to have low point defect densities. The data of solar cells prepared from the Si LPE layers may confirm their high perfection. Selective epitaxial growth on defect-free substrates combined with epitaxial lateral overgrowth provides us with

completely defect-free silicon-on-insulator layers whose properties are evaluated by measuring the characteristics of MOS transistors fabricated in them. Mechanisms for defect formation during epitaxial growth are studied in order to find ways to eliminate defects or to minimize their densities. Attempts to correlate dopant and impurity incorporation with the microstructure of the interface will be described. Heteroepitaxial growth of  $Si_{1-x}Ge_x$  ( $0 \leq x \leq 1$ ) on Si is studied. The dislocation-free Si substrates prove favorable for investigating basic processes of misfit dislocation formation during early stages of epitaxial growth.

---

## STRUCTURE OF THE GROWTH SURFACE OF GaAs GROWN ON (001) GaAs BY LIQUID PHASE EPITAXY

*H.P. Strunk and T. Marek*

Institut für Werkstoffwissenschaften VII,

Universität Erlangen, Haberstr. 2, DW-8520 Erlangen, Germany

Understanding the molecular processes that occur at a growing surface requires the surface structure to be known, i.e. the actual surface topology is to be microscopically investigated. We choose GaAs-epilayers grown onto GaAs substrates by liquid phase epitaxy (Ga-solution). Nominal substrate normal is (001); however, in order to analyse the topology, that develops during epitaxial growth, in dependence of the misorientation, frequently spherically shaped substrates with up to  $\approx 50^\circ$  deviation are used.

After growth the surface is investigated in the Nomarski differential interference optical microscope and, frequently at accordingly preselected areas, in the reflection electron microscope. The latter method is readily applied to GaAs contrary to

Si surfaces, in which case the natural oxidation leads to charging effects.

Observations on the monomolecular growth step structure on the (001) facettes are described first, especially in areas where dislocations serve as growth promoters. The observations are discussed in the light of current models of growth at dislocations. Then the micro- and nano-structure of terrace risers and treads will be considered. We show as a new result, that the microstep structure of both differs essentially only in scale, not in geometry. Implications of these findings for modelling crystal growth and for interaction between growth steps will be discussed.

## SESSION 5D

### CRYSTALLIZATION OF OXIDE SUPERCONDUCTORS FROM MOLTEN HYDROXIDE

*Angelica M. Stacy, Sarah L. Stoll, Linda N. Marquez and Steven W. Keller*

Department of Chemistry, University of California  
Berkeley, California 94720

The copper oxide superconductors generally have been prepared by solid state reactions at temperatures above 800°C. Unfortunately, there are many disadvantages with the use of solid state reactions, several of which are especially detrimental to the performance of the oxide superconductors. Here we report the crystallization of cuprate superconductors by selective precipitation from molten salts at substantially lower temperatures than have been reported previously. Specifically,

$\text{La}_{2-x}\text{Na}_x\text{CuO}_4$ ,  $\text{La}_{2-x}\text{K}_x\text{CuO}_4$ , and  $\text{EuBa}_{2-x}\text{Na}_x\text{Cu}_3\text{O}_7$  were precipitated from molten NaOH and/or KOH at temperatures between 320°C and 450°C. All three exhibit superconductivity. Among the many advantages of this synthetic route are the preparation of the products at relatively low temperatures, and simplicity in the formation of solid oxide materials. Furthermore, in contrast to most solid state reactions, single crystals are obtained; the properties of these crystals will be described.

---

### HIGH OXYGEN PRESSURE ( $\text{P}_{\text{O}_2} \leq 3000$ bar) P-T-x PHASE DIAGRAM OF THE Y-Ba-Cu-O SYSTEM

*E. Kaldis, J. Karpinski, S. Rusiecki and E. Jilek*

Laboratorium für Festkörperphysik ETH 8093-Zürich

In the YBaCuO system, three superconducting phases have been discovered up to now:  $\text{YBa}_2\text{Cu}_3\text{O}_{7-x}$ (123),  $\text{Y}_2\text{Ba}_4\text{Cu}_7\text{O}_{15-x}$ (247) and  $\text{YBa}_2\text{Cu}_4\text{O}_8$ (124). At present, after the optimization of their synthesis, the  $T_c$ 's of all these phases have reached similar values between 90 and 95K.

In order to find the conditions necessary for the synthesis and crystal growth of the various phases in the YBaCuO system, we have to determine the multidimensional P-T-X phase diagram [1,2]. In such system all parameters: Y, Pa, Cu content, T,  $\text{P}_{\text{O}_2}$  and hydrostatic pressure itself influence the stability of the phases. One should also remember, that Cu appears with various valences, which introduce additional variables. We have limited our investigations to compositions corresponding to the points of the line 123-CuO on the ternary phase diagram  $\text{CuO-BaO-Y}_2\text{O}_3$   $1 < \text{P}_{\text{O}_2} \leq 3000$  bar and  $T < 1200^\circ\text{C}$ . An important conclusion is that the P-T phase diagrams depend strongly on composition and, therefore, the stability regions of 124 and 247 phases are different for various composition. This quite

obvious conclusion has not been always recognize in the literature. Further, this phase diagrams show that under normal conditions the 123 phase is metastable.

The phase boundary of 124 has different slopes at  $\text{P}_{\text{O}_2} \leq 1$  bar and  $\text{P}_{\text{O}_2} > 1$  bar. This is important, because it indicates a difference in the free energy  $\Delta G$  of the reaction at high and low pressure[2]. Most important is the dependence of the  $T_c$  of the 247 phase on the synthesis conditions. Conditions of synthesis leading to partial reorientation of the single Cu-O chains are very important for  $T_c$ .

Several others properties of the single crystals of the double chains YBCO compounds will be briefly discussed[1].

1. E. Kaldis, J. Karpinski, S. Rusiecki, Proceed. "Toshiba Intern. School of Superconductivity," Kyoto, July 1991; Springer 1991.
2. J. Karpinski, E. Kaldis, K. Conder, S. Rusiecki, E. Jilek, Proceed. NRS Symposium Dec. 1991; Elsevier 1992.

## PHASE DIAGRAM AND CRYSTAL GROWTH OF $(Y_{1-x}Pr_x)Ba_2Cu_3O_{7-y}$

Chen Changkang, B.M. Wanklyn, Hu Yongle, A.K. Pradham, J.W. Hodby, S. Hazell and F.R. Wondre

Clarendon Laboratory, University of Oxford, Parks Road, Oxford, UK

A. Boothroyd

Department of Physics, University of Warwick, Coventry, UK

$(Y,Pr)BCO$  is an unique superconductive material for investigation of the relationship between structure, composition and properties. In order to grow big crystals with high quality, a physico-chemical research has been carried on the growth system of  $Y_2O_3$  -  $BaO$  -  $CuO$ . The eutectic composition of flux with  $BaO:CuO = 7:18$  (Mol.) was confirmed by the improved thermogravimetric analysis (ITGA). And the pesudo-binary phase diagram of  $(Y,Pr)BCO$  -  $(7BaO+18CuO)$  was established by means of differential thermal analysis (DTA), X-ray technique and the experiments of crystal growth. According to the phase diagram, suitable composition and the temperature pro-

gram were set up for the growth of large crystal and for the separation of crystals from the flux. Single crystal with wide range of Pr doping level have been obtained from the flux of  $BaO-CuO$  with eutectic composition. The crystals were identified by X-ray powder diffraction pattern. The dependance of the Pr concentration in crystals on it in the starting composition was shown by electron probe microanalysis (EPMA) and X-ray microanalysis. The superconductivity measurement indicated that the superconducting transition temperatures were related to the doping concentrations.

## CRYSTAL GROWTH MECHANISM OF $YBa_2Cu_3O_y$ SUPERCONDUCTORS WITH PERITECTIC REACTION

Teruo Izumi, Yuichi Nakamura and Yuh Shiohara

Superconductivity Research Laboratory, International Superconductivity  
Technology Center, 1-10-13 Shinonome Koto-ku, Tokyo 135, Japan

$YBa_2Cu_3O_y$  (123) crystal rods were prepared by a zone melt method under several different growth rates to investigate the growth mechanism. Calcined powders with the ratio of  $Y:Ba:Cu=1.2:2.1:3.1$  were pressed into rods which were about 2mm in diameter. The precursor rod was suspended by a clip and inserted into a furnace at high speed. The partial melting zone in the furnace was controlled at  $1030^\circ C$  which is within the partial melting temperature range where  $Y_2BaCuO_5$  (211) and liquid phases coexist. The unidirectional solidification was performed by pulling the samples upward at 1, 2, 3, 6, and 10mm/h. Then the samples were dropped into a quench tank by releasing the clip during steady state solidification in order to observe the growth interface morphology.

The samples grown at growth rates lower than 6mm/h showed a continuous structure and faceted interfaces were observed in the samples grown at 1 and 2mm/h. Furthermore, the volume of the 211 phase changed drastically from liquid to

the 123 crystals. This suggests that for a typical peritectic reaction of this system, the necessary solute is provided through the liquid. The solidification model based on the liquid diffusion control was developed. According to this model, if the initial size distribution of 211 particles, the initial composition, and several thermo-physical properties are given, then the balanced velocity for steady state directional solidification and the size distribution change of 211 particles from liquid to 123 crystal can be estimated. The expected balance velocities and distribution change are in good agreement with the experimental results.

Additionally, the effects of platinum doping to the precursor on the growth of 123 crystal will be discussed.

This work has been supported by the New Energy and Industrial Technology Development Organization under management of Research and Development of Basic Technology for Future Industries.

## CZ GROWTH OF $\text{YBa}_2\text{Cu}_3\text{O}_7$ SINGLE CRYSTALS

*C.T. Lin<sup>a</sup>, E. Schönherr<sup>b</sup>, H. Bender<sup>b</sup> and W.Y. Liang\**

<sup>a</sup>IRC in Superconductivity, University of Cambridge,

Madingley Road, Cambridge CB3 OHE, UK

<sup>b</sup>Max-Planck-Institut für Festkörperforschung,

Heisenbergstr. 1, 7000 Stuttgart 80, Germany

We report the growth of  $\text{YBa}_2\text{Cu}_3\text{O}_{7-x}$  single crystals by a modified Czochralski technique. A particular high temperature muffle furnace has been designed to heat an Y-Ba-Cu-O flux in an alumina crucible. The closed end of an alumina tube was used as a seeding center. A large radial and axial temperature gradient was maintained by cooling the tube end with a cold air flow. The crystal growth was controlled by an extremely low pulling rate (0.2 mm/h) together with a low cooling rate (0.1  $^{\circ}\text{C}/\text{h}$ ) rate (0.1  $^{\circ}\text{C}/\text{h}$ ) of the flux.

An optimum flux composition was found at about Y:Ba:Cu = 1:6:13. In the first step the non-123 phases were pulled off from the flux. In the second step large  $\text{YBa}_2\text{Cu}_3\text{O}_{7-x}$  single crystals were formed at the surface of the flux. For crucibles with a diameter of 5 cm the area of some single crystals reached about  $6 \text{ cm}^2$ . The oxygen content of the single crystal was determined by Raman Spectrum to amount 6.8. We also report the magnetic properties of the single crystal.

---

## ON ROLE OF ELECTRON AND OPTICAL MICROSCOPY IN THE STUDY OF PREGROWTH AND POSTGROWTH HISTORY OF SOME CUPRATE CRYSTALS

*A.J.S. Chowdhury and B.M. Wanklyn*

National Crystal Growth Facility for Superconducting Oxides

Clarendon Laboratory, Department of Physics

University of Oxford, Oxford OX1 3PU, UK

Crystals of  $\text{YBa}_2\text{Cu}_3\text{O}_{7-z}$ ,  $(\text{Y},\text{Pr})\text{Ba}_2\text{Cu}_3\text{O}_{7-z}$ ,  $\text{NdBa}_2\text{Cu}_3\text{O}_{7-z}$ ,  $\text{Bi}_2\text{Sr}_2(\text{Ca},\text{Gd})\text{Cu}_2\text{O}_z$ ,  $(\text{Nd}_{1-x-y}\text{Ce}_x\text{Sr}_y)_2\text{CuO}_{4-z}$  were grown by the flux method. Some crystals were superconducting, others were not. The Hot Stage Optical microscopy played an important part during the pregrowth studies of the starting materials. This was used to determine the peritectic and eutectic temperatures of some of the systems. The informations obtained could be used either on their own or in conjunction with DTA to draw phase diagrams of a system. Both the optical and the electron

microscopy were useful during the postgrowth assessment and the characterisation of the product crystals. The techniques used for this study involved Hot Stage Optical Microscopy, Interference Microscopy, and SEM, TEM, EPMA and microanalysis using different electron microscopes. The advantages and the disadvantages of these methods to carry out routine analysis and the assessment of the crystals will be discussed in some detail.

**SURFACE ANALYSIS OF  $Kb_{2-x}Ce_xCuO_4$  (Ln=Pr and Nd) SINGLE CRYSTALS  
GROWN BY THE TOP SEEDED SOLUTION METHOD**

*L.C. Sengupta\* and S. Sengupta\*\**

*\*U.S. Army Materials Technology Laboratory,  
Ceramics Research Branch, Watertown, MA 02172-0001  
\*\*Laboratory for Advanced Solid State Laser Materials,  
Center for Materials Science and Engineering,  
Massachusetts Institute of Technology, Cambridge, MA 02139*

N-type cuprate superconductors have generated scientific interest for the past few years. Due to the unavailability of large single crystals, a thorough study of the electronic properties and optical properties of the material has been somewhat limited.

Large single crystals of  $Ln_{2-x}Ce_xCuO_4$  (Ln=Pr and Nd), average size approximately 5 mm. x 5 mm. x 1 mm. were grown by the Top Seeded Solution Growth TSSG technique<sup>1</sup>. The optical constants of the crystals were determined by Variable Angle Spectroscopic Ellipsometry (VASE). The compositions of the crystals were verified by Rutherford backscattering Spectrometry (RBS) and the orientation was verified by X-ray diffraction. Also susceptibility measurements were performed using a SQUID magnetometer. We will present the results which show that the crystals grown by the TSSG method are very uniform in composition and well-oriented. A comparative

study with equivalent ceramic specimens will also be presented. These single crystals were also used to study the effect of Ce concentration and annealing parameters on the 1.5 ev electronic transition of  $Ln_{2-x}Ce_xCuO_4$  using the VASE technique. The results seem to indicate that the 1.5 ev transition appears as the doping concentration decreases. The excitation can be assigned to the charge transfer (CT) between the Cu (3d) and the O (2p) state. This charge transfer has also been observed for p-type cuprate superconductors. Also an increase in the Ce concentration increases the spectral weight near 4 ev which suggests a change in the Cu-related transitions. The effect of oxygen reduction on the transition was also studied.

<sup>1</sup>The single crystals were grown by Dr. Arlete Cassanho at the CMSE at M.I.T. and the authors gratefully acknowledge her generosity in lending the crystals.

---

**REAL STRUCTURE OF  $La_{2-x}Sr_xCuO_4$  SINGLE CRYSTALS**

*K.V. Gamayunov\**

*General Physics Institute, Vavilov St. 38, 117942, Moscow, USSR*

Real structure of crystals is quite significant for the experimental data interpretation of all kinds electric, magnetic and others measurements.

In this report we present some results of investigation of real structure of the  $La_{2-x}Sr_xCuO_4$  single crystals.

Ordering of the Sr atom distribution over La sites in single crystals of  $(La_{1-x}Sr_x)_2CuO_{4.8}$  has been established by X-ray structural analysis. The ordering can be: full-La( $La_0.76Sr_{0.24})_2CuO_{3.92}$  partial - ( $La_{0.94}Sr_{0.06}) (La_{0.86}Sr_{0.14})CuO_{4.8}$  or it can be missing - ( $La_{0.97}Sr_{0.03})_2CuO_{4.8}$ . The ordering leads to Sr concentration in certain layers of the structure, -La-La-Cu-(La,Sr)-(La,Sr)-Cu-La-La-, and the loss of some oxygen atoms in the same layers. The latter accounts for a lowering of  $T_c$  in single crystals with an ordered Sr atom distribution. The superconducting transition temperature of  $(La_{1-x}Sr_x)_2CuO_{4.8}$  depends not only on the Sr content in a sample but also on its distribution over La sites. That is why the superconducting transition temperature of ceramic samples is, as a rule, higher than that of single crystals with the same Sr content.

Real structure of  $La_{1.92}Sr_{0.08}CuO_4$  superconducting single crystal has been investigated by method of reflectory X-ray diffraction topography. Investigation was carried out in two perpendicular planes, one of which contents "c" axis. We have found that the sample which was determined by integral diffraction data as single crystal in reality is the conglomerate of large quite perfect (60") blocks of lamellar form. Clear layered structure with period of 50-60  $\mu m$  and layers oriented perpendicularly to "c" axis was observed for planes which containted "c" axis.

The data on the electrical resistivity vs T along and perpendicular to "c" axis have shown that superconducting transition exists in both directions but transition are sharper for measurements in the direction of "c" axis.

---

*\*In collaboration with Institute of Crystallography (Moscow) and Physical-Technological Institute (St-Peterburg).*

TECHNOLOGICAL PARAMETERS INFLUENCE ON THE MORPHOLOGY AND THE  
TEMPERATURE OF SUPERCONDUCTING TRANSITION IN  
 $\text{La}_{2-x}\text{Sr}_x\text{CuO}_{4-\delta}$  SINGLE CRYSTALS  
V.V. Voronov, K.V. Gamayunov, V.I. Zorya, A.L. Ivanov, V.V. Osiko,  
V.M. Tatarintsev, A.I. Chernov and Yu P. Yakovets  
General Physics Institute, Academy of Sciences of the USSR  
117942 Moscow, Vavilov Street 38, USSR

In this paper we have investigated the influence of the temperature distribution in the melt region and the rate of melt cooling on the shape and the dimensions of growing  $\text{La}_{2-x}\text{Sr}_x\text{CuO}_{4-\delta}$  crystals, their composition and superconducting transition temperature. Single crystals of pyramid-like shape of dimensions  $5 \times 4 \times 7 \text{ mm}^3$  and of plate-like shape of dimensions  $11 \times 10 \times 1.4 \text{ mm}^3$  were obtained by spontaneous crystallization from CuO flux. Grown crystals were investigated by X-ray diffraction and electron-probe analysis. The critical tempera-

ture was determined by DC susceptibility measurements. We have obtained both pure and Sr doped  $\text{La}_2\text{CuO}_{4-\delta}$  single crystals with maximal  $T_c$ -25 K. It has been found that Sr does not principally affect on the shape of  $\text{La}_{2-x}\text{Sr}_x\text{CuO}_{4-\delta}$  crystals. It's shown that the rate of melt cooling for the growth of relatively large pyramidal crystals must be rather slow than for plate-like crystals of the same dimensions. The hypothesis on the difference between growth processes along "c" and "a" directions has been proposed.



## SESSION 6

### ROLE OF INSTABILITIES IN DETERMINATION OF THE SHAPES OF GROWING CRYSTALS

*Robert F. Sekerka*

Depts. of Physics and Mathematics  
Carnegie Mellon University, Pgh., PA 15213

The shapes of growing crystals are determined by an interplay of complex processes that include transport of energy and matter through bulk phases, usually by diffusion or convection, and kinetic processes that take place local to the interface at which the crystal is forming from the nutrient phase. These processes take place in the context of local equilibrium conditions of a thermodynamic origin, which at the interface depend on considerations of capillarity (surface tension) in a manner expressed by the Gibbs-Thomson equation. A mathematical description of crystal growth therefore results in a free boundary problem (the free boundary being the location and shape of the interface as a function of time) for thermal and compositional fields, governed by partial differential equations and subject to boundary conditions on the free boundary and at the extremities of the system. This free boundary problem is not only difficult to solve but often displays multiple solutions; i.e., its solutions are not unique. Although one could seek to restore uniqueness by accounting for new physical phenomena, this approach has generally been unsuccessful. Instead, one attempts to select from among the multitude of possible solu-

tions by invoking matters of dynamic stability. Matters of hydrodynamic instability, which may be important when the nutrient phase is a fluid, are covered in other parts of this conference and will not be considered in this lecture. We shall concentrate on matters of instability that govern the shape of the interface through an interplay of diffusive transport, capillarity, and interface kinetics. The interplay of diffusive transport and capillarity is the basis of classical morphological stability theory; whereas, the interplay of diffusive transport and interface kinetics leads to well-known dynamical instability criteria for faceted crystals. Studies of the interplay of capillarity and interface kinetics are more recent, and lead to interesting modifications of the classical work of Frank that describes the evolution of crystal growth shapes under conditions for which capillary effects are negligible. Theories that treat all three phenomena simultaneously are rare but lead to interesting effects that deserve further exploration.

---

This work was supported by the National Science Foundation under grant DMR9043322.



## SESSION 6A

### GROWTH MORPHOLOGIES IN DIFFUSION FIELD

*Yukio Saito, Makio Uwaha\* and Tomoko Sakiyama*

Department of Physics, Keio University

3-14-1 Hiyoshi, Kohoku-ku, Yokohama 223, Japan

\*Institute for Materials Research, Tohoku University

2-1-1 Katahira, Aoba-ku, Sendai 980, Japan

Crystals growing in a diffusion field undergo a morphological instability to form intricate structures with full variety. The stability of planar interface can be studied with the linear theory, but the well-developed nonlinear structures can most appropriately be handled by numerical simulations.

Simulations of an aggregation growth from a lattice gas revealed that the growth rate is governed by the gas density and the fractal dimension of the diffusion-limited aggregation[1]. Effects of other factors such as noise, anisotropy[2] and flow[3] are also investigated. Inclusion of surface tension and surface kinetics produces more regular structures, but the two effects cannot be separated[4].

For a crystal with a rough interface, the dendritic growth is simulated by a continuous model, and there the effects of surface tension and kinetics can be separately controlled. The crossover in the scaling behavior of the dendritic growth is observed by increasing the kinetic coefficient[5].

---

- [1] M. Uwaha and Y. Saito, *Phys. Rev. A* **40** (1989) 4716.
- [2] M. Uwaha and Y. Saito, *J. Crystal Growth* **99** (1990) 175.
- [3] S. Seki, M. Uwaha and Y. Saito, *Europhys. Lett.* **14** (1991) 397.
- [4] Y. Saito and T. Ueta, *Phys. Rev. A* **40** (1989) 3408.
- [5] Y. Saito and T. Sakiyama, unpublished.

---

### SIMULATION OF MICROSCOPIC SEGREGATION AND GROWTH MORPHOLOGIES IN BINARY SYSTEMS

*Rong-Fu Xiao, J. wan D. Alexander, Franz Rosenberger and Ma-Ben Ming*

Center for Microgravity and Materials Research

University of Alabama in Huntsville

Huntsville, Alabama 35899, USA

We have used a Monte Carlo model to simulate microscopic segregation and growth morphologies in binary solidification. The model combines species transport in the melt, based on a modified diffusion-limited aggregation (DLA) process, with anisotropic growth kinetics at the solid-melt interface. The interfacial processes considered include attachment, surface diffusion and detachment. The transition probabilities for these processes are calculated from the thermodynamic driving forces and pairwise particle interactions, considering up to second-nearest neighbors. The driving forces in the binary solution are dependent on the applied undercooling and transport-dependent melt concentration distribution at the interface. For selected cases we have superimposed a drift on the random walk (DLA) process to explore the trends resulting from convective transport.

Through variation of the interaction energies, undercoolings and initial melt composition, a broad range of microstructures has been obtained, including faceted and non-faceted

lamellar systems of spacing  $\lambda$ , and layered and ionic compounds. For lamellar eutectics we have found that at higher undercoolings, the product of  $\lambda^2$  and the solidification rate is constant and has the same order of magnitude as that found in experiments. For off-eutectic growth we have observed oscillations in the lamella widths at certain growth conditions. In addition, we have obtained tilted growth for both eutectic and off-eutectic compositions by suddenly changing the undercooling.

This work has been supported by the State of Alabama through the Center for Microgravity and Materials Research at the University of Alabama in Huntsville, and by NSF Grant INT-89031 73.

---

\*Laboratory of Solid State Microstructures, Nanjing University, Nanjing 210008, People's Republic of China.

**MONTE CARLO SIMULATION OF MORPHOLOGICAL INSTABILITY  
IN STEP FLOW GROWTH**  
**C.C. Hsu**  
 Department of Electronic Engineering  
 The Chinese University of Hong Kong  
 Shatin, NT, Hong Kong

In the epitaxial growth process on vicinal surface, steps provide the nucleation sites. If the supersaturation is sufficiently low, the growth will commence in a lateral fashion, according to the BCF theory. This is the so-called "step flow." It is important to maintain the morphological stability of these moving steps during growth. In the conventional morphological stability theory, diffusion and Gibbs-Thompson effect are the destabilizing and stabilizing factors. However, instability was reported on the growth of Si on (111) surface by MBE and GaAs by MOCVP. The steps have anisotropic character. It shows that anisotropy is a stronger stabilizing/destabilizing

factor than those considered in isotropic morphological stability theory.

Using the Monte Carlo method developed by Gilmer and Bennema, we simulate the crystal growth on the (111) vicinal surface. Surface morphology generated by simulation is similar to that observed by TEM, provided that proper simulation growth parameters (temperature, bond strength and supersaturation) were chosen. In the Monte Carlo method crystal symmetry and anisotropy are inherently reflected in its attachment kinetics.

**FLUCTUATION OF STEPS IN SURFACE DIFFUSION FIELD**

*Makio Uwaha*  
 Institute for Materials Research, Tohoku University  
 2-1-1 Katahira, Aoba-ku, Sendai 980, Japan  
*Yukio Saito*  
 Department of Physics, Keio University  
 3-14-1 Hiyoshi, Kohoku-ku, Yokohama 223, Japan

Crystal growth from the vapor has been studied for a long time since the classic work of BCF (W.K. Burton N. Cabrera and F.C. Frank, *Philos. Trans. R. Soc. London, Ser. A* 243 (1951) 299). Recent advancement of the observation technique made direct observation of thermal fluctuation of atomic steps possible. Step stiffness and interaction between steps on the Si(111) face have been estimated from the equilibrium fluctuation of steps. We study nonequilibrium fluctuation of steps, where the growth mechanism plays an important role in determining fluctuation.

In the BCF type model we use a linear stochastic equation to describe the step fluctuation  $\delta y_k(t)$ . The spectrum of the random force is determined by the equipartition law at equilibrium. The amplitude of the step fluctuation is given by a generalized partition law as  $\langle |\delta y_k|^2 \rangle = T/v_k(f)$ , where  $v_k(f)$  is an

effective force constant controlled by the impingement frequency  $f$ .

With an asymmetry in step kinetics, the step becomes smooth when it melts, whereas it becomes rough when it grows. The roughness diverges when the supersaturation approaches the Mullins-Sekerka instability point. These effects are very pronounced if the surface diffusion length is large.

We perform Monte Carlo simulations with a lattice model (Fig. 1). The growth velocity agrees very well with the theoretical value, and the expected step smoothing and roughening are confirmed with a reasonable accuracy.

Fluctuation of equidistant parallel steps in a vicinal face is also studied.

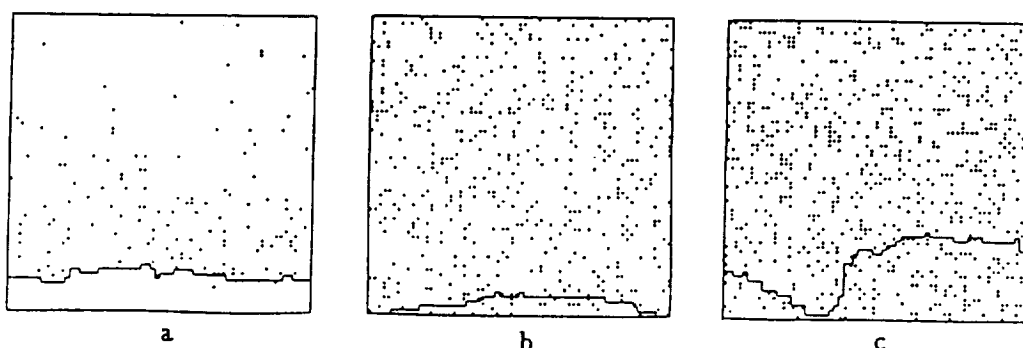


Figure 1. Position of adsorbed atoms and the step in the atmosphere of a) vacuum, b) equilibrium and c) supersaturated vapor.

## HOW DO INTERFACE KINETICS AND FLOW WITHIN BOUNDARY LAYER TOGETHER INFLUENCE MORPHOLOGICAL STABILITY OF A VICINAL FACE

A.A. Chernov

Institute of Crystallography, Russian Academy of Sciences  
59 Leninsky Prospekt, Moscow 117333, Russia

Analyzing morphological stability one assumes an infinitely fast interface kinetics or stagnant mother liquor. In this work, both the anisotropic interface kinetics and the flow within the boundary layer have been considered for the first time.

A flat vicinal face declined from singular orientation by a small angle  $\arctan p$  is characterized by incorporation surface ( $\beta$ ) and step ( $\beta_{st}$ ) kinetic coefficients,  $\beta = \beta_{st}p$ .

The vicinal face grows from a solution that flows parallel to the face and perpendicular to steps on it with the velocity  $u(z)=u_0[1-\exp(-\alpha z)]$ . Here  $z$  is the distance to the face,  $\alpha^{-1}$  is the boundary layer thickness,  $u_0$  is the velocity in the solution bulk. The perturbation of the vicinal has the wavenumber  $k$ . The problem is: when the vicinal is stable against the perturbation? For the profile  $u(z)$  above, the convective diffusion equation has analytical solution in Bessel functions allowing to find that the vicinal is stable against perturbations with

$$k > k_0 = [2 \cdot 3^{1/4} \Gamma(2/3)/\Gamma(1/3)]^{1/2} p^{3/2} (\alpha u_0/D)^{1/2} \quad (1)$$

This is valid if  $u_0 \gg Dk$ ,  $D$  being diffusivity in solution. The numerical coefficient is  $\sim 2.5$ . At  $p=10^{-3}$ ,  $u_0=30$  cm/s,  $\alpha=10$  cm $^{-1}$ , eq. (1) gives  $2\pi/k_0=14$  cm. Cappillarity provides stability only if the perturbation wavelength is  $\leq 2 \cdot 10^{-3}$  cm. This dramatic stabilization comes from the drift of concentration waves excited by growing face along the flow if the step flow direction is opposite to the one of the solution. If the directions are parallel, the same drift provides strong destabilization. The effect typical of solution growth was found experimentally [A.A. Chernov: *Cont. Phys.* 30(1989)251]. In vapor, the effect is possible at high flow rates. In melt, the flow and step velocities are comparable and further analysis is needed.

Publication: A.A. Chernov, *J. Crystal Growth* 1992, in print.

---

## NONLINEAR ANALYSIS IN RAPID SOLIDIFICATION

R.J. Braun

National Institute of Standards and Technology

G.J. Merchant

Stanford University

K. Brattkus

California Institute of Technology

S.R. Davis

Northwestern University

In the rapid directional solidification of a dilute binary alloy, analysis reveals that in addition to the Mullins and Sekerka cellular mode there is an oscillatory instability. Coriell and Sekerka first analyzed the linear stability of the planar melt/solid interface with nonequilibrium effects and found that the oscillatory mode had a nonzero wavenumber. For the model analyzed by Merchant and Davis, the preferred wavenumber is zero; the mode is one of pulsation. Restricting the experimental and material parameters to be in certain

regimes allows nonlinear analyses to be performed that describe this pulsatile mode. Nonlinear equations govern the position of the interface to leading order, and the resulting oscillations may produce high speeds. These oscillations in the speed of the interface may help explain microstructures in the solid resulting from rapid solidification processes such as laser surface remelting. Extension of the model to concentrated alloys may explain some experimental behavior not captured in the model.

## THERMAL EFFECTS IN RAPID DIRECTIONAL SOLIDIFICATION

*D.A. Huntley and S.H. Davis*

Northwestern University

We study the morphological instability of a planar solid/liquid interface for a unidirectionally-solidified dilute binary mixture. We use a model formulation suggested by Boettger *et al.* (1985), Aziz (1982) and Jackson *et al.* (1980), which allows for nonequilibrium effects in the interfacial solute segregation and the liquidus slope and takes into account the effects of attachment kinetics. Our analysis introduces the effects of latent heat and the full temperature distribution but assumes no flow in the system. The two types of instabilities found are the cellular instability, a slight modification of that found by Mullins and Sekerka (1964), and an oscillatory instability related to

that found by Coriell and Sekerka (1983) and driven by disequilibrium effects at the interface. We compare the character of these instabilities to those found by Merchant and Davis (1990), who used the frozen temperature approximation, and find that the addition of thermal effects slightly postpones the onset of the cellular instability but dramatically postpones the onset of the oscillatory instability. The coupling of these instabilities may be responsible for the appearance of banding phenomena in rapid solidification. We investigate different material systems and compare experimental observations of banding with our linear theory predictions.

---

## CELLULAR SOLIDIFICATION WITH ANISOTROPIC DIFFUSION

*Douglas A. Kurtze*

Department of Physics, North Dakota State University

In the simplest model of directional solidification – with a fixed thermal gradient and no diffusion in the solid phase – numerical calculations of steady-state cells often show that the concentration field is only weakly dependent on position transverse to the growth direction. In order to take advantage of this fact, I consider directional solidification with anisotropic diffusion, with the diffusion coefficient in the transverse direction much larger than that in the growth direction. Since the transverse concentration gradient is already small in the isotropic case, and increasing the transverse diffusion coefficient can only make it smaller, this change should not affect the solutions

much. I report numerical calculations which test how close the solutions of the isotropic and anisotropic models are. I then solve the anisotropic problem perturbatively, with the ratio of diffusion coefficients as a small parameter, to reduce it to an effective one-dimensional diffusion equation for the concentration, coupled to equations for the shape of the cell and the position of the cell tip. I will discuss the implications of this analytical calculation for the local constitutional supercooling conjecture of Weeks and van Saarloos, for the stability of the grooves, and for oscillatory instabilities of the cell tips and the cell-to-dendrite transition.

## SESSION 6B

### CRYSTAL GROWTH OF $\text{FeBO}_3$ BY TOP SEED SOLUTION METHOD

*Daiqin Ni and Dezhong Shen*

Research Institute of Synthetic Crystals  
P.O. Box 733, Beijing 100018, P.R. China

Ferric borate,  $\text{FeBO}_3$  (FB) is a crystal which has a spontaneous ferromagnetic moment at room temperature and is transparent well into visible spectrum. The ratio of the Faraday rotation to the optical absorption coefficient of FB at room temperature is  $25^\circ/\text{dB}$  in the green wavelength. It is the highest value obtained in any other materials at room temperature. This crystal possesses many important potential applications for microwave magneto-optical modulation of visible lasers, optical deflection and isolation, magneto-optic display, and hologram<sup>[1]</sup>.

There are two methods to grow FB crystal: traditional flux growth and chemical vapour deposition<sup>[2]</sup>. However, none of both can be used to grow single FB crystal in good optical

quality up to now. This situation seriously hampers the application of FB crystal.

In order to get good single FB crystal, we used the top seed solution (TSS) method to grow this crystal. This is the first time to grow FB crystal with TSS method to our knowledge. The flux was chosen, the ratio of solute and solvent was studied. The conditions for crystal growth and the results will be reported.

[1] R. Wolee, et.al., *J. Appl. Phys.* 41(3) (1970) 1218.

[2] R. Diehl, *Solid State Comm.* 17, (1975) 743.

---

### CRYSTAL GROWTH OF $\text{PbTiO}_3$ BY A SELF-FLUX TECHNIQUE

*B.N. Sun, Y. Huang and D.A. Payne*

Department of Materials Science and Engineering, Materials Research Laboratory, and Beckman Institute, University of Illinois at Urbana-Champaign, Urbana, IL 61801, USA

Highly polar lead titanate ( $\text{PbTiO}_3$ ), a potential ferroelectric material with a displacive phase transformation, is of interest for energy sensing and transducing applications. Large crystals ( $4 \times 4 \times 5.5 \text{ mm}^3$ ) were grown from high-temperature solutions using  $\text{PbO}$  as a self-flux. The optimized growth conditions were determined to be: 18 mol%  $\text{PbO}$  + 82 mol%  $\text{TiO}_2$  for the starting composition, 1050-930 °C as the growth temperature range with 0.4-1.5 °C as the cooling rates. Evaporation of  $\text{PbO}$

was significantly reduced by use of a double-crucible technique. Growth mechanisms will be discussed in terms of crystal habits and surface morphology, which were investigated by optical and scanning electron microscopy. The grown crystals were characterized by X-ray diffraction, chemical analysis, differential scanning calorimetry, infrared spectroscopy and electrical measurements. The results are compared with those of the crystals grown from a KF-flux system.

## THE GROWTH OF BARIUM-STRONTIUM TITANATE ( $Ba_{1-x}Sr_xTiO_3$ ) SINGLE CRYSTALS BY THE FZ METHOD

Hironao Kojima, Minoru Watanabe and Isao Tanaka

Institute of Inorganic Synthesis, Faculty of Engineering  
Yamanashi University, Miyamae 7, Kofu, Yamanashi 400, Japan

Barium titanate ( $BaTiO_3$ ) has three polymorphs of tetragonal, cubic and hexagonal phases. Tetragonal  $BaTiO_3$  is known as a ferroelectric material, and its single crystals are expected of application for the nonlinear optical materials. However, normal melt growth induces formation of the hexagonal phase. Formation of the hexagonal phase is prevented by substitution of Sr for part of Ba in  $BaTiO_3$ . In this study, single crystals of  $Ba_{1-x}Sr_xTiO_3$  were grown by the floating zone method.

Stoichiometric amounts of  $BaCO_3$ ,  $TiO_2$  and  $SrCO_3$  were mixed, and calcined at 1000°C for 10 hours two times repeatedly. The preheated powder was formed to a cylindrical shape, and then used as a feed rod. The apparatus for crystal growth was an infrared heating furnace with two 1.5 kW halogen lamps used as the heat source. The growth conditions were the growth rates of 1.0~2.0 mm/h and the growth atmosphere of oxygen.

As the analysis result of the grown crystals with several compositions between 0.5 and 5.0at%Sr, it was found that  $Ba_{1-x}Sr_xTiO_3$  melts congruently at 1.5at%Sr. The crystal growth of  $Ba_{0.985}Sr_{0.015}TiO_3$  was performed. Fig.1 shows an

as-grown crystal of  $Ba_{0.985}Sr_{0.015}TiO_3$ . The as-grown crystal was 5 mm diameter by 25 mm long, transparent and light yellow. The grown crystals were indicated as a tetragonal phase by XRD. Furthermore, it was confirmed that the grown crystals transform reversibly between the tetragonal and the cubic phases at 126°C.

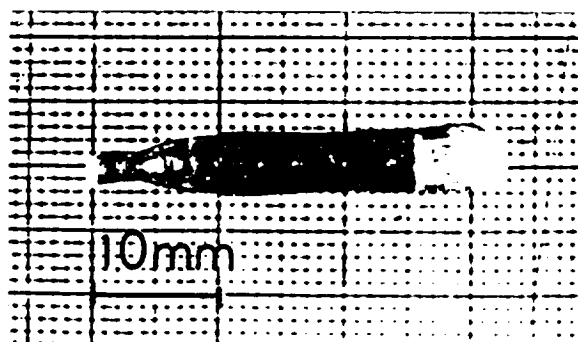


Figure 1. As-grown boule of  $Ba_{0.985}Sr_{0.015}TiO_3$ .

## HYDROTHERMAL GROWTH OF BISMUTH SILICATE

John J. Larkin, Meckie T. Harris, J. Emery Cormier, R.N. Brown and A.F. Armington\*

Rome Laboratory, Hanscom AFB, MA 01731

\*Parke Mathematical Laboratory, Carlisle, MA 01734

Bismuth Silicate (BSO) in the sillenite structure  $Bi_{12}SiO_{20}$ , is a non-linear optical material which has many applications including four-wave mixing and optical memories. As obtained by melt growth methods, at approximately 900°C, it is orange-brown in color and exhibits the photorefractive effect. Hydrothermal growth of this material has been accomplished at the Rome Laboratory hydrothermal facility. Specimens cut from crystals produced by this method are colorless, transparent, free of inclusions and strain and thus might provide a starting point to engineer materials superior to commercial crystals

produced by growth methods such as Czochralski (CZ) and gradient freeze. The hydrothermal process may permit "tailoring" of the properties of this material since growth takes place at a relatively low temperature and properties regarded as intrinsic in melt grown materials may be the result of a high temperature defect absent at the hydrothermal processing temperature (~400°C). Growth conditions will be described for this material. Some electrical and optical characteristics and chemical analyses will also be presented. Preliminary results on doped materials will be described.

## SOLID-LIQUID INTERFACE IN THE GROWTH OF SILENITE-TYPE CRYSTALS

*J. Martínez-López and M.A. Caballero*

Dpto. Estructura y Propiedades de Los Materiales  
Universidad de Cádiz, 11510 Pto. Real, Cádiz, Spain

*M.T. Santos, L. Arizemendi and E. Dieguez*

Dpto. Física Aplicada, Universidad Autónoma, 28049 Madrid, Spain

It is known that the maintenance of a flat crystal/melt interface during Czochralski (CZ) growth can clearly yield high quality single crystals.

In this work some sillenite-type crystals have been grown:  $\text{Bi}_{12}\text{SiO}_{20}$ ,  $\text{Bi}_{12}\text{GeO}_{20}$  and  $\text{Bi}_{12}\text{TiO}_{20}$  by CZ method using a control diameter system. Several growth parameters have been studied: crystal orientation, crystal rotation rate, crystal dia-

ter, pulling rate, vertical/radial temperature gradients, temperature fluctuations, melt depth, etc.

In order to perform the core phenomena, periodic bands, growth striations, bubble entrapment, facet formations and other variables, optical microscopy, S.E.M. and X-ray diffraction topography analysis have been carried out.

---

## MODELLING OF DIRECTIONAL SOLIDIFICATION OF BSO

*C. Lin and S. Motakef*

Massachusetts Institute of Technology, Cambridge, MA 02139

Bismuth Silicate ( $\text{Bi}_{12}\text{SiO}_{20}$ ) possesses the common characteristics of electro-optical oxides: high reactivity of the molten phase with all crucible materials except Pt, low thermal conductivity in crystalline and molten phases, and semi-transparency of the solid to infra-red radiation. Thermal transport during growth of this matrix in vertical Bridgman configuration is numerically investigated. Radiative heat transfer is modelled by a two-band model in the crystal (using room-temperature spectral transmittance data) and is neglected in the melt where heat transfer is by buoyancy-induced convection. Heat transfer through the solid is found to be much larger

than that in the melt, resulting in a growth interface shape concave into the melt. The high thermal conductivity of the Pt crucible is found to exert an overwhelming influence on the planarity of growth interface morphology and the deviation between growth and charge lowering rates. A multilayered crucible structure consisting of a thin layer of Pt on a ceramic host which is externally covered by an infra-red absorbing coating is found to result in significant reduction of growth interface nonplanarity and an axial temperature profile in the charge which closely follows that of the furnace.

---

## TWINNING AND DISLOCATION IN THE BRIDGMAN-GROWN $\text{Li}_2\text{B}_4\text{O}_7$ CRYSTALS

*Sun Ren-ying, Fan Shi-ji and Xu Yi-bin*

Shanghai Institute of Ceramics, Chinese Academy of Sciences  
Shanghai 200050, P.R. China

The laminar twinning in the Bridgman-grown  $\text{Li}_2\text{B}_4\text{O}_7$  crystals of direction has been observed by the etching method for the first time. The laminar twins range along  $\langle 100 \rangle$  and  $\langle 010 \rangle$  directions and their interfaces are  $(010)$  and  $(100)$  faces respectively. The different etching rates and figures in the relative twin areas are demonstrated. The nuclei of original laminar twins create at the enlarged region between the seed and grown crystal due to the thermal partial stress of the crucible. The secondary twins in grown crystals propagate mainly from the seed containing twins. The dislocation, sub-boundary and large angle boundary in the crystal have also been observed by the

etching method. The square etch pits and the deformed pentagonal etch pits have been demonstrated on the  $(001)$  and  $(110)$  faces of the crystals respectively. The densities of dislocations and sub-boundaries in the different regions of the crystal are quite different. The high density of etch pits of  $10^5 \text{ cm}^{-2}$  appears in the core region and the areas containing inclusions and growth cracks however the low density of  $10^3 \text{ cm}^{-2}$  in the perfect region. The dislocations in the grown crystals propagate mainly from the dislocations in the seed so that the minimum of the density of etch pits can be reached by the selection of  $\text{Li}_2\text{B}_4\text{O}_7$  seed.

## CRYSTAL GROWTH AND MAGNETO-STRUCTURAL CHARACTERISATION OF

### $Zn_{1-x}Mn_xCr_2O_4$ SINGLE CRYSTALS

*F. Leccabue, B.E. Watts, G. Bocelli<sup>1</sup>, G. Calestani<sup>1</sup>, D. Fiorani<sup>2</sup> and V. Sagredo<sup>3</sup>*

<sup>1</sup>Istituto Maspes/CNR, Via Chiavari 18A, 43100 Parma, Italia

<sup>1</sup>Centro di Strutture Diffrattometrica/CNR, Parma Italia

<sup>2</sup>ITSE/CNR, Area della Ricerca di Roma, Roma, Italia

<sup>3</sup>Departamento de Fisica, Universidad de Los Andes, Merida, Venezuela

Magnetic oxide spinels with the general formula  $M'_{1-x}M''_{x}Cr_2O_4$  ( $M'$  and  $M''$  are divalent metals) are being extensively studied because of their interesting properties. The system  $Zn_{1-x}Mn_xCr_2O_4$  seems particularly attractive because of the coexistence of competitive Cr-Cr, Cr-Mn and Mn-Mn anti-ferromagnetic interactions. The pure compounds  $ZnCr_2O_4$  (antiferromagnetic,  $T_N = 16$  K,  $\theta = -424$  K) and  $MnCr_2O_4$  (non-collinear ferromagnet,  $T_c = 43$  K) are normal spinels with the chromium ions occupying the octahedral sites; the substitution of  $Zn$  by  $Mn$  ions, by changing the spin structure and the resulting magnetic interactions, leads to a magnetic moment on the tetrahedral sites.

In this work single crystals of  $Zn_{1-x}Mn_xCr_2O_4$ , up to  $1 \times 1 \times 1$  mm, in the range of compositions  $x = 0$  to  $1$ , have been grown by the chemical vapour transport (CVT) technique using chlorine as the transport agent. A thermodynamic study of the closed tube system has been done in order to determine the most favourable conditions for growth. The gaseous species taken into consideration were  $Cl_2$ ,  $O_2$ ,  $MnCl_2$ ,  $CrCl_2$ ,  $CrCl_3$ ,

$CrCl_4$ ,  $CrO_2Cl_2$  and  $Cr_2Cl_4$ . In addition the calculations also take into account the presence of  $MnCl_2$  liquid, a spurious species which may modify the crystal perfection and stoichiometry.

Single crystals of different compositions were analyzed by X-ray diffractometric methods using  $MoK\alpha$  radiation. All the crystals examined showed a spinel structure (space group  $Fd\bar{3}m$ ), with zinc which partially substitutes manganese in tetrahedral sites. The variation of the parameters of the cells does not appear to be linear.

Susceptibility measurements as a function of temperature from 4 to 300 K for the different compositions are reported. The magnetic phase diagram has been determined as a function of  $x$  and  $T$ : it was observed that the antiferromagnetic and ferromagnetic states are progressively perturbed and then destroyed, leading to a spin-glass like state in an intermediate composition range.

## A GAS PHASE SUPPORTED LIQUID PHASE SINTERING PROCESS APPLIED GROWING BIG HOMOGENEOUS EuO SINGLE CRYSTALS

*K.J. Fischer, U. Köbler, B. Stroka\*, K. Bickmann and E. Wenzl*

Forschungszentrum Jülich, IFF, Postfach 1913, W-5170 Jülich, Germany

\*Universität Karlsruhe, Physikalisches Institut, Postfach 6980, W-7500 Karlsruhe

The methods of directional freezing from the melt or flux by lowering of the temperature which have been used previously for the preparation of EuO single crystals yield inhomogeneous crystals [1,2,3].

To minimize inhomogeneity of  $cm^3$ -sized crystals of defined stoichiometry a method has been applied in which the growth takes place at nearly constant temperature with a small temperature gradient over the charge volume. The crystal is in equilibrium with a metal-rich liquid (flux, consisting of  $Eu_{1+x}O$ ) and a gas phase. Contrary to the common flux method, however, where the major fraction of the charge consists of flux and the minor fraction of solid this method applies for solid to flux ratios of about 9:1 to 4:1.

Mostly, nominal composition of  $Eu_{1.050}O$  has been used consisting of either  $Eu_2O_3$  powder plus Eu metal or pre-prepared oxygen-rich inhomogeneous EuO pieces plus Eu metal. Crystal growth runs have been performed for 1:1 stoichiometry (at  $1780^\circ C$ ), oxygen- ( $1820^\circ$ ) and metal-rich ( $1740^\circ C$ ) material [1] in sealed molybdenum ampoules and

have been studied by interruption at different stages of the growth process.

The growth features observed in cleaved pieces taken from interrupted runs are substantially the same as for liquid phase sintering [4,5]. For the  $CdS:Te$  system this growth process has been described previously by the term "coalescence process" [6]. Magnetization-and specific heat-measurements have been used to confirm homogeneity. The structural perfection of the crystals has been studied by  $\gamma$ -ray diffractometric and shows low angle grain boundaries.

- [1] M.W. Shafer, J.B. Torrance, T. Penney, *J. Phys. Chem. Solids* 1972, Vol. 33, 2251-2266.
- [2] T.B. Reed, R.E. Fahey, *J. Crystal Growth* 8, 1971, 337-340.
- [3] K.G. Barraclough, G. Garton, P.J. Walker, *J. Crystal Growth* 35, 1976, 321-322.
- [4] W.J. Huppmann, G. Petzow, *Elementary Mechanisms of Liquid Phase Sintering in Materials Science Research* Vol. 13, 1980, Plenum Press.
- [5] R.M. German, *Liquid Phase Sintering*, Plenum Press 1985.
- [6] R.M. Mikulyak, *J. Crystal Growth* 8, 1971, 149-152.

## GROWTH OF $TiO_2$ RIBBON SINGLE CRYSTALS BY EDGE-DEFINED FILM-FED GROWTH METHOD

Hiroshi Machida\*, Keigo Hoshikawa and Tsuguo Fukuda

Institute for Materials Research, Tohoku University, Sendai, 980, Japan

Rutile ( $TiO_2$ ) crystals have attracted much attention because of their applications as polarizers and in other optical devices. The crystals have been grown only by the Verneuil and floating zone methods. Their crystal qualities have been reported<sup>1)</sup> to be usually degraded by the small-angle grain boundary produced as a result of high temperature gradient growth. Moreover, in these methods the growth direction is restricted to the z-axis due to the thermal conductivity in that direction being much greater than in the others. The attempt has been made to grow  $TiO_2$  single crystals by the Czochralski method<sup>2)</sup>, since this permits low temperature gradient growth, but it has been unsuccessful due to the great difficulties encountered with diameter control. We have investigated  $TiO_2$  single crystal growth by the edge-defined, film-fed growth (EFG) method, which could potentially permit control of the crystal shape by use of the die and could create a wide range of temperature gradient near the growth interface. The EFG method has already applied to  $Al_2O_3$  ribbons and other crystals. However, the growth of  $TiO_2$  by the EFG method has not yet been reported.

A typical EFG ribbon crystal grown under conditions similar to the  $Al_2O_3$  ribbon crystal is shown in Fig. 1(a). The characteristics of this crystal were that the cross-sectional shape easily became unstable and that the ribbon width and thickness changed periodically. As a result of theoretical and experimental studies on these instabilities, it proved possible to grow well-formed ribbon crystals under the modified growth conditions [see Fig. 1(b)]. It was confirmed that no small-angle grain boundaries existed in these crystals. The growth conditions and characteristics of  $TiO_2$  ribbon crystals will be shown and discussed.

1) M. Higuchi et al., *J. Crystal Growth* 112(1991)354.

2) H. Machida and T. Fukuda, *J. Crystal Growth* 112(1991)835.

Present address: Fine Ceramics R&D Division, Chichibu Cement Co. Ltd., Mikajiri, Kumagaya, 360, Japan.

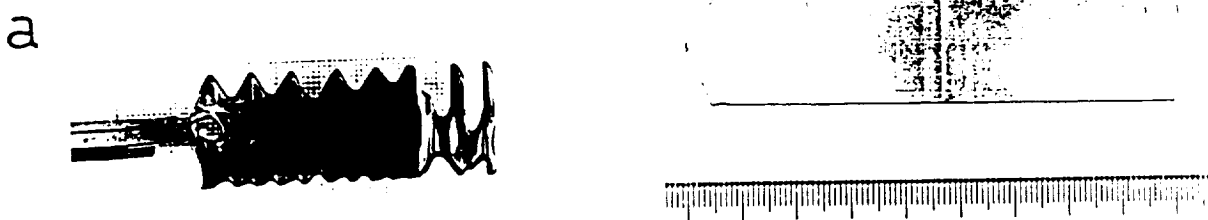


Figure 1.  $TiO_2$  ribbon single crystals grown under standard conditions (a) and modified conditions (b).

## THE GROWTH OF DOME-SHAPED SAPPHIRE CRYSTALS BY THE GSM

A. Horowitz, S. Biderman, D. Gazit, Y. Einav, G. Ben Amar and M. Weiss

Crystal Growth Division, Nuclear Research Center-Negev

P.O. Box 9001, Beer Sheva 84190, Israel

The excellent optical and mechanical properties of sapphire make it the preferred choice for IR domes, necessary as an external window of missiles operating in the 3-5  $\mu m$  optical region. However, the inherent advantage of extreme hardness, makes the fabrication of such domes from single crystal boules difficult, time consuming and expensive.

In our laboratory, near-net-shaped sapphire domes have been grown for many years, in a variety of size (up to 6 inches in diameter), shapes (hemispherical and others) and orientations (including the c-axis orientation). The domes are grown in double wall molybdenum crucibles by the Gradient Solidifi-

cation Method. For each dome geometry, size and orientation, a special furnace and growth course are designed. This is necessary, in view of the non-linearity of the temperature gradient, surface energy effects that arise in large-diameter crystals and the very high temperature involved. By optimizing the growth condition it is possible to achieve premium grade domes, free of grain-boundaries, scattering centers and stresses.

The paper will describe the principles of this growth technique, demonstrate its advantages and some of the difficulties overcome.

## HYDROTHERMAL SYNTHESIS AND MORPHOLOGY OF $\text{Li}_2\text{B}_4\text{O}_7$ CRYSTALS

*K. Byrappa and K.V.K. Shekar*

The Mineralogical Institute, University of Mysore  
Manasagangotri, Mysore-570 006, India

Lithium tetraborate ( $\text{Li}_2\text{B}_4\text{O}_7$ ) is becoming a substitute for the traditional  $\alpha$ -quartz in the recent years, because of its excellent piezoelectric and non-ferroelectric properties which are highly attractive for Surface Acoustic Wave (SAW) and Bulk Acoustic Wave (BAW) devices with a low temperature coefficient of delay and higher electromechanical coupling constants. Several methods have been successfully employed in growing single crystals of lithium tetraborates. In this work the hydrothermal synthesis of  $\text{Li}_2\text{B}_4\text{O}_7$  crystals is reported for the first time. The crystallization was carried out through spontaneous nucleation by adopting some effective measures in order to control the nucleation centres. The crystals obtained were

highly transparent and vary in size from 1mm to 12mm. In general the morphology of the hydrothermally grown  $\text{Li}_2\text{B}_4\text{O}_7$  is very interesting and varies widely depending upon the experimental conditions, particularly the starting materials and percent fill. The morphology varies from polycrystalline form to a single crystal form as the molarity of the solvent and internal pressure change. A detail morphological study including the surface morphology has been discussed in the present work. The main thrust of this paper is the suitability of the hydrothermal technique to overcome some of the problems being faced in the Czochralski and Bridgman techniques, and the morphological variation with reference to the growth parameters.

## SESSION 6C

### GROWTH OF GaN AND AlGaN BY MOVPE FOR UV/BLUE P-N JUNCTION DIODES

*I. Akasaki, H. Amano and H. Murakami*

Nagoya University, Department of Electronics  
Furo-cho, Chikusa-ku, Nagoya 464-01, Japan

Recent progress of the technique and understanding of the mechanism of the heteroepitaxial growth on highly mismatched substrate (HGHMS) have developed a new field in the semiconductor physics and devices. Growth of GaN and AlGaN on sapphire using buffer layer is the typical example of such a newly developed HGHMS. In spite of the large lattice and thermal mismatches between GaN and sapphire, high quality  $Al_xGa_{1-x}N$  ( $0 \leq x \leq 0.4$ ) can be grown on sapphire (0001) or (1120) substrate using thin AlN buffer layer deposited at low temperature. TEM observation revealed that even though many dislocations exist in the AlN buffer layer and near the interface between GaN epitaxial film and the buffer layer, most of them are terminated at the initial stage of the growth of GaN. Undoped GaN films show high resistivity, indicating that our GaN films are very pure and nearly intrinsic. PL spectra of these films show strong band edge emission, and very weak deep level related emission, indicating that the concentration of impurity and/or point defect is very few in the GaN film. Stimulated emission from highly excited undoped GaN film grown in this way has been clearly observed at RT for the first

time. As concerns the conductivity control, electron concentration can be controlled linearly by doping of Si using  $SiH_4$  in both cases of GaN and AlGaN. GaN doped with acceptor impurity such as Zn or Mg usually shows high resistivity. In 1989, we succeeded for the first time to prepare Mg-doped GaN film having distinct p-type conductivity by the low energy electron beam irradiation (LEEBI). High power UV/blue p-n junction LED have been fabricated using n-type GaN:Si and LEEBI treated p-type GaN:Mg. These LEDs emit blue emission peaking at about 420nm and UV emission peaking at about 375nm. The output power of our LED is more than 0.1mW, and the external quantum efficiency is more than 0.2% at the DC-forward current of 30mA, which are the highest value to date. Recently, GaN/AlGaN multiheterostructure showing quantum size effect has been achieved. All these results are promising for the realization of UV/blue laser diode which can operate at RT. DH devices using AlGaN as the cladding layer also shows high power. The performance of these DH devices will be presented in detail.

---

### MORPHOLOGICAL PROPERTIES OF CVD AlN FILMS

*R. Rodríguez-Clemente\*, B. Aspart†, N. Azemá‡ and B. Armas\*\*,  
C. Combescure†, J. Durand‡ and A. Figueras\**

\*Institut de Ciencia de Materials de Barcelona, CSIC,

Campus U.A.B., 08193 Cerdanyola, Spain

†ISGMP-CNRS, 66120 Odeillo, France

‡Laboratoire de Physicochimie des Matériaux, ENSC-CNRS,  
8, rue de l'Ecole Normale, 34053 Montpellier, France

Aluminum nitride is a material with applications in piezoelectric devices, gas-turbine blades, surface acoustic-wave substrates, and several other. Its high mechanical strength, high melting point, good resistance to oxidation and good thermal conductivity, make this material suitable for coating in composites employed in aerospace applications and environments with extreme thermal, chemical and physical conditions.

AlN films deposited on silicon and graphite have been produced by PEMOCVD (Plasma Enhanced Metal-Organic Chemical Vapour Deposition) and LPMOCVD (Low Pressure Metal Organic Chemical Vapour Deposition) respectively. The crystal size increases with the increase in temperature for LPMOCVD. In the case of PEMOCVD, the crystal size increases with decreasing excitation frequency (varying in the range 13.56 MHz to 35 mHz). The rate of deposition also

increases with decreasing excitation frequency. It seems as if the surface processes such as growth site creation, surface diffusion, by-products desorption, etc, are favored by low excitation frequencies, which give the ions energies similar to those existing in the crystal lattice. In both systems, the rate of deposition depends on the partial pressure of the organometallic reactants. The hydrogen liberated during the pyrolysis process has a strong morphological influence. The thickening of the layers leads to preferential orientations, resulting from the specific kinetic of growth of different crystal faces and their interaction with the hydrogen. It has been observed that a high concentration of hydrogen in the reacting systems leads to the blockage of the (0001) face and the growth of the faces parallel to the [0001] axis leading to lamellar crystals. In this paper, a model is proposed to explain the morphologies obtained with these two methods of synthesis.

## SiC-AlN SOLID SOLUTION GROWTH BY METALORGANIC CHEMICAL VAPOR DEPOSITION

V.A. Dmitriev\*, K.G. Irvine, I. Jenkins, X. Tang and M.G. Spencer

Materials Science Research Center of Excellence  
School of Engineering, Howard University  
Washington, DC, USA  
\*and A.F. Ioffe Institute, St. Petersburg, USSR

We report the first epitaxial growth of  $(\text{SiC})_x(\text{AlN})_{1-x}$  solid solution by MOCVD. This solid solution has an electronic bandgap in the range 3 eV to 6 eV. At high values of  $x$ , the bandgap undergoes a transition from indirect to direct.<sup>1</sup> The solid solution of  $(\text{SiC})_x(\text{AlN})_{1-x}$  has a lattice constant that varies between 3.081 Å (the values for 6H SiC) and 3.114 Å (the value for 2H AlN), the maximum mismatch in this system is about 0.5 percent. Because of the excellent lattice match and the possibility of direct gap material, this system looks attractive for ultraviolet optoelectronic devices and for wide bandgap heterojunction devices.

$(\text{SiC})_x(\text{AlN})_{1-x}$  layers composition and crystalline quality have been investigated as a function of growth conditions. At optimum growth conditions, single crystalline layers up to 5 microns have been grown on (100) Si substrates and (0001) 6H SiC substrates. Growth of  $(\text{SiC})_x(\text{AlN})_{1-x}$  was accomplished

using the hydrogen, silane, propane, ammonia, and trimethylaluminum system. Depositions were carried out in a stainless steel vertical reactor at reduced pressures. The growth temperature was varied between 1100°C and 1400°C. The dependence of the layer morphology and growth rate on temperature and gas flow will be presented.

It has been shown in other growth systems, that the polytype structure for solid solutions of  $(\text{SiC})_x(\text{AlN})_{1-x}$  depends on concentration of AlN. We will discuss the dependence of the solid solution polytype on growth conditions.

1. Nurmagamedov, S.A. et al. *Sov. Phys. Semicon.*, 22(1), 1989.

This work has been supported by the National Science Foundation and the Office of Naval Research.

## GROWTH OF LARGE SiC SINGLE CRYSTALS

D.L. Barrett, R.G. Seidensticker, J.P. McHugh, H.M. Hobgood and R.H. Hopkins

Westinghouse Science and Technology Center  
1310 Beulah Road, Pittsburgh, PA 15235, USA  
W.J. Choyke  
Department of Physics, University of Pittsburgh  
Pittsburgh, PA 15260, USA

Silicon carbide is the semiconducting material of choice for high power microwave, high temperature, and radiation hard applications due to its large bandgap, high dielectric strength, large saturated drift velocity and high thermal conductivity. The large bandgap (2.86 eV for 6H polytype SiC, compared with 1.1 eV for Si and 1.4 eV for GaAs) results in semiconducting devices which will operate at a higher temperature (650°C has been demonstrated) than Si or GaAs devices, and which exhibit improved radiation resistance. SiC exhibits a critical electric-field breakdown strength 10 times that of Si, a high-field electron velocity equal to that of GaAs, and a thermal conductivity near that of copper; qualities which will enable microwave transistors with up to 10X the power density of today's Si devices to be fabricated.

Recent advances in crystal growth technology to prepare single crystal, single polytype crystals of SiC, and the promise of silicon-like wafer processing, heralds a new age in the fabrication of practical devices using SiC. We have grown 1.5-inch diameter single crystal boules of 6H polytype SiC up to 3

inches in length using a sublimation-source physical vapor transport (PVT) technique. The SiC sublimation-source supplies vapor for transport and growth onto 6H polytype single crystal seeds. Undoped crystals were grown using SiC Lely-grown platelets as the source material after pre-purification by vapor transport, while  $\text{N}^+$  crystals were grown using a partial nitrogen atmosphere. Al is used to provide p-type doping. Wafers were prepared for subsequent epitaxial layer growth and device fabrication by slicing the boules with an ID-diamond saw, and polishing using diamond grit lapping and polishing.

We have designed our system for high purity growth by using a water-cooled quartz-wall system and an induction heated arrangement. Pre-purified graphite materials was used in hot-zone construction to provide a vacuum in the mid  $10^{-6}$  torr at 2000°C after degassing at higher temperatures. Vacuum-tight integrity of the system, and a high temperature degassing step was important in reducing the nitrogen donor concentration and achievement of high purity SiC material. Growth and characterization of the crystals will be described.

BLUE PHOTOLUMINESCENCE AT ROOM TEMPERATURE IN  
Zn-DOPED SINGLE CRYSTALS OF CuAlS<sub>2</sub>  
*Igor Aksenov and Katsushi Sato*  
Faculty of Technology, Tokyo University of Agriculture and Technology  
Koganei, Tokyo 184, Japan

We have succeeded for the first time in observing a very bright blue and green photoluminescence (PL) from CuAlS<sub>2</sub> crystals, grown by chemical vapor transport and subsequently doped with Zn.

Single crystals of undoped technique in a closed system using iodine as a transporting agent. The starting materials employed were the powders of CuAlS<sub>2</sub> prepared by the direct melting of constituent elements in a pBN crucibles held in a sealed silica ampoule. The maximum temperature used was 1300°C.

Zn-doping has been carried out for 50 h at different temperatures in the range 700-900°C in evacuated silica ampoules, containing the as-grown crystals and Zn, as well as sulphur or a powder of the CuAlS<sub>2</sub> compound. PL was excited by the 325nm-line of a He-Cd laser (50 mW), with the samples being put into an Oxford Instruments continuous flow cryostat.

The typical PL spectrum of undoped CuAlS<sub>2</sub> exhibits a series of sharp lines at 346nm-357nm, caused by free- and bound-exciton recombination, intense purple DA-emission band at 410nm, as well as a broad orange band, originated from the DA pair recombination, involving deep centers. Usually, the orange band dominates the spectrum, and the resulting colour of emission is orange.

The spectra of the crystals, annealed at 700°C in the presence of Zn and sulphur with the vapour pressure of about 5 atm exhibit three new bands V, B, and G<sub>2</sub> at 380nm, 445nm, and 520nm, respectively, which were not observed in the as-grown

crystals. The thermal quenching curves for the strongest V-band reveal the existence of two energy levels with the activation energies of 50 meV and 180 meV, involved in this emission. Hence, the violet emission is supposed to be caused by DA-recombination.

The annealing of the crystals in the presence of Zn plus CuAlS<sub>2</sub> powder being added into the ampoule greatly strengthens the green emission band G<sub>2</sub> and gives rise to G<sub>1</sub>-emission band, peaked at 480nm. The resulting green-coloured emission from the crystals is very bright even at room temperature and is observable up to T = 250°C.

Rising of the annealing temperature up to 900°C causes drastic changes in the PL spectra, the luminescence in this case being dominated by a very strong B-emission, which is believed to be also originating from DA pair recombination, including deep levels, formed in the band gap of the CuAlS<sub>2</sub> by Zn-related defects. The resulting blue emission is very bright and, like in the case of the green emission, is observed up to T = 250°C.

Since Zn-doped CuAlS<sub>2</sub> crystals exhibit low resistivity values of about 1 Ωcm, and since the lattice mismatch between the CuAlS<sub>2</sub> and ZnS compounds is quite small (1.5%), the PL results obtained point out that the CuAlS<sub>2</sub> compound can be regarded as a perspective materials for the fabrication of homojunction or CuAlS<sub>2</sub>/ZnS-heterojunction blue and green light emitting device.

## FLOATING ZONE GROWTH OF MONOCHROME GRADE CRYSTALS OF YB<sub>66</sub>

Yutaka Kanimura, Takaho Tanaka, Shigeki Otani and Yoshio Ishizawa

National Institute for Research in Inorganic Materials, Tsukuba, Japan

Zofia U. Rek

Stanford Synchrotron Radiation Laboratory, Stanford, USA

Joe Wong

Lawrence Livermore National Laboratory, Livermore, USA

YB<sub>66</sub>, cubic with a cell parameter of 23.44 Å, is suitable as a soft X-ray (1~2keV) monochromator for dispersing synchrotron radiation<sup>(1)</sup> as a result of its large d-spacing (5.86 Å) of the (400) reflection and it having no intrinsic absorption due to its constituent elements in that energy range. For this purpose, we are investigating growth methods of obtaining the monochromator grade crystals. The YB<sub>66</sub> crystals have been grown by an indirectly heating floating zone (IHFZ) method previously reported<sup>(2)</sup>, where the molten zone is heated by radiation from an inductively heated tungsten ring.

To achieve high perfection in the YB<sub>66</sub> crystal, there are two key factors. One is the growth conditions; the temperature of the molten zone, the direction of drive, the rates of growth and rotation, and the atmosphere. These conditions have a great influence on the shape of the molten zone. A convex shape of the growth interface is important for growing high quality crystals and has been achieved by keeping low heating power and downwards drive.

The other is the chemical composition of the YB<sub>66</sub> feed rod and the molten zone. We have been successful in growing several monochromator grade crystals with congruent composition of [B]/[Y]=62, while recent preliminary experiments suggest that the same grade crystal of YB<sub>66</sub> is able to be grown even with incongruent composition.

An example of soft-Xray rocking curve of the highest quality crystals of YB<sub>66</sub> shown in Fig. 1, indicating this crystal is suitable for monochromator use.

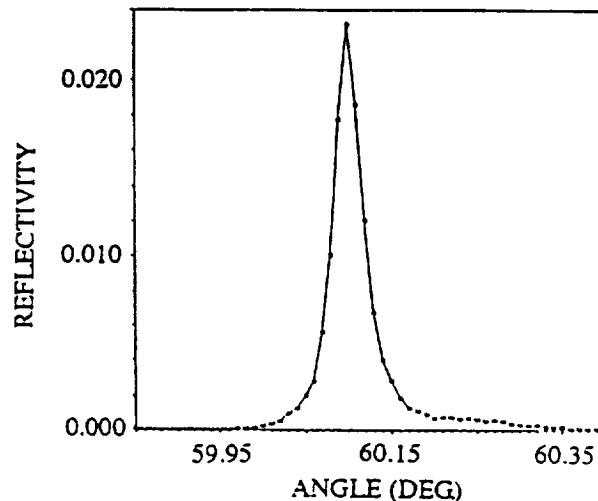


Figure 1. Soft X-ray rocking curve of YB<sub>66</sub> measured at 1.25 keV (mgka). FWHM is about 110 arc sec.

(1) J. Wong, G. Shimkaveg, W. Goldstein, M. Eckart, T. Tanaka, Z.U. Rek and H. Tompkins, *Nucl. Instrum. Methods Phys. Res. A291* (1990) 243.

(2) T. Tanaka, S. Otani and Y. Ishizawa, *J. Crystal Growth* 99 (1990) 994.

## PREPARATION OF BOUNDARY-FREE $\text{LaB}_6$ SINGLE CRYSTALS BY THE TRAVELING SOLVENT FLOATING ZONE METHOD

Shigeki Otani, Shigeru Honma, Takaho Tanaka and Yoshio Ishizawa  
National Institute for Research in Inorganic Materials  
1-1, Namiki, Tsukuba, Ibaraki 305, Japan

$\text{LaB}_6$  single crystals are widely used as thermionic electron emitters of high brightness and longevity. The crystals are mainly prepared by the floating zone method because of high purity and large size. However, the crystals contain many sub-grain boundaries, and accordingly the emitters must be made from only boundary-free parts in the crystal.

In this presentation, boundary-free  $\text{LaB}_6$  crystals were prepared by the traveling solvent floating zone method, that is, by decreasing the growth temperature, as shown in Fig. 1. A feed sintered rod was set to the upper shaft in the furnace. A  $\langle 100 \rangle$

seed crystal was set to the lower shaft. A Lanthanum metal lump was put on the seed crystal to control composition of an initial molten zone. In several atmospheres of argon, the molten zone was passed along the feed rod at a rate of 0.5 cm/h. During the zone pass, evaporation did not change the zone composition. The boundary-free crystals were obtained when the growth temperature was lower than  $2400^\circ\text{C}$ ,  $300^\circ\text{C}$  lower than the melting point of  $\text{LaB}_6$ . The grown crystals were 5 cm long and about 0.9 cm in diameter. In addition, the influence of the growth conditions on the crystal quality was examined.

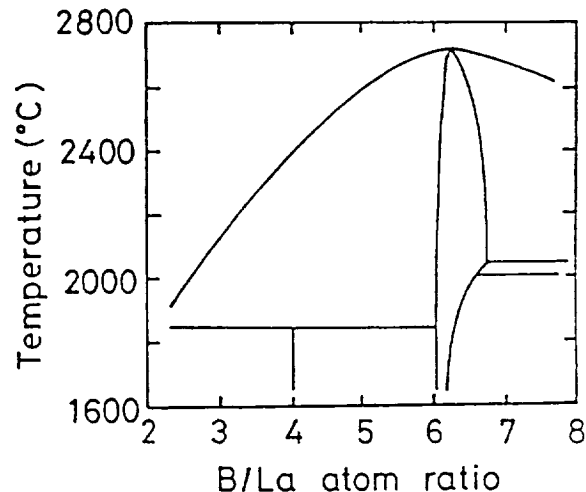
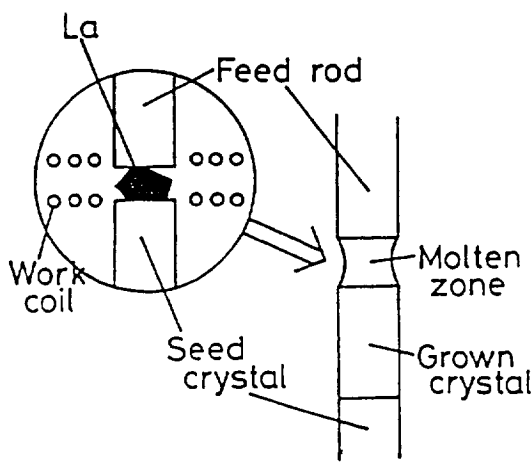


Figure 1. Preparation of  $\text{LaB}_6$  crystals by the traveling solvent floating zone method.

## USE OF THE BRIDGMAN METHOD FOR GROWTH OF PERITECTIC COMPOUNDS

Thierry Caillat\*, Jean-Pierre Fleurial and Alex Borshchevsky  
Jet Propulsion Laboratory\*\*  
California Institute of Technology, Pasadena, California, USA

Crystal growth of peritectic compounds from solutions requires excellent control over the processing conditions. A high temperature two-zone Bridgman furnace was designed and built to obtain a temperature gradient of about  $40^\circ\text{C}/\text{cm}$  and achieve growth rates as low as 1 mm/day. Single crystals of the peritectic compound  $\text{Cr}_{11}\text{Ge}_{19}$  were grown in this furnace. The crystals were investigated by optical microscope, microprobe

analysis and X-ray diffractometry. Density and some electrical properties were measured and are reported.

\*This work was done while the author held a National Research Council-Jet Propulsion Laboratory Research Associateship.

\*\*Carried out under contract with the National Aeronautics and Space Administration.

**ELEKTRODEPOSITION OF MOLYBDENUM ONTO THE BENT SINGLE CRYSTAL  
MOLYBDENUM SUBSTRATES FROM MOLTEN SALTS**

*N.O. Esina, A.N. Baraboshkin, V.O. Esin, Z.J. Vales,  
L.M. Minchenko, A.A. Pankratov and D.M. Tagirova*  
Institute of Electrochemistry, Ekaterinburg, 620219, USSR

It has been established that during the transition from the autoepitaxial single crystal growth of molybdenum to the polycrystalline one with the axial growth texture the gradually incline of the growing single crystal to the direction of the texture axis occurs [1].

This work shows the principal possibility of the receipt of the monocrystalline molybdenum layers at the bent single crystal molybdenum substrates of the different orientations.

The plate-like (5x10x0.15mm) monocrystalline molybdenum substrates with <110>, <100>, <112> and <111> orientations were bent with the radius of curvature R=20mm.

The electrodeposition was carried out from the molten salts KCl-NaCl-MoCl<sub>3</sub> at temperature 800-830°C, at the conditions when the layers with (111) axial growth texture on the nonoriented substrates have been formed. The thickness of the deposits was from 50 to 500μm.

It was found by X-ray and metallographic methods that these deposits were the monocrystalline ones. The morphology of the growing bent surface corresponded to the morphology of the growing straight surface at the same condition.

It is interesting that the sizes of the pits (pyramids) of growth at the concave surface were two times as large than at the convex growing surface. The thickness of the deposit on the concave surface is the same on the convex one. Besides, due to the X-ray topography data we can propose that the self-organization and the self-perfection of the growth bent crystal structure take place.

---

[1] A.N. Baraboshkin, N.O. Esina. 30th Meeting, International Society of Electrochemistry. Extended Abstracts, Yugoslavia, 1981. V.1, 349-352p.

## SESSION 6D

### TOWARDS AN UNDERSTANDING OF THE PRECRYSTALLIZATION AND EARLY STAGES OF CRYSTAL GROWTH OF BIOLOGICAL MACROMOLECULES

#### The influence of macromolecular homogeneity

Richard Giege<sup>a</sup>, Bernard Lorber<sup>a</sup>, Mohammed Skouri<sup>b</sup>, Jean-Pierre Munch<sup>b</sup> and Sauveur Candau<sup>b</sup>

<sup>a</sup>Institut de Biologie Moléculaire et Cellulaire du CNRS,

15 Ne René Descartes, F-67084 Strasbourg Cedex, France

<sup>b</sup>Laboratoire d'Ultrasons et de Dynamique des Fluides Complexes,

URA 851 du CNRS, Université Louis Pasteur, 4 rue Blaise Pascal,

F-67070 Strasbourg Cedex, France

Biological macromolecules are always difficult to obtain in a highly pure and homogeneous state as would be required for optimal crystallization experiments (1). Since contaminants are known to affect nucleation and crystallization of small molecules as well as of macromolecules (e.g. 1-4), we have investigated the effect of trace amounts of macromolecular impurities on the nucleation and crystal growth of a model protein, hen egg white (HEW) lysozyme. The purity and activity of various preparations of HEW lysozyme were evaluated by various biochemical methods. The precrystallization (5), nucleation and early growth stages of crystallization (6) were analyzed by dynamic light scattering, video microscopy and photomicrography and compared for several apparently pure and monodisperse preparations. Additional experiments were conducted on highly pure protein solutions in which trace amounts of the natural HEW lysozyme contaminant (ovalbumin) or foreign proteins were added on purpose.

Data will be presented that illustrate the influence of purity and homogeneity of HEW lysozyme on its phase diagram,

solubility, aggregation under precrystallization conditions in under- or supersaturated solutions before appearance of macroscopic crystals, and on crystal number, size and habit. Implications for reproducibility of protein crystal growth experiments will be emphasized.

- (1) R. Giegé, A.C. Dock, D. Kern, B. Lorber, J.C. Thierry and D. Moras (1986) *J. Crystal Growth*, **76**, 554-561.
- (2) A.A. Chernov (1984) *Modem Crystallography III*, Springer Series in Solid-State Sciences 36, Springer-Verlag, Berlin.
- (3) A.S. Myerson and K. Toyokura (1990) *Crystallization as a Separation Process*, ACS Symposium Series 438 Washington DC.
- (4) C. Abergel, M.P. Nesa and J.C. Fontecilla-Camps (1991) *J. Crystal Growth*, **110**, 11-19.
- (5) M. Skouri, J.P. Munch, B. Lorber, R. Giegé and S. Candau (1992) *J. Crystal Growth*, in press.
- (6) M. Skouri, M. Delsanti, J.P. Munch, B. Lorber and R. Giegé (1991) *FEBS Lett.*, **295**, 84-88.

## GROWTH AND DISSOLUTION KINETICS OF LYSOZYME

*Lisa A. Monaco, Franz Rosenberger and Nai-Ben Ming\**

Center for Microgravity and Materials Research

University of Alabama in Huntsville

Huntsville, Alabama 35899

High resolution optical microscopy with digital image storage and processing was used to study in-situ the growth and dissolution kinetics of lysozyme in a 25  $\mu\text{l}$  solution bridge inside a temperature controlled cell. Employing transmission differential interference contrast and reflection interferometric techniques, the real-time evolution of interfacial features was studied with a depth resolution of 300  $\text{\AA}$ . For the control of super- and undersaturation, we used the solubility data determined with the light scintillation technique developed in our laboratory. The solutions contained 50 mg/ml of protein and 2.5% w/v NaCl at pH=4.5.

Normal growth (and etching) rates of facets were determined, revealing increasing anisotropies with increasing supersaturation  $\sigma$ . At low  $\sigma$ 's growth is kinetically controlled and occurs through layer spreading. At higher  $\sigma$ 's interfacial kinetics and bulk transport become equally important for the growth morphology. The interferometric data show that the comers that overlie regions in which growth striations intersect growth sector boundaries become more active sources for growth steps. The propagation velocities of macrosteps (originating

from dislocations and 2-d nucleation) depend on  $\sigma$  in a manner similar to that observed in inorganic systems. However, comparable growth rates (100  $\text{\AA/sec}$ ) require  $\sigma$ 's that are orders of magnitude higher. Below  $\sigma \approx 2$  macroscopic growth rates become exceedingly small.

The etching experiments revealed morphological anisotropies on crystallographically seemingly identical faces. These anisotropies can be interpreted in terms of a bond structure analysis. Correlations between layers of irregularly incorporated solution (growth striations) and growth temperature variations were established. Striations are more pronounced in the growth sectors that possess higher growth rates.

---

\*Laboratory of Solid State Microstructures, Nanjing University, Nanjing 210008, People's Republic of China.

This work has been supported by the Microgravity Science and Applications Division of NASA (Grants NAG8-868 and NGT-50129) and by NSF (Grant INT-8903173).

---

## NUCLEATION PHENOMENA IN CRYSTALLIZATION OF SATELLITE

### TOBACCO MOSAIC VIRUS (STMV)

*Alexander J. Malkin and Alexander McPherson*

Department of Biochemistry, University of California at Riverside  
Riverside, CA 92521, USA

**1. Methods.** The nucleation phenomena and postnucleation events in the crystallization of satellite tobacco mosaic virus (STMV) was investigated by quasi-elastic light scattering (QELS) using photon correlation spectroscopy.

**2. Elementary parameters of STMV crystallization.** Under conditions of relatively moderate supersaturation  $\sigma = 100\text{-}140\%$ , the continuous aggregation process leading to the appearance of a new phase does not become established immediately. The definite supersaturation dependent induction period,  $t_{\text{ind.}} = 4\text{-}155\text{min}$  was necessary for the appearance of aggregates in solution with a size  $R$  more than that of the critical nucleus  $R_c$ . At  $\sigma > 140\%$  large aggregates composed of more than  $10^3$  virus particles appeared immediately. The critical nuclear size supportive of stable crystal growth,  $R_c$ , was estimated from time dependent size distribution analyses to be in the range of 20 ( $\sigma$  at 100%) to 5 virus particles ( $\sigma$  at 140%). From the same data, the molar interfacial free energy and the activation energy for STMV crystal growth was deduced to be 2.2 kcal/mol and 10 kcal/mol, respectively. These, we believe

represent the first such estimates for virus crystal growth. The acceleration of nucleation and crystal growth by the introduction of heterogeneous nucleants (latex microspheres) was demonstrated.

**3. Postnucleation growth.** The size of the aggregates,  $R$ , increases with time as  $R \approx t^{1/2}$ , i.e. STMV crystal growth is limited by volume diffusion rather than by kinetics of surface processes. The data is consistent with a probable pathway for STMV crystal growth that proceeds through accretion of clusters of virus particles. Our experiments demonstrate that for STMV, the aggregation process leading to crystal formation is distinctly different than that producing amorphous precipitate. The aggregation rate for crystallization is substantially higher with a power law exponent of  $n \approx 0.5$  while that associated with eventual amorphous precipitate was in the range of  $n = 0.1\text{-}0.2$ . Our results provide additional evidence that QELS can be a useful tool for the rapid and nondestructive determination of the ultimate fate of solutions supersaturated with respect to macromolecules.

## THERMAL METHODS IN PROTEIN CRYSTALLIZATION

R.C. De Mattei and R.S. Feigelson

Center for Materials Research

105 McCullough Building, Stanford, CA 94305-4045

The controlled nucleation and growth of protein crystals has only recently begun to be investigated. These studies are driven by the need to better understand and control the nucleation and growth process in order to produce better crystals.

The solubility diagrams of the proteins canavalin<sup>[1]</sup> and lysozyme<sup>[2]</sup> show a strong dependence on temperature as well as precipitating agent. This temperature dependence indicates that thermal methods of crystal growth can be applied to proteins. This paper will discuss two of those methods that apply to nucleation and growth.

The Thermonucleator was developed as a means to control and localize nucleation using a temperature field. This apparatus was designed to separately control the temperature at the point of nucleation (600 $\mu$  diameter spot) and the bulk of the crystallizing solution. The thermal profiles around the cold spot have been measured in water and gradients as high as 200°C/cm were obtained. The Thermonucleator has been used to nucleate and grow crystals of ice, Rochelle salt, lysozyme in both the normal and retrograde solubility regions, and horse

serum albumin (retrograde solubility). In the latter two examples, the solubility diagram was not known.

The thermal gradient transport method has been used to grow lysozyme crystals. The apparatus used for the growth consisted of two microscope slides (1in x 3in) separated by a 0.0625in spacer. The temperatures at the two end of the apparatus were controlled using water baths. The supersaturation along the apparatus was calculated from the temperature gradient and the actual growth rate was compared to that calculated from the supersaturation. Seeded crystals were grown for periods of up to 9 weeks.

It is possible to combine these two techniques to grow protein crystals for molecular structure determinations.

1. R.C. De Mattei and R.S. Feigelson, *J. Crystal Growth*, 110 (1991) 34

2. M.L. Pusey, private communication.

This research was supported by NASA Grant NAG 8-774 and by the NSF-MRL program.

---

## CRYSTALLISATION OF NORTRIPTYLINE HYDROCHLORIDE, A TRICYCLIC ANTIDEPRESSANT

M.L. MacCalman and K.J. Roberts

Department of Pure and Applied Chemistry  
University of Strathclyde, Glasgow G1 1X1, UK

B. Hendriksen

Lilly Research Centre Ltd, Windlesham, Surrey, GU20 6PH, UK

Crystallisation represents an essential unit-operation for the preparation and definition of many pharmaceutical products. The performance of such a product is fundamentally dependent on structural factors such as absolute solubility, bioavailability, stability, compressibility and flow. In the formulation, tabletting and packaging crystal habit can play a significant role and product performance can be directly influenced and improved with the correct choice of crystallisation parameters such as temperature, solvent, supersaturation etc.

In this paper we present an examination of the role of such parameters on the crystallisation characteristics of the antidepressant drug nortriptyline hydrochloride. The crystal habit of commercially available materials together with samples recrystallised as a function of crystal growth conditions has

been examined using scanning electron microscopy and compared to theoretically derived morphologies using the intermolecular force modelling package HABIT [1]. The results are presented and discussed in terms of the surface chemistry of nortriptyline hydrochloride in terms of the molecular recognition processes taking place between the crystal surfaces and the mother liquor phase. Morphologies are compared and contrasted to predicted morphologies based on geometry and lattice energy calculations.

[1] HABIT - A computer program to predict the Morphology of Molecular crystals. G. Clydesdale, R. Docherty and K.J. Roberts, *Computer Physics Communications* 64 (1991) 311-328.

## GROWTH AND MORPHOLOGY OF CHOLESTEROL IN MODEL BILES

*F.C. Voogt, R.M. Geertman and H. Meekes*  
Laboratory of Solid State Chemistry, University of Nijmegen  
*B. Groen*  
Academical Medica Centre, Amsterdam, The Netherlands

For the formation of gallstones the transport, nucleation and growth of cholesterol monohydrate plays an important role. Human bile consists mainly of bile salts, phospholipids (lecithin) and cholesterol in water. The cholesterol is for the largest part present in vesicles or micelles formed by the phospholipids and bile salts. The formation of cholesterol crystals, which on their turn can conglomerise into gallstones, is not fully understood yet. The question is whether the growth is determined by actual growth kinetics, nucleation or transport from the vesicles and micelles.

Therefore, we started to investigate the growth and nucleation of cholesterol monohydrate crystals in different systems more or less corresponding to human bile. From the theoretical side we worked on the above question by performing periodic

bond chain analysis and studying the interaction between cholesterol crystal faces and the solvent using computer calculations and graphical tools. Special attention in the PBC analysis and calculations will be given to the stabilising role of the crystal water. The incorporation of the bile salts in the crystals is investigated both theoretically and experimentally.

We will present results on the macroscopic morphology which turns out to depend clearly on the solvent system used. Furthermore, growth rate and nucleation times will be given for the different systems.

The interpretation of the experimental results will be based on the computer calculations. The relevance of human bile will be discussed.

---

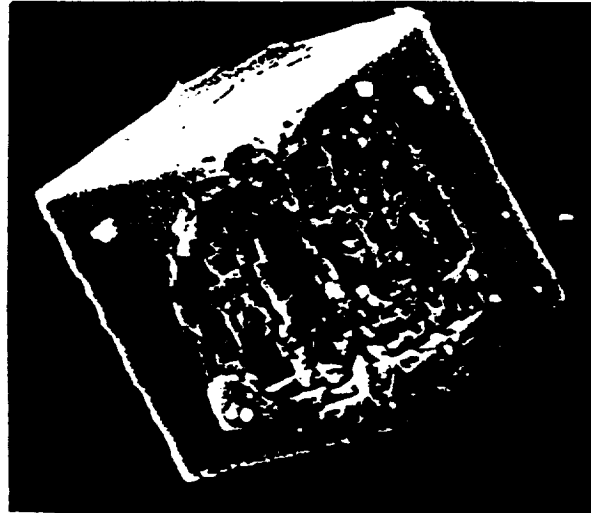
## GROWTH-RELATED MORPHOLOGY OF POROUS INORGANIC SALTS

*S. Halász, S. Farkas\* and K. Kincses*  
Research Institute for Technical Chemistry of the Hungarian  
Academy of Sciences, H-8201 Veszprém, P.O. Box 125, Hungary  
*\*Veszprém University, H-8200 Veszprém*

The morphological stability or instability of the growing crystal is related to the interface kinetics (Brice and Bruton, 1974). The degree of deformation depends on various process parameters i.e. supersaturation, solvents, impurities etc.

Chernov (1989) stated . . . "The shape of the growing crystal serves as the simplest indicator of the atomic growth mechanism" therefore we only have to make it "visible." By applying the gold evaporation technique in scanning electron microscopy, the good quality detailed micrographs well informed us about the steps and parameter dependent growth rates of the dendrite and inclusion formation as it will be demonstrated.

By controlling these processes regular patterns of macro defects were developed within inorganic salts thus producing valuable, high porosity specialty chemicals from the cheap raw materials.



*Porous NaCl crystal.*

## FACTORS AFFECTING THE MORPHOLOGY OF ISOCITRATE LYASE CRYSTALS

Robert C. DeMattei and Robert S. Feigelson

Center for Materials Research, Stanford University, Stanford, CA 94305-4045

Patricia Weber

Experimental Station, Du Pont Merck Pharmaceutical Company

Wilmington, DE 19880-0228

Isocitrate lyase (ICL) crystals for molecular structure studies have been grown by the hanging drop vapor equilibration method<sup>[1]</sup> both on earth (1-g) and in low gravity ( $\mu$ g) on space shuttle missions<sup>[2]</sup>, and by vapor equilibration in small capillaries. The drop sizes studied were 4 and 30 $\mu$ l in 1-g and 30 $\mu$ l in  $\mu$ g. The ICL crystals grown in 1-g all exhibited dendritic morphologies whether grown in 4 $\mu$ l or 30 $\mu$ l drops while those grown in  $\mu$ g had much improved morphology. The ICL crystals grown in the capillaries showed a highly regular crystal morphology consistent with an orthorhombic crystal bounded by low index planes.

Preliminary experiments indicated that the dendritic morphology did not arise due to sedimentation effects. The most likely cause of the dendritic growth was excessive supersaturation. Since supersaturation in these growth experiments was related to the rate of evaporation, the models developed by Sibille and co-workers<sup>[3,4]</sup> for hanging drop and capillary evaporation were applied to the ICL crystal growth system. The results of the calculations showed that a 30 $\mu$ l drop evaporates 5 times more slowly than a 4 $\mu$ l drop and that a crystallizing solution in a 1.88mm diameter capillary evaporates two orders of magnitude more slowly than the same volume in a drop. These calculations gave a reasonable explanation for the quality of the ICL crystals grown in the capillaries, but did not account for the improvement seen in the crystals grown in the hanging drops in  $\mu$ g.

Sibille<sup>[3]</sup> pointed out that hanging drops evaporated more slowly than anticipated in space due to the formation of a highly saturated layer at the solution-vapor interface in the absence of thermal-solutal convection. The decrease in evaporation rate of a factor of two was not enough to explain the change in ICL crystal morphology observed. Experiments with inverted capillaries which would tend to stabilize any dense layers formed at the liquid-vapor interface developed amorphous layers at the interface which could only be attributed to the precipitation of isocitrate lyase. In the  $\mu$ g experiments, similar removal of the ICL from solution due to precipitation acted to lower the supersaturation at which the crystals were growing and, thus, promoted more controlled growth and improved morphology.

---

1. A. McPherson, *Preparation and analysis of Protein Crystals*, John Wiley & Sons, NY 1982.
2. L.J. DeLucas, et al., *J. Crystal Growth*, 110 (1991) 302.
3. L. Sibille and J.K. Baird, *J. Crystal Growth* 110 (1991) 72.
4. L. Sibille, J.C. Clunie and J.K. Baird, *J. Crystal Growth* 110 (1991) 80.

This research was supported by NASA Grant NAG 8-774 and the NSF-MRL program.



## SESSION 7

### MASS PRODUCTION OF REFRACtORY OXIDE CRYSTALS:

#### CUBIC ZIRCONIA

*Joseph F. Wenckus*

Ceres Corporation, North Billerica, MA 01862

Large-scale production of refractory oxide crystals using skull-melting techniques has undergone dramatic development during the past decade. These developments have been promoted in large measure by the growing demand for Cubic Zirconia (CZ) crystals used to fashion the "fake" diamonds which have become popular in the gem/jewelry industry worldwide.

Since the introduction of CZ gems in 1977, the production of CZ crystals has increased steadily and present annual world output is estimated to be well in excess of 250 tons.

The discussion will include a brief history of the skull-melting process and focus upon current production technology.

### DEVELOPMENT OF SKULL MELTING AND CRYSTALLIZATION, PARTIALLY STABILIZED ZIRCONIA

*V. Osiko*

1. Concise history of direct RF melting in cold container.
2. Present state of skull melting.
3. Partially stabilized zirconia (PSZ), melting, crystallization, and solid phase transformation.
4. Phase composition and micro structure of PSZ.
5. Useful properties of PSZ:
  - high hardness and shock resistance;
  - high wear and tear resistance;

- high chemical and temperature stability;
- low friction coefficient.

6. Accomplished and possible applications:
  - medical instruments (scalpels, perforators and drills);
  - cutting and abrasive instruments for processing of some metallic and non-metallic materials;
  - draw plates, rollers, mills and mortars;
  - thread leading tools, bearings.



## SESSION 8

## NON-LINEAR EFFECTS IN IMPURITY INCORPORATION IN SEMICONDUCTOR MELT GROWTH

V.V. Voronkov

Institute of Rare Metals, Moscow, Russia

Impurity incorporation by some semiconductor crystals (Ge, GaAs) turns out strongly nonlinear at low concentration in the melt,  $N_m$ . On the contrary, the range of relatively high  $N_m$  corresponds to simple proportional dependence of captured concentration  $N$  on  $N_m$ . This phenomenon can be well explained by the correlated incorporation of impurity atoms and vacancies both at nonequilibrium concentration. Every moving step creates a fresh part of the surface atomic layer with some initial concentrations of impurity and vacancies. Then the created layer, being exposed to the melt, exchanges the intrinsic and impurity atoms with the melt, these atoms fill the surface vacancies and, reversely, produce new vacant sites by jumping into the melt. So the final (incorporated into the crystal) vacancy concentration  $C$  is dependent on the impurity concentration - if the intrinsic filling is hindered by high enough energy barrier. Likewise the captured impurity concentration  $N$  is dependent on  $C$ . The  $N(C)$  function is determined not only by impurity filling the surface vacancies but also by

diffusion exchange of impurity between the near interface crystal layers, as the diffusion rate is proportional to  $C$ . The calculated  $C(N_m)$  and  $N(N_m)$  functions are of peculiar nonlinear character that strongly depends on the growth rate and on the step distribution. The latter can be either regular (equidistant) or chaotic depending on the step source. The  $N(N_m)$  function becomes simple proportional at  $N >> C$  when the filled surface vacancies give small contribution to  $N$ .

For binary crystals (such as GaAs there exists a new type of nonlinear correlation between impurity and vacancies: the surface point defects of the first sublattice can catalytically influence the filling acts for the vacancies of the second sublattice. In that way the impurity - even it populates only one of the two sublattices - constitutes the correlated nonlinear system with both kinds of vacancies. This phenomenon can account for some complicated effects of isoelectronic impurities on the properties of binary semiconductors.



## SESSION 8A

### FORMATION OF PATTERNS DURING GROWTH OF SNOW CRYSTALS

*Etsuro Yokoyama*

Kyushu Institute of Technology, Iizuka 820 Japan

We discuss recent progress in the understanding of the formation of patterns of snow crystals. In particular, we focus on the morphological instability of snow crystals that occurs with an increase in the degree of supersaturation. At low supersaturation, a hexagonal prism of snow crystals can grow in a stable manner and retains its form. For higher supersaturations, however, it changes form by means of preferred growth of edges and corners, becoming a dendrite for temperature between -10°C and -22°C. To explain the transition from the hexagonal to the dendritic pattern, we present a numerical model<sup>[1]</sup> that takes into account the following elementary processes relevant to the growth: (1) a surface kinetic process for incorporating water molecules into a crystal lattice, and (2) a process for diffusing molecules through air toward the crystal surface. We demonstrate that the anisotropy of surface kinetics, for which

the kinetic coefficient has singularities in the form of deep cusps that depend on the supersaturation at the surface, plays a very important part in the formation of faceted shapes of snow crystals as hexagonal prism and facets seen at the tips of dendrite. Furthermore, we show that the critical conditions for the transition from hexagonal to dendritic pattern are given by the supersaturation and the dimensionless crystals size, relative to the mean free path of a water molecule in air, and finally discuss how the ratio of the step energy to the surface diffusion distance of an admolecule influences the patterns of snow crystals.

[1] E. Yokoyama and T. Kuroda, *Phy. Rev.* 41(1990)2038.

---

### CAPILLARY EFFECTS AT DYNAMIC CRYSTAL/MELT INTERFACES

*M.E. Glicksman*

Department of Materials Engineering

Rensselaer Polytechnic Institute, Troy, New York 12180-3590

*S.P. Marsh*

Code 6325, Naval Research Laboratory, Washington, D.C. 20375-3590

Of particular interest in the field of crystal growth is the effect of interfacial energy on the local thermodynamic properties (capillary effects). These effects play an important role in the microstructural development and evolution of solidifying materials. In this paper we present experimental results on the thermal evolution of solid-liquid mixtures of pure materials, and discuss some thermodynamic aspects of these nonequilibrium systems.

A novel experimental method has been developed to monitor, *in situ*, the progress of interface coarsening via the thermocapillary effects in pure materials. Solid-liquid mixtures of white phosphorus ( $\alpha$ -P<sub>4</sub>) and ethylene carbonate crystals were created by rapid isenthalpic solidification of the undercooled melts. These mixtures were held adiabatically, and a platinum resistance temperature detector with a resolution of 100  $\mu$ K was used to monitor the average temperature. The mean tem-

perature was observed to rise a few mK toward an asymptotic value, reflecting the decay of the mean capillary undercooling. Analysis of the data confirms the  $(\text{time})^{1/3}$  kinetics predicted by theory. However, the observed volume fraction dependence of the kinetic rate is qualitatively inconsistent with that obtained by a mere averaging of the local temperatures determined by the equilibrium Gibbs-Thomson relationship.

A possible source of this discrepancy is the presence of additional global energy constraints not accounted for by the mathematical variation used to derive the canonical (isothermal) Gibbs-Thomson relationship. To quantify the capillary effects, we consider the average properties of a unit volume of the solid-liquid mixture and its subsequent evolution during coarsening. The aim of this analysis is to predict the mean temperature,  $\langle T \rangle$  and volume fraction of solid,  $V_v$ , consistent with the amount of excess interfacial energy present.

PRECEDING PAGE BLANK NOT FILMED

## SURFACE TENSION ANISOTROPY AND CELL-LIKE STRUCTURE FORMATION IN FREE SOLIDIFICATION

V. Pines, M. Zlatkowski and A. Chait

NASA Lewis Research Center  
Cleveland, OH 44135, USA

This work addresses the role of a surface tension anisotropy during solidification of a pure materials from a supercooled melt. We study the formation of a predendritic cell-like structure using fully time-dependent nonlinear numerical solutions of the thermodiffusion model avoiding simplifications of mathematical nature. The introduction of surface tension anisotropy in the model results in changes in cell tip radii as well in some

variations in the morphology of the solid-liquid interface. Time-dependent phenomena leading to the establishment of near constancy of cell tip radii, the restoration of cell tip radii following induced tip perturbations, and the recently found solitary wave generation during solidification are found in cases both of zero and of nonzero surface tension anisotropy parameter values.

## THREE-DIMENSIONAL PATTERN FORMATIONS AT GROWTH OF ICE DENDRITES

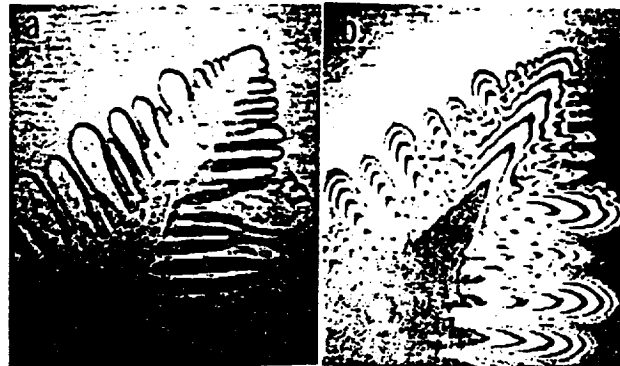
Yoshinori Furukawa and Wataru Shimada

Institute of Low Temperature Science  
Hokkaido University, Sapporo 060, Japan

It is well known that the morphology of ice crystal growing from the supercooled pure water changes sequentially with time from circular disk, to disk with perturbed periphery, and finally to developed dendrite with hexagonal symmetry<sup>1,2</sup>. Many researchers<sup>3</sup> have watched the ice crystal growth with keen interest as a typical case in the problems of pattern formations. However, though all of them considered that the ice crystals are grown in two dimensions, actual ice dendrites have three-dimensional structures.

In order to analyze the three-dimensional pattern formations of ice dendrites, in-situ observations were carried out for ice crystals growing in supercooled water, using a new optical system which was constructed by the alternation of Schlieren and Mach-Zehnder interferometer<sup>4</sup>. In addition to the sharp images of the outline of ice dendrites, the interference fringes (see the picture) corresponding to the ice crystal thickness were obtained. We were able to obtain the time-sequent growth patterns in three dimensions by analyzing the observational results.

Tip radii of ice dendrites,  $\rho_1$  and  $\rho_2$  which were in the basal plane and in the plane perpendicular to the basal plane, respectively, were independently determined from the three-dimensional analysis of morphology. Growth rates  $V$  at the tip of dendrite and the supercoolings  $DT$  were also measured. As a result, the formation mechanism of ice dendrite will be discussed on the basis of the previous theoretical considerations about the pattern formations.



An ice crystal observed by Schlieren System (a) and Mach-Zehnder interferometer (b).

1. K. Arakawa and K. Higuchi: *J. Fac. Sci., Hokkaido Univ., Ser. II*, 4(1952)201.
2. S.H. Tirmizi and W.N. Gill: *J. Crystal Growth*, 85(1987)488; 96(1989)277.
3. J.S. Langer, R.F. Sekerka and T. Fujioka: *J. Crystal Growth*, 44(1978)414.
4. Y. Furukawa and W. Shimada: Proc. Int. Sympo. Phy. Chem. Ice, Hokkaido Univ. Press (1992) in print.

**DENDRITIC GROWTH OF CYCLOHEXANE**  
*R.M. Geertman, E.P.G. van der Berg and P. Bernnema*  
 Laboratory of Solid State Chemistry University of Nijmegen  
 The Netherlands

The growth of cyclohexane from a pure melt and benzene-cyclohexane mixtures has been studied. The formation of dendrites has been focused on and compared with theoretical models, resulting in a reasonable agreement. The cyclohexane had a purity of 99.95%. The amount of benzene present - in the studied mixtures varied from 0.1 to 3%. The growth of cyclohexane crystals started with a seed of approximately 80  $\mu\text{m}$ . The undercoolings used ranged from 0.05 to 0.5 K. After the initial formation of pseudo faces, and in the case of pure cyclohexane, cellular fronts, dendrites developed. The tip curvature and the growth speed of the dendrites were determined and used to calculate the capillary length ( $d_o$ ) and the diffusion constant ( $D$ ).  $d_o$  had a constant value of 2.0 nm, while  $D$  varied from  $1.0 \times 10^{-6} \text{ m}^2/\text{s}$  in the case of pure cyclohexane to  $4.2 \times 10^{-8} \text{ m}^2/\text{s}$  for the melt containing three percent benzene. The standard deviation of these values is typically 90%. This

means that the Langer-Müller Krumbhaar theory describes this case quite well, even though it does not take the fact into account that heat flow and particle diffusion occur simultaneously. The values are compared with data from literature for  $d_o$  and  $D$ , both thermal and chemical. The value of  $d_o$  is fairly constant but an order of magnitude to small when compared with literature data. This could be attributed to the value used for  $\sigma$  which is 0.025 according to theory. Bilgram and Saito have already proven that this value can differ upon the compounds studied. The measured value of  $D$  for the pure cyclohexane and the mixture with 0.1% benzene differs also an order of magnitude with literature data. This could be explained in the same way. When more benzene is present  $D$  is getting smaller, which can be expected, seen the fact that  $D$ (thermal) is much larger than  $D$ (chemical).

**EFFECTS OF HIGH MAGNETIC FIELDS OF FRACTAL GROWTH  
 OF LEAD METAL-LEAVES**

*Iwao Mogi, Susumu Okubo and Yasuaki Nakagawa*  
 Institute for Materials Research, Tohoku University  
 Katahira, Sendai 980, Japan

Growth patterns of lead metal-leaves were investigated in high magnetic fields up to 8 T as an experimental approach to the anisotropic diffusion-limited aggregation (DLA) with lateral drifts of particles.

The lead metal-leaves were grown around a piece of zinc metal from a lead acetate aqueous solution between two glass plates by means of electrodeless reduction of lead ions. Magnetic fields were produced by a superconducting magnet with a large bore of 200 mm in the High Field Laboratory of Tohoku University, and were applied perpendicularly to the glass plates.

Growth patterns of the lead metal-leaves are shown in Fig. 1. In the absence of magnetic fields (a), dendritic pattern is observed, where sidebranches grow symmetrically on both sides of main branches. On the other hand, the growth pattern at 8 T (b) becomes denser, and the most sidebranches develop on one side of main branches. These drastic change in growth pattern was explained in terms of the magnetohydrodynamic effect on the diffusive motion of lead ions and the interface kinetic process.

Fractal dimension  $D_f$  of the metal-leaf was estimated by means of the box-counting method;  $D_f$  increases with increasing magnetic field from 1.59 at zero field to 1.66 at 8T.

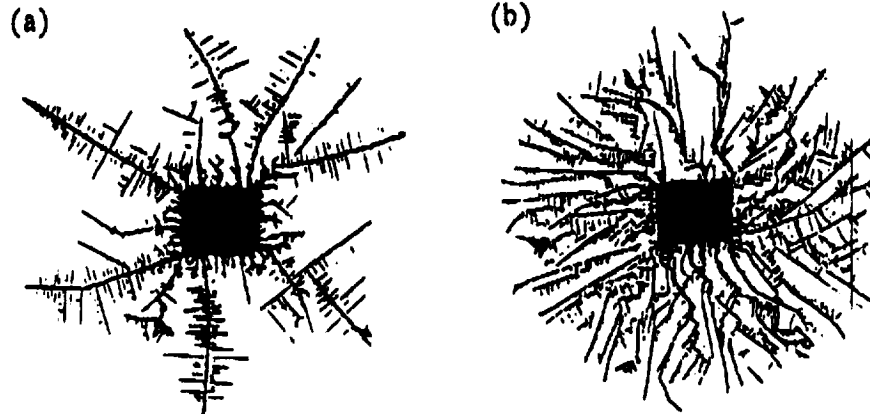


*Figure 1.*

## EXPERIMENTAL STUDIES ON THE PATTERN FORMATION IN AQUEOUS SOLUTION FILM SYSTEM

*Mu Wang and Nai-ben Ming*

National Laboratory of Solid State Microstructures,  
and Department of Physics, Nanjing University,  
Nanjing 210008, People's Republic of China

Growth of fractals, dendrites and faceted crystals are studied in a thin isothermal aqueous-solution film system of  $\text{Ba}(\text{NO}_3)_2$ , using *in-situ* observation method. Kinetic phase diagrams to show the dependence of pattern formation on the supersaturation, the solute concentration and the thickness of the aqueous solution film have been investigated. Micromorphology and the growing process of fractals, as well as the

process of the pattern evolution from faceted crystal to dendrite and then to fractals, have been studied. The experiments indicate that the high driving force and the self-sustained perturbation are necessary for the growth of the fractal pattern. Local growth conditions, including the thickness of the aqueous solution film near the growing interface, are responsible for the micromorphology of the fractals.

---

## THERMAL EVOLUTION OF EQUILIBRIUM CRYSTAL SHAPE OF $\alpha\text{-Ag}_3\text{S}$

*Tadashi Ohachi and Ichirou Taniguchi*

Department of Electrical Engineering  
Doshisha University, Kyoto 602, Japan

Equilibrium crystal shape (ECS) is related to the surface free energy density and thermal evolution of facet size of ECS is related to the roughening transition temperatures. The purposes of this report are to study about the ECS of the high temperature phase of silver sulfide, to improve the experimental equilibrium conditions, and to discuss the existence of different roughening transition temperatures depending on a given equilibrium condition.

Single crystals of  $\alpha\text{-Ag}_3\text{S}$  were grown by a solid vapor reaction developed for ionic-electronic mixed superionic conductors[1-3]. The improvement of uniformity of the temperature of the system is performed by a new growth system of two zones. A sphere of silver of about 1 mm diameter was reacted with sulfur vapor directly within a capsule and capillary tube of 0.3 mm  $\phi$ . The uniformity was kept by the small capsule and uniform winding of heater wire. Grown symmetrical crystal shape shows the confirmation of uniform temperature distribution. ECS of  $\alpha\text{-Ag}_3\text{S}$  is given by temperatures of an equilibrated crystal and sulfur liquid  $T_g$  and  $T_v$ . ECS is defined for each  $T_g$  and  $T_v$ . Both  $\{110\}$  and  $\{110\}$  facet were observed.

The area of facets was decreased at higher  $T_g$ . ECS is determined by the temperature and the vapor pressure at the surface. This means ECS is given by each equilibrium condition. Roughening transition temperature, therefore, is given for each facet of a crystal and given vapour pressure. The relationship between the facet area and crystal temperature at given vapor pressure is measured.

This experimental macroscopic technique is one of tools to know the surface information related atomic level surface reaction. Facet shape or crystal shape of a bcc  $\alpha\text{-Ag}_3\text{S}$  crystal was examined optically.

---

- [1] T. Ohachi and I. Taniguchi, *J. Crystal Growth*, 65(1983)84.
- [2] T. Ohachi and I. Taniguchi, Morphology and Growth Unit of Crystals (Tera Sci. Pub. Comp., 1988) Ed. I. Sunagawa p.185.
- [3] T. Ohachi, Proc. of 4th Topical Meeting on Crystal Growth Mechanism (Tokyo Univ., 1991) Ed. T. Nishinaga p.13.

## THE FINITENESS EFFECT ON CRYSTAL EQUILIBRIUM SHAPE

*D. Aquilano\*, R. Kern\*\* and M. Rubbo\**

\*Dipartimento di Scienze Mineralogiche e Petrologiche

Università di Torino-via V.Caluso 37-I-10125 Torino Italy

\*\*CRMC2-CNRS, Campus Luminy-F-13288 Marseille Cedex 9 France

The surface energy  $\phi$  of a finite crystal can be expressed, according to Stranski, by means of specific energies of surface ( $\sigma^*$ ), edge ( $\kappa^*$ ) and corner ( $\varepsilon^*$ ), corresponding to a subdivision of the infinite crystal space surrounding the finite shape.

We treated the equilibrium of an ideal orthorhombic crystal limited by three pinacoids and defined according to  $\phi = 2\sum \sigma_{ij} \cdot \frac{1}{h_i}$ , a new specific surface energy  $\sigma_{ij} = \sigma_{ij}^* \sigma_{ij}^*$ ,  $\kappa_j^*$ ,  $\kappa_j^*$ ,  $\varepsilon^*$ ,  $h_j$ ,  $h_j$ ,  $h_k$ , where the central distances  $h$  can vary independently each other and  $\sigma_{ij}$  are not constant with the face size.

The sole condition on the surface properties concerns the normal derivatives of  $\sigma^*$ ,  $\kappa^*$  and  $\varepsilon^*$ , which are considered negligible with respect to  $\sigma^*$ ,  $\kappa^*$ ,  $\varepsilon^*$ .

Under the condition:  $\Delta F = -8\lambda h_1 h_2 h_3 + \phi = \text{extremum}$ , it ensues that the ratios among the central distances of the faces belonging to the equilibrium shape are determined by a set of three equations:

$$h_i/h_j = \frac{\sigma_{jk}^* \left( 1 + \frac{\kappa_j^*}{\sigma_{jk}^* h_k} \right)}{\sigma_{ik}^* \left( 1 + \frac{\kappa_i^*}{\sigma_{ik}^* h_k} \right)} \quad (1)$$

Hence the equilibrium shape is no longer homotetic due to the finiteness of the crystal, and the Wulff theorem is recovered only when the infinity conditions are fulfilled ( $\varepsilon^*$ ,  $\kappa^*$ ,  $\ll \sigma^*$ ).

Moreover from (1) it follows that equilibrium shape is the only one for which the separation work of crystal from a semi-infinite column underlying a given face is equal for all faces.

Numerical examples are given ( $\text{CaSO}_4$  anhydrite,  $\text{CaCO}_3$  aragonite) within the Born-Stern approximation and without relaxation.



## SESSION 8B

### VAPOR GROWTH AND CHARACTERIZATION OF CdTe BULK SINGLE CRYSTALS

*H. Wiedemeier and G.H. Wu*

Department of Chemistry, Rensselaer Polytechnic Institute  
Troy, New York 12180-3590, USA

The intrinsic experimental conditions of the melt growth of CdTe contribute to its current problems in terms of contamination, thermal stress, dislocation density, and segregation. Vapor growth of this material (PVT) can reduce these problems, but is generally limited by much lower growth rates relative to those of melt growth. This investigation deals with an increase of the vapor growth rate of CdTe by about an order of magnitude relative to typical values reported in the literature, while maintaining low etch pit densities and formation of lamellar twins only. These results are based on high purity source material, and on suitable thermal gradient and growth temperature conditions.

For the bulk growth of CdTe, in-situ grown seed crystals were employed. Growth temperatures from about 830°C to 900°C and temperature gradients of about 5 to 40°C/cm were used. Under these conditions, previous CdTe growth rates of about 2-3 mm per day observed in this laboratory could be increased to about 25 mm per day. The predominant growth direction of the single crystalline boules was in or near the

<100> or <111> B directions. The boules of up to 10 g were grain-free and contained only a limited number of lamellar twins. Etch pit densities from less than  $10^4 \text{ cm}^{-2}$  to about  $10^5 \text{ cm}^{-2}$  were observed. SEM and X-ray diffraction techniques confirmed the high quality of these crystals. These results can be explained in terms of the thermal conductivity and interface stability of CdTe. In addition, the necessary surface migration required for single crystalline growth (for otherwise same conditions) is provided by the appropriate growth temperature. In the present work, we have been able to effectively eliminate lateral twinning and to observe lamellar twins only, even at the highest growth rates. The grouping of lamellar twins suggests that they may be caused by some periodic disturbances. Further investigations concerning the origin of the twinning phenomenon are in progress.

The combined results are comparable to those observed for the melt growth technique. This makes vapor growth of II-VI compounds particularly attractive for applications.

**CONDITION FOR GROWING SINGLE AND TWINNED CRYSTALS  
IN CdTe VAPOR PHASE EPITAXY**  
Masanobu Kasuga, Lin Li and Yasushi Yoshioka  
Department of Electronics, Yamanashi University, Kofu, 400 Japan

In the VPE growth of CdTe on CdTe, creation of twinned layer is strongly influenced by the substrate orientation and the supersaturation of the vapor, i.e. large offset angle from {111} plane and small source-to-substrate temperature difference has proved to favor formation of single crystal.

This paper clarifies theoretically the condition for the single and twinned crystal formation on the assumption that step flow growth mode is essential for single crystal growth and two dimensional nucleation independent of steps are responsible for the formation of twinned layers. We can define three growth modes where monomers, polymers and stable two-dimensional nuclei play the main role in the growth mecha-

nism as is calculated and is typically shown in Fig. 1 as a function of step distance  $\lambda$  and supersaturation ratio  $\alpha$ .

Although there are some unknown parameters to compare this theoretical estimation exactly to the observed data, it seems to be the formation of dimers and not the formation of 2-D stable nuclei that result in twinned layers since experimental boundary comes around the curve of criteria for monomer-dimer transition.

This criteria has also been estimated by a Monte Carlo solid on solid simulation and are plotted in the same figure. It guarantees indirectly the validity of the theoretical curve.

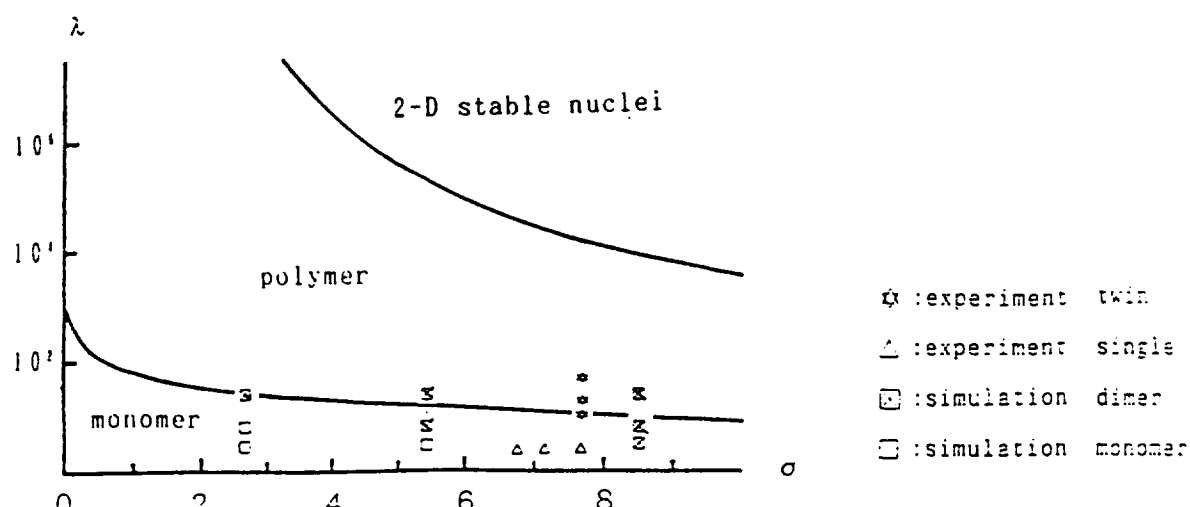


Figure 1. Three growth modes where monomers, polymers and 2-D nuclei dominates vs  $\lambda$  and  $\alpha$ .

## CHARACTERIZATION OF LARGE-DIAMETER SINGLE-CRYSTAL CdTe

GROWN BY THE VERTICAL BRIDGMAN METHOD

*Louis G. Casagrande, Don Di Marzio and David J. Larson, Jr.*

Grumman Corporate Research Center, Bethpage, NY 11714-3580

*Michael Dudley and Thomas Fanning*

Department of Materials Science and Engineering, SUNY, Stony Brook, NY 11794

We report on the growth of 64 mm diameter single-crystals of CdTe using a large-bore, high-thermal mass, multizone Vertical Bridgman furnace. Ampoules are carefully prepared so that the probability of melt adhesion or spurious nucleation is reduced. The longitudinal thermal gradient imposed on the solidifying boule is less than 10°C/cm and the hot and cold zone temperatures have been adjusted to levels designed to reduce the interface curvature and the thermal stress on the growing crystal and the solidified portion of the boule. A seed crystal is utilized in order to control growth orientation, and several ampoule geometries have been investigated. Post-solidification processing of the boule, including annealing and cooling rate, is designed to reduce the size and density of

precipitates as well as residual strain. Wafers taken from the crystals have been structurally and chemically characterized. The emphasis of our analysis has been on correlating the various characterization techniques in order to determine the relationships between specific features observed with different methods. We have been able to establish a correspondence among features identified on high quality surfaces of CdTe using Synchrotron White Beam Topography (SWBT), x-ray rocking curve maps, and Nakagawa-etch-pit micrographs. We propose that the use of SWBT together with x-ray rocking curve mapping provides important structural information and can be utilized as an alternative to destructive etch pit analysis for the characterization of the surface defect structure.

---

## LARGE (Cd,Zn)Te INGOTS GROWN BY THE HORIZONTAL BRIDGMAN TECHNIQUE

*Pok-Kai Liao, Men-Chee Chen and Carlos Castro*

Texas Instruments Incorporated, Central Research Laboratories

P.O. Box 655936, MS 154, Dallas, TX 95265

Because of its unique characteristics, the ternary compound (Cd,Zn)Te is the most suitable substrate material for the epitaxial growth of (Hg,Cd)Te and related infrared detector materials. However, historically, difficulties in growing large single crystals have limited substrate sizes and made this material less affordable. The horizontal Bridgman technique provides several advantages over other techniques for the growth of high quality (Cd,Zn)Te ingots having large single crystals portions. Up to 4 Kg (Cd,Zn)Te ingots are grown by the horizontal Bridgman technique at Texas Instruments and large single crystal, (111) oriented (Cd,Zn)Te substrates with areas up to 2 inches by 3 inches are routinely obtained from these ingots. Monthly production of over 3,000 cm<sup>2</sup> (111) oriented (Cd,Zn)Te substrates has been achieved with two horizontal Bridgman furnaces<sup>1</sup>.

In this paper, (Cd,Zn)Te crystal growth and substrate preparation will be discussed. Material properties such as dislocation etch pit densities, tellurium precipitate concentrations, Hall effect data, and FTIR transmissions will also be presented. In addition post growth annealing under Cd overpressure has been studied to improve the substrate properties. The defect chemistry of this ternary system has been experimentally investigated and correlated to the thermodynamic parameters such as annealing temperatures and Cd overpressures.

---

<sup>1</sup>P.-K. Liao, L. Colombo, C.A. Castro, B.E. Dean, C.J. Johnson, P.R. Boyd, W. Mozar and R. Comtols, 1991 Meeting of the IRIS Specialty Group on Infrared Materials, October, 1991, pp. 245-257.

## STATE AND DISTRIBUTION OF POINT DEFECTS IN DOPED AND UNDOPED BRIDGMAN - GROWTH CdTe SINGLE CRYSTALS

K.W. Benz<sup>1</sup>, D. Sinerius<sup>1</sup>, C. Eiche<sup>1</sup>, B.K. Meyer<sup>2</sup>, D.M. Hofmann<sup>2</sup>,  
C. Albers<sup>3</sup>, R. Boyn<sup>3</sup>, P. Rudolph<sup>3</sup> and H. Zimmermann<sup>3</sup>

<sup>1</sup>Crystallographic Institute, University of Freiburg, Hebelstr. 25, D-7800 Freiburg, F.R.G.

<sup>2</sup>Department of Physics E 16, Technical University of Munich, James - Franck - Str. 1, D-8046 Garching, F.R.G.

<sup>3</sup>Section Physics, Humboldt - University of Berlin, Invalidenstr.110, O-1040 Berlin, F.R.G.

The axial distribution of the free carrier concentration, the tellurium excess precipitation and inclusion density from IR extinction analysis the concentration of substitutionally incorporated shallow acceptors and donors (deduced from PL - measurements) and the total impurity concentrations (from mass spectroscopy) is investigated in undoped and doped (Ag, Cl) CdTe crystals grown without and with an overpressure of Cd.

A characteristical correlation exists between the crystal growth conditions, in particular the deviations of stoichiometry, the incorporation of impurities, the distribution of intrinsic point defects and the interaction between these intrinsic and extrinsic point defects. It can be shown that the kinetic distribu-

tion coefficient of dopants is controlled by the vacancy concentration at the melt - solid interface.

The resistivities of Cl - doped CdTe - crystals were investigated depending on the dopant - concentrations added. The analysis of deep centers (by photo induced current transient spectroscopy) showed, that the electrical properties are mainly governed by intrinsic defects. Vacancy - donor - complexes (A - centers) play an important role in the compensation behaviour of II - VI compounds. By optically detected magnetic resonance (ODMR) investigations in the luminescence band at 1.42 eV the structure of A - centers in Cl - doped CdTe has been determined.

---

## DEFECTS IN CdTe BRIDGMAN MONOCRYSTALS CAUSED BY NONSTOICHIOMETRIC GROWTH CONDITIONS

P. Rudolph, M. Neubert and M. Mühlberg

Humboldt University of Berlin, Department of Physics  
Institute for Crystallography and Materials Science  
Invalidenstraße 110, Berlin 0-1040, Germany

CdTe single crystals are important for technical applications as, for example, substrates in (Hg,Cd)Te epitaxy, IR-windows and prisms, electro-optical modulators and gamma-ray detectors. To achieve parameters as high resistivity and transmission exact stoichiometry control during growth is unavoidable. This may be done successfully by using an additional Cd source during growth [1].

In contrast, growth without Cd source tends to change to nonstoichiometry. CdTe melt evaporates incongruently, the free volume inside the ampoule fills with Cd-gas and, in consequence, the melt composition changes to tellurium excess. Correlations between free volume, melt volume and tellurium excess atoms in the melt/crystal will be discussed.

There may be observed two phenomena occurring during growth from slightly tellurium-rich melts: i) inclusions of tellurium rich melt, caused by morphological instabilities at the

growth interface (particles  $\geq 1 \mu\text{m}$  in diameter) and ii) precipitations originated during cooling of the crystal, caused by the retrograde slope of the solidus (particles 0.01 to  $0.1 \mu\text{m}$  in diameter). An axial distribution profile of the total amount of included/precipitated tellurium excess had been observed by IR-transmission microscopy (i) and extinction spectrometry (ii) respectively. The distribution of (ii) may be approximated by Pfann's segregation profile with a segregation coefficient of about 0.5 [2].

Summarizing this, growth from nonstoichiometric melts can provide useful hints about the shapes of solidus and liquidus near the congruent melting point.

[1] M. Mühlberg, P. Rudolph, A. Wenzel, *Crystal Properties and Preparation*, in press.

[2] U. Becker, P. Rudolph, R. Boyn, M. Wienecke, I. Utke, *phys. stat. sol. (a)* 120 (1990) 653.

PHOTOLUMINESCENCE AND SIMS MEASUREMENTS OF CdTd AND CdZnTe  
SAMPLES SUBJECTED TO THERMAL ANNEALING

*M. Azoulay, R. Tenne\* and H. Feldstein*

Soreq Nuclear Research Center, Yavne 70600, Israel

\*Weizman Institute of Science, Rehovot 76100, Israel

High quality CdZnTe single crystal was proved to be a good candidate as a lattice matched substrate for the growth of HgCdTe epitaxial layers<sup>(1)</sup>. The evaluation of both, the free carrier concentration and the conductivity type in the substrate is difficult due to the high resistivity of ultra high pure CdZnTe crystal ( $10^7 \Omega\text{cm}$ )<sup>(2)</sup>. PL analysis was found to be a sensitive tool for determining both the crystalline quality and the chemical purity<sup>(3,4)</sup>. It has been shown<sup>(5,6)</sup> that deviation from stoichiometry or post growth annealing of CdZnTe crystals can be clearly observed in the PL spectra.

In this paper, it is shown that the PL spectra of the near edge emission (up to 100 meV from the band edge) and SIMS measurements of impurities in CdZnTe substrates can be correlated. Sodium which was found to be present in the as grown crystal was reduced by an annealing process as determined by SIMS. This reduction of sodium is apparently accompanied by

reducing the PL relative intensity of the DAP recombination peak around 1.5618eV.

1. S.B. Qadri, E.F. Skelton, J.J. Kennedy. *App. Phys. Let.* 46, (1985) 257.
2. P. Cheuvart, U. El-Hanani and R. Triboulet. *J. Crystal Growth* 101 (1990) 270.
3. J.M. Figuera and O. Zelayer. *J. Appl. Phys.* 60(1), (1966) 452.
4. K.M. James, J.D. Flood and J.L. Merz. *J. Appl. Phys.* 59(10), (1986) 3596.
5. I. Gonzalez-Fernandez and W.V. Allred. *J. Val. Sci. Tec.* A8(4), (1990) 3255.
6. S. Seto, A. Tanaka and M. Kawashima. *J. Appl. Phys.*, 64(7), (1988) 3658.

---

MICROGRAVITY CRYSTAL GROWTH EXPERIMENTS OF CdTe ON  
THE SOVIET PHOTON 7 MISSION

*M. Salk, B. Lexow and K.W. Benz*

Kristallographisches Institut der Universität, Hebelstr. 35, D-7800 Freiburg, Germany

*D.C. Matioukhin*

Riga Scientific Research Institute for Radioisotope Apparatus, Riga, Latvia

*J.M. Gel'fgat and M.Z. Sorkin*

Institute of Physics, Latvian Academy of Sciences, Riga, Latvia

*A.S. Senchenkov, A.V. Egorov and I.V. Barmen*

SPLAV Technical Center, Glavcosmos USSR, 107497, Moscow, USSR

*P. Sickinger, P. Hofmann and R. Klett*

Kayser-Threde GmbH, Wolfratshauser Str. 48, D-8000 München 70, Germany

In October 1991 two CdTe crystal growth experiments took place during the unmanned Soviet PHOTON 7 mission. Both experiments were prepared and carried out in the short time of 18 months. This was possible due to the effective scientific cooperation between the Technical Center SPLAV, Kayser-Threde and the research institutes in Riga and Freiburg.

The Travelling Heater Method was chosen for the growth experiments. A tellurium solution zone, which was formed as a result of dissolving the compound CdTe in the Te-solvent, was positioned between a seed crystal and a solid feed rod. The solution zone moved along the ampoule axis at the constant velocity of 0.2 mm/h. Dissolution of the polycrystalline feed is caused by the undersaturation of the solution and the crystal growth is caused by supercooling of solution.

The following experiments were performed in the zone melting facility ZONA 4:

- CdTe crystal growth by the Travelling Heater Method under 1g- and  $\mu\text{g}$ -conditions,
- CdTe crystal growth within a rotating magnetic field by the Travelling Heater Method under 1g- and  $\mu\text{g}$ -conditions.

Results on the material transport in the liquid zone within and without the rotating magnetic field will be given in comparison to the 1g-reference experiments. All experiments are accompanied by theoretical modeling of temperature profiles, phase boundaries, flow patterns in the solution zone and growth kinetics.

CRYSTAL GROWTH OF SEMIMAGNETIC-SEMICONDUCTORS IN  
VERY HIGH MAGNETIC FIELDS

*Giyuu Kido, Nobuyasu Adachi and Masahiro Inoue*  
Institute for Materials Research, Tohoku University  
Katahira, Sendai 980, Japan

High magnetic fields up to 12 T were applied during the crystal growth process of semimagnetic semiconductors  $Cd_{1-x}Co_2Te$  and  $Cd_{1-x}Mn_2Te$  to homogenize the concentration of magnetic ion and to acquire a large single crystal grain.

A vertical Bridgman furnace with 25 mm clear bore was incorporated in a 15 T water-cooled-resistive magnet at the High Field Laboratory, Tohoku University. The length of the SiC heater part is 150 mm. A temperature as high as 1200°C could be obtained continuously at 12 T.

Crystals are grown as the following: A mixture of Cd, Te and Co (or Mn) granules was sealed in a graphitized quartz ampoule under  $10^{-6}$  Torr at 400°C. The ampoule placed in the upper part of the heater was heated up to 1170°C in 12 hours at the zero field, and then was lowered vertically in the rate of 2 cm/hour at 10 T for 10 hours. The control was made in the same condition except the magnetic field. We found that the grain size becomes significantly larger by the application of field. It is possibly due to the suppression of the convection of fluid mixture by the magnetic field.

---

SEEDLESS SEEDING AND ZERO TELLURIUM PRECIPITATES IN  
VERTICAL BRIDGMAN GROWN CdZnTe (3-5%)\*

*Arthur J. Socha, Sr. and Daniel W. Bakken*  
Johnson Matthey Electronics Inc., Spokane, Washington

Seedless methods for seeding CdZnTe (3-5%) utilizing Vertical Bridgman techniques are discussed. Ingots 55mm and 75mm in diameter were investigated with variations in crucible bottom design, growth procedures, and crucibles of quartz and PEN. Ingot rotation and its effect of grain development was also investigated. The growth and annealing (*in situ*) pro-

cedures to produce routine crystals with zero tellurium precipitates ( $<0.8 \mu$ ) and defects  $<5 \times 10^4$  are also discussed.

---

\*Supported in part by DARPA contract MDA972-91-C-0046.

## VACANCY DIFFUSION IN MERCURY CADMIUM TELLURIDE

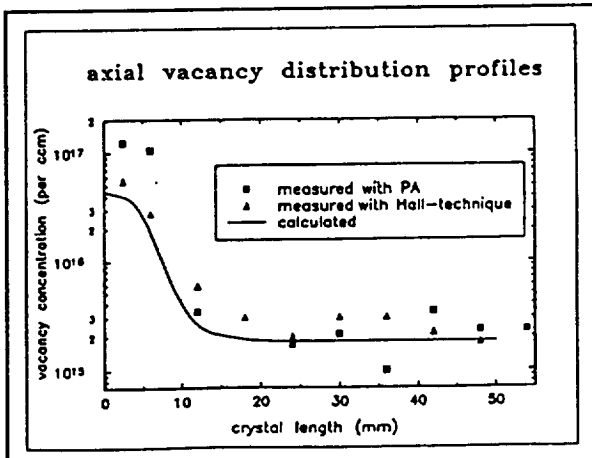
*M. Neubert, F.H. Kiessling and K. Jacobs*

Humboldt University of Berlin, Department of Physics  
Institute for Crystallography and Materials Science  
Invalidenstraße 110, 0-1040 Berlin, Germany

In THM-grown  $Hg_{0.8}Cd_{0.2}Te$  crystals a significant increase in Hall-measured p-type carrier concentration can be observed along their axis in the last solidified parts. This increase is assumed to be caused by mercury vacancies. Positron annihilation measurements (PA) exclusively detecting vacancies, lead to similar results and confirm the assumption made above.

These experimental results can be understood in the following way: During growth from a tellurium rich solution a certain number of mercury vacancies is built in corresponding to the tellurium saturated boundary of the existence region at growth temperature. Because of the retrograde solubility of native point defects and the lacking interaction of the inner parts of the crystal with the surrounding atmosphere, the built-in vacancies precipitate during cooling. This process goes more or less to completion depending on the individual thermal history of each part of the crystal. Almost complete precipitation results in a very low residual vacancy concentration. Incomplete precipitation leaves more vacancies. Obviously, the last solidified parts of the crystal had been cooled down faster and therefore possess higher residual vacancy concentrations.

Precipitation has been modelled as a diffusion limited process assuming precipitations as inner sinks in the crystal. The numerically calculated axial vacancy distribution profiles show a reasonable agreement to experimental results (Fig.). The process can only be understood assuming a diffusion co-efficient depending on actual vacancy concentration.



## TEM INVESTIGATION OF PRECIPITATES IN $HG_{0.8}CD_{0.2}TE$ GROWN BY THM

*F.-M. Kiessling*

Humboldt University of Berlin, Department of Physics  
Invalidenstr. 110, 0-1040 Berlin, Germany

*H.S. Leipner*

Martin Luther University of Halle/Wittenberg  
Department of Physics, Friedemann-Bach Platz 6, 0-4010 Halle, Germany

The ternary intermetallic compound  $(Hg,Cd)Te$  (MCT) is of particular importance to infrared technology. Growing crystals at the Hg deficiency side of the phase diagram the strongly retrograde solid solubility of native point defects causes inevitably in a significant second phase precipitation. Such precipitation has been investigated in material mostly prepared by solid-state recrystallization, but there is a considerable lack of information on precipitates in crystals grown by the travelling heater method (THM). The differences between both crystal growth methods being most important for the precipitation process are growth temperature and time-dependent cooling down procedure.

Transmission electron microscopy (TEM) investigations were carried out on samples received from as-grown MCT crystals as well as on samples post-growth annealed under

mercury saturated conditions to search for precipitates. Unexpectedly, a very high precipitation density of about  $10^{15} \text{ cm}^{-3}$  was found in as-grown samples. These defects were identified as loops with a diameter up to 25 nm consisting of aggregated Hg vacancies. This type of precipitation process has not been described for other bulk growth methods of MCT material before.

The peculiarities of the THM growth were correlated to the precipitation process. Simple calculations were made to compare the concentration of vacancies precipitated with the tellurium excess in the solid at the very beginning of the solidification process. Results of Hall-effect measurements and positron annihilation techniques were taken into consideration to understand the diffusion processes of mercury vacancies.



## SESSION 8C

### FUNDAMENTAL PROBLEMS OF CVD DIAMOND

B.V. Spitsyn

Institute of Physical Chemistry, Russian Academy of Sciences  
Moscow, Russia

A violent evaluation of research and development on chemical crystallization of diamond from activated vapor phase started ten years ago [1,2] make very challengeable to found common approaches in theoretical and experimental CVD diamond investigations.

According to author's opinion, despite of wide spectrum of elaborated methods of diamond growth from vapor phase, (activated by heat, electrical and electromagnetic fields, by chemical reactions etc.) it is reasonable to concentrate the discussion about basic regularities, connected with most important parameters.

We discuss from theoretical and experimental points of view linear growth rate and quality of grown diamond on:

- temperature of crystallization,

- carbon-contained component concentration,
- total pressure in vapor phase,
- middle range between region vapor activation and surface of crystallization,
- level of activation of vapor phase.

On base of our and another works we will discuss doping of diamond in the course of its growth and kinetics of early stages of diamond growth on non-diamond surfaces.

1. B.V. Spitsyn, L.L. Boulov and B.V. Derjaguin. *J. Crystal Growth*, 1981, vol. 52, p. 219.
2. S. Matsumoto, Y. Sato, M. Tsutsumi and N. Setaka. *J. Mater. Sci.*, 1982, vol. 17, p. 3106.

---

### GROWTH OF DIAMOND BY SEQUENTIAL DEPOSITION AND ETCHING PROCESS USING HOT FILAMENT CVD

J. Wei and Y. Tzeng

Department of Electrical Engineering, Auburn University  
Auburn, Alabama 36049

High quality and higher growth rate diamond films have been grown by sequential deposition and etching process using hot filament CVD system. Since oxygen is very effective in etching the non-diamond components, a computer can be used to control the cycle between oxygen-rich gas mixture and deposition reaction gas mixture in order to achieve higher growth rate diamond deposition without sacrificing diamond quality. During the deposition part of the cycle, higher carbon (C) concentration in reaction gas mixture than that used to deposit high quality diamond was used to deposition. During the etching part of the cycle, oxygen-rich gas mixture was used

to etch the non-diamond components that was deposited simultaneously with diamond components when using a high C concentration gas mixture. Results according to SEN and Raman spectroscopy show that by decreasing the cycling time, better crystallites of diamond film is obtained. Using a cycling time of less than one minute, high quality and higher growth rate film is obtained. We speculate that short cycling time is advantageous to grow high quality and high growth rate diamond film by hot filament CVD. The sequential deposition and etching process also leads to the understanding of nucleation and growth of CVD diamond.

## SELECTIVE AREA GROWTH OF DIAMOND FILM USING ION PLANTATION

*Ken Kobayashi, Shiro Karasawa, Takeshi Watanabe and Fumitaka Togashi\**

Industrial Research Institute of Kanagawa Prefecture

3173 Showa-machi, Kanazawa-ku, Yokohama 236, Japan

\*Science University of Tokyo

1-3 Kagurazaka, Shinjuku-ku, Tokyo 162, Japan

Many studies have been reported on the synthesis of diamond films, but the reports on the selective area growth have been very few. If one could grow diamond film at any area, many applications of diamond film would increase.

We investigated the influence of ion implantation on the nucleation density of diamond.  $\text{Ar}^+$  ions were implanted after scratch of Si surface. The experimental process is as follows:

- (1) Surface scratch of Si substrate for 5min.
- (2) Ion implantation at accelerating energy of 100KeV.
- (3) Synthesizing diamond film by electron-assisted CVD method for 2h.

We used a metal mask easily made, but a photo-lithography or an EB-lithography could be usable. Dose amount was varied from  $1\text{E}14$  ions/ $\text{cm}^2$  to  $1\text{E}16$  ions/ $\text{cm}^2$ .

The nucleation density decreased according as dose amount increased. Fig. 1 shows images of optical microscopy. The upper part was the area  $\text{Ar}^+$  ions were implanted. There seems to be three levels of the nucleation density decreased by ion implantation. 1st level was that incomplete film grew. 2nd was that there were many particles. 3rd was that there were very few particles. 1st level occurred when dose amount was under  $5\text{E}14$ . 2nd, 3rd level occurred  $1\text{E}15$  and over  $5\text{E}15$ , respectively.

To investigate the reason why ion implantation obstructs the growth of diamond, we used an atomic force microscopy. Surface morphology differed in accordance with the three levels.

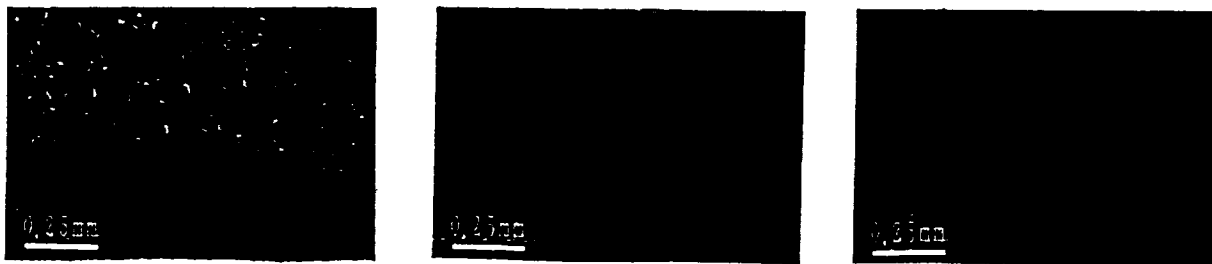


Figure 1. Images of selective area growth.

**LOW PRESSURE DEPOSITION OF DIAMOND FILMS  
THE INFLUENCE OF GROWTH PARAMETERS ON THE FORMATION  
OF A TEXTURED SURFACE MORPHOLOGY**  
*H. Walcher, Ch. Wild, W. Müller-Sebert, N. Herres,  
T. Eckermann and P. Koidl*  
Fraunhofer-Institut für Angewandte Festkörperphysik  
Tullastr. 72, D-7800 Freiburg, Germany

Low pressure deposition of diamond is recently finding increasing interest. Several 100  $\mu\text{m}$  thick layers or free-standing films are of special importance for mechanical, thermal or optical applications.

It is known, that the morphology and crystalline structure of polycrystalline diamond films generally are thickness-dependent<sup>[1]</sup>. Fibre textures with preferred growth along the  $\langle 110 \rangle$  or  $\langle 100 \rangle$  directions are frequently observed<sup>[2]</sup>. The latter (100)-textured growth is of special importance, since it may lead to a flat surface formed by (100)-facet<sup>[2]</sup>.

We report on the microwave plasma deposition of (100)-textured diamond films. The texture development has been

analyzed as a function of nucleation density and the deposition conditions, such as process gas composition and deposition temperature. Texture formation has been characterized by X-ray diffraction and the evaluation of the surface topography. It is shown that under optimum conditions highly oriented films with (100)-faceted surface can be grown with an angular variation of the  $\langle 100 \rangle$  crystallite direction of the order of  $\pm 1$  degree.

---

[1] C. Wild, N. Herres, P. Koidl; *J. Appl. Phys.* 68, (1990) 973.  
[2] C. Wild, P. Koidl, N. Herres, W. Müller-Sebert, T. Eckermann; *Electrochem. Soc. Proc.* 91-8 (1991) 224.

---

**CHARACTERIZATION OF THIN FILM DIAMOND GROWTH BY SCATTERING  
OF LIGHT AND SURFACE REFLECTANCE SPECTROSCOPY**

*A.M. Bonnot, T. Lopez-Rios, B. Mathis, L. Magaud and F. Cyrot-Lackmann*  
Laboratoire d'Etudes des Propriétés Electroniques des Solides,  
CNRS, BP 166, 38042 Grenoble Cedex 9, France

The growth of diamond on silicon making use of a hot filament and methane-hydrogen (0.1% - 2%) was monitored by reflectivity and elastic scattering of 1.96 eV radiation. A systematic study of the influence of the experimental parameters governing the diamond growth has been undertaken and correlated to the in-situ optical measurements. Noticeable changes on the reflectivity due to the growth of an intermediate layer prior to the diamond growth will be discussed. The formation of the transition layer produces little changes on the scattered light. On the contrary, the beginning of the diamond growth

gives rise to a strong increase of the scattered light intensity which varies as the square of the deposition time allowing to determine the diamond growth rate. Afterwards, Mie scattering takes place giving rise to oscillations allowing through modelling the determination of the dimension of the diamond crystals. Deterioration of the diamond quality, related to the presence of amorphous carbon phases, manifests itself by damping of the Mie oscillations. Complementary scanning electron microscopy and Raman scattering measurements will be discussed.

## CRYSTAL GROWTH IN THE MINERAL KINGDOM

*Ichiro Sunagawa*

Yamanashi Institute of Gemmology and Jewelry Arts

Tokoji-machi 1955-1, Kofu, 400 Japan

It has been the main interests of modern science and technology of crystal growth to understand the growth mechanisms at atomic level and to synthesize single crystals or thin films with desired property, perfection and homogeneity. To achieve this, efforts have been made to realize precisely controlled growth conditions, mainly near equilibrium. Conditions under which mineral crystals nucleate, grow or dissolve are just opposite to this. They are not controlled at all; they range from very close to equilibrium to far apart from that; may fluctuate greatly; the chemical systems are extremely multi-components, with full of impurity elements; the process is impossible to be observed directly. However, we must remember that the science of crystal growth was born from pure curiosity on morphology of mineral crystals. It started from the work of N. Steno, who put forward in 1669 a concept of growth rate anisotropy to account for the origin of a variety of external forms exhibited by natural quartz crystals. Investigations of mineral growth give us not only a pleasure to decode a detective story of the Earth's history, but also provide useful information for modern science and technology of crystal growth, since the Earth acted as a ceaseless crucible to grow crystals

under extremely wide range of conditions. At the same time, the knowledge achieved by the modern science of crystal growth plays an important new role in understanding our Earth, where equilibrium thermodynamic analysis had been the main and unique methodology in the past.

The key codes to decipher the detective story are properties of mineral crystals which deviate from the ideal state such as growth morphology of crystals surface microtopography of crystal faces, internal textures, such as growth sectors growth banding and distribution of lattice defects and impurities, textures of crystal aggregates, etc. Although principal methodology is deductive, it has been possible to decode growth and post-growth histories of mineral crystals based on the results of their characterization. Diamond is a successful example of investigations of this type. In addition to these, various experimental investigations have recently been made to reproduce textures of terrestrial and extra-terrestrial materials and to *in-situ* observe magmatic crystallization, which enriched our understanding on the formation of the Earth and Planetary materials.

---

## THE SEPARATION OF NATURAL FROM SYNTHETIC GEM-QUALITY DIAMONDS ON THE BASIS OF CRYSTAL GROWTH CRITERIA

*Emmanuel Fritsch and James E. Shigley*

GIA Research, Gemological Institute of America  
1660 Stewart Street, Santa Monica, CA 90404-4088

One of the most important challenges faced by the gemologist is the separation of natural from synthetic gem materials. When properly identified, synthetic gem materials are worth only a small fraction of their natural counterparts. This is a particularly sensitive issue for near-colorless diamonds, since they represent such a large segment of the jewelry sold today. Using magnification, luminescence, and spectroscopy techniques, a number of characteristic properties of synthetic diamonds have been found which help confirm their identity.

During their growth, synthetic diamonds trap small amounts of the metal flux (generally iron-nickel) they crystallize in. These geometric shaped, metallic inclusions are a tell-tale sign of synthetic origin. Synthetic diamonds are inert to longwave, but fluoresce moderately to shortwave ultraviolet light, a behavior very unusual in natural gem diamonds.

Most useful, however, are identification criteria based on the morphology of the crystals. Synthetic diamonds show cubic growth sectors, which are always absent from natural diamond crystals. When the diamond is faceted, these cubic growth sectors can be recognized through "graining," color zoning, or irregular distribution of the photo or cathodo-luminescence.

Infrared and ultraviolet-visible absorption spectroscopies can be useful in detecting the nature of the impurities present in a particular diamond, for example if nitrogen aggregates, typical of natural diamonds, are present.

Gem quality synthetic diamonds are increasingly clean, and the latest commercial production ( $^{12}\text{C}$  diamonds from General Electric) contains no nitrogen, which is at the origin of many of the gemological criteria used to separate natural from synthetic diamonds. Luminescence remains a very useful criterion. We are cautiously optimistic that we will be able to separate natural from synthetic near-colorless diamonds in the future. Further work would be needed if there was a large production of commercially available crystals of gem-quality, near-colorless synthetic diamonds.

The new low-pressure synthesis of diamond has already produced materials of potential gemological interest, such as faceted, near-colorless, natural diamonds covered with a thin film of blue synthetic diamond. This film can be recognized by the irregularities it creates at facet junctions.

## WHO FIRST GREW DIAMOND: "THE DOG THAT DID NOTHING"

*Kurt Nassau*

Nassau Consultants, Lebanon, NJ 08833

*'Is there any other point to which you would wish to  
draw my attention?'*

*'To the curious incident of the dog in the night-time.'*

*'The dog did nothing in the night-time.'*

*'That was the curious incident,' remarked Sherlock Holmes.  
Silver Blaze; Sir Arthur Conan Doyle*

The synthesis of diamond was first achieved by H. Tracy Hall at General Electric on December 16, 1954. Only after the GE announcement (F.P. Bundy et al., *Nature* 176, 51, 1950) did the Swedish Company ASEA (Allen Anna Svenska Elektriska Aktie-bolaget) announce that H. Liander and E. Lundblad had in 1953 used a cubic press to contain a thermite reaction which

produced some very small diamond particles (H. Liander, *ASEA Journal* 28, 97, 1955). Details were not published until 1960 (H. Liander and E. Lundblad, *Arkiv for Kemi*, 16, 139, 1960), long after GE had published full details.

This naturally raises the question of the title quotation. Possible reasons are discussed for this lack of public announcements on the part of ASEA in 1953, which would undoubtedly have brought them much acclaim, as well as their seven year delay to release details. Also discussed are the conventional criteria for claims of priority of invention. Since these were not met, scientists in general recognize the priority of the GE diamond synthesis work.



## SESSION 8D

### EFFECT OF IMPURITIES ON CRYSTAL GROWTH

K. Sangwal

Department of Physics, Technical University of Lublin  
ul. Nadbystrzycka 38a, 20-618 Lublin, Poland

The influence of impurities inherently present in growth media and deliberately added to them on crystal growth is manifested during the process of crystallization in a number of ways [1-3]. An impurity may lead to changes in three-dimensional nucleation rate as well as growth rates of different faces of the growing crystal. In the latter case, since the magnitude of the change in growth rates of different faces is usually anisotropic, the growth habit of a crystal is modified by impurities. Apart from causing changes in nucleation and growth rates, impurities may also be trapped at the growing interface. The trapping or segregation of an impurity may be random and homogeneous in the crystal bulk or may be preferential along certain planes as impurity striations. Homogeneous trapping of impurities takes place when growth proceeds under well stabilized conditions. However, even under well stabilized conditions, the presence of large clusters of impurities and

inhomogeneities often produce voids and other defects (e.g. stacking faults). Impurity striations are produced in poorly stabilized conditions.

The presentation will describe the following topics: effect of impurities on growth kinetics (layer and face displacement rates), growth habit and growth morphodroms, effect of inhomogeneities on the growth of epitaxial layers, and formation of impurity striations.

1. H.E. Buckley, *Crystal Growth* (Wiley, New York, 1951).
2. A.A. Chernov et al. *Modern Crystallography III: Crystal Growth* (Springer, Berlin 1984).
3. K. Sangwal and R. Rodriguez-Clemente, *Surface Morphology of Crystalline Solids* (Trans Tech, Zurich 1991).

---

### MOLECULAR DYNAMICS SIMULATIONS OF INTERFACES BETWEEN CRYSTALLINE UREA AND AQUEOUS UREA SOLUTIONS

E.S. Boek, W.J. Briels, J.van Eerden and D. Feil

Chemical Physics Laboratory, University of Twente  
PO Box 217, 7500 AE Enschede, The Netherlands

In crystal growth from solution the structure and dynamics of the solvent close to the crystal surface play a fundamental role. The morphology of crystals from solution may deviate dramatically from vapour-grown crystals: it has been shown that preferential adsorption of solvent molecules on specific faces may lead to retardation of the growth of these faces<sup>1</sup>. In this study the structural and dynamical behaviour of water molecules near several urea crystal surfaces is investigated by means of M.D. simulations.<sup>2</sup> There were several reasons for choosing this system:

- 1) From aqueous solution urea crystallizes as long needles with large (110) and small (001) faces. Vapour-grown crystals show the same faces but are more equidimensional, which is in good agreement with theoretical habits derived from PBC and Ising theory, using *ab initio* charge models.<sup>3</sup> We want to investigate whether water adsorption is strongest on (110), causing retardation of the growth of this face.
- 2) A famous crystallographic problem is why only one of the faces (111) and (111) appears on urea crystals and the other one is never observed. PBC theory does not discriminate between these two faces since their slice energies are the same. Specific adsorption of water molecules may be an explanation.

The M.D. runs have been analysed in terms of density profiles, positional and orientational distribution functions and diffusion coefficients. It appears that the water structure at the interface is strongly determined by the crystal surface structure: the (001) and (111) interfaces show high density peaks revealing strong adsorption while the (110) and (111) interfaces do so to a lesser extent. Therefore the appearance of only (111) on the growth form is predicted. In the same way we might expect that the growth of (110) is enhanced relative to that of (001). On the solution growth form however (110) is dominant. We argue that this cannot be explained using a simple layer growth model. Furthermore M.D. simulations of aqueous urea solutions of various concentrations near urea surfaces have been performed to investigate whether the water structure close to the interface is influenced by the presence of urea in solution. Finally some results on free energy calculations of the desorption of solid urea molecules from the surface into the solution will be presented.

<sup>1</sup>Z. Berkovich-Yellin, *J. Am. Chem. Soc.* **107**, 8239 (1985).

<sup>2</sup>E.S. Boek, W.J. Briels, J.van Eerden and D. Feil, *J. Chem. Phys.*, submitted for publication.

<sup>3</sup>E.S. Boek, D. Feil, W.J. Briels and P. Bennema, *J. Crystal Growth* **114**, 389 (1991).

## BUNDLING CRYSTALLIZATION OF ASPARTAME FROM STAGNANT AQUEOUS SOLUTIONS

Noriaki Kubota and Tetsushi Mori

Department of Applied Chemistry, Iwate University  
4-3-5 Ueda, Morioka, 020 Japan

Sou Abe, Shin'ichi Kishimoto and Satoshi Kumon  
Process Development Laboratories, Ajinomoto Co. Ltd.  
1-1 Suzuki-cho, Kawasaki-ku, Kawasaki, 210 Japan

An artificial sweetener aspartame [L- $\alpha$ -aspartyl-L-phenylalanine-methyl ester] crystallizes from a non-stirred aqueous solution as bundles of thin needle crystals. The larger bundles, both in length and diameter, are obtained from a highly-concentrated solution when it is cooled at higher cooling rates without stirring [1]. Such crystallization behavior looks rather strange, since rapid cooling of the highly-concentrated solution generally produces many small crystals even without stirring. The nucleation and growth rates were deduced from previously reported data of the waiting time for the primary nucleation in stagnant solutions of aspartame sealed into glass ampoules [2]. These rates are shown as a function of supercooling respectively. Crystallization behavior in a stagnant solution was observed in a small cell under optical microscope at different cooling rates for different concentrations of aspartame aqueous solution. Photographs of the crystals were taken. Crystalliza-

tion in test tubes were also observed by naked eyes under non-stirring condition. During cooling, crystals appeared one after another from place to place in the cell or in the test tube, but the convection flow, which was expected to be induced by heat of crystallization, was not observed in the crystallizing solution. The secondary nucleation, which could be induced by the convection flow, did not occur. A mechanism is proposed for explaining the strange crystallization behavior that the larger bundles are obtained from a highly-concentrated solution at higher cooling rate without stirring.

[1] Kishimoto, S. and M. Naruse, *J. Chem. Tech. Biotechnol.*, 43 (1988) 71.

[2] Kubota, N. et al., *J. Crystal Growth*, 100 (1990) 491.

## GROWTH KINETICS OF SODIUM CHLORATE CRYSTALS GROWN FROM PURE AND SODIUM DITHIONATE DOPED SOLUTION

R.J. Ristic\*, B. Shekunov and J.N. Sherwood

Department of Pure and Applied Chemistry, University of Strathclyde  
295 Cathedral Street, GLASGOW G1 1XL, UK

By the interferometric method *in situ* and X-ray topography, the growth of the {100}, {110} and {111} faces of  $\text{NaClO}_3$  crystals from pure and doped solution have been studied. It was shown that these faces grow in both cases by a dislocation mechanism.

Significant variations have been found in the slopes of dislocation hillocks on the {110} and {111} faces. An ex-situ X-ray topographic investigation reveals helicoidal dislocations in both {110} and {111} growth sectors. The crowding of these dislocations into bunches generating a growth source is the main reason for oscillations of the steepness and its growth rate of crystals grown either from pure or doped solution.

The addition of a certain amount of sodium dithionite as an impurity produces a characteristic morphological change leading to tetrahedral form. The habit faces of a such tetrahedron are rounded {111} faces which are not morphologically stable in the pure solution. The growth mechanism and stability of these faces in the presence of different levels of sodium dithionite as an impurity has also been considered.

\*Permanent address: Institute of Physics, P.O. Box 57, 11000 Belgrade, Yugoslavia.

## STUDIES OF THE NATURE OF DIFFUSION LAYER NEAR KDP CRYSTAL GROWING IN SOLUTION

Mariusz J. Krasinski

Institute of Physics, Technical University  
Wolczanska 219, 93 005 Lodz, Poland

The properties of crystal-solution interface and properties of transition layer in solution very near crystal face are of special interest for proper understanding of crystal growth process. Because systematic investigations of diffusion layer are still rare it is reasonable to make new systematic experiments.

Here we present results of investigations of nature of interfacial layer near growing KDP crystal in solution. Small ( $10 \times 5 \times 1 \dots 5 \text{ mm}^3$ ) KDP crystals were grown (dissolved) in thin ( $1 \dots 5 \text{ mm}$ ) cell assuring near two dimensional conditions. Experiments were conducted at constant temperature for various super(under)saturations in static conditions. The distribution of concentration near crystal face was detected with the use of Mach-Zehnder interferometer and moire fringes method for better detection of concentration gradients.

Thanks to interferometric method it was possible to detect real supersaturation  $\sigma_{\text{real}} = (c_{\text{interface}} - c_{\text{equilibrium}})/c_{\text{bulk}}$  existing on the crystal face. This supersaturation is more suitable for description of crystallization process than bulk supersaturation  $\sigma_{\text{bulk}}$  and it is also possible to calculate supersaturation index  $I_s = \sigma_{\text{real}}/\sigma_{\text{bulk}}$  what enables us to determine relation between surface kinetics and mass transport in solution.

The results of investigation can be summarized as below:

- diffusion layer thickness varies from 100 to 400  $\mu\text{m}$  and slightly increases on supersaturation only for small super(under)saturations
- the supersaturation index  $I_s$  for growth decreases from 0.8 for small supersaturations (surface kinetics regime) to 0.45 for  $\sigma_{\text{bulk}}=16\%$  (mixed regime)
- dissolution process is not fully diffusion controlled
- the growth rate  $R$  dependence on concentration gradient  $(dc/dx)_{\text{int}}$  near crystal face is linear but for big gradients (connected with big supersaturations) nonlinearity can be detected. The calculated on this basis diffusion coefficient in the diffusion layer is approx 50% higher than for pure solution and slightly decreases for big supersaturations
- even for thin cells convection remains significant way of mass transport
- surface kinetic coefficient  $\beta$  (0.00088 m/s) was calculated from experimental data.

In the paper the analysis of results with the use of hydrodynamics properties of the cell is presented. It can be shown that results can be quite well explained with the use of diffusion-convection concept.

---

## THE INFLUENCE OF CRYSTAL PERFECTION ON THE GROWTH KINETICS OF POTASH ALUM SINGLE CRYSTALS

### 1. Dislocation characterisation in crystals grown by seeded solution growth under conditions of low supersaturation

H.L. Bhat<sup>(1)</sup>, R.J. Ristic<sup>(2)</sup>, J.N. Sherwood and T. Shripathi<sup>(3)</sup>

Department of Pure and Applied Chemistry, University of Strathclyde  
Glasgow G1 1XL, Scotland

An experimental analysis has been carried out of the genesis and character of growth dislocations present in all growth sectors of single crystals of potash alum. The crystals, grown from seeded solutions by the temperature lowering method under conditions of low supersaturation, presented the well developed forms: {111} dominant, {100} and {100}. Growth dislocations formed predominately during refacetting of the edges and corners of the seed, rounded during preparation and insertion into the supersaturated solution. From here they become refracted into the {111} sectors which proved to be the most defective. Smaller numbers of dislocations form at the {111}, {100} and {110} seed interfaces and propagate in these sectors. In crystals of inferior quality a number of inclusions were found predominantly in the fast growing {100} sectors

which become the source of additional dislocations. Dislocations present in the original seed did not propagate across the interface into the developing crystal. Dislocations of all characters were observed. The principal Burgers vectors were found to be  $\langle 100 \rangle$ ,  $\langle 110 \rangle$  and  $\langle 111 \rangle$ .

---

#### Permanent Addresses:

<sup>1</sup>Department of Physics, Indian Institute of Science, Bangalore-560012, India

<sup>2</sup>Institute of Physics, P.Box 57 11000 Belgrade, Yugoslavia.

<sup>3</sup>Inter University Consortium, University Campus, Indore (MP) 452001, India.

## THE STUDY OF THE GROWTH MECHANISM OF POTASH ALUM CRYSTALS

*R.J. Ristic\*, B. Shekunov and J.N. Sherwood*  
Department of Pure and Applied Chemistry  
University of Strathclyde, 295 Cathedral Street  
Glasgow G1 1XL UK

Previous studies of the growth kinetics of potash alum crystals have indicated a significant variation of growth rate and highlighted the role played by dislocations.

In the current work, by using Michelson interferometry combined with X-ray topography, a more detailed examination of the growth kinetics of the {100}, {110} and {111} faces of potash alum is made. It was shown that these faces grow by dislocation mechanism.

The dislocation hillocks can spontaneously change their slopes and have a short lifetime. This phenomenon was typical for those hillocks observed on the {110} faces. As a consequence, the source activity and values of normal and tangential velocities of movement of the hillock slopes change periodically. Also, the variation of number of active growth centres on

the {100} faces at constant external growth conditions have been observed.

Step velocity was measured over a large range of supersaturation and shows well defined a linear dependence for all faces. At higher supersaturations the steps develop a zig-zag form due to the competition between anisotropic step velocity and variation of supersaturation along the growing surface.

Kinetic growth parameters for the observed faces were determined and the obtained results have been considered in the broader context of growth rate variation in potash alum crystals.

---

Permanent address: Institute of Physics, P.Box 57, 11000 Belgrade Yugoslavia.

---

## CRYSTAL GROWTH AND CHARACTERIZATION OF $\text{MgHPO}_4 \cdot 3\text{H}_2\text{O}$ \*

*B.C. Sales, B.C. Chakoumakos, L.A. Boatner and J.O. Ramey*  
Solid State Division, Oak Ridge National Laboratory, Oak Ridge, TN

Synthetic crystals of the mineral newberryite ( $\text{MgHPO}_4 \cdot 3\text{H}_2\text{O}$ ) were grown from an aqueous solution containing  $\text{Mg}(\text{NO}_3)_2 \cdot 6\text{H}_2\text{O}$ ,  $\text{H}_3\text{PO}_4$  and urea. The slow thermal decomposition of urea (at 60°C) was used to increase the solution pH which resulted in the nucleation and growth of relatively large, optically clear newberryite crystals ( $5 \times 5 \times 5 \text{ mm}^3$ ). The mineral newberryite is currently found in bat guano, urinary stones and animal calculi. In the ancient ocean, before the development of life, newberryite was probably the dominant phosphate mineral and, hence, may have played a role in the evolution of life on the planet. The present interest in newberryite, however, is related to an unusual crystalline-to-amorphous transition that occurs during heating. This transition is investigated using high-performance liquid chromatography (HPLC), x-ray diffraction (XRD), differential scanning calorimetry (DSC), and thermogravimetric analysis (TGA). The dehydration of newberryite results in amorphous x-ray diffraction (XRD) patterns that remain essentially unchanged over the

interval between 150 and 600°C. In contrast, over the same temperature interval, the HPLC results show a dramatic evolution in the distribution of chains of corner-linked  $\text{PO}_4$  tetrahedra resulting in the formation of chains up to 13  $\text{PO}_4$  tetrahedra in length. Above 600°C, crystalline  $\text{Mg}_2\text{P}_2\text{O}_7$  is formed. At each annealing temperature the distribution of phosphate anions is in agreement with theory. During the crystalline-to-amorphous transition the original crystal shape is preserved even though the crystals lose up to 36% of their original weight. High pressure DSC experiments with newberryite resulted in the formation of a unique crystalline phosphate phase that contained equal amounts of orthophosphate and pyrophosphate anions.

---

\*Research sponsored by the Division of Materials Sciences, U.S. Department of Energy under contract no. DE-AC05-84OR21400 with Martin Marietta Energy Systems, Inc.

## GROWTH MORPHOLOGY OF BERLINITE CRYSTALS OBTAINED UNDER HYDROTHERMAL CONDITIONS

*J. Gomez-Morales\*, R. Rodriguez\*, J. Durand\*\* and L. Cot\*\**

\*Institut de Ciencia dels Materials de Barcelona,

C.S.I.C. Campus U.A.B., 08193 Cerdanyola, Spain

\*\*Laboratoire de Physicochimie des Matériaux, CNRS-ENSC,

8, rue Ecole Normale, 34053 Montpellier Cedex 1, France

The growth morphology of Berlinite ( $\text{AlPO}_4$ ) crystals obtained under hydrothermal conditions depends of the solvent employed ( $\text{H}_3\text{PO}_4$ ,  $\text{HCl}$ ,  $\text{H}_2\text{SO}_4$ , and their mixtures) and the crystallization temperature. We have constructed a morphological diagram (morphogram) showing the habits resulting by changing the relative rates of growth of the  $r$ ,  $\{10\bar{1}1\}$ , and  $\pi$ ,  $\{10\bar{1}2\}$ , faces respect to  $m$ ,  $\{10\bar{1}0\}$ , and keeping constant and equal to 0.9 the relations between the first two types of faces and the rates of growth of the  $z$ ,  $\{0111\}$ , and  $\pi'$ ,  $\{01\bar{1}2\}$ , faces respectively. In the morphogram we distinguish 4 zones:  $R_1$  where the most important faces are  $r$  and  $z$ ,  $R_2$  where the

crystal habit is dominated mainly by  $m$ ,  $\pi$  and  $\pi'$ . In  $R_3$  the main faces are  $\pi$  and  $\pi'$ , with a little development of  $m$ . Finally sector  $R_4$  is composed by  $\pi$ ,  $\pi'$ ,  $r$  and  $z$ .

From the resulting crystals and the morphogram, it can be observed that the crystals grown from  $\text{H}_3\text{PO}_4$  fall in the  $R_1$  region, those grown from  $\text{HCl}$  solutions fall in the  $R_2$  region and those grown in  $\text{H}_2\text{SO}_4$  in the  $R_3$  region. The crystals grown in  $\text{H}_3\text{PO}_4\text{-HCl}$  mixtures present morphologies situated between  $R_1$  and  $R_2$ , while those obtained from mixtures  $\text{H}_2\text{SO}_4\text{-HCl}$  are in between  $R_2$  and  $R_3$ . The rise of temperature usually produce a greater development of the prismatic face  $m$ .

---

## CRYSTAL GROWTH, MORPHOLOGY, STRUCTURE AND PROPERTIES OF SOME SUPERSONIC PYROPHOSPHATES

*K. Byrappa, B.V. Umesh Dutt and G.S. Gopalakrishna*

The Mineralogical Institute, University of Mysore

Manasagangotri, Mysore-570 006, India

*S. Gali*

Departament de Crystallografia i Dipòsits Minerals Universitat de Barcelona

Facultat de Geologia Martí i Franques s/n 08028 Barcelona, Spain

Sodium superionic conductors find great applications in high temperature batteries, fuel cells, gas sensors, electrochromic displays etc. Several new compounds with mixed framework structures based on the structure of NASICON have been reported in the literature. However, all these superionics belong to the orthogroup. Recently, the research group at the University of Mysore has reported high ionic conductivity in a series of condensed phosphates, especially in pyrophosphates. This has opened a new trend in the search for sodium superionic conductors in other condensed radicals, not only among phosphates but also among silicates, germanates, vanadates and other related tetrahedral complexes. In the present report the authors describe the crystal growth, morphology, structure and properties of  $\text{Na}_2\text{M}\text{Zr}(\text{P}_2\text{O}_7)_2$  (where  $\text{M} = \text{Ni, Co, Zn, Cd}$ ),  $(\text{Na}_{2/3}\text{Zr}_{1/3})_2\text{P}_2\text{O}_7$ ,  $\text{Na}_2\text{H}_3\text{Al}(\text{P}_2\text{O}_7)_2$ ,  $\text{Na}_2\text{CaMn}_2(\text{P}_2\text{O}_7)_2$  and  $\text{NaMP}_2\text{O}_7$  (where  $\text{M} = \text{Co, Fe, Ni}$ ).

All these new superionics have been obtained by hydrothermal technique through spontaneous nucleation within a wide range of PT conditions ( $T = 240\text{-}600^\circ\text{C}$ ,  $P = 50\text{-}2000$  bars). An emphasis is made on the search for optimum growth conditions in order to obtain these compounds in the form of single crystals. Crystal growth with reference to the suitable solvent selection, solvent-solute interaction has been discussed. The crystal morphology of these pyrophosphates is very interesting and it varies depending upon the nutrient composition, growth conditions and structure of these compounds. A brief survey of the crystal structure of these new superionic pyrophosphates, which usually crystallize in the lower symmetry will be given. Ultimately the electrical conductivity and other related properties of these new superionics would be discussed.

## HYDROTHERMAL SYNTHESIS OF NEW POTASSIUM NEODYMIUM SILICATES

*S.M. Haile and B.J. Wuensch*

Massachusetts Institute of Technology

Department of Materials Science and Engineering, 77 Massachusetts Avenue

Cambridge, MA 02139

*T. Siegrist and R.A. Laudise*

AT&T Bell Laboratories,

600 Mountain Avenue, Murray Hill, NJ 07974

We have hydrothermally synthesized micro-crystals of eight potassium neodymium silicates (PNS's) as possible fast ion conductor's (FIC's). PNS's are interesting as FIC's because some of them have open channels in their structure. In addition, as in the case of NASICON, it should be possible to substitute framework cations of different size or valence, thus tailoring the structure to optimum transport properties. Procedures for the preparation of (1)  $K_3NdSi_6O_{15}$  (Pbam), (2)  $K_6Nd_3Si_{20}O_{44}$  (Bb\*\*), (3)  $K_8Nd_3Si_{12}O_{32}OH$  (P1), (4)  $K_{10}Nd_4Si_{14}O_{39}$  (Pn\*\*), (5)  $KNd_9(SiO_4)_6O_2$  (P6<sub>3</sub>), (6)  $K_3NdSi_8O_{18}$  (P3\*\*), (7)  $K_4Nd_2Si_8O_{21}$  (C222<sub>1</sub>), and (8)  $K_{12}Nd_2Si_{18}O_{45}$  (2/mI\*\*n) were discovered. (2), (4), (6), (7) and (8) are previously unreported and the growth conditions for (1), (3) and (5) have not been given previously. We report the conditions under which each phase has been synthesized, and discuss some aspects of the relevant silicate phase equilibria. In general, synthesis was carried out using a glass of high silica content ( $4K_2O \cdot Nd_2O_3 \cdot 17SiO_2$  or  $4K_2O \cdot Nd_2O_3 \cdot 34SiO_2$ ) or a mixture of the appropriate oxides as the precursor material. The glass was prepared by mixing, calcining and then melting the required amounts of  $Nd_2O_3$ , vitreous  $SiO_2$ , and  $K_2CO_3$ . Aqueous solutions of  $KOH$ ,  $K_2CO_3$ ,  $K_2B_4O_7$ ,  $KF$ , or  $KHF_2$ ,

served as the solvent. Pressures employed ranged from 0.5 to 1.3k bar, and temperatures from 350-600°C. Isothermal synthesis, typically conducted in a Tuttle type autoclave, yielded crystalline powders. Synthesis carried out under a temperature gradient, typically in a Morey autoclave, yielded crystals as large as 3mm x 2mm x 2mm for some phases. Composition measurements were made on electron micro-probe and X-ray powder diffraction data were collected on a powder diffractometer and single crystal intensity data for  $K_3NdSi_6O_{15}$  and  $K_8Nd_3Si_{12}O_{32}OH$  on a four-circle diffractometer. Crystallographic data for the remaining phases were determined from precession x-ray camera photographs.

Conductivity measurements are reported for six of the compounds. (4) has the highest conductivity which however was much lower than practical superionic conductors like beta alumina. However the correlation of structural and conductivity data enables one to begin to understand how to design better open channel conductors. The potential for hydrothermal growth in the exploration and understanding of ionic conductors is emphasized.

## SESSION 9A

### MICROSCOPIC CONDENSATION PROCESSES OF NIOBIUM MICROCLUSTERS IN SPUTTERING

Kozo Obara

Faculty of Engineering, Kagoshima University  
Korimoto, 1-21-40, Kagoshima 890, Japan

Microscopic data and analyses of condensation of sputtered niobium particles are presented. Niobium particles were formed by a conventional magnetron sputtering system. Sputtered particles are composed of negative, positive and neutral particles. The sputtering chamber was separated from the growth chamber, in which the pressure is four order lower than that in the sputtering one, by the orifice with a diameter 1mm. The momentums of particles through the orifice were obtained by magnetic field deflection method. The energies of particles were obtained by retarding-potential method. From the obtained momentums and energies, the masses and speeds of particles were estimated. The number of particle was estimated from the detected ion current intensity. Figure 1 shows the particle density distribution of negative particles in momentum space at 0.3 Torr argon. The peaks indicated by  $N_i$  ( $i=1,2,3$ ) show negative particles. The speed distribution of the particles with the same mass in the broad peak  $N_3$  is approximately expressed by the Maxwell distribution of speeds but the peaks

$N_1$  and  $N_2$  are not. The peaks  $N_1$  and  $N_2$  are considerably sharper than the Maxwell distribution. The speed of the peak  $N_2$  is nearly equal to that of the peak  $N_1$ . The number of niobium atoms of the peak  $N_1$  and  $N_2$  are 2 and 20, respectively. we found six peaks with the same speed. The masses of these peaks are  $N=2, 8, 20, 40, 58$  and 138, respectively. These series of mass numbers were explained by the electronic shell model. The region indicated by  $P_i$  ( $i=1,2$ ) shows the positive particles. These features show two condensation processes from niobium atoms with high temperature. Finally, we conclude that there are two condensation processes for the sputtered particles with high energies. One is the process for thermalization, in which the kinetic energy is lost by the collision of between particles. The other is the process, in which the kinetic energy of particle is conserved when the particles collide. These two processes depend on the electronic structures of clusters and influence the morphology of the microcrystals.

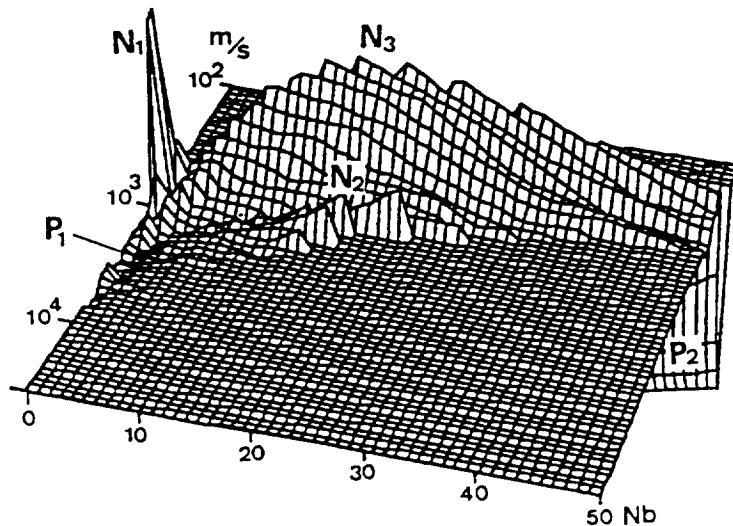


Figure 1. Particle density distribution.

OPTICAL ABSORPTION SPECTRA OF  $\text{Au}_2$  AND  $\text{Cu}_2$  IN  
GAS EVAPORATION TECHNIQUE

Tsugio Okazaki and Yahachi Saito\*

Department of Physics, Meijo University, Nagoya 468, Japan

\*Department of Electrical and Electronic Engineering,  
Mie University, Tsu 514, Japan

When a metal is evaporated in an inactive gas at a low pressure, a smoke consisting of ultra fine particles is formed (called gas evaporation technique)[1]. Emission of light is observed from a vapor zone around the evaporation source. The color of light is characteristic of metal, e.g. green for Au and blue for Cu. The visible light are attributed to the electronic transition of dimers from excited states to the X state[2]. In order to take an absorption spectrum, the vapor zone in a smoke is shined by a collimated white light beam from a xenon lamp and the light which passes through the smoke is analyzed by a monochromator. A typical spectrum of  $\text{Au}_2$  from 222 to 229nm is shown in Fig. 1. The D-X band system reported by Klotzbucher and Ozin [3] is observed. However, precise

molecular constants are not known. We derived the constants of band origin and vibrational constants of D state as follows:  $\nu_{00}=44462.2 \text{ cm}^{-1}$ ,  $\omega_0=168.3 \text{ cm}^{-1}$ ,  $\omega_{00}=0.63 \text{ cm}^{-1}$ . The constants of the lower state is coincident with the constants of ground state. In the study of the  $\text{Cu}_2$ , unknown constants of H, I and J states are also determined and revised.

- [1] R. Uyeda: Morphology of Crystal, e. I. Sunagawa (Terra Scientific, Tokyo, 1987) Chap. 6.
- [2] Y. Saito: *Jpn. J. Appl. Phys.* 28(1989) L2024.
- [3] W.E. Klotzbucher and G.A. Ozin: *Inorg. Chem.* 12(1980) 3767.

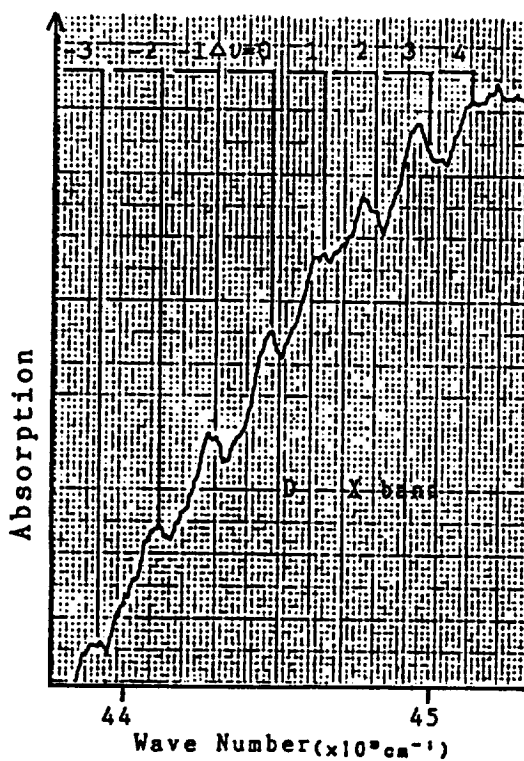


Figure 1. Absorption spectrum of D-X band system of  $\text{Au}_2$

STRUCTURE OF ALLOY AND OXIDE PARTICLES PRODUCED BY THE  
REACTION BETWEEN ULTRAFINE PARTICLES AND FILMS

*Y. Saito, K. Ohtsuka, T. Watanabe and C. Kaito*

Department of Electronics and Information Science

Kyoto Institute of Technology, Matsugasaki, Sakyo-ku, Kyoto, 606, Japan

The ordered phase of  $Fe_{50}Ni_{50}$  which is called tetrataenite was the one of the important mineral in meteorite. It is not possible to produce tetrataenite phase in laboratory by conventional heating of laboratory Fe-Ni alloys. We produced the tetrataenite particles by the gas evaporation method by using the coalescence in smoke[1,2]. The ordered particles can be produced above 200°C by the coalescence of Fe and Ni particles in short time of  $10^{-2} \sim 10^{-3}$  sec. Another method to produce the ordered structure were neutron[3] or high energy electron[4] irradiations.

In this paper, the extraterrestrial important materials such as  $Fe_{50}Ni_{50}$  ordered phase and  $MgSiO_3$ (enstatite) have been produced by the reaction between particles and thin films. Since both ultrafine particles and thin film are transparent for electron beam, the production process of the alloy or the compound oxide can be directly observed by an electron microscope.

Fe thin films were prepared by a vacuum evaporation method on NaCl substrates. After Ar gas at 13kPa was introduced to the vacuum chamber, Ni ultrafine particles were deposited onto the Fe films. The Fe films with the Ni particles were heated at various temperature without exposure to air. An ordered phase of  $Fe_{50}Ni_{50}$  was clearly produced by the heating at 300°C for 1 hour. The alloy produced by the reaction between the films and the particles by the mutual diffusion of Fe and Ni atoms. In the initial stage, the alloys are formed at the interface between the Fe films and the Ni particles. With the initial formation of the alloys by the mutual diffusion, Fe

and Ni atom vacancies are formed in the film and the particles, respectively. The vacancies produced by the mutual diffusion more accelerate the diffusion. Since the diffusion rate of Ni in Fe is faster two order than that of Fe in Ni, the reaction proceed into the Fe films predominantly. As a result, the ordered phase particles are produced in the Fe films. It can be concluded that the ordered phase can be produced at low temperature for short time, because the vacancies reduce the reaction temperature or accelerate the atom diffusion in the Fe film.

In the case of production of  $MgSiO_3$  particles, Mg ultrafine particles and SiO thin film were used. By the heating at 400°C  $MgO$  particles about ~100 nm in size have been produced by the reaction between the Mg particles and the SiO films. Above 450°C in addition to the  $MgO$  particles,  $MgSiO_3$  particles were produced. At 500°C,  $MgSiO_3$  particles were predominantly produced by the diffusion of Mg atoms into the SiO films.

[1] C. Kaito and Y. Saito, *Proc. Jpn. Academy* 65 Ser. B (1989) 125-128.  
[2] T. Nagata, C. Kaito, Y. Saito and M. Funaki, *Proc. NIPR Symp. Antarct. Meteorites.* 4 (1991) 404-419.  
[3] L. Néel, J. Pauleve, R. Pauthenet, J. Lugier and D. Dautreppe, *J. Appl. Phys.* 35 (1964) 873-877.  
[4] A. Chamberod, J. Laugier and J.M. Penisson. *J. Magn. Magn. Mineral.* 10 (1979) 139-144.

A NEW EXPERIMENTAL STUDY ON THE PRODUCTION OF CLUSTERS DUE  
TO CHEMICAL REACTION OF COPPER ULTRAFINE PARTICLES

C. Kaito, T. Watanabe K. Ohtsuka, H. Chin and Y. Saito

Department of Electronics and Information Science

Kyoto Institute of Technology, Matsugasaki, Sakyo-ku, Kyoto, 606, Japan

One of the advanced method for producing clusters is the so-called "gas evaporation technique" in which a material is heated in an atmosphere of inert gas. Since almost all of the particles produced are 30-200nm in size, the production of the clusters of the order of 10nm is very difficult. In this paper, it has been shown that copper clusters of ~10nm in size can be produced through oxidation and reduction process of ultrafine copper particles.

The ultrafine copper particles produced in Ar gas pressure at 13kPa were collected on carbon or SiO thin films supported on stainless steel electron microscope grids. The particles were oxidized in air at 200°C for a few minutes. After that, the specimen was heated at 300°C for about 30 minutes in an electron microscope by Hitachi H-8101 specimen heater holder. Oxidation took place on the surface of the ultrafine particles. The particles were covered with Cu<sub>2</sub>O layer which were composed of crystallites of a few nm in size. The thickness of the oxide layer increased by the oxidation time. Completely oxidized particles became the spherical shell with oxide layer[1]. By the heating, the oxidized particles having the spherical shell in vacuum at 300°C, reduction of the Cu<sub>2</sub>O layer took place[2]. Almost all of the particles were rebirth to copper clusters with the size of ~10nm. The coalescence of the formed copper clusters took place, then 100nm size of the

copper particles sometimes appeared. A reduced Cu<sub>2</sub>O small cluster of ~5nm size has been sometimes observed even when the specimen was reduced about 1 hour. The cluster has a super structure which is due to the reduction of oxygen atom layer in Cu<sub>2</sub>O crystal.

The copper particles covered with oxide layer contain voids or void clusters. These particles were recovered to the original copper particles by the reduction. The void clusters were also filled up with copper atoms. For example, a copper particle of 86nm in size was covered with oxide layer of 11nm by heating at 200°C for 1 minute in air. Then the size of the particles covered with oxide layer become 108nm. By the reduction at 300°C for 15 minutes, the oxide layer disappeared and the copper particles of 86nm size appeared. The number of the copper atoms moved in the process is  $8 \times 10^6$  which corresponds to the number including in a copper crystal particle of 30 nm in size.

[1] C. Kaito, K. Fujita and H. Hashimoto, *Jpn. J. Appl. Phys.*, 12, (1973), 489-496.

[2] C. Kaito, Y. Nakata, Y. Saito, T. Naiki and K. Fujita, *J. Crystal Growth*, 74, (1986), 469-479.

## FUNDAMENTAL CRITERION FOR SURFACE MELTING

*J.P. van der Eerden, T.H.M. van de Berg, J. Huinink and H.J.F. Knops\**

Laboratory of Interfaces and Thermodynamics, Padualaan 8, 3584CH Utrecht, The Netherlands

\*Institute of Theoretical Physics, Toernooiveld, 6525ED Nijmegen, The Netherlands

During ICCG9 we proposed to use the vanishing of a properly defined surface shear modulus as a fundamental criterion for surface melting [1]. This idea has been worked out now, and it has been applied to the surface of a Lennard-Jones crystal model.

In the course of our research it turned out that a proper definition of local stress and (bi)local elastic constants is not trivial. Of course a minimum requirement of such definitions should be that integration of the local stress and elasticity fields over the whole system volume should give the average value of these fields multiplied with the system volume. For these average values exact expressions (*virial expressions*) are readily available in text books [2]. Our original idea [1] basically was to decompose the global virial expressions, and to define a local field at  $r$  as the contribution from atoms in the neighborhood of  $r$ .

This type of definition, however turns out to be inconsistent. E.g., in a liquid Lennard-Jones system we found that the global value of the shear modulus was zero, but the value of the local shear modulus (averaged over a slice of atomic thickness) was positive when calculated with the decomposition type of definition. Closer inspection of the derivation of the virial expressions revealed that the decomposition is reliable only when the field vary slowly on the scale of the range of the interaction potential. As the range of our modified Lennard-Jones potential corresponds to several atomic layers, we can

not use the decomposition method to calculate the elasticity tensors per atomic layer.

The essential new idea is to describe the interatomic forces in terms of momentum transfer. Conceptually one introduces a virtual particle current between the interacting atoms. This current contributes to the total force on a plane when it crosses the plane. In this spirit a local stress tensor as well as a bi-local elasticity tensor can be defined for arbitrary positions in space (even when no atom is present at that particular position). It is then a matter of mathematics to show that integrating the thus defined local stress and elasticity tensors over the system volume leads to the global virial expressions found in the standard literature.

We have applied the new definitions to the Lennard-Jones system [3]. As required we found that the local shear modulus of a liquid system vanishes. Moreover we studied the (001) surface of a Lennard Jones crystal and the results pointed at a surface melting point of  $(69 \pm 1)K$  which would be below the bulk melting point of  $(72 \pm 1)K$ . Work is in progress for the (111) surface as well.

- [1] J.P. van der Eerden, A. Roos and J.M. van der Veer, *J. Crystal Gr.* 99(1990)77.
- [2] L.D. Landau and E.M. Lifshitz, *Theory of elasticity*, Pergamon Press (1959).
- [3] J.P. van der Eerden, H.J.F. Knops and A. Roos, *J. Chem. Phys.* (1991).

---

## ELECTRON MICROSCOPY STUDY OF GROWTH AND AGGREGATION OF MICROCLUSTERS OF AgI AND HgI<sub>2</sub>

*M. Abdulkhadar and K.C George*

School of Pure and Applied Physics, Mahatma Gandhi University  
Cheruvandoor, Ettumanoor - 686 631, India

Clusters represent a new class of material particles expected to have chemical and physical properties that span the range from molecular to bulk and have invited intense interest in recent years. One of the reasons by which the properties of clusters are of intrinsic interest is that we can understand the crystal growth processes on a microscopic level. In the case of polydisperse systems non-steady state processes like Ostwald ripening and recrystallisation may occur. Every time a new atom or a molecule or a small aggregate of these condenses on to a cluster, the atoms in the cluster may completely rearrange themselves and the cluster may reconstruct. It will be interesting to know the sequence of structures a cluster assumes as it grows and also to understand whether a unique structure exists in a cluster. The process of aggregation of small particles to form larger clusters falls into two regimes, viz, DLA and RLA, determined by the nature of interparticle interaction which in

turn control the sticking probabilities for two colliding clusters. The authors report the study of aggregation and growth of clusters of AgI and HgI<sub>2</sub> in aqueous suspensions using TEM and electron diffraction. The aggregates formed have been found to be random, tenuous and could be termed as fractals. The electron diffraction patterns of fresh and aged clusters have been found to be different. Electron diffraction patterns of fresh HgI<sub>2</sub> clusters consist of two discontinuous rings while that of aged samples consist of a number of rings. But fresh AgI samples show a number of diffraction spots while aged samples give two diffraction rings. These observations are explained on the basis of aggregation of finer particles aided by surface relaxation and it has been shown that as the clusters grow, rearrangement of molecules takes place within the clusters leading to a unique crystal structure.



## SESSION 9B

### SELF-LIMITING MONOLAYER EPITAXY (SME): A NEW APPROACH TO THE GROWTH OF WIDE GAP II-VI HETEROSTRUCTURES

*W. Faschinger*

Institut für Halbleiterphysik, University of Linz, Austria

*P. Juza, S. Ferreira\* and H. Sitter*

Inst. für Experimentalphysik, Univ. of Linz, Austria

Wide gap II-VI heterostructures containing S or Se are currently a topic of major interest for blue laser applications. In order to obtain high quality heterostructures with well defined thickness and abrupt interfaces an UHV growth method with precise thickness control in a monolayer scale is desirable. This technological challenge motivated us to develop a new technique, which we call Self-limiting Monolayer Epitaxy (SME). It combines the advantages of a self regulating growth mechanism, as achieved in Atomic Layer Epitaxy (ALE), with a feature typical for Molecular Beam Epitaxy (MBE), namely that both constituents of a compound are simultaneously present at the surface. The combination of both the characteristics of ALE and MBE allows us to avoid the problems connected with each of these methods: The occurrence of fractional monolayer growth, which seems to limit the possibilities of ALE, and the problem of interface roughness as reported many times for MBE grown superlattices, which is a consequence of the lack in accuracy of MBE growth rate control.

SME is achieved by offering the more volatile constituents S or Se permanently, while the group II constituents Cd or Zn are offered in a pulsed mode. In analogy to ALE we call the

growth time from one group II evaporation pulse to another a cycle. Since X-ray diffraction of superlattices is the most accurate method to measure the growth rate per cycle, short period superlattices of  $ZnS/ZnS_{1-x}Te_x$  and  $ZnSe/CdSe$  were grown at various beam fluxes, evaporation pulse times and substrate temperatures. The X-ray results show that growth in discrete compound monolayer steps can be easily achieved by SME: The growth rate per cycle for all superlattices is an integer number of monolayers of the compound. It is exactly one monolayer per cycle as long as the amount of material offered within one cycle is kept between one and two monolayers, but increases to exactly  $n$  monolayers per cycle ( $n$  being an integer) if the offered material within one cycle is kept between  $n$  and  $n+1$  monolayers.

In addition to the X-ray diffraction measurements we will present in situ RHEED investigations and discuss a model of the growth process based on these results.

---

\*Permanent address: Inst. de Pesquisas Espaciais, CP 515, 12201-S.J.C., Brazil

---

### GROWTH OF ZINC SELENIDE CRYSTALS BY THE LIQUID ENCAPSULATED VERTICAL BRIDGMAN TECHNIQUE

*Yasunori Okano, Keigo Hoshikawa and Tsuguo Fukuda*

IMR, Tohoku University, Sendai 980, Japan

*Hideto Unuma and Kazuhiko Tono-Oka*

GID Lab., Hokkaido, Sapporo 062, Japan

Zinc Selenide (ZnSe) has a wide band gap of 2.7 eV at room temperature and is one of the materials for practical use in blue light-emitting diodes. Many studies on growth of bulk ZnSe crystals by the Bridgman<sup>1,2)</sup> and liquid encapsulated Czochralski<sup>3)</sup> techniques have been reported, however, twins due to phase transformation at 1425 °C have been observed. This study aims at fundamental study for growth of ZnSe bulk crystals with high quality. In order to avoid the twins, low temperature growth and usage of liquid encapsulated materials are performed.

Crystals are grown by a conventional vertical Bridgman furnace with a single hot zone in Ar atmosphere (10 or 200 kgf/cm<sup>2</sup>). A pBN crucible available for setting a seed crystal with 25 mm in diameter is used. Starting materials are stoichiometric poly ZnSe crystals or Zn and excess Se powders. Liquidus in Zn-Se system was determined. As the encapsulant,

$B_2O_3$  and fluoride compounds such as  $AlF_3$ ,  $BaF_2$ ,  $CaF_2$ ,  $KF$ ,  $LiF$ ,  $MgF_2$ ,  $NaF$  and  $ZrF_4$  were examined, and we found that  $CaF_2$ (60 wt %)+ $AlF_3$ (40 wt %) was more suitable for the encapsulant than other materials from view point of chemical reaction with ZnSe and the crucible, and stability around melting point of ZnSe.

Grown crystals with the encapsulant was easy to take out from the crucible and boundary between ZnSe and the encapsulant was very clear. Crystals grown from flux with excess Se at 1400 °C was free from twins.

---

- 1) M. Shone et al : *J. Crystal Growth* 86 (1988) 132.
- 2) I. Kikuma and M. Furukoshi: *J. Crystal Growth* 41 (1977) 103.
- 3) A.G.Fischer: *Crystal Growth* Vol. 16, edited by B. Pamplin p.379 Pergamon Press (1980).

## THE GROWTH AND CHARACTERISATION OF CADMIUM SELENIDE AND ZINC CADMIUM SELENIDE EPILAYERS BY MOVPE

P.J. Parbrook, A. Kamata and T. Uemoto

Research and Development Center, Toshiba Corporation  
1, Komukai Toshiba-cho, Sawai-ku, Kawasaki 210, Japan

In order to obtain blue light emitting devices using II-VI materials it can be advantageous to grow multilayer structures. Considerable success has been achieved recently using MBE based techniques to grow ZnCdSe alloy layers for use as quantum wells [1]. However to date ZnCdSe alloys have not been studied using MOVPE.

In this presentation the growth of CdSe and ZnCdSe alloys is described. The epitaxial layers were grown by atmospheric pressure MOVPE using dimethylcadmium, dimethylzinc and dimethylselenide onto (100) oriented GaAs substrates. The growth temperature was between 300 and 550°C.

CdSe growth was found to be possible at much lower temperatures than for ZnSe growth under similar conditions. This is due to the lower temperature pyrolysis of dimethylcadmium which induces the breakdown of the dimethylselenide. X-ray diffraction studies showed the CdSe layers were always cubic despite its preference to grow in the hexagonal phase. Comparison with previous attempts to grow CdSe by MOVPE, where mixed phase growth was obtained [2], suggests that critical

factor in obtaining cubic epitaxial CdSe on (100) GaAs is the growth mechanism at the surface.

ZnCdSe alloys have successfully been grown across the entire composition range. The layers were zinc rich in comparison to the gas phase composition. This effect becomes stronger with increasing growth temperature. The strength of this effect, coupled with the behaviour of the growth rate as the temperature or the Zn:Cd gas phase ratio was changed suggests that the presence of zinc strongly inhibits cadmium incorporation into the layers. Structural analysis showed that the alloys were always cubic in structure but that layer quality tended to deteriorate with increasing Cd composition.

Transmission electron microscopy has confirmed the cubic nature of the samples. However many defects were observed. The nature of these defects and their effect on strain relief within the epilayer will be discussed.

[1] M.A. Haase et al: *Appl. Phys. Lett.* 59 (1991) 1272.

[2] M.P. Halsall et al: *J. Crystal Growth* 91 (1988) 135.

## EPITAXIAL GROWTH OF HIGH QUALITY ZnSe AND ZnSe/ZnS SUPERLATTICES FOR OPTICAL PROCESSING

Chungdee Pong, R.C. DeMattei\* and R.S. Feigelson

Department of Materials Science and Engineering, Stanford University, Stanford, CA 94305

\*Center for Materials Research, Stanford University, 105 McCullough, Stanford, CA 94305

High quality epitaxial films of ZnSe and ZnSe/ZnS strained layer superlattices (SLS) have been grown on (100) GaAs substrates using diethylzinc, diethylselenide, and propylenesulfide as precursors in a low pressure MOCVD reactor. Results of the growth of ZnSe films demonstrated the influence of process conditions, such as reagent flow ratio ( $f_{VI}/F_{II}$ ) and substrate temperature, on the film stoichiometry, surface morphology, and crystalline quality. The surface morphology of the films was usually faceted, and the degree of facetedness was decreased with increased growth temperature and  $f_{VI}/f_{II}$ . Photoluminescence (PL) studies at 2.8K showed a strong near band edge peak (NBE) at 2.802eV and a shallow deep level emission band between 2.0 and 2.2eV for a stoichiometric ZnSe film. Detailed investigation of NBE peaks indicated both donor- and acceptor-related emissions due to the interdiffusion of substrate atoms into film during growth. Rutherford backscattering spectrometer, cross-sectional TEM, and x-ray diffraction indicated that the ZnSe films had very low structural defects.

Low temperature PL was used to study samples of ZnSe/ZnS strained layer superlattices. The quantum size effect was observed on samples of single and multiple (10 layers) ZnSe(1.5 nm)/ZnS(8.5 nm) quantum well structures. A curve of peak energy vs. well thickness ( $L_w$ ) was determined and fit well with theoretical calculations. A new deposition procedure was developed which effectively reduced the PL linewidth of multiple quantum wells. The preliminary results showed a reduction in linewidth of nearly 40%. It was determined that 15nm of barrier material (ZnS) was sufficient to eliminate coupling effect between the quantum wells. Atomic force microscopy (AFM) was applied to study surface morphology of multilayer samples. Peak-to-valley values were within several nanometers; these results can be correlated with the PL results. Finally, a novel prototype device for second harmonic generation of blue light was demonstrated.

\*Research funded by NSF-MRL Thrust Program through CMR at Stanford University.

**LARGE-GRAINED CuInSe<sub>2</sub> CRYSTAL GROWTH USING COMPUTER-CONTROLLED,  
HIGH-PRESSURE LEDS FURNACES**  
*C.R. Schwerdtfeger and T.F. Ciszek*  
National Renewable Energy Laboratory  
Golden, Colorado 80401 USA

Earlier, we reported a simple high-pressure furnace system for the liquid-encapsulated directional solidification (LEDS) of chalcopyrites such as Cu<sub>x</sub>Ag<sub>1-x</sub>InSe<sub>2</sub> and III-V's such as InP<sup>1</sup>. We have incorporated precise motion and temperature control on this furnace system using geared stepper motors, custom built heaters, and interfaced computer control for the purpose of growing CuInSe<sub>2</sub> crystals with improved homogeneity and structural integrity. The system has been designed with the capability for cooling rates below 1°C/hr, although higher rates have been used with favorable results. CuInSe<sub>2</sub> crystal growth was carried out under B<sub>2</sub>O<sub>3</sub> encapsulant, in open-top quartz

ampoules, with an argon ambient at 70-80 bars pressure to confine volatile Se. Vertical directional solidification was conducted in both small (<15°C/cm) and large (30-90°C/cm) thermal gradients and with a range of crystal cooling rates. Compositional, crystallographic, electrical, and mechanical (cracking) characteristics of the ingots will be presented.

---

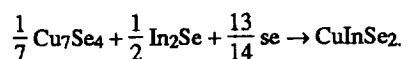
1. T.F. Ciszek and C.D. Evans, *J. Crystal Growth* **91** (1985) 533.

**METHOD OF SELENIZING LIQUID Cu-In ALLOY IN GROWING  
CuInSe<sub>2</sub> SINGLE CRYSTALS**

*Shigetaka Nomura and Takeo Takizawa*  
College of Humanities Sciences, Nihon Univ., Tokyo 156

Growth of single-crystalline CuInSe<sub>2</sub> has been performed by selenizing liquid Cu-In alloy. This is an effective method of stoichiometry-controlled growth of CuInSe<sub>2</sub> in the two-zone-temperature system with the control of selenium vapor pressure. In the normal melting method, it has been found that copper selenides and indium selenides produced in the reaction processes of elements cause non-stoichiometry before the solution of Cu-In-Se is formed.<sup>1)</sup> On the other hand, in our method, the liquid Cu-In alloy is perfectly selenized above the melting point of CuInSe<sub>2</sub> without decomposition of binary selenides such as In<sub>2</sub>Se<sub>3</sub>. However, when selenized at temperatures below the melting point, a small amount of binary phases of Cu<sub>7</sub>Se<sub>4</sub> and In<sub>2</sub>Se is formed in addition to CuInSe<sub>2</sub> owing to the incomplete selenization. This is consistent to the chemical

reaction process proposed for the final step of reaction by the normal melting method as,



During the cooling process for crystal growth, vapor pressure of selenium is controlled. Both n- and p-type crystals having variation in carrier concentration or electrical resistivity are grown by the control of selenium vapor pressure together with the change in Cu/In ratio at the initial charge. Application of selenium vapor pressure is effective for reducing imperfections in p-type crystals.

---

- 1) S. Nomura et al: *Jpn. J. Appl. Phys.* **30**(9A) (1991) 2040.

## CHARACTERIZATION OF $\text{CuInSe}_2$ SINGLE CRYSTALS WITH VARIOUS DEVIATIONS FROM STOICHIOMETRY

H. Nakanishi, A. Tamai, S. Ando, S. Endo and T. Irie

Science University of Tokyo, Noda, Chiba 278 (Japan)

Recently, the ternary semiconducting compound  $\text{CuInSe}_2$  has considerable attention because of its potential uses. Numerous experimental studies have been made to explain the electrical and optical properties of  $\text{CuInSe}_2$  in terms of an intrinsic defect model. The parameters of this model are the deviation from molecularity  $\Delta m$  and the deviation from valence stoichiometry  $\Delta s$ , which have been defined by Groenink and Janse for the nearly stoichiometric ternary compounds (see Fig. 1).<sup>1</sup> In the present communication we report the results of characterization of as-grown  $\text{CuInSe}_2$  single crystals with the compositional deviation of  $\Delta m$  for  $\Delta m < 0$  in the  $\text{Cu}_2\text{Se}-\text{In}_2\text{Se}_3$  system and those with the deviation of  $[\text{Cu}]/[\text{In}]$  ratio ( $=R$ ) from 1 in the  $\text{CuSe}-\text{InSe}$  system within the single phase region of chalcopyrite structure. Single crystals of  $\text{CuInSe}_2$  were prepared by

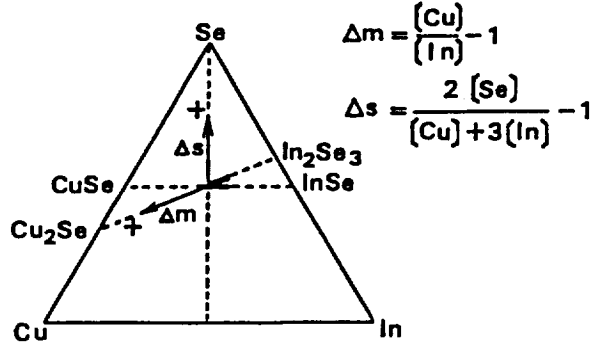


Figure 1. Triangle diagram for the system Cu-In-Se.

melting the elements in an evacuated quartz ampoule followed by directional freezing. P-type samples were obtained for  $\Delta m > 1$ , while n-type samples were obtained for  $\Delta m < 1$ . Figure 2 shows the absorption spectra for various  $\Delta m$  in the vicinity of fundamental absorption edge at room temperature. It can be seen that the logarithm of absorption coefficient varies linearly with photon energy, and that the gradient of each curve decreases with an increase of  $\Delta m$ . Thus, the exponential tail in the absorption edge may be attributed to the defects in  $\text{CuInSe}_2$ .

1. J.A. Groenink and P.H. Janse, *Z. Phys. Chem.*, 110 (1978) 17.

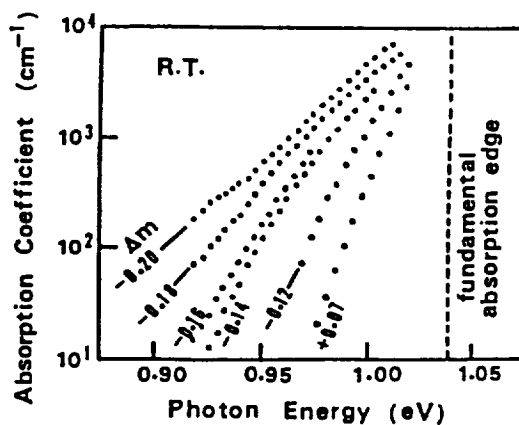


Figure 2. Exponential tail of the absorption edge for various  $\Delta m$

## SESSION 9C

### THE APPLICATION OF X-RAY TECHNIQUES TO PROBLEMS IN CRYSTAL SCIENCE

*K.J. Roberts*

Department of Pure and Applied Chemistry  
University of Strathclyde, 295, Cathedral Street  
Glasgow G1 1XL, UK and  
SERC Daresbury Laboratory, Warrington, WA4 4AD, UK

There has been an increasing awareness in recent years of the importance and utility of crystal characterisation techniques in aiding our understanding, definition and optimisation of crystallisation and related processes. For such applications X-ray based techniques are most useful in that they are non-destructive and can provide essential information to the crystal grower concerning bulk and surface micro-structure structure for a wide range of atomic correlation length scales.

In this paper a number of X-ray techniques using both laboratory and synchrotron sources are presented and include:

- EXAFS and its application to studies of ionically adsorbed habit modifiers and dopants in semiconductors;

- high resolution powder diffraction and its application to studies of polymorphism and phase separation in n-alkanes;
- X-ray topography and its application to probing the growth history of solution and flux grown crystals;
- surface fraction and X-ray standing waves and their application to studies of semiconductor surfaces.

In addition the use of high energy synchrotron radiation to probe crystal growth processes *in-situ* using energy dispersive diffraction will be reviewed through the example of studies of the crystallisation of long chain hydrocarbons from solution.

---

### REAL-TIME OBSERVATION OF STRESS-INDUCED DEFECT FORMATION AND MOVEMENT IN Si, GaAs AND CdTe SINGLE CRYSTALS

*R. Balasubramanian and W.R. Wilcox*

Center for Crystal Growth in Space  
Clarkson University, Potsdam, NY 13699, USA  
*G. Long*  
National Institute of Standards and Technology  
Gaithersburg, MD

The generation of slip-bands indicating motion of dislocations in Si, GaAs and CdTe single crystals was observed in real-time by synchrotron X-ray topography. Experiments were carried out in the temperature ranges 1023-1173 K, 673-873 K, and 373-673 K, for Si, GaAs and CdTe respectively. A high temperature tensile apparatus was constructed with provision for stressing 'dog-boned' shaped samples of single crystal. In Si and GaAs, dislocations were locally generated and immediately developed slip-band structures in the pre-yield stage of the stress-strain diagram. Consequently slip-band structures were observed over the entire sample at stresses corresponding

to the yield point of the material. It was not possible to observe the generation of the slip-bands in CdTe, since yield occurred very rapidly. Preliminary results suggest that the limiting stress permissible in the growth of single crystals is only a fraction of the critical resolved shear stress measured from the stress-strain curve. A more detailed analysis of the results is underway<sup>1</sup>.

---

<sup>1</sup>This work was conducted at beam-line X-23A3 of the National Synchrotron Light Source, Brookhaven National Laboratory, Upton, NY.

**A COMMON ORIENTING ACTION OF ELECTRICAL FIELD AND SUBSTRATE  
PATTERNING IN ARTIFICIAL EPITAXY (GRAPHOEPITAXY)**

*E.I. Givargizov, A.I. Pankrashov and L.A. Zadorozhnaya*  
Institute of Crystallography, USSR Academy of Sciences  
Leninsky pr. 59, Moscow 117333, USSR

Artificial epitaxy (graphoepitaxy) is a broadly-based phenomenon. Studies of its mechanisms have both fundamental and applied aspects [1]. Of particular interest is the case when a topographic relief and an electrostatic field are acting simultaneously.

In this paper, experiments are described on deposition of antimonium sulpho-iodide (SbSI) films onto substrates with and without striated microrelief under electrical field applied both parallel and normal to the substrates.

It was found, in some preliminary experiments, that the films deposited onto such substrates consisted of single crystallites with their C-axis oriented along the striations while, without the relief, the crystallites were randomly oriented. It was, further, found that, at least in the initial stages, the growth proceeded with participation of a liquid phase, under action of capillary forces. The crystallites floated and "moored" to the sides of the grooves [2,3].

When an electrical field of 2.5 kV/cm was applied parallel to the substrate having no relief, a significant part of the crystallites (up to 30%) became oriented along the field. Under similar conditions on striated substrates, the azimuthal orientation of the crystallites depended on the angle between the field vector and the direction of the striations. A maximal change of the orientation in comparison with non-field conditions was

observed when the field was perpendicular to the striations. Three sets of crystallites were observed in this case: those normal to the striations, and those with angles +67 or -67° relative to the striations.

Basing on the results obtained, an orientation mechanism is assumed for this case, namely: SbSI crystallites, being polarized, are arranged so that their C-axes are directed along the field, whereas tile crystallites are "nestled" by their {001} or {001} faces to the sides of the grooves.

When the field is perpendicular to the striated substrate, rather high ratio of the crystallites becomes oriented with their axis normal to the substrate, faces {121}, {211} and to {011} being parallel to sides of the grooves in accordance with the mechanism considered above.

1. E.I. Givargizov, "Oriented Crystallization on Amorphous Substrates," (Plenum Press, N.Y., 1991).
2. A.I. Pankrashov, L.A. Zadorozhnaya and E.I. Givargizov, *Soviet Phys.-Crystallogr.* 32, 429 (1987).
3. E.I. Givargizov, A.I. Pankrashov and L.A. Zadorozhnaya, *Heteroepitaxy of Dissimilar Materials*, eds. R.F.C. Farrow, J.P. Marbison, P.S. Peercy, and A. Zangwill, Proc. MRS 221 (MRS Press, Pittsburgh, PA 1991), pp. 123-128.

## FORMATION OF $Ge_{1-x}Si_x$ SOLID SOLUTION BY POWDER METALLURGY AND HOT-ISOSTATIC PRESSING

*J. Schilz and M. Langenbach*

German Aerospace Research Establishment (DLR), Institute for Materials Research  
P.O. Box 906058, W-5000 Köln 90, Germany

Ge-Si alloys have a large number of important applications in several fields, such as its use as thermoelectric material, extrinsic photodetectors, solar cells, substrate material for other semiconductor compounds, or monochromators for thermal neutrons. The latter two applications require highly perfect single crystals - an aim that has not been achieved up to now. As long as the use of  $Ge_{1-x}Si_x$  is concerned on its electronic properties, it is often sufficient to have a polycrystalline alloy.

In the case of the exploitation of heavily doped  $Ge_{1-x}Si_x$  alloys as thermoelectric material, it is even desirable to have a large amount of grain boundaries in order to decrease the thermal conductivity. Therefore, thermoelectric elements are often made of compacted, small sized germanium-silicon grains, which are achieved by ball milling of casted  $Ge_{1-x}Si_x$  and hot pressing.

This investigation on such "powder crystals" is motivated by the lack of understanding on the formation of powder metallurgically prepared  $Ge_{1-x}Si_x$  material. The present paper tries to shed light on the milling and compacting process, because these steps have received minimal attention to date. Therefore,

instead of using the usual preparation method, to mill an already casted and possibly doped  $Ge_{1-x}Si_x$  compound, we start from the pure elements Ge and Si, which are mechanically comminuted in a planetary mill together in the desired composition.

Objectives of the experiments include the observation of the mixing and possibly blending of the two constituents and the detection of solid state phases after a cold- or hot-pressing process. SEM investigations revealed the different microstructures of the Ge and the Si and by means of TEM we found that the lattice is partly amorphous. Each grain consists of Ge and Si regions on a typical length scale of 100 nm. X-ray diffraction showed a broadening of the peaks as a function of milling time. However, in contrast to earlier publications, the ball milling did not induce any compound formation. Hot-isostatic pressing and further heat treatment of the samples showed a formation of mixed crystal regions. Microhardness of the hot-pressed and tempered samples was measured. Additionally, electrical transport measurements were performed in order to find out the amount of impurities incorporated into the material during the whole preparation procedure.

## A NEW DEVELOPMENT OF LASER-HEATED PEDESTAL GROWTH TECHNIQUE

*S.Ja. Rusanov, I.A. Shcherbakov and E.V. Zharikov*

General Physics Institute Acad. Sci. USSR  
117342, Moscow Vavilov Str. 38, USSR

*G.R. Grigorian, I.N. Sisakian*

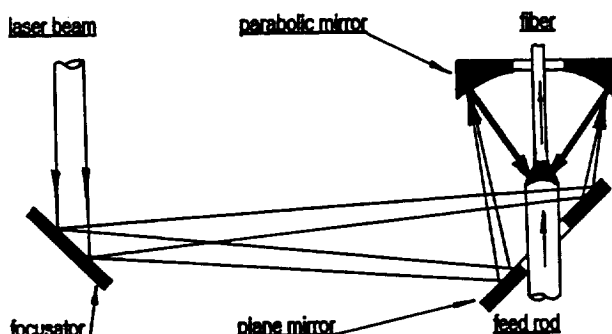
Central Bureau for Unique Instrumentation 117342, Moscow, Butterov Str. 15, USSR

Laser-heated minipedestal growth (LHPG) method is universal technique for growth of variety single crystalline fibers [1]. The paper presents new original technical development of LHPG technique. The growth apparatus with heating arising from continuous-wave  $CO_2$ -laser with power 90W has been made.

The main problem of practical realization of LHPG technique is creation of axial symmetry heating of pedestal. This task has been solved by using of special optical element (so called focusator) in combination with parabolic mirror. The focusator transforms the nonuniform cross-section of laser beam into a ring with high grade of uniformity of laser power density. Then the parabolic mirror forms the cone beam which meet at the end of initial feed rod (see figure).

The advantage of this version of LHPG-technique is that complicative optical system is exchange by only one element (focusator), which do not need the fine adjusting and effectively works independently on mode structure of laser emission.

Single fibers of sapphire and doped rare-earth scandium garnets have been successfully grown by this apparatus. The fibers have diameter from 100 to 300  $\mu m$  and length up to 300 mm. Details of apparatus design and features of fibers growth will be presented.



R.S. Feigelson "Opportunities for Research on Single-crystal Fibers." *Material Since and Engineering*, B1, (1988) p67-75.

THE INFLUENCE OF  $Pb^{2+}$  ION ON THE RADIATION  
DISTANCE OF  $BaF_2$  CRYSTAL

*G. Chen, S.X. Ren, H. Xiao, S.Q. Man and J.Q. Zhang*

Beijing Glass Research Institute

Dongdai 1, Chongwenmenwai, Beijing 100062, P.R. China

It is well known that  $Pb^{2+}$  can make the absorption at 205nm in  $BaF_2$  crystal which is harmful to export of the fast component of  $BaF_2$  crystal. This ion, we studied recently, is also deteriorated to the radiation resistance of  $BaF_2$  crystal.

There is an obvious difference of  $Pb^{2+}$  content between Pb-containing and pure  $BaF_2$  crystals but other metal ions impurities, which were cut from same crystal and  $Pb^{2+}$  ion was located at the bottom of crystal. The content of  $Pb^{2+}$  of Pb-containing sample was about 4.8ppm. We could find an absorption peak at 205nm in this Pb-containing crystal. Comparing with pure crystal, the Pb-containing one caused a strong radiation

damage. It is obvious that this difference was not the result of other metal ions impurities. The fluorescence spectra report that the valence of  $Pb^{2+}$  was not changed after  $\gamma$ -ray irradiated, and it is hardly possible of lattice vacancy introducing when  $Pb^{2+}$  occupy sides of  $Ba^{2+}$ , because the ion radius of  $Pb^{2+}$  and  $Ba^{2+}$  are very similar and their valences are same. We consider that the remains of  $Pb^{2+}$  can lead to increase content of  $O^{2-}$  because of polarize between them. The vacancy of anion, which is the one of basic factors of nature of color centres, will be reached when  $O^{2-}$  occupying the sides of  $F^-$  ion. The analysis result about oxygen content by TEM has proved this point.

## SESSION 9D

### INVESTIGATIONS OF THE EFFECTS OF SOME ADDITIVES ON THE CRYSTALLIZATION OF TETRAHYDRATE SODIUM PERBORATE

*C. Frances, B. Biscans, N. Gabas and C. Laguerie*

*E.N.S.I.G.C.-LGC (URA CNRS 192)*

*Chemin de la Loge - 31078 Toulouse Cedex France*

Sodium perborate, commercially available as a tetrahydrate and a monohydrate, is the most widely used solid peroxygen compound. Its main applications are in safety bleach formulations, detergents and tooth powders. It is also extensively used in Europe in washing powders formulations.

The work is especially concerned with tetrahydrate sodium perborate (SPB). SPB is produced by reactive crystallization between aqueous solutions of sodium metaborate (SMB) and hydrogen peroxide. Crystals of a good quality with respect to their chemical stability, morphology, shape and size are required. In order to improve these properties various additives have been used. Additives as well as impurities in a system can modify the growth rates of crystals grown from solutions and hence the characteristics of the crystals. So, in order to analyse the effect of some additives on the crystallization of SPB, crystal growth experiments have been carried out in a batch fluidized bed crystallizer.

In industrial processes, the reaction described above is often performed with an excess of SMB with respect to stoichiometry. So the effect of SMB on the solubility and the crystallization of SPB have been first tested. It has been observed that SMB drastically affects the solubility of SPB in water. For concentrations of SMB lower than 3% in mass, the effect of the

common ion  $\text{Na}^+$  is predominant and provokes a decrease of the solubility by moving the chemical equilibrium. For higher concentrations of SMB, the decrease of the activity coefficients of ionic species becomes the main factor and reverses the tendency. Related to this, SMB also modifies the growth rate of SPB crystals, exerting an inhibiting effect.

Then, the influence of various kinds of mineral additives, surfactants and a polymer on growth rate have been investigated. These additives are either impurities usually present in commercial product, or additives known as crystallization modifiers. The retarding action observed in the presence of magnesium sulphate as additive and in the presence of a polymer has been interpreted in terms of a Langmuir-type adsorption isotherm. It has been concluded that these additives are adsorbed on active growth sites on the faces of the crystals. The accelerating effect obtained with aluminum sulfate and cetyltrimethyl ammonium bromide (CTAB), a cationic surfactant, is supposed to be related to an accelerating effect on nucleation and agglomeration processes. Habit modification is observed with crystals grown from solutions containing trace amounts of CTAB. In presence of this additive crystals have a quite regular and spherical shape whereas they have a dendritic habit without additive.

### GROWTH OF GYPSUM

#### III. INFLUENCE AND INCORPORATION OF TRIVALENT IONS

*C.H. de Vreugd, G.J. Witkamp\* and G.M. van Rosmalen*

*Delft University of Technology, Leeghwaterstraat 44, 2628 CA Delft*

*The Netherlands*

The growth of gypsum ( $\text{CaSO}_4 \cdot 2\text{H}_2\text{O}$ ) has been performed by the constant composition technique in 0.1 M  $\text{NaNO}_3$  at 25 °C and by continuous crystallization experiments in 1 M  $\text{NaNO}_3$  solutions.

The effect of lanthanide, chromium and chromate ions on the growth kinetics was studied as well as the uptake of these impurities and of cadmium ions in the crystals. In addition the adsorption of  $\text{La}^{3+}$  on gypsum was studied.

The growth of gypsum is retarded by lanthanide ions present in the solution as impurities. The crystal faces show macrostep formation. At relative supersaturations of 0.2 the growth retarding influence of the ions decreases in the order  $\text{La}^{3+} \approx \text{Ce}^{3+} \approx \text{Eu}^{3+} > \text{Er}^{3+} > \text{Cr}^{3+} > \text{Cr}_2\text{O}_7^{2-}$ , with a maximal difference of a factor 10 between the blank and  $\text{La}^{3+}$  at a

concentration of  $3 \cdot 10^{-4}$  M. At increasing supersaturations this difference becomes smaller and finally disappears at  $\sigma=1$ . The uptake of lanthanides increases with increasing ionic radius, with a maximum for  $\text{Ce}^{3+}$ . The sequences of growth retardation performance and uptake of the ions are therefore roughly similar. At higher supersaturations the uptake becomes higher.

From the growth retardation as a function of the  $\text{La}^{3+}$  concentration an adsorption energy of 30 kJ per mole was calculated. From adsorption experiments no adsorption energy could be derived.

The incorporation of  $\text{Cd}^{2+}$  ions in the presence of lanthanides behaves similarly as without these ions.

\*Author to whom correspondence should be addressed.

CHARACTERISING THE EFFECT OF GROWTH CONDITIONS AND CRYSTAL  
HABIT ON THE DISTRIBUTION OF IMPERFECTIONS AMONGST  
POPULATIONS OF CRYSTALS

C.J. Price

Separation Processes Service, AEA Technology  
Harwell Laboratory, Didcot, Oxfordshire, OX11 ORA UK

The variation of crystal habit with growth conditions is widely documented. However the variation of the distribution of gross imperfections amongst populations of crystals grown from solution is much less well documented. This paper seeks to examine how the frequency of twinning, agglomeration and breakage varies with growth temperature and solution purity.

The material selected for this study was copper sulphate pentahydrate. It has been shown that the habit of near perfect crystals of copper sulphate changes significantly with both the presence of impurities and the growth temperature. (Price and Hallas 1990). The crystals characterised in this study were grown isothermally at a range of temperatures from both pure and impure solutions. The crystals were segregated into size fractions by sieving. These sieve fractions were then further segregated by hand into six defect categories; near perfect single crystals, crystals with a small adhering fragment, twinned crystals, agglomerates, broken single crystals and agglomerate fragments.

For each sieve fraction the number and mass distributions and volume shape factors of each defect category was determined. An overall volume shape factor was also determined.

The populations of crystals grown from impure solution contained significantly more imperfect crystals than those grown from pure solution. Amongst the crystals grown from impure solution the proportion of imperfect crystals decreased

as the growth temperature increased. This finding was unexpected since the crystal habit becomes more plate-like and apparently more fragile at higher temperature. There was also variation in the number and type of imperfections with crystal size for crystals grown under near identical conditions: the proportion of near-perfect crystals decreased with decreasing size. This was usually balanced by a corresponding increase in the number of agglomerates.

During this study a considerable body of data has been gathered allowing the causes of these variations in imperfection distribution to be explored. The variation in the imperfection distribution amongst populations of crystals has significant implications for the users of crystallization as an industrial separation technique. Two areas are worthy of specific mention; the purity of the product is likely to be influenced by imperfect crystals through changes in the solid-liquid separation and washing characteristics. The product's performance in subsequent processing stages will also be affected by differences in the imperfection distribution.

---

Price, C.J. and Hallas, N.J., "The Influence of crystal habit and size measurement and its implications for deriving kinetic parameters." p 583-588, Industrial Crystallization '90, Proceedings of the 11th Symposium on Industrial Crystallization, Ed. A. Mersmann, Garmisch-Partenkirchen 18-20th September 1990.

## ADSORPTION BEHAVIOUR OF POLYELECTROLYTES IN RELATION TO THEIR GROWTH INHIBITING PERFORMANCE

*M.C. van der Leeden and G.M. van Rosmalen*  
Delft Technical University, Laboratory for Process Equipment  
Leeghwaterstraat 44, 2628 CA Delft, The Netherlands

Polycarboxylate-type additives are commonly applied for the growth retardation of inorganic or mineral salts. Although preferential adsorption of a growth inhibitor at the crystal surface is known to be an essential step in its specific performance, the precise nature of the various factors influencing this step and the role they play in the adsorption process are not yet fully disclosed. Important factors which can be distinguished in the adsorption process are the level and rate of adsorption. These factors are influenced by parameters as type and strength of the bonds between mineral ions and functional groups of the inhibitor, their electrostatic interaction, the inhibitor configuration, and the matching of the interatomic distances and orientation of the lattice ions with the functional groups of the inhibitor.

For two polyphosphinoacrylates PPAA-I ( $M_w=3800$ ) and PPAA-II ( $M_w=1100$ ), and a random copolymer of maleic acid and vinylsulphonic acid PMA-PVS ( $M_w=1730$ ), the level of adsorption on  $\text{BaSO}_4$  has been determined as a function of time and concentration. Their adsorption levels and adsorption rates have been related to the growth inhibiting effectiveness of

these compounds in  $\text{BaSO}_4$  crystallisation. The adsorption plateau values of the best growth retarder PMA-PVS and the moderate inhibitor PPAA-II appear to be only slightly different, but the time needed to establish plateau coverage is considerably shorter in case of PMA-PVS. It is found that the adsorption rate of PPAA-II interferes with the attachment rate of  $\text{BaSO}_4$  growth units under the experimental conditions of initial supersaturation ratio  $S=5.6$ ,  $\text{pH}=5$  and  $t=25^\circ\text{C}$ .

To find out whether matching between the inhibitor molecules and the crystal surface layer plays a role in its performance, the shape and morphology of  $\text{BaSO}_4$  crystals were examined after long-term growth experiments in the presence of PMA-PVS and PPAA-II. The development of {011} and {101} faces in the presence of PMA-PVS points at easy replacement of lattice sulphate ions with one S-O bond orientated perpendicular to the crystal surface by sulphonate ions of PMA-PVS. In the presence of PPAA-II, striations are observed in <010> directions which might be related to fitting of interatomic lattice distances by the mutual distances of the functional groups of the inhibitor.

---

## CRYSTAL GROWTH MODIFIERS FOR BARITE AND GYPSUM: BINDING MOTIFS AT CRYSTAL SURFACES

*S.N. Black, L.A. Bromley, D. Cottier, R.J. Davey, B. Dobbs and J.E. Rout*  
Research and Technology Department, ICI Chemicals and Polymers Limited  
The Heath Runcorn Cheshire WA7 4QD, UK

The use of crystal morphology as an assay for specific interactions between crystal surfaces and auxiliary molecules has received considerable attention in the last decade. Thus, in the case of molecular crystals, it is now possible to design tailor made additives for the control of morphology and polymorphic form (1) based on an appreciation of stereo-chemical recognition factors which operate at specific crystal surfaces (2). In the parallel field of recognition at inorganic surfaces research has been directed mainly towards an understanding of the ways in which organic molecules control biomimetic processes. For example the role of simple carboxylic acids and carboxylate rich macromolecules in the mineralisation of calcium carbonate has been extensively studied (3,4). The more general aspects of the role of stereochemistry at the surface of inorganic crystals has received little attention since the earlier work of Whetstone (5) on habit modification by dyes. In this

contribution we examine the stereochemical nature of specific interactions between organic phosphonate molecules and the mineral phases barite and gypsum using a combination of morphological data and molecular modelling. The data illustrate the importance of charge, geometry, stereochemistry and H-bonding as driving forces for recognition at inorganic surfaces.

1. R.J. Davey, L.A. Polywka and S.J. Maginn in 'Advances in Industrial Crystallisation' Butterworths London 1991.
2. L. Addadi, Z. Berkovitch-Yellin, I. Weissbuch, M. Lahav and L. Leiserowitz, *Topics in Stereochemistry* **16** (1986) 1.
3. S. Mann, J. Didymus, N.P. Sanderson, B. Heywood and E.J. Aso Sanper, *J Chem Soc Farad Trans* **86** (1990) 1873.
4. L. Addadi and S. Weiner, *Proc Natl Acad Sci USA* **82** (1985) 4110.
5. J. Whetstone *Nature* **168** (1951) 663.

## THE STUDY OF TRANSPORT PHENOMENA IN ZEOLITE CRYSTAL GROWTH

*Simon Ostrach, Yasuhiro Kamotani and Hao Zhang*

Department of Mechanical and Aerospace Engineering  
Case Western Reserve University, Cleveland, Ohio 44106, USA

Zeolite synthesis is a unique crystal growth process which usually takes place within an amorphous solid gel plus aqueous solution. The growth mechanism is studied by carefully examining the structure of the gel portion and the interaction between growing zeolite crystals and the diminishing solid gel. It is found that a white and opaque portion containing amorphous solid gel, crystals and aqueous solution does not settle under gravity as it appears to be. Instead, it shrinks to the bottom of the hydrothermal reactor leaving the clear solution above it due to depletion of the flocculated gel particles. Based on the assumption of solution phase nucleation and crystallization, a correlation for the shrinkage is derived. Zeolite A was synthesized in our lab since it is a typical example of the solution phase mechanism. The observed shrinkage curves agree very well with the derived correlation. The curves basically consist of two exponentially decayed stages correspond-

ing to induction and crystallization, because one has very different activation energy from the other. According to our experiments, secondary nucleation which has been believed to be one of the detrimental effects due to crystal sedimentation occurs only within the shrinking gel portion. Based on the correlation and the calculation of mass transfer rate for an individual zeolite, a non-dimensional parameter is suggested as a criterion for the occurrence of secondary nucleation. In addition to other physical variables, there are two variables upon which the parameter is strongly dependent, the height of the reaction mixture (geometry) and the number of nuclei per unit volume (nucleation rate). This parameter can serve as a constraint when zeolite crystal growers intend to minimize the number of nuclei in order to produce larger resultant zeolites. Additionally, scaling analysis is used to compare zeolite crystal growth under microgravity with that under centrifugal force.

## AUTHOR INDEX

M. Abdulkhadar – 183  
 Sou Abe – 174  
 H.N. Acharya – 24  
 Nobuyasu Adachi – 164  
 Joseph A. Adamski – 41  
 I. Akasaki – 137  
 Igor Aksenov – 139  
 C. Albers – 162  
 M. Albrecht – 20  
 J. van D. Alexander – 127  
 H. Amano – 137  
 G. Ben Amar – 135  
 A.C. Anderson – 72  
 T.J. Anderson – 68  
 M. Ando – 68  
 S. Ando – 188  
 F. W. Anger – 112  
 D. Aquilano – 157  
 D. Arivuoli – 25  
 L. Arizemendi – 133  
 B. Armas – 137  
 A.F. Armington – 132  
 William A. Arnold – 100  
 H. Asano – 59  
 B. Aspar – 137  
 L.J. Atherton – 85  
 N. Azema – 137  
 M. Azoulay – 163  
 M.A. Azouni – 49

Daniel W. Bakken – 164  
 R. Balasubramanian – 189  
 A.A. Ballman – 10  
 K. Balzuweit – 47  
 K. Balzuweit – 48  
 A.N. Baraboshkin – 142  
 I.V. Barmin – 163  
 D.L. Barrett – 138  
 K. Baskar – 23  
 E. Bauser – 118  
 Roger F. Belt – 9, 105  
 H. Bender – 121  
 P. Bennema – 32, 48, 53, 155  
 K.W. Benz – 67, 162, 163  
 E. Beregi – 53  
 E.M. Berends – 4  
 G.W. Berkstresser – 71  
 H.L. Bhat – 175  
 K. Bickmann – 134  
 S. Biderman – 135  
 R.M. Biefeld – 89  
 B. Biscans – 193  
 G. Bisshopink – 67  
 S.N. Black – 64, 195  
 David F. Bliss – 41  
 L.A. Boatner – 176  
 G. Bocelli – 134

E.S. Boek – 173  
 A.M. Bonnot – 169  
 A. Boothroyd – 120  
 Alex Borschhevsky – 141  
 M.M.R. Boutz – 111  
 R. Boyne – 162  
 C.D. Brandle – 71, 108  
 S. Brandon – 79, 85  
 K. Brattkus – 130  
 R.J. Braun – 130  
 S. Brennan – 77  
 W.I. Briels – 173  
 L.A. Bromley – 195  
 Robert A. Brown – 81, 132  
 E. Brück – 11  
 O.S.L. Bruinsma – 4  
 R. Burrows – 19  
 K. Byrappa – 136, 177  
 P. Byszewski – 73

M.A. Caballero – 133  
 E. Cabrera – 4  
 Thierry Caillat – 141  
 G. Calestani – 134  
 D. Camel – 79  
 Sauveur Candau – 143  
 Torbjörn Carlberg – 99  
 Frederick Carlson – 100  
 Warren E. Carlson – 55  
 Louis G. Casagrande – 161  
 A. Cassanho – 74, 84  
 Carlos Castro – 161  
 Z. Cecil – 70  
 V.C. Cestone – 92  
 Bruce H.T. Chai – 83  
 Arnon Chait – 100, 154  
 B.C. Chakoumakos – 92, 176  
 J.P. Chaminade – 84  
 Chen Changkang – 120  
 G. Chen – 192  
 Huanchu Chen – 12  
 Men-Chee Chen – 161  
 L.K. Cheng – 10  
 L.T. Cheng – 10  
 T.A. Cherepanova – 33  
 A.A. Chernov – 54, 129  
 A.I. Chernov – 123  
 H. Chin – 182  
 T.P. Chin – 117  
 V.W.L. Chin – 88  
 Zheng Chongzhong – 10  
 Jason K. Chow – 50  
 A.J.S. Chowdhury – 121  
 W.J. Choyke – 138  
 Luo Chuhua – 10  
 T.F. Ciszek – 19, 187  
 J.E. Clemans – 42

B. Cockayne – 48  
 R. Collongues – 111  
 C. Combescure – 137  
 S.R. Coriell – 99  
 J. Emery Cormier – 132  
 L. Cot – 177  
 D. Cottier – 195  
 John E. Creamer – 105  
 F. Cyrot-Lackmann – 169

A. Dabkowski – 73  
 H. Dabkowski – 73  
 R.J. Davey – 64, 195  
 S.H. Davis – 130  
 S.R. Davis – 130  
 William J. Debnam, Jr. – 81  
 L.D. DeLoach – 85, 86  
 Robert C. DeMattei – 147, 186  
 I.I. Derby – 85  
 J.J. Derby – 79  
 William J. DeSisto – 92  
 J.J. DeYoreo – 85  
 S.A. DiCarolis – 91  
 E. Dieguez – 133  
 V.A. Dmitriev – 138  
 B. Dobbs – 195  
 G.A. Dolgikh – 104  
 Michael Dudley – 161  
 J. Durand – 137, 177  
 Stephen D. Durbin – 55  
 B.V. Umesh Dutt – 177

Raymond S. Eachus – 21  
 T. Eckermann – 169  
 R.J. Egan – 88  
 A.V. Egorov – 163  
 Minoru Eguchi – 17  
 C. Eiche – 162  
 L.G. Eidelman – 25  
 Y. Einav – 135  
 S. Endo – 188  
 S. Erdei – 112  
 V.O. Esin – 142  
 N.O. Esina – 142  
 Leon Esterowitz – 105

R.E. Fahey – 72  
 Thomas Fanning – 161  
 S. Farkas – 146  
 W. Faschinger – 185  
 J.J. Favier – 79  
 R. Feenstra – 92  
 Luo Fei – 10  
 Robert S. Feigelson – 11, 22, 91, 145,  
     147, 186  
 D. Feil – 173  
 Martin Fejer – 65

## AUTHOR INDEX (Cont'd)

H. Feldstein – 163  
A.I. Feonychev – 104  
S. Ferreira – 185  
A. Figueras – 137  
D. Fiorani – 134  
K.J. Fischer – 134  
Jean-Pierre Fleurial – 141  
R. Fornari – 41  
C. Frances – 193  
V.J. Fratello – 108  
Archibald L. Fripp – 81  
Emmanuel Fritsch – 170  
K. Fujikawa – 50  
J. Fujioka – 4  
H. Fujiwara – 16  
T. Fujiwara – 16  
T. Fukuda – 39, 44, 61, 106, 135, 185  
P.H. Fuoss – 77  
Yasunori Furukawa – 37  
Yoshinori Furukawa – 154  
I. Fusegawa – 14, 18  
  
N. Gabas – 193  
S. Gali – 177  
M. Gally – 4  
K.V. Gamayunov – 122, 123  
R. Ganesha – 25  
J.P. Garandet – 79  
A. Garcia – 84  
Juan Manuel García-Ruiz – 80  
D. Gazit – 135  
R.M. Geertman – 146, 155  
J.M. Gel'fgat – 163  
K.C. George – 183  
Richard Giege – 143  
George H. Gilmer – 3, 30  
E.I. Givargizov – 190  
M.E. Glicksman – 23, 153  
M. Göbbels – 107, 109  
G.S. Gopalakrishna – 177  
V.I. Goriletsky – 25  
R.J. Gorman – 45  
J.E. Greedan – 73  
G.R. Grigorian – 191  
B. Groen – 146  
R. Gutmann – 35  
  
S.M. Haile – 178  
S. Halász – 146  
P. Halfpenny – 64  
R. Hamacher – 63  
J.C. Han – 100  
Th. Hangleiter – 21  
Meckie T. Harris – 132  
E. Hartmann – 53  
J. Hatano – 50  
Y. Hayakawa – 68  
  
H. Hayashi – 59  
Shigeyuki Hayashi – 94  
T. Hayashi – 38  
S. Hazell – 120  
B. Hendriksen – 145  
T. Henningsen – 63  
R.L. Henry – 45, 92  
N. Herres – 169  
Taketoshi Hibiya – 17  
Matthias Hierlemann – 87  
Robert M. Hilton – 41  
Katsuyuki Hirai – 15  
A. Hirata – 61  
R. Hiskes – 91  
H.M. Hobgood – 138  
J.W. Hodby – 120  
D. Hofmann – 103  
D.M. Hofmann – 162  
P. Hofmann – 163  
P.H. Holloway – 68  
Shigeru Honma – 141  
F.K. Hopkins – 63  
R.H. Hopkins – 63, 138  
Hiroyuki Horiuchi – 94  
A. Horowitz – 135  
Keigo Hoshikawa – 39, 44, 106, 135, 185  
C.C. Hsu – 128  
Baibiao Huang – 89  
Y. Huang – 131  
J. Huinink – 183  
J. Hulliger – 35, 62  
D.A. Huntley – 130  
D.T.J. Hurle – 1  
  
E. Iino – 14, 18  
Yoshihiro Imamura – 88  
Y. Imashimizu – 49  
S. Inoto – 12  
P. Imperatori – 77  
T. Inada – 43  
S. Inami – 16  
Kimio Inaoka – 56  
John B. Ings – 9  
Masahiro Inoue – 164  
Tetsuo Inoue – 94  
I.P. Ipatova – 90  
T. Irie – 188  
K.G. Irvine – 138  
Manabu Ishimaru – 115  
Yoshio Ishizawa – 140, 141  
Kohei Ito – 37  
A.L. Ivanov – 123  
N. Iyi – 38, 59  
Alexander F. Izmailov – 7  
F. Izumi – 59  
Teruo Izumi – 120  
  
Kenneth A. Jackson – 30  
K. Jacobs – 165  
R.D. Jacowitz – 91  
Richard H. Jarman – 36  
R. Jayavel – 95  
I. Jenkins – 138  
H.P. Janssen – 74, 84  
Minhua Jiang – 89  
Quanzhong Jiang – 12  
E. Jilek – 119  
Barry C. Johnson – 36  
O.C. Jones – 23  
A.S. Jordan – 42, 114  
Li Jun – 10  
T. Jung – 103  
P. Juza – 185  
  
Bart Kahr – 50  
Gu Kaihui – 10  
C. Kaito – 181, 182  
Koichi Kakimoto – 17  
E. Kaldis – 21, 22, 119  
J.P. Kalejs – 13  
A. Kamata – 186  
Yutaka Kamimura – 140  
Yasuhiro Kamotani – 196  
S. Kan – 39  
H. Kanai – 19  
Shiro Karasawa – 168  
Norbert Karl – 61  
J. Karpinski – 119  
Masanobu Kasuga – 160  
Tomoji Kawai – 93  
Steven W. Keller – 119  
R. Kern – 157  
Giyuu Kido – 164  
F.-M. Kiessling – 165  
F.H. Kiessling – 165  
C.T. Kim – 23  
M. Kimura – 19  
S. Kimura – 38, 40, 59, 107, 109  
K. Kincses – 146  
Thomas A. Kinney – 81  
P.D. Kirchner – 117  
Shin'ichi Kishimoto – 174  
D.W. Kisker – 77  
Kenji Kitamura – 37  
K. Kitamura – 38, 59  
P. Klavins – 95  
C. Klemenz – 75  
R. Klett – 163  
H.J.F. Knops – 183  
David J. Knuteson – 81  
Ken Kobayashi – 168  
S. Kobayashi – 16  
U. Köbler – 134

## AUTHOR INDEX (Cont'd)

Z. Kodejs – 70  
J. Kohout – 70  
P. Koidl – 169  
Hironao Kojima – 132  
E.N. Kolesnikova – 82  
Hiroshi Komatsu – 94  
A. Refik Kortan – 47  
F.K. Koschnick – 21  
Miroslav Kotrla – 33  
P.N. Kotru – 72  
S. Kou – 80  
H. Kouta – 12  
Mariusz J. Krasinski – 175  
M. Kremers – 48  
W.F. Krupke – 85, 86  
T. Kubo – 16  
Noriaki Kubota – 174  
Thomas F. Kuech – 87  
S. Kuma – 43  
M. Kumagawa – 68  
Satoshi Kumon – 174  
Douglas A. Kurtze – 130  
Noriyuki Kuwano – 115  
Y. Kuwano – 12  
Yu.G. Kuznetsov – 54, 57  
W.L. Kway – 85, 86

C. Laguerie – 193  
M. Lahav – 7  
F.J. Lamelas – 77  
C.W. Lan – 80  
M.D. Lan – 95  
M. Langenbach – 191  
K. Langer – 107  
John J. Larkin – 132  
M. Larrousse – 101  
David J. Larson, Jr. – 161  
R.A. Laudise – 178  
F. Leccabue – 134  
H.S. Leipner – 165  
L. Leiserowitz – 7  
A.M. Lejus – 111  
A.G. Leonov – 70  
Marten Levenstam – 99  
Andrea C. Levi – 33  
B. Lexow – 163  
Lin Li – 160  
Li Lian – 6, 15  
B.W. Liang – 117  
W.Y. Liang – 121  
Pok-Kai Liao – 161  
C. Lin – 117, 133  
C.T. Lin – 121  
I.T. Lin – 23  
J.Z. Liu – 95  
Shiwen Liu – 89  
Xiang-Yang Liu – 32

G. Long – 189  
T. Lopez-Rios – 169  
J. Martínez-López – 133  
Bernard Lorber – 143  
Douglas H. Lowndes – 92  
Z. Lu – 91

Xiaoyan Ma – 36  
M.L. MacCalman – 145  
R.M. Macfarlane – 84  
Hiroshi Machida – 135  
L. Magaud – 169  
Alexander J. Malkin – 144  
V.G. Malyshkin – 90  
S.Q. Man – 192  
R.A. Manente – 108  
T. Marek – 118  
S.A. Markgraf – 109  
Linda N. Marquez – 119  
S.P. Marsh – 153  
Don Di Marzio – 161  
V.A. Maslov – 11  
A.Yu. Maslov – 90  
B. Mathis – 169  
D.C. Matioukhin – 163  
Ichiro Matsubara – 93  
Syo Matsumura – 115  
R.C. De Mattei – 22, 145  
R. Mazelsky – 63  
E.M. McCarron, III – 10  
W. Gordon McDugle – 21  
G.B. McFadden – 99  
J.P. McHugh – 138  
Alexander McPherson – 144  
H. Meekes – 47, 48, 146  
C.L. Melcher – 108  
G.J. Merchant – 130  
B.K. Meyer – 90, 162  
Kohji Mimura – 56  
L.M. Minchenko – 142  
Ma-Ben Ming – 127  
Nai-Ben Ming – 3, 144, 156  
S. Miyahara – 16  
Satoru Miyashita – 94  
S. Miyazawa – 74  
Iwao Mogi – 155  
Lisa A. Monaco – 144  
E.M. Monberg – 42  
J. Gomez-Morales – 177  
Frantisek Moravec – 68  
Tetsushi Mori – 174  
Kazuo Moriya – 15  
P.R. Morley – 64  
P.A. Morris – 9  
S. Motakef – 100, 133  
S. Motoyama – 19  
M. Mühlberg – 162

M. Mukaida – 74  
Georg Müller – 27, 31, 101, 103  
W. Müller-Sebert – 169  
Jean-Pierre Munch – 143  
H. Murakami – 137  
B.T. Murray – 99  
P. Murugakoothan – 95  
Boyan Mutaftschiev – 51  
A.Z. Myaldun – 104  
Allan S. Myerson – 7

Yasuaki Nakagawa – 155  
Yuichi Nakamura – 120  
H. Nakanishi – 188  
Nobuhito Nango – 15  
Ranga Narayanan – 81  
Kurt Nassau – 171  
Charles C. Nelson – 110  
M. Neubert – 162, 165  
H.S. Newman – 92  
Daiqin Ni – 131  
Dumitru Nicoara – 102  
Irina Nicoara – 102  
T. Nishinaga – 97  
Fumio Nitanda – 37  
Yukio Nobe – 107  
Shigetaka Nomura – 187  
P.E.R. Nordquist – 45  
Robert H.D. Nuttall – 21  
Marianne Nyman – 50

Kozo Obara – 179  
Matsuyuki Ogasawara – 88  
Tomoya Ogawa – 6, 15  
Tadashi Ohachi – 156  
K. Ohtsuka – 181, 182  
Toshio Okabe – 5  
Yasunori Okano – 39, 44, 61, 185  
Tsugio Okazaki – 180  
Kensuke Oki – 115  
Susumu Okubo – 155  
L.A. Olkhovaya – 11  
Myra T. Olm – 21  
P. Omling – 90  
A. Oppenländer – 84  
V.V. Osiko – 11, 123, 149  
M.S. Osofsky – 92  
Simon Ostrach – 196  
A.G. Ostrogorsky – 31, 101  
Fermín Otálora – 80  
Shigeki Otani – 140, 141  
T. Ozawa – 68

P. Pacák – 70  
A. Pajaczkowska – 73  
T. Pal – 24  
A.I. Pankrashov – 190

## AUTHOR INDEX (Cont'd)

A.A. Pankratov – 142  
 P.J. Parbrook – 186  
 B. Pathaney – 68  
 D.A. Payne – 131  
 S.A. Payne – 85, 86  
 C.A. Peterson – 108  
 G. Pétré – 49  
 P.M. Petroff – 113  
 G.D. Pettit – 117  
 M. Piechotka – 21, 22  
 V. Pines – 154  
 T.M. Pollak – 64  
 Chungdee Pong – 186  
 A.K. Pradham – 120  
 C.J. Price – 194  
 V.G. Protsenko – 25

Xie Qiuixiang – 10  
 Gregory J. Quarles – 105

A.V. Radkevich – 25  
 K.S. Raju – 24  
 P. Ramasamy – 23, 25, 95  
 J.O. Ramey – 176  
 Mark H. Randles – 105  
 C.R. Venkateswara Rao – 95  
 R.J. Raymakers – 11  
 Ashok K. Razdan – 72  
 Liya L. Regel – 100  
 Zofia U. Rek – 140  
 Hongwen Ren – 89  
 S.X. Ren – 192  
 Sun Ren-ying – 133  
 R.I. Ristic – 174, 175  
 R.J. Ristic – 176  
 H. Riveros – 4  
 D.H. Roberts – 85  
 K.J. Roberts – 145, 189  
 A. Robertson – 114  
 R. Rodríguez – 177  
 R. Rodríguez-Clemente – 137  
 Franz Rosenberger – 127, 144  
 V. Rosicka – 70  
 J.E. Rout – 195  
 R.K. Route – 11  
 M. Rubbo – 157  
 P. Rudolph – 162  
 C. Ruiz-Mejia – 4  
 B. Rupp – 86  
 S.Ja. Rusanov – 191  
 S. Rusiecki – 119

V. Sagredo – 134  
 Yahachi Saito – 180  
 Yukio Saito – 127, 128  
 Y. Saito – 181, 182

Shigeru Saito – 5  
 Yasuyuki Saito – 45, 69  
 Kazufumi Sakai – 6  
 M. Sakamoto – 39  
 Tomoko Sakiyama – 127  
 B.C. Sales – 176  
 M. Salk – 163  
 K. Sangwal – 173  
 M.T. Santos – 133  
 T. Sasaki – 106  
 M. Sasaura – 74  
 H. Sato – 50  
 Katsuaki Sato – 139  
 Kiyotaka Sato – 56  
 Masayoshi Sato – 37  
 G.A. Satunkin – 70  
 B.V. Saunders – 99  
 S. Scharl – 101  
 Hans J. Scheel – 71  
 H.J. Scheel – 75  
 J. Schilz – 191  
 F. Scholz – 90  
 E. Schönherz – 121  
 Y. Schumacher – 62  
 P.G. Schunemann – 64  
 J.S. Schweitzer – 108  
 C.R. Schwerdtfeger – 187  
 J. Sedlacek – 70  
 R.G. Seidensticker – 138  
 C. Sekar – 95  
 Robert F. Sekerka – 125  
 H.I. Sell – 101  
 A.S. Senchenkov – 163  
 L.C. Sengupta – 122  
 S. Sengupta – 74, 122  
 S.L. Sharma – 24  
 E.A. Shcherbakov – 11  
 I.A. Shcherbakov – 191  
 V.A. Shchukin – 90  
 K.V.K. Shekar – 136  
 B. Shekunov – 174, 176  
 R.N. Shelton – 95  
 Dezhong Shen – 36, 131  
 J.N. Sherwood – 63, 64, 174, 175, 176  
 Fan Shi-ji – 133  
 M. Shibata – 43  
 James E. Shigley – 170  
 Wataru Shimada – 154  
 K. Shimamura – 106  
 Yuh Shiohara – 120  
 T. Shripathi – 175  
 P. Sickinger – 163  
 T. Siegrist – 178  
 G.S. Simpson – 63  
 D. Sinerius – 162  
 N.B. Singh – 63

I.N. Sisakian – 191  
 H. Sitter – 185  
 Mohammed Skouri – 143  
 L.K. Smith – 85, 86  
 Yongyuan Song – 12  
 M.Z. Sorki – 163  
 J-M. Spaeth – 21  
 M.G. Spencer – 138  
 B.V. Spitsyn – 167  
 Arthur J. Socha, Sr. – 164  
 Angelica M. Stacy – 119  
 L.A. Stefanova – 82  
 A.V. Stekolnikov – 33  
 G.B. Stephenson – 77  
 Sarah L. Stoll – 119  
 N.R. Storozhev – 104  
 A.J. Strauss – 72  
 G.B. Stringfellow – 87  
 B. Stroka – 134  
 H.P. Strunk – 20, 118  
 C. Subramanian – 95  
 Shigeho Sueno – 94  
 T. Sugimoto – 61  
 T. Sukegawa – 19  
 Daliang Sun – 12  
 B.N. Sun – 131  
 Ichiro Sunagawa – 6, 170  
 E.P. Supertzi – 63  
 T. Suzuki – 43, 44, 97

M. Tachibana – 61  
 D.M. Tagirova – 142  
 Lu Taigin – 6, 15  
 K. Takano – 14, 18  
 H. Takayama – 14  
 Takeo Takizawa – 187  
 A. Tamai – 188  
 Isao Tanaka – 132  
 Takaho Tanaka – 140, 141  
 A. Tanaka – 19  
 X. Tang – 138  
 Ichiro Taniguchi – 156  
 T.L. Tansley – 88  
 J.B. Tassano – 85, 86  
 V.M. Tatarintsev – 123  
 Dmitri E. Temkin – 30  
 R. Terne – 163  
 Kazutaka Terashima – 40  
 I. Théry – 111  
 William A. Tiller – 60  
 M. Timoshchkin – 106  
 Fumitaka Togashi – 168  
 Eiji Tokizaki – 40  
 N.K. Tolochko – 104  
 Koichi Toyoda – 15  
 V.V. Trofimenko – 25

## AUTHOR INDEX (Cont'd)

Katsuo Tsukamoto – 29  
C.W. Tu – 117  
Y. Tzeng – 167

Takashi Uchida – 116  
Tetsuya Uchida – 116  
Satoshi Uda – 60  
T. Uemoto – 186  
Makio Uwaha – 127, 128

A.J. Valentino – 71  
Z.I. Vales – 142  
G.M. van Rosmalen – 4, 193, 195  
T.H.M. van de Berg – 183  
E.P.G. van der Berg – 155  
J.P. van der Eerden – 32, 48, 173, 183  
M.C. van der Leeden – 195  
M.G. Vasil'ev – 82  
P.G. Vekilov – 54  
J.J. Venkrbec – 70  
M.A. Verheijen – 48  
J.C. Vial – 84  
A. Virzi – 104  
D. Vivien – 111  
Daniel Vizman – 102  
L.J.P. Vogels – 48  
F.C. Voogt – 146  
V.V. Voronkov – 20, 151  
V.V. Voronov – 123  
C.H. de Vreugd – 193  
  
Hideo Wada – 15  
Koh Wada – 116  
Toshiaki Wada – 5

H. Walcher – 169  
Mu Wang – 156  
T.H. Wang – 19  
B.M. Wanklyn – 24, 72, 120, 121  
J. Watanabé – 49  
Masahito Watanabe – 17  
Minoru Watanabe – 132  
T. Watanabe – 50, 134, 181, 182  
Takeshi Watanabe – 168  
B.E. Watts – 134  
Patricia Weber – 147  
Barry A. Wechsler – 110  
J. Wei – 167  
M. Weiss – 135  
Joseph F. Wenckus – 149  
E. Wenzl – 134  
C. Wetzel – 90  
A.A. Wheeler – 99  
H. Wiedemeier – 159  
William R. Wilcox – 100, 101, 189  
Ch. Wild – 169  
H.H. Wills – 1  
G.J. Witkamp – 193  
A.F. Witt – 69  
C.F. Woensdregt – 111  
E. Woermann – 107  
F.R. Wondre – 120  
Joe Wong – 140  
J.M. Woodall – 117  
Glenn A. Woodell – 81  
G.H. Wu – 159  
B.J. Wuensch – 178  
H. Wüest – 35

Rong-Fu Xiao – 127  
H. Xiao – 192  
Xiangang Xu – 89  
  
Yu P. Yakovets – 123  
Kiyoshi Yamagishi – 107  
H. Yamagishi – 14, 18  
Yasuhide Yamaguchi – 107  
J.K. Yamamoto – 38, 59  
Mikihiro Yamanaka – 56  
Hiroshi Yamashita – 93  
Kiyoshi Yase – 56  
M. Yemou – 49  
Xu Yi-bin – 133  
Etsuro Yokoyama – 153  
Hu Yongle – 120  
Yasushi Yoshioka – 160  
J.L. Young – 91  
V.S. Yuferev – 82  
H. Yumoto – 50  
  
L.A. Zadorozhnaya – 190  
D.E. Zelmon – 63  
J.Q. Zhang – 192  
Hao Zhang – 196  
Lu Zhang – 95  
E.V. Zharikov – 104, 191  
X.-Y Zheng – 92  
J. Zhou – 101  
Shen Zhu – 92  
H. Zimmermann – 162  
M. Zlatkowski – 154  
V.I. Zorya – 123

## ACTIVITIES - LOCATION

CONFERENCE REGISTRATION .....	GRAND BALLROOM ENTRANCE FOYER
WELCOME RECEPTION .....	POOL GROUNDS
VENDOR RECEPTION .....	CHAMPAGNE BALLROOM
CONFERENCE OFFICE .....	ROSE ROOM
PUBLICATION OFFICE .....	SAUVIGNON ROOM
SLIDE PREVIEW CENTER .....	SAN ANTONIO ROOM
PLENARY SESSIONS .....	GRAND BALLROOM
TECHNICAL SESSIONS "A" .....	CUYAMACA ROOM
TECHNICAL SESSIONS "B" .....	LAGUNA ROOM
TECHNICAL SESSIONS "C" .....	PALOMAR ROOM
TECHNICAL SESSIONS "D" .....	WHITE WINES ROOM (Chenin, Colombard, Gamay and Riesling Rooms)
POSTER SESSIONS .....	EXHIBIT HALL
ACCOMPANYING PERSONS HOSPITALITY .....	CABERNET/CHARDONNAY ROOMS
INDUSTRIAL EXHIBIT .....	CHAMPAGNE BALLROOM
PHOTOGRAPH EXHIBIT .....	CHAMPAGNE BALLROOM
CRYSTAL EXHIBIT .....	CHAMPAGNE BALLROOM
BANQUET .....	GRAND BALLROOM





